ROR1 AS A TARGET FOR CANCER IMMUNOTHERAPY

Solange Rosa Paredes Moscosso

UCL

A thesis submitted to University College London (UCL) for the degree of Doctor of Philosophy

Supervisors: Prof Amit Nathwani and Dr Martin Pule
September 2017

Declaration

I, Solange R. Paredes Moscosso, confirm that the work presented in this thesis is my own. Where information has been derived from other sources, I confirm that this has been indicated in the thesis.

Solange R. Paredes Moscosso

Abstract

Receptor tyrosine-kinase like orphan receptor (ROR1) is a member of the tyrosine kinase family. Importantly, ROR1 is absent in healthy, critical tissue but overexpressed in various solid and haematological malignancies, including Chronic Lymphocytic Leukaemia (CLL). Moreover, recent studies suggest ROR1 is expressed on cancer stem cell-like cells (CSCs). The overriding aim of this study was therefore to combine the unique features of ROR1 with the exquisite specificity/therapeutic potential of monoclonal antibodies (MAbs) and/or their derivatives.

To this end, our group generated a rat hybridoma library and screened >150 anti-ROR1^{+} clones. I then cloned 16 of our novel antibodies to human IgG1, kappa constant regions, of which 12 recognised ROR1 on different cell types. Based on functional/characterisation data, it was identified that clone SA1 exhibited significant CDC activity on primary CLL cells, whilst clone F was the only MAb able to bind the Frizzled domain of ROR1. Further investigation, however, revealed clone SA1 bound non-specifically to ROR1^{-} cells. Therefore, my investigation focused instead on clone F, which was developed in parallel as a bispecific T-cell engager (BiTE) within our group.

Having shown F BiTE elicited potent and specific cytotoxicity of ROR1^{+} cells on various solid cancer cell lines, including pancreatic cancer (PaCa), ROR1 BiTE was tested on PaCa cell line-derived CSCs using an *in vitro* tumoursphere model. Immunocytochemistry data confirmed specific elimination of cells expressing both CSC biomarkers and ROR1.

As a whole, ROR1 MAb-based immunotherapy, particularly using BiTEs, seems to not only target ROR1^{+} cells present in the bulk of the tumour but, crucially, it also eliminates ROR1^{+} CSC subsets in PaCa. This approach represents a relevant and much needed addition to the current options for cancer treatment. Further preclinical and clinical studies will ultimately reveal the true therapeutic potential of ROR1 BiTEs alone and in combination.

Acknowledgements

I would like to start by thanking both my supervisors Prof Amit Nathwani and Dr Martin Pule. Amit, I particularly want to say thank you for believing in me and giving me the opportunity to join the group more than 5 years ago, and for encouraging me to pursue a PhD!

I would also like to thank all the people I was blessed to work with in the ACN group (present and past), and that made the lab such an enjoyable place to work in. The list is long, but I cannot help mentioning: Jenny M., Marc, Polly, Sara, Allison, Azadeh. Doyoung, Cecilia, Rebecca, Marco, Sat, Micaela, Moh, Adriana, Susi, Jonathan, Sajjida, Gavin and Kinda. Special thanks go to the CLL T-eam, originally composed by Marc and I (thanks for all the lessons, conversations, laughter and support, Marc!). The team was then enriched by the presence of Sat (your enthusiasm and productivity were always refreshing and inspiring).

The CLL T-eam soon became the ROR1 T-eam, led by Marco (you gave us a new perspective, solid expertise and good advice! I'm truly grateful for having learnt from you). Months passed by and Micaela joined our little group (Miccita, you gave a new colour to my days! Your attentiveness and hardworking attitude are impressive. I'm sure you'll go far!). Recently, the group welcomed Moh and Leo (you guys have brought the "coolness" to our group…thanks for that!).

But what's science without collaborations? Therefore, I'd like to thank Jenny Y., Maha and Fatemeh from Prof K. Chester's lab and all the people from the Haematology department; among them: Oscar and Theresa for the philosophical and enjoyable conversations. Gordon, Eva, Leyla, Farhaan and all the Pule group. Your friendship (and sometimes, reagents) made my days more enjoyable!

A wholeheartedly thank you goes to Sara, Leyla, Eva, and more recently, Micaela. I found in you, my lovely girls, true friendship and an oasis of honesty, fun, a bit of alcohol, and the craziest yet insightful conversations. I feel truly blessed for having met you!

Yet, my biggest thank you goes to Daddy and Ma! To my sisters: Erika, Shirley, Kelly, and to the light of my eyes -my niece and goddaughter- Anna Lucía. Daddy and Ma; your vision, sacrifice, contagious braveness, “unique” personalities and parenting (hahah), support (in every single sense), trust and words of wisdom, have sculptured the person I am today and encouraged me to cross the ocean just to follow a dream… Your sisterly banter (E and Shir), your most needed visits (Kelly) along our little “expeditions” and getaways rebooted my system! Mi Nunú, your very existence and laughter have been an inspiration since the very day you were born!

Needless to say that my love and profound gratitude goes to you, Claudio. Thanks for all your love, patience and intellectual stubbornness, you challenge me and make me a better person. Your strength, awesomeness and unique sense of humour make life so much easier and happier. In moments of darkness, your love and presence were a safe haven!

Last, but definitely not least, I need to publicly say thank you to Whom is the very reason of my existence and everything in it. This is to You, my Lord. During all my life, You have made Your love, gentleness, fatherly correction and pure sweetness known to me. No matter what comes our way, Your love makes it all worth it. Ad Maiorem Dei Gloria!

Table of contents

List of figures

List of tables

List of abbreviations

5’RACE	5’ Rapid amplification of cDNA ends
5-FU	5- fluoruracil
ABC	ATP-binding cassette transporters
ACT	Adoptive cell transfer
ADC	Antibody-drug conjugate
ADCC	Antibody-dependent cellular cytotoxicity
ADCP	Antibody-dependent cellular phagocytosis
AF488	AlexaFluor 488
AKT	Protein kinase B
ALDH1	Aldehyde dehydrogenase 1
ANOVA	Analysis of variance
APC	Antigen presenting cell
APRIL	Tumour necrosis factor ligand super family member 13
BAFF	Tumour necrosis factor ligand super family member 13B
B-ALL	B-cell acute lymphoblastic leukaemia
BCR	B cell receptor
BiTE	Bispecific T-cell engager
CAR	Chimeric antigen receptor
CD	Cluster of differentiation
CD40L	CD40 ligand
CDC	Complement-dependent cytotoxicity
cDNA	Complementary DNA
CDR	Complementary determining regions
CIE	Clathrin-independent endocytosis
CK1ε	casein kinase 1 epsilon
CLL	Chronic Lymphocytic Leukaemia
CME	Clathryn-mediated endocytosis
CR	Complete remission
CREB	cAMP-response-element-binding protein

CRS	Cytokine release syndrome
CSC	Cancer stem cell-like cell
c-Src	Cellular Src kinase
Ct	Cycle threshold
CTLA-4	Cytotoxic T lymphocyte-associated protein 4
CXCL12	CXC-chemokine ligand 12
CXCR4	CXC-chemokine receptor 4
DAMP	Damage-associated molecular pattern molecules
DAPI	4’,6-diamidino-2-phenylindole
DC	Dendritic cells
DFS	Disease-free survival
E:T	Effector to target ratio
EBV	Epstein-Barr virus
ECM	Extracellular matrix
EDTA	Ethylenediaminetetraacetic acid
EGFR	Epidermal growth factor receptor
EMT	Epithelial-mesenchymal transition
eROR1	Extracellular ROR1
EV	Extracellular vesicle
Fab	Fragment antigen binding
FAP	Fibroblast activation protein
Fc	Fragment crystalline
FcRn	Neonatal Fc receptor
FcγR	Fc gamma receptor
FPLC	Fast protein liquid chromatography
GM-CSF	Growth and differentiation factor granulocyte macrophage colony-stimulating factor
GPCR	G-coupled protein cell receptor
GPCR	G-protein-coupled receptors
HAT	Hypoxanthine-aminopterin-thymidine
HD	Healthy donor

HGPRT	Hypoxanthine-guanine-phosphoribosyltransferase
HI-FBS	Heat-inactivated foetal bovine serum
HLH	Haemophagocytic lymphohistiocytosis
HRP	Horseradish peroxidase
IFN-γ	Interferon gamma
IL-2	Interleukin 2
IMGT	Immunogenetics information system
IPMN	Intraductal papillary mucinous neoplasm
ITAM	Immunoreceptor tyrosine-based activation motif
ITIM	Immunoreceptor tyrosine-based inhibitory motif
K_D	Dissociation rate constant
K_{off}	Dissociation rate constant
K_{on}	Association rate constant
LGR	Leucine-rich repeat-containing GPCR
MAb	Monoclonal antibody
MAC	Membrane attack complex
MAS	Macrophage activation syndrome
MCL	Mantle-cell lymphoma
MCN	Mucinous cystic neoplasm
MDSC	Myeloid-derived suppressor cells
MFI	Median fluorescence intensity
MFIR	Median fluorescence intensity ratio
MHC	Major histocompatibility complex
miRNA	MicroRNA
MMP	Matrix metalloproteinases
MSKCC	Memorial Sloan Kettering Cancer Centre
NFκB	Nuclear factor-κB
NK	Natural killer cells
NKT	Natural killer T-cells
NPC	Nasopharyngeal carcinoma
NR	Non-reducing conditions

o/n	Overnight
ORR	Objective response rate
OS	Overall survival
OV	Oncolytic virus
PaCa	Pancreatic cancer
PAGE	Polyacrylamide gel electrophoresis
PAMP	Pathogen-associated molecular pattern molecules
PanIN	Pancreatic intraepithelial neoplasia
PAO	Phenyalrsine Oxide
PBMCs	Peripheral blood mononuclear cells
PBS	Phosphate-buffered saline
PCP	Planar cell polarity
PCR	Polymerase chain reaction
PD-1	Programmed cell death protein 1
PDAC	Pancreatic ductal carcinoma
PDGF	Platelet-derived growth factor
PD-L1	PD-1 Ligand
PI	Propidium iodide
PI3K	Phosphatidylinositol 3-kinase,
PSC	Pancreatic stellate cells
qPCR	Quantitative polymerase chain reaction
qPSC	Quiescent pancreatic stellate cells
R	Reducing conditions
ROR1	Receptor tyrosine kinase-like orphan receptor 1
ROR2	Receptor tyrosine kinase-like orphan receptor 2
RTKs	Receptor tyrosine kinases
Rtx	Rituximab
scFv	Single chain variable fragment
sCRS	Severe cytokine release syndrome
SD	Standard deviation
SEM	Standard error of the mean

SDS	Sodium dodecyl sulphate
SHH	Sonic hedgehog
SPR	Surface plasmon resonance
TAA	Tumour-associated antigen
TB	Trypan blue
TCR	T-cell receptor
TIL	Tumour infiltrating lymphocytes
TME	Tumour microenvironment
TNF	Tumour necrosis factor
TRUCK	T-cells redirected universal cytokine killing
TTF-1	Thyroid transcription factor
VCAM1	Vascular cell adhesion protein 1
VEGF	Vascular endothelial growth factor
VH	Variable heavy antibody region
Vim	Vimentin
VL	Variable light antibody region
αSMA	α-smooth muscle actin

Chapter 1 Introduction

1.1 Cancer immunosurveillance, immunoediting and immunotherapy

As defined by Hanahan and Weinberg almost two decades ago, cancer is not one but more than a hundred diseases bearing unanticipated high levels of complexity (Hanahan and Weinberg, 2000). It has now become evident that malignant tumours, rather than insular masses of proliferating cancer cells, are complex tissues composed of multiple distinct cell types that interact with one another. These various cell types actively contribute to tumourigenesis and disease progression, and constitute the tumour microenvironment (TME) (Hanahan and Weinberg, 2011). Consequently, in order to grow and expand, cancer tumours exploit several strategies, including immune escape; a feature that has become a hallmark of cancer.

Extensive investigation of the relationship between immunity and cancer has been carried out for over a century, since (Coley, 1893) reported successful treatment of inoperable sarcoma by mixed bacterial toxins (*S. erysipelas* and *B. prodigiosus*). A few years later, Paul Ehrlich postulated for the first time in 1909 the concept of 'tumour surveillance', whereby tumour cells can be distinguished from healthy cells and could therefore be eliminated by the immune system before clinical detection (Ehrlich, 1909). Unfortunately, no convincing experimental evidence supported this notion. It was only on the second half of the last century where homograft rejection studies led Lewis Thomas (Thomas, 1959) but mostly Frank MacFarlane Burnet to champion the 'cancer immunosurveillance' hypothesis (Burnet, 1967).

On the following years, contradicting experimental data began to emerge and most immunologists were still sceptical. This changed since the 1990s as evidence in favour of effective tumour-specific immunity became increasingly compelling, amongst them: i) identification of various tumour-associated

antigens (TAA) (Urban and Schreiber, 1992, Rosenberg, 1999), ii) presentation of TAAs by dendritic cells (DCs) to the adaptive immune system (Flamand et al., 1994, Steinman and Dhodapkar, 2001, Parmiani et al., 2002), and iii) immunodeficient murine models (e.g. $RAG^{-/-}$, $STAT1^{-/-}$, $perforin^{-/-}$ mice) with much higher incidences of tumour than their wild-type counterparts (van den Broek et al., 1996, Dighe et al., 1994), etc.

A greater understanding of cellular immunity and the availability of better animal models not only supported the immunosurveillance concept, but led to the realisation that it only represented one dimension of the complex relationship between the immune system and cancer (Dunn et al., 2002, Dunn et al., 2004). Evidence showing that the immune system promoted the formation of primary tumours with reduced immunogenicy, able to escape immune recognition and destruction (Shankaran et al., 2001) prompted the development of the 'cancer immunoediting' hypothesis. The latter encompasses potential host-protective and tumour-sculpting functions; it is a dynamic process composed of three phases: elimination, equilibrium and escape (**Fig. 1. 1**).

The *Elimination* phase refers to what was originally described as 'cancer immunosurveillance'; whereby natural killer (NK) cells and NKT cells produce IFN-γ in response to local tumour inflammation. These interactions have direct anti-proliferative and apoptotic effects on malignant cells, whilst indirectly preventing angiogenesis. In turn, DCs acquire tumour antigens and migrate to the lymph node in order to present antigens to T-cells. These TAA-specific T-cells migrate from the lymph node to the tumour and mediate tumour regression. In parallel, to induce tumour cell death, the escalating immune response recruits NK cells and macrophages (Dunn et al., 2002). Despite its effectiveness, this immune response is not aways successful in preventing tumour development.

Equilibrium takes place when the immune system controls tumour growth but cannot eliminate the tumour. In line with this, a study by (Koebel et al., 2007) revealed that the immune system of a naive mouse can also restrain cancer growth for extended time periods. In their experiments, these researchers injected mice with a chemical carcinogen, methylcholanthrene (MCA), to induce tumourigenesis. There was a group of mice, however, that did not develop tumours. This group was then treated with antibodies that depleted CD8 or CD4 T-cells or neutralised IFN-γ, resulting in the development of sarcomas. These observations suggested that microscopic tumours were controlled by the immune system and were able to grow only when this control was disrupted.

Escape occurs when tumours accumulate new and several mutations that prevent their recognition and subsequent elimination by the immune system. An important escape mechanism is the reduced expression of the tumour antigen, or of the proteins involved in antigen presentation such as the downregulation of human leukocyte antigen (HLA) directly (Algarra et al., 2000) or of the components of the antigen processing pathways (Seliger et al., 2001). Alternatively, the tumour and/or the TME can promote immune dysfunction by overexpression of immunosuppressive cytokines (Khong and Restifo, 2002) or the recruitment of immunosuppressive cells like regulatory T-cells (Tregs), NKT cells (Terabe and Berzofsky, 2004), dysfunctional DCs (Pinzon-Charry et al., 2005) and tumour-resident myeloid derived suppressor cells (MDSC) (Gabrilovich, 2004).

The knowledge that: i) expression of the inhibitory receptor cytotoxic T lymphocyte associated antigen 4 (CTLA-4) on Tregs is an important regulator of T-cell activation (Schwartz, 1992); and ii) overexpression of the immuno-modulatory receptor programmed death-ligand 1 (PD-L1) promotes dysfunction of tumour-infiltrating T-cells (Chen and Flies, 2013), has led to the targeting of these molecules using monoclonal antibodies. Certainly, cancer

patients treated with checkpoint blockade antibodies against CTLA-4, PD-L1 or, its receptor on T-cells, PD-1, have achieved great clinical outcomes (Pardoll, 2012). Certainly, this type of therapy represents an illustrative example of what can be achieved when the escape phase of immunoediting is disrupted. This is discussed in more detail in **section 1.1.3.1**.

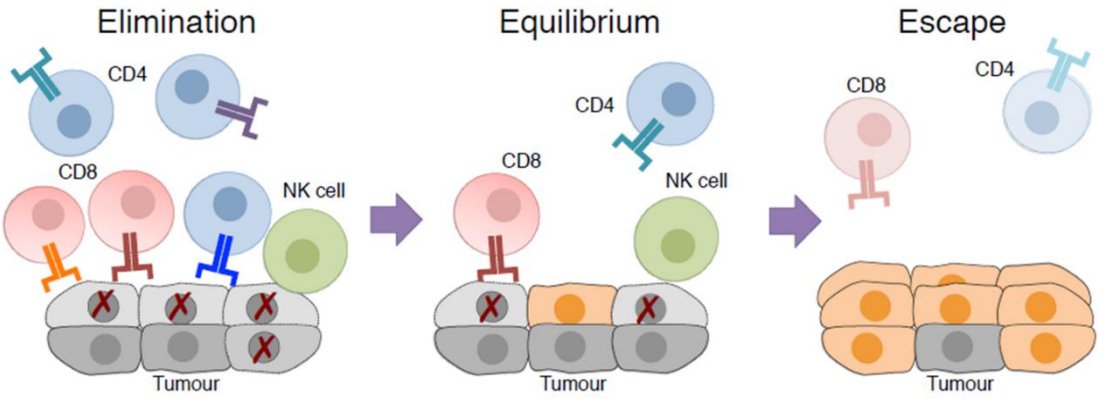

Fig. 1. 1. Cancer immunoediting. Elimination phase; where the immune response is able to kill tumour cells and reject the tumour. Equilibrium; tumour cells are still present due to incomplete elimination but still controlled by the immune system. Escape; genomic instability within the tumour and/or an immunosuppressive TME prevent malignant cells from being recognized by the immune system. TME= Tumour microenvironment. Modified from (Hotblack, 2016).

The great amount of evidence supporting the 'cancer immunoediting' theory has led both clinicians and immunologists to utilise the potential of the immune system to control and ultimately eliminate tumours in cancer patients. Recently, this has resulted in significant advances in the use of monoclonal antibodies (MAbs), therapeutic vaccines and adoptive cellular therapy (Lowdell and Thomas, 2017). The unprecedented clinical benefit that checkpoint blockade antibodies and other strategies have attained in patients with advanced-stage tumours strongly support the concept that immunotherapy represents a promising treatment for cancer (Chen and Mellman, 2013, Voena and Chiarle, 2016).

Cancer immunotherapy can be defined as the approach to treating cancer by generating or augmenting an immune response against malignant tumours (Khalil et al., 2016), whereby both the innate and adaptive arms of immunity can target tumour cells. Importantly, this approach has broad potential and offers the possibility of achieving durable and robust responses across a diverse spectrum of malignancies. In the next paragraphs, the main strategies in cancer immunotherapy, including oncological vaccines, oncolytic viruses, monoclonal antibodies and adoptive cell therapy will be summarised.

Additionally, in **Fig. 1. 2**, an overview of the current immunotherapeutic agents in cancer, categorised by their ability to directly target tumour cells or activate immune cells is presented.

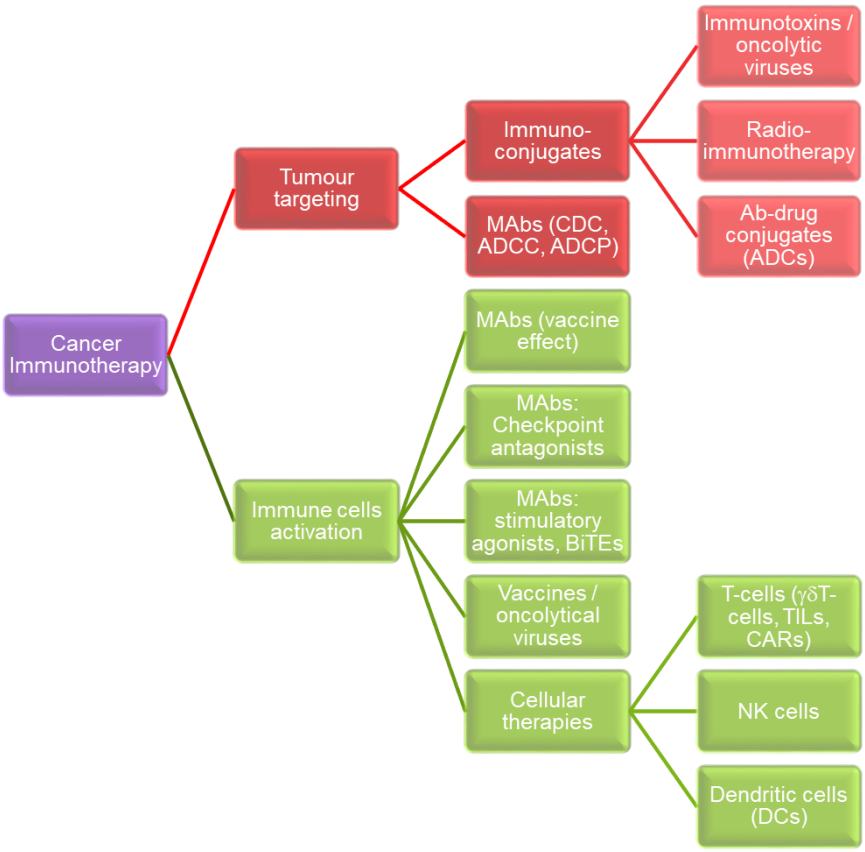

Fig. 1. 2. Conceptual palette of cancer immunotherapy agents. Different approaches for cancer immunotherapy are presented and classified based on their tumour targeting and immune cell activation effects. MAbs= Monoclonal antibodies, CDC= Complement-dependent cytotoxicity, ADCC= Ab-dependent cellular cytotoxicity, ADCP= Ab-dependent cellular phagocytosis, BiTE= Bispecific T-cell engager, ADC= Ab-drug conjugate, TILs= Tumour infiltrating lymphocytes, CAR= Chimeric antigen receptor, NK= Natural killer cells.

1.1.1 Cancer vaccines

The knowledge that cancer patients could harbour $CD8^+$ and $CD4^+$ T-cells capable of recognising tumour antigens (Rosenberg et al., 1988), prompted the possibility of developing cancer vaccines (Boon et al., 2006). This was supported by clinic-pathological studies that demonstrated a strong association between the presence of intratumoural T-cells, an IFN-γ signature and prolonged patient survival (Galon et al., 2006, Zhang et al., 2003).

The main goal of therapeutic cancer vaccines is to induce T-cell cytotoxicity by immunising patients against tumour-associated antigens (TAA). Unfortunately, their long history of failure has tainted this strategy. Many of the initial attempts were compromised by a lack of understanding of immunisation mechanisms, particularly the role of DCs (Mellman et al., 2011). DCs are known as the most effective antigen presenting cells (APCs) and are pivotal in coordinating innate and adaptive immune responses.

Another key consideration in vaccine therapy is the identification of suitable antigens. In the past, the use of short peptides derived from TAA (usually without effective DC-activating adjuvants) resulted in minimal clinical success (Sathyanarayanan and Neelapu, 2015). It is likely that vaccination with this type of antigens induced low to moderate affinity T-cells because of self-tolerance mechanisms. In contrast, the use of tumour-specific antigens could be recognised as foreign and lead to induction of high affinity T-cells and robust anti-tumour immunity (Cohen et al., 2015). Also, another major deficiency seen in clinical trials was the lack of suitable co-treatment during vaccination in order to overcome the highly immuno-suppressive tumour microenvironment (van der Burg et al., 2016).

To date, Sipuleucel-T is the only FDA-approved DC-based therapeutic cancer vaccine. It has been indicated for the treatment of asymptomatic or minimally symptomatic castrate resistant prostate cancer. Sipuleucel-T consists of

autologous $CD54^+$ APCs co-cultured and activated with a fusion protein of prostatic acid phosphatase conjugated with the DC growth and differentiation factor granulocyte macrophage colony-stimulating factor (GM-CSF). Although this therapy achieved an approximately 4-month improvement in median survival, randomised clinical trials failed to show effects on the time to disease progression (Kantoff et al., 2010).

In this context, the ideal cancer vaccine would be one able to trigger the maturation of DCs, which would in turn promote the production of tumour-reactive $CD8^+$ cytotoxic T-cells by using immunogenic tumour specific antigens. Since many of the standard-of-care chemotherapies can shape the immuno-suppressive cancer microenvironment, combinations of vaccines and chemotherapy would probably be the first step for improving clinical effects of therapeutic vaccines. For instance, treatment with an antimicrotubule agent, Paclitaxel (Taxol), in advanced ovarian cancer was shown to upregulate cytotoxic T-cell function (Emens and Jaffee, 2005). Similarly, (Shurin et al., 2012) has shown that many chemotherapeutic agents can directly stimulate functional activity of DCs. Furthermore, the inclusion of checkpoint therapy is likely to boost the tumour-specific immune response of vaccines (van der Burg et al., 2016).

With regards to ROR1 vaccines, (Imani Fooladi et al., 2015) designed *in silico* a ROR1 endotoxin B chimeric protein capable of stimulating ROR1-specific T- and B-cell mediated immune responses. Evaluation of this approach in *in vitro* and *in vivo* models remains to be performed.

1.1.2 Oncolytic virus therapy

Oncolytical viruses (OVs) are natural or genetically modified viruses that selectively infect and replicate in tumour cells, leading to immunogenic tumour cell death (Kaufman et al., 2015). Oncolysis is followed by activation of adaptive anti-tumour immunity through the release of anti-tumour antigens and

danger signals (e.g. damage-associated molecular pattern [DAMPs] and pathogen-associated molecular pattern [PAMPs] molecules) (Bartlett et al., 2013).

Hence, anti-tumour responses are promoted mainly through two mechanisms of action: i) non-immunogenic cell death; acute tumour debulking due to tumour cell infection followed by lysis, and ii) immunogenic cell death; presentation of danger signals and TAAs by dendritic cells to T-cells in order to induce/initiate systemic anti-tumour immunity. Additionally, OVs can be engineered to express specific cytokines able to stimulate immune cell recruitment/activation or to facilitate stimulation of intra-tumoural T-cells by the production of T-cell costimulatory molecules on infected tumour cells (Farkona et al., 2016, Hu et al., 2006, van Rikxoort et al., 2012).

Up to date, several types of viruses have been evaluated as vectors for OV immunotherapy. Viruses such as Newcastle disease virus, reovirus or Seneca valley virus are naturally non-pathogenic to humans. Others (like vaccinia virus, herpes simplex virus or measles virus) need to be genetically manipulated to become non-pathogenic (Chiocca and Rabkin, 2014). Accordingly, Talimogene laherparepvec (T-VEC), a modified oncolytic herpes simplex virus type I, is the most advanced OV agent in clinical development and it is now the first oncolytic immunotherapy to be FDA-approved for the treatment of advanced melanoma.

T-VEC has been modified in order to prevent neuronal involvement and to allow the secretion of GM-CSF. Enhanced production of this cytokine favours APC recruitment to the tumour microenvironment and induces anti-tumour immunity. Thus, T-VEC promotes viral replication, antigen presentation and increases oncolytic therapeutic activity overall (Johnson et al., 2015). Nevertheless, some limitations in terms of its application have been associated to this type of therapy. For example, OVs could not be used in immunocompromised patients as antitumour immunity could be compromised

(Senzer et al., 2009). Also, low levels of efficiency have been reported in patients with advanced disease. Furthermore, since OVs are injected locally, organs that are difficult to reach could not be treated (Ledford, 2015).

All in all, OV therapy possess a favourable risk-benefit ratio and its FDA-approval in 2015 (Ledford, 2015) is already a milestone in the field. It is anticipated that the targeting of immune-modulatory circuits involved in promoting tumour tolerance, such as CTLA-4 and PD-1/PD-L1 in combination with OVs would considerably augment anti-tumour immunity (Bartlett et al., 2013).

1.1.3 Monoclonal antibodies (MAbs)

As reviewed by (Strebhardt and Ullrich, 2008), Paul Ehrich first proposed the “magic bullet” hypothesis over a century ago; yet, it was the development of the hybridoma technology by (Kohler and Milstein, 1975) that the generation of monoclonal antibodies (MAbs) became feasible.

In the past two decades, the use of monoclonal antibodies has become an established strategy for the treatment of both haematological and solid malignancies (Scott et al., 2012), either as monotherapy or in combination with chemotherapy, small-molecule inhibitors and other antibodies (Loisel et al., 2011). Certainly, naked antibodies have improved overall response rate, complete remission rates, and progression-free as well as overall survival in multiple cancers including breast cancer, colon cancer, lymphomas, amongst others (Sathyanarayanan and Neelapu, 2015).

One of the first MAbs that showed encouraging results on clinical trials was Rituximab, an anti-CD20 chimeric mouse-human antibody used on non-Hodgkin lymphoma patients (Maloney et al., 1997, O'Brien et al., 2001). It is now evident that, in combination with chemotherapy, Rituximab has revolutionised the treatment of B-cell malignancies (Keating et al., 2005, Rai

and Jain, 2015). Recently, advances in antibody engineering and the discovery of better tumour-associated targets have contributed to the expansion of the field of antibody-based therapeutics. As of July 2017, more than 24 MAbs, most of them human IgG-based, have been FDA-approved for cancer therapy and ≥150 mAbs and/or antibody fragments are in clinical development (Pandey and Mahadevan, 2014).

Based on their target, antibodies used in cancer treatment can be classified into two categories: i) direct targeting MAbs; comprised of conventional antibodies that target tumour cells by direct binding to either lineage-specific antigens (such as CD20 or CD52), tumour neoantigens (e.g. glycans) or oncogenic biomarkers (e.g. epidermal growth factor receptor [EGFR]); which upon antibody engagement, eliminate tumour cells via Fc-signalling (Yu et al., 2017). ii) immunomodulatory MAbs; do not directly engage tumour cells but target receptors on immune cells in an attempt to stimulate the immune system, particularly $CD8^+$ T-cells (Lee et al., 2013, Berman et al., 2015). Accordingly, researchers in the field of cancer immunotherapy are now focussing not only on the induction/activation of the immune system but also on overcoming immunosuppression from the tumour microenvironment (Nicholas et al., 2016b). This type of therapy will be discussed in the next paragraphs.

1.1.3.1 Immune checkpoint blockade

One of the main reasons why cancer immunotherapy has come under the spotlight is the remarkable clinical benefits observed after cancer patients were treated with immune checkpoint therapy. This approach is based on the notion that anti-tumour T-cells are generated by the organism in response to tumour antigens (mutated neo-antigens); moreover, these are likely to be high affinity T-cells (Cohen et al., 2015, Gros et al., 2014). These cells however could be rendered ineffective due to several immune resistance mechanisms, collectively called immune checkpoints (Sledzinska et al., 2015). Crucially,

blocking the immune checkpoints enhances the function of anti-tumour T-cells and tilts the balance in the tumour microenvironment from immunosuppressive and immune resistance to immune destruction of the tumour.

It is now accepted that activated T-cells upregulate various co-inhibitory receptors on their cell surface in order to regulate their function and prevent unwanted immune responses against normal tissues. Many such receptors have been identified over the last years, including CTLA-4, PD-1, TIM-3, BTLA, LAG-3, among others (Tsiatas et al., 2016). In acute infections, for instance, once the antigen has been eliminated, T-cells downregulate their inhibitory receptors and a subset of T-cells persist as memory T-cells. In chronic infections and cancer, however, chronic antigenic stimulation leads to overexpression of inhibitory receptors on T-cells, which results in impaired function or even T-cell exhaustion (Wherry, 2011, Blackburn et al., 2009).

Not surprisingly, several tumour escape mechanisms use immune checkpoint pathways to evade the immune response. The most relevant examples are the interactions between CTLA-4 on activated T-cells and CD80/86 on DCs, which results in T-cell inhibition. Similarly, binding of PD-1 on activated T-cells to PD-L1 on tumour cells results in T-cell signalling attenuation and inhibition of T-cell proliferation and function (**Fig. 1. 3**).

The use of Ipilimumab and Nivolumab -monoclonal antibodies against CTLA-4 and PD-1, respectively- has become paradigm-shifting in the treatment of solid tumours. Several reports indicate these blocking MAbs promoted prolongation of overall survival (Hodi et al., 2010) and durable clinical responses, with some patients remaining free from disease progression for many years (Topalian et al., 2014).

For instance, according to (Phan et al., 2003, Hodi et al., 2010) anti-CTLA-4 MAbs unleash pre-existing anticancer T-cell responses, trigger potent antitumour properties and prolong overall survival. Similarly, antibodies

against PD-1 and PD-L1 have attained long-lasting clinical responses within a broad range of human cancers (Brahmer et al., 2012, Mahoney et al., 2015).

Despite these unprecedented results, concomitant immune-related toxicities have also been observed, particularly with CTLA-4, where severe adverse events have been observed in up to 35% patients (Phan et al., 2003, Hodi et al., 2010). Futhermore, a major disadvantage of checkpoint blockade MAbs is that only a relatively small fraction of patients obtains clinical benefit. Current efforts are on-going to identify novel immune modulators with similar efficiency but less toxicity (Farkona et al., 2016).

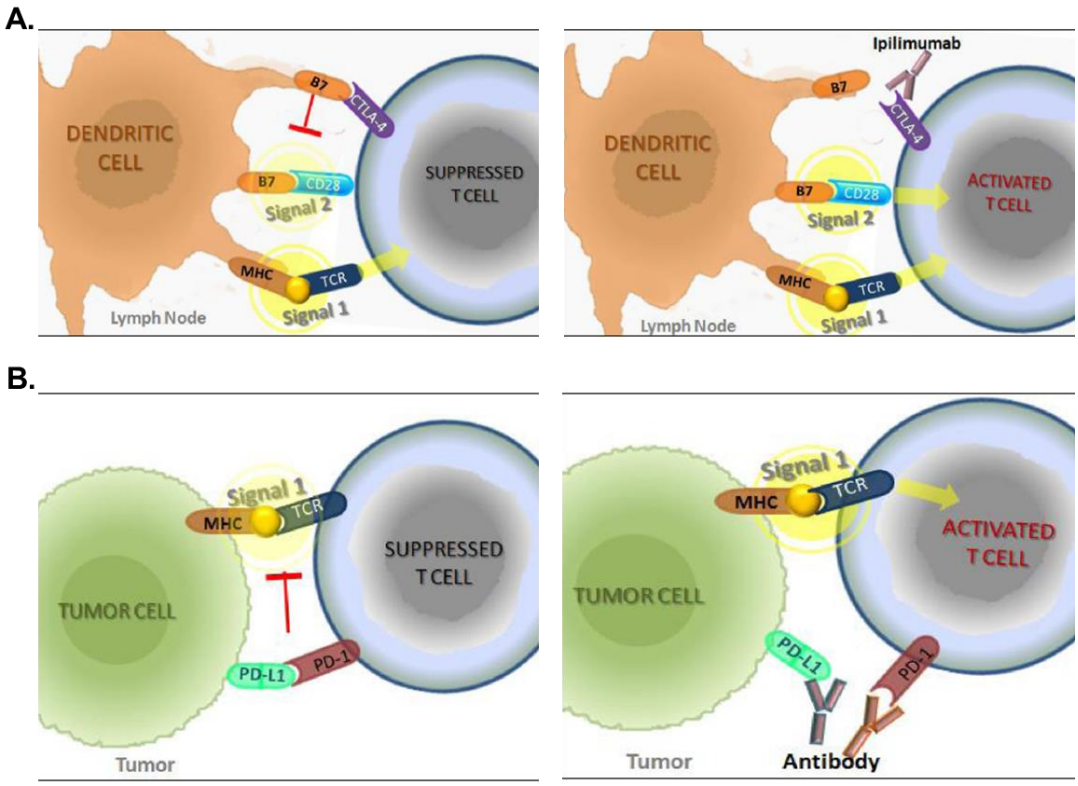

Fig. 1. 3. Immune checkpoints and blocking antibodies. (A) In the lymph node. Both immunological signals 1 (TCR recognition of antigens through MHC) and 2 (CD28-B7 costimulation) are required for T-cell activation in the lymph node. Interaction between B7 and CTLA-4 suppresses T-cells by blocking immunologic signal 2. Anti-CTLA-4 antibodies (Ipilimumab) allow T-cell activation. (B) In the tumour microenvironment; PD-1 is an inhibitory receptor expressed on antigen-activated T-cells and its interaction with PD-L1 blocks anti-tumour response. MAbs targeting PD-1 impede activation of the PD-1 pathway, thereby allowing T-cell activation. TCR= T-cell receptor, MHC= Major histocompatibility complex. Modified from Farkona et al., 2016.

1.1.4 Adoptive cell transfer (ACT)

Another form of immunotherapy is the adoptive transfer of lymphocytes – that have firstly been isolated from patients' peripheral blood, tumour draining lymph nodes or tumour tissue, expanded *ex vivo*, and reinfused back into the patient (Hinrichs and Rosenberg, 2014).

An example of this approach is the ACT of NK cells, which are phenotypically defined as CD3-CD56+ lymphocytes. This type of therapy has been more successful in haematological malignancies than solid tumours. In 2011, Curti et al. reported that out of 13 acute myeloid leukaemia (AML) patients, 6 achieved transient complete remission (CR) responses (Curti et al., 2011); thereby suggesting this infusion of NK cells was feasible in elderly patients. For solid tumours, (Parkhurst et al., 2011) reported results of a clinical trial where 8 patients with metastatic melanoma or renal carcinoma were treated with autologous NK cells. Although no clinical responses were observed, adoptively transferred NK cells persisted for at least one week and, in some patients, for several months after transfer. Taken together, NK cell-based therapies have achieved modest clinical success in cancer patients and more developments are necessary to improve clinical efficacy.

Tumour-infiltrating lymphocytes (TILs) represent a more successful example of ACT. TILs are mixtures of $CD8^+$ and $CD4^+$ T-cells from resected tumours, and are expanded in presence of a cocktail of various cytokines. This is done in an attempt to reverse the functional impairment of these T-cells caused by the immunosuppressive tumour microenvironment (Gilham et al., 2015). TIL infusion after a lympho-depleting conditioning regimen resulted in an objective response rate (ORR) of more than 50%, as well as durable, complete regression of metastatic melanoma (Geukes Foppen et al., 2015). Importantly, host lymphodepletion is thought to improve TIL functionality by eliminating immunosuppressive cells such as Tregs and myeloid-derived suppressor cells (MDSCs) in the TME. Plus, it promotes overexpression of homeostatic

cytokines IL-7 and IL-15 (Gattinoni et al., 2005). Nevertheless, one of the major limitations of this approach is the cost and time required to develop these cell populations. Plus, TIL therapy is largely restricted to melanoma, as it is the only malignancy where clear clinical benefit has been achieved (Hinrichs and Rosenberg, 2014).

Another form of ACT is the transfer of T-cells expressing a chimeric antigen receptor (CAR). This CAR technology combines the antigen recognition domain of an antibody with T-cell intracellular signalling domains into a single chimeric protein (**Fig. 1. 4**). Patients' own T-cells are first activated, genetically modified to express a CAR, then expanded *ex vivo* and transferred-back into the patient. CAR T-cells will then be specifically redirected against cells expressing a tumour-associated antigen in a major histocompatibility complex (MHC)-independent manner (Riches and Gribben, 2014, Suryadevara et al., 2015).

Most clinical trials have used second generation CAR T-cells (i.e. engineered T-cells bearing two intracellular domains) against CD19, a cell membrane protein uniformly expressed on normal and malignant B-cells. In a hallmark study, (Porter et al., 2011) showed that these CD19 CARs have potent anti-tumour activity, even in high-risk patients. Notably, the introduction of the 4-1BB signalling domain resulted in increased persistence of CAR T-cells partly explained by the generation of memory CAR T-cells, which retained anti CD19-effector functionality (Kalos et al., 2011). An important aspect to consider when interpreting the results of this and other trials is that patients received lymphocyte-depleting chemotherapy that might have contributed to the reported remissions (Kochenderfer and Rosenberg, 2013). In line with this, inferior rate responses were observed in trials that did not include conditioning chemotherapy, such as those carried out at MD Anderson (Kebriaei, 2014).

One of the most successful CAR programs is the one designed at University of Pennsylvania and the Children's Hospital of Philadelphia (Maude et al.,

2014, Porter et al., 2015). Data from 48 evaluable pediatric patients treated with conditioning chemotherapy followed by CD19 CAR have shown 94% CR, whilst 6-month disease-free survival (DFS) was 76%. In terms of toxicity, severe cytokine-release syndrome (sCRS) reached 29% cases, plus there were 67% of patients that presented CD19-negative relapses. Certainly, some of the most toxic adverse events related to this type of immunotherapy are sCRS, macrophage activation syndrome (MAS; or haemophagocytic lymphohistiocytosis, HLH) and neurological toxicities. Selection of patients with low tumour burdens might minimise the occurrence of CRS and related toxicities in the future (Khalil et al., 2016).

With regards to solid tumours, CAR therapy faces three unique challenges not seen in B-cell malignancies. First, the microenvironment in malignancies such as B-cell acute lymphoblastic leukaemia (B-ALL), where CAR therapy has achieved impressive clinical outcomes, is not as immunosuppressive as in solid cancers. Second, antigen selection tends to be more challenging since antigen heterogeneity in the tumour and the TME is higher in solid malignancies (Fidler and Hart, 1982, Marusyk and Polyak, 2010). Third, the 'on-target, off-tumour' toxicity is usually more problematic as potential antigens in solid tumours are more likely to be expressed in other critical organs. Nevertheless, CARs targeting mesothelin for the treatment of mesothelioma (Adusumilli et al., 2014), pancreatic and ovarian cancer are now entering clinical trials.

Due to the immunosuppressive nature of the TME in cancer, a fourth generation CAR has been proposed recently, when (Chmielewski et al., 2011) demonstrated that production of CAR T-cells bearing a CAR-inducible IL-12 cassette secreted this cytokine upon CAR engagement. Therefore, CAR T-cells that release a transgenic product (usually a pro-inflammatory cytokine) and accumulate in the targeted tissue are called 'T-cells redirected for universal cytokine killing' (TRUCKs) (Chmielewski et al., 2014). Although systemic administration of IL-12 was shown to be toxic in early phase clinical

trials (Leonard et al., 1997), local administration could be achieved by IL-12 TRUCKs. The first clinical trial using armoured CAR T-cells targeting mucin-16 and secreting IL-12 in patients with ovarian cancer has opened (NCT02498912) (Koneru et al., 2015a) and is currently recruiting patients as final data will be collected in August 2018. Results are now awaited as IL-12 secretion in preclinical studies has been shown to enhance CAR T-cell persistence, resistance to Tregs and MDSC inhibition which provide enhanced antitumour efficacy *in vivo* (Kerkar et al., 2011, Chinnasamy et al., 2012, Koneru et al., 2015b).

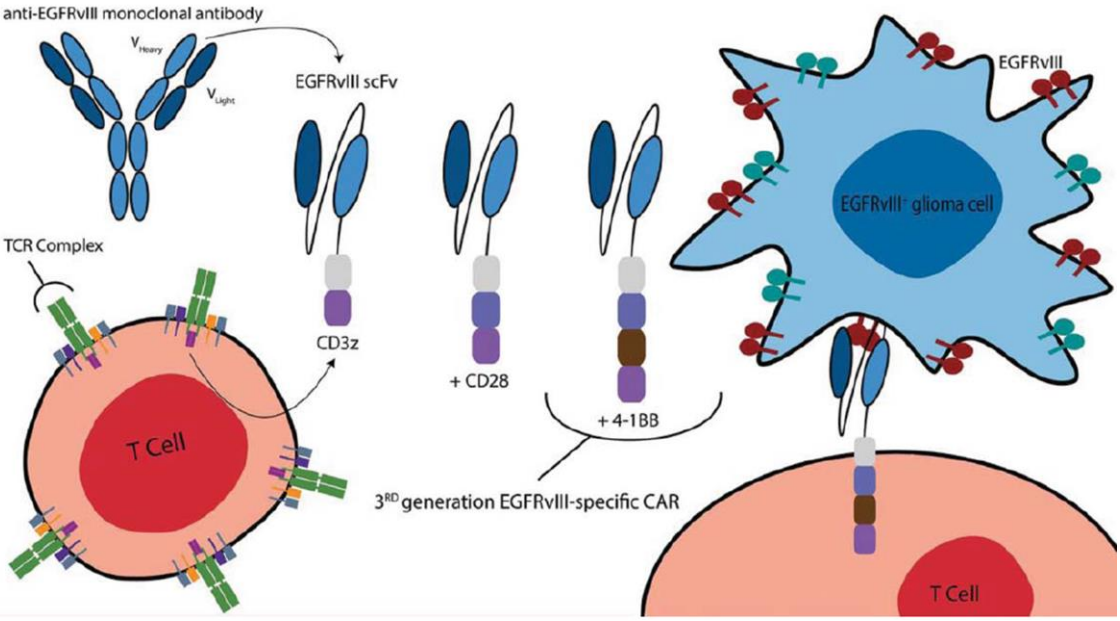

Fig. 1. 4. CARs are produced by combining the scFv specificity of an antibody, a transmembrane stalk and the intracellular signalling domains of a T-cell receptor (TCR). A schematic of an anti-EGFRvIII CAR is shown. For 1st generation CARs, CD3z was the intracellular domain of choice. More recently, additional costimulatory moieties (CD28 and/or 4-1BB) are being included to improve T-cell persistence, proliferation and anti-tumour activity, where 2nd and 3rd generation CARs are defined by their number of intracellular moieties. Reproduced from Suryadevara et al., 2015.

In this thesis, the ROR1-based immunotherapies generated were tested in both haematological and solid malignancies, namely: Chronic lymphocytic leukaemia and Pancreatic cancer. In the following sections, the disease biology, TME and current status of clinical applications will be discussed for both cancer types.

1.2 Focus on: Chronic lymphocytic leukaemia (CLL) and pancreatic cancer (PaCa)

1.2.1 Chronic lymphocytic leukaemia (CLL)

CLL is a chronic haematological malignancy characterised by the progressive accumulation of $CD5^+$ $CD19^+$ B-cells (Van Bockstaele et al., 2009) in blood, bone marrow, lymph nodes or other lymphoid tissues (Chiorazzi et al., 2005). It is the most common leukaemia diagnosed in the Western world among the elderly. Despite the current availability of novel small molecule inhibitors, including B-cell receptor antagonist such as Ibrutinib, and new monoclonal antibodies including Obinutuzumab, CLL remains incurable (Park and Brentjens, 2013). To date, allogeneic stem cell transplantation represents the only curative option due to the graft-versus-leukaemia effect mediated by the allogeneic T-cells. Nevertheless, the age-related excess in morbidity and mortality of this treatment –due to concomitant graft-versus-host disease (GvHD)– restricts its application.

1.2.1.1 CLL biology

More than a decade ago, chronic lymphocytic leukaemia was considered as a homogenous disease, where high counts of mature B-cells were mainly due to a fault in the mechanisms that lead to apoptosis. Nonetheless, research advances in the past few years have revealed that the accumulation of lymphocytes is not only characterised by prolonged B-cell survival but also by high cell proliferation (Chiorazzi, 2007).

CLL has now been demonstrated to be a heterogeneous disease with survival ranging from months to decades depending on age, gender, diversity of cell morphology, bone marrow histology, cytogenetics (mutation status of immunoglobulin heavy chain variable region (*IGHV*) genes, *TP53*, etc.), epigenetic alterations and immunophenotype, amongst others (Rodriguez-Vicente et al., 2013). Remarkably, high levels of Lactate dehydrogenase

enzyme (LDH), deletion of the short arm of chromosome 17 (del17p), high CD38 expression and increased ZAP70 (Zeta-associated protein of 70kDa) are associated with a reduced survival time (Van Bockstaele et al., 2009).

Genetic alterations in CLL can include chromosomal alterations, somatic mutations, changes in the expression of microRNAs (miRNAs) and epigenetic modifications. A study by (Dohner et al., 2000) revealed that ~80% of CLL patients carry at least one of four common chromosomal alterations: a deletion in chromosome 13q14.3 (del(13q)), del(11q), del(17p) and trisomy 12. Of these, del(13q) is the most common one (>50% of patients) and is associated with good prognosis. Trisomy 12 is associated with an intermediate prognosis and is found in 16% of patients, whilst del(11q), del(17p) are less common but are associated with adverse clinical outcome. A report by (Van Dyke et al., 2016) revisiting the Dohner classification in CLL, however, has shown that in general the overall survival has improved in recent years.

A series of studies involving next generation and whole-exome sequencing have increased our understanding of the genetic heterogeneity of CLL (Landau et al., 2015, Puente et al., 2015). Recurrent somatic mutations have been observed in genes with a role in: DNA damage (e.g. *TP53, ATM*), mRNA processing (e.g. *SF3B1, XPO1*), chromatin modification (e.g. *HIST1H1E, CHD2, ZMYM3*), Wnt and Notch signalling pathways, as well as *BRAF*, which can affect B-cell related signalling and transcription (Damm et al., 2014). Interestingly, somatic mutations can be induced after chemotherapy or small molecule inhibitors. A recent study reported that CLL patients treated with Ibrutinib (a BTK inhibitor) showed mutations associated with drug resistance as they were different from those detected in CLL patients treated with standard chemotherapy (Burger et al., 2016).

(Calin et al., 2002) reported for the first time the involvement of miRNAs in any human disease. The study described that the most common lesion in CLL is the downregulation/deletion of two closely linked miRNAs: *mir-15-1* and *mir-*

16a. Since both miRNAs target BCL2 and MCL1 (Cimmino et al., 2005), their loss enhances the expression of the target genes -which encode anti-apoptotic proteins of the BCL2 family- thereby prolonging CLL cell survival (Fabbri et al., 2011). Reduced expression or loss of other miRNAs can promote CLL development, amongst them: miR-29a/b, miR-29c, miR-34b, miR-181b and miR-3676 (Balatti et al., 2015). In contrast, (Costinean et al., 2006, Cui et al., 2014) has shown that overexpression of *mir-155* is associated with enhanced B-cell receptor (BCR) signalling, B cell proliferation and lymphomagenesis.

CLL heterogeneity also includes epigenetic changes. Recent studies (70, 71) have linked disordered methylation to genetic aberrations in CLL, thereby contributing to the accumulation of somatic mutations and adverse clinical outcome. Not surprisingly, methylation signatures can be used to classify distinct clinical CLL subgroups (Bhoi et al., 2016, Kulis et al., 2012).

With regards to the BCR signalling in CLL, it has been shown *in vivo* that the surface immunoglobulin of CLL cells is engaged by autoantigen, which results in constitutive BCR signalling (Duhren-von Minden et al., 2012). Certainly, the importance of this interaction is supported by the success of kinase inhibitors in the clinic. These types of therapies will be further discussed in **section 1.2.1.4**.

1.2.1.2 Tumour microenvironment in CLL

In CLL, the TME is mainly composed of neighbouring non-malignant stromal cells, nurse-like cells (lymphoma-associated macrophages), T-cells ($CD4^+$, $CD8^+$, Tregs), NK cells, DCs, endothelial cells and mesenchymal stromal/stem cells (Nicholas et al., 2016a). Importantly, CLL cells depend on the survival signals released by the TME. Therefore, CLL cells follow chemokine gradients into lymph nodes (usually mediated by CXCR4 in response to nurse-like cell-secreted CXCL12), where ‘proliferation centres’ are formed (Herishanu et al., 2011). Migration of CLL cells into lymph nodes can also occur via CCR7 in

response to CCL19 and CCL21 (produced by endothelial cells of high endothelial venules (HEVs)).

Once in the proliferation centres, the TME promotes CLL cells proliferation and are exposed to chemokines, integrins, cytokines and survival factors, such as: BAFF (TNF ligand superfamily member 13B) and APRIL (TNF ligand superfamily member 13B), which activate NF-κB (nuclear factor-κB) before they go back to the bloodstream (Endo et al., 2007). Activation of the latter results in *mir-155* expression which enhances BCR signalling, and in turn, CLL cell proliferation (Cui et al., 2014). CLL survival is also promoted through CD31 and CD38 activation, as well as interaction of ROR1/2 and/or various Frizzled receptors with Wnt factors produced by stromal cells. Consistent with this, high expression of ROR1 has been associated with accelerated disease progression (Cui et al., 2016). In parallel, mesenchymal stromal cells expressing VCAM1 (vascular cell adhesion protein 1) interact with CLL cells via binding to α4β1 integrin, which contributes with CLL survival.

CLL cells can also secrete chemokines to recruit T-cells and monocytes to the CLL TME. Activated T-cells send proliferative signals to CLL cells through CD40L (CD40 ligand) and CD40 interactions. Adding to the complexity of CLL cell-TME interactions, (Smallwood et al., 2016) showed that CD40/IL-4-stimulated CLL cells released extracellular vesicles (EVs) enriched with specific miRNAs, including miR-363. Transfer of these EVs to autologous $CD4^+$ T-cells exhibited enhanced migration and immune synapse formation interactions with tumour cells. This study revealed that CLL-EVs could modify T-cell function, highlighting the bidirectional effects of $CD4^+$ T-cell:tumour interactions. In parallel, amongst the cytokines that are secreted by T-cells, namely IL-2, IL-10 and IL-4, the latter can upregulate IgM on CLL cells, thereby facilitating the interaction of CLL cells with their autoantigen (Aguilar-Hernandez et al., 2016). Importantly, IL-10 (a known immunosuppressive cytokine) may also be secreted by CLL cells (DiLillo et al., 2013). Additionally,

(Ramsay et al., 2012) showed that CLL cells express high levels of both PD-L1 and PD-L2. These findings underline the immunosuppressive interactions in CLL that lead to T-cell exhaustion and impaired cellular immune function.

The high heterogeneity and complex CLL cell-TME interactions observed in this disease have to be therefore taken into account when designing the treatment strategy as it can have a direct impact on clinical course and response to treatment (Zenz et al., 2010). Current standard therapy and research on novel treatment options for CLL will be therefore discussed below.

1.2.1.3 Standard therapy

A meta-analysis study performed by the CLL Trialists' Collaborative Group more than 15 years ago found that the single-agent chlorambucil was the most effective treatment in terms of survival and, that inclusion of anthracycline gave no evidence of added benefit. Monotherapy with alkylating agents –in this case– chlorambucil, was recommended as the first line of treatment and it was, for several years, the gold standard (CLL trialists' collaborative group [(1999)]).

It is noteworthy to mention that, based on that same report; asymptomatic patients with early-stage disease are usually not offered treatment as no advantage was ascertained when early treatment with chlorambucil was compared to observation and/or late treatment. Indeed, up to a third of CLL patients never require treatment and yet have a near-normal life expectancy, with death resulting from causes other than CLL. Importantly, no studies on asymptomatic patients using current therapies have been performed (Rozovski et al., 2014). However, according to (Zenz et al., 2010), new clinical trials are selecting high-risk subgroups of CLL patients at early stages based on biological and clinical criteria with the aim to reassess the effects of early treatment.

Nevertheless, ever since that seminal publication in 1999, there has been a transition from single-agent therapy with alkylating compounds to nucleosides,

multidrug combinations and chemo-immunotherapy (Zenz et al., 2010). Accordingly, results from a clinical phase III trial (Hallek et al., 2010) showed for the first time that addition of an anti-CD20 antibody (Rituximab) to a combinatorial chemotherapeutic approach (i.e. Cyclophosphamide, an alkylating agent, and Fludarabine, a purine analogue that inhibits DNA repair of interstrand crosslinks caused by the former) had better efficacy in overall survival despite the increased toxicity. As reviewed by (Nabhan et al., 2014), this chemo-immunotherapeutic approach (known as FCR) is currently recommended to be used in fit patients with normal renal function as the standard upfront treatment.

Notably, a variety of drug combinations are currently available. Chemo-immunotherapeutic regimens would have to be adjusted depending on patients' performance status, renal function and comorbidities (Hallek, 2013). Nevertheless, due to the considerable toxicity of this sort of approach, alternative treatment options are being explored.

1.2.1.4 New therapies

Emerging research and evolving understanding of CLL biology have allowed the generation of new compounds that are currently in clinical development. In the next paragraphs, small-molecule inhibitors targeting the B-cell receptor and tyrosine kinases, along with immunotherapies encompassing the development of novel monoclonal antibodies, immunomodulatory drugs and chimeric antigen receptors will be discussed.

1.2.1.4.1 Small-molecule inhibitors

As reviewed by Tsubata, 2001, the B-cell receptor (BCR) signalling pathway is involved in cell proliferation, differentiation and antibody production in normal B-cells. Similarly, in CLL cells, this receptor plays a pivotal role in cell survival, proliferation and trafficking (Tsubata, 2001). Importantly, chronic lymphocytic leukaemia, along with other haematological malignancies, display aberrantly phosphorylated proteins involved in the BCR signalling pathway, mimicking

activated B-cells. This has led to the generation of kinase inhibitors targeting spleen tyrosine kinase (SYK) (Friedberg et al., 2010), mammalian target of rapamycin (mTOR) (Zent et al., 2010), Bruton's tyrosine kinase (BTK) (Honigberg et al., 2010) and phosphoinositide 3'-kinase (PI3K) (Lannutti et al., 2011).

Possibly the most impressive responses have been achieved by inhibitors developed against BTK, PI3K and SYK; namely, Ibrutinib, Idelalisib and Fostamatinib (Davids and Brown, 2012, Kipps et al., 2017b). These molecules have been found, in preclinical models, to reduce CLL cell viability through modulation of the stromal microenvironment. More recently, these drugs have been evaluated in patients with CLL. A brief summary of the clinical findings is presented below.

Ibrutinib is a highly potent BTK inhibitor. It is an orally bioavailable small molecule that have shown to be well tolerated in relapsed/refractory patients of all ages, including elderly patients. It has been reported that Ibrutinib works in part by disrupting the protective effect that stromal cells have on CLL cells (Herman et al., 2011). A randomised study of Ibrutinib versus Ofatumumab in patients with relapsed CLL revealed that Ibrutinib was highly effective even in high-risk patients bearing the del(17p) (Byrd et al., 2014). Results from this study led to the approval of Ibrutinib for the treatment of patients with relapsed CLL or as initial therapy of patients with del(17p). Similarly, a randomised study of Ibrutinib versus Chlorambucil as initial therapy showed that the BTK inhibitor was more effective than chemotherapy in patients ≥65 years of age without del(17p). This resulted in the approval of Ibrutinib for the initial treatment of CLL patients (Burger et al., 2015). Some adverse effects of this therapy, however, include fatigue, diarrhoea, bleeding, ecchymoses, rash, arthralgia, myalgia, increased blood pressure and atrial fibrillation. Second generation BTK inhibitors, such as Acalabrutinib (Byrd et al., 2016) or ONO/GS-4059 (Walter et al., 2016), are now in clinical trials in order to determine whether any

of these drugs has a superior therapeutic effect and/or less toxicity (Wu et al., 2016).

Similarly, Idelalisib (CAL-101), a potent and highly specific inhibitor of the PI3K delta isoform, promotes apoptosis in CLL cells in a time- and dose-dependent manner without inducing apoptosis of normal T-cells or natural killer cells. CAL-101 has been shown to disturb the interaction of several microenvironmental factors, such as nurse-like cells, cytokines and chemokines with the cancer cells (Wiestner, 2012). Remarkably, in a large phase I study, clinical benefit was observed even in patients with poor prognostic factors, as reviewed by (Davids and Brown, 2012). Idelalisib was approved in the United Stated and Europe after data from a clinical trial revealed that patients treated with Rituximab and Idelalisib had significantly higher response rates and overall survival than patients treated with Rituximab and placebo (Furman et al., 2014). Adverse effects of Idelalisib include transaminitis, pneumonitis and colitis, which tends to be severe enough to require therapy discontinuation (Lampson et al., 2016). Recently, the FDA recommended the closure of clinical trials investigating the Idelalisib and Rituximab combination as first-line treatment for CLL patients due to a high number of infections and deaths associated to this treatment (Buensalido and Chandrasekar, 2014). Currently, other PI3K inhibitors, such as Duvelisib, TGR-1022 and ACP-319 are also being evaluated in clinical trials (Blunt and Steele, 2015).

As reviewed by (Kipps et al., 2017a), treatment with Fostamatinib, an oral SYK inhibitor, caused reduction in lymphadenopathy with concomitant lymphocytosis in phase I/II clinical trials (Friedberg et al., 2010). Side effects of this treatment include neutropenia, thrombocytopenia and diarrhoea. Entospletinib, another SYK inhibitor, is currently being evaluated in preclinical and clinical studies.

Although small-molecule inhibitors have shown very promising results in pre-clinical models and clinical trials, a limitation to bear in mind is the development of resistance to treatment often seen in patients treated with monotherapies (Mani et al., 2015). More recently, new clinical trials exploring the use of these inhibitors in combination with monoclonal antibodies and/or chemotherapy are being carried out (Hallek, 2013). Such is the case of Venetoclax (ABT-199), an orally administered agent that selectively inhibits BCL-2 and does not target other members of the BCL family –preventing growth of lymphocytes without interfering with platelet homeostasis. This BCL-2 inhibitor has been recently tested in combination with Rituximab in a phase 1b trial, attaining an ORR of 88% (Roberts et al., 2014). The most common grade 3 to 4 adverse events however were neutropenia, thrombocytopenia and anaemia (Owen et al., 2015). Studies examining the use of Venetoclax with or without an anti-CD20 MAb, and with or without Ibrutinib are ongoing (Cervantes-Gomez et al., 2015, Thijssen et al., 2015). It is expected these combinations will provide higher response rates to therapy than with Venetoclax alone.

1.2.1.4.2 Immunotherapies: Immuno-modulatory drugs, Monoclonal antibodies & CAR T-cells

Despite the encouraging data obtained so far with both chemo-immunotherapy and small-molecule inhibitors, the former cannot be used in frail or elderly patients due to its toxicity. Small-molecule inhibitors, although better tolerated, produce relatively low rates of complete remission (CR, obtained in <10% of patients) and still do not seem to represent a cure for CLL (Riches and Gribben, 2014). Hence, new options of treatment need to be explored.

Immune-based therapies seek to boost or redirect the patient's own immune system in order to break tolerance to cancer cells and eliminate them (Makkouk and Weiner, 2015). As most malignancies, CLL presents defective immunological processes. As reviewed by (Emole et al., 2015), recent studies suggest that an immunotherapeutic approach can target and overcome these

aberrant processes without the toxicity of chemotherapy. In CLL, this could be achieved by: i) immunomodulatory therapy and ii) adoptive transfer of anti-tumour/checkpoint blockade monoclonal antibodies or chimeric antigen receptor (CAR) T-cells. These strategies will be briefly discussed below.

Lenalidomide, a derivative of thalidomide, is a chemically modified drug with enhanced immunomodulation and decreased neurologic toxicity (Carballido et al., 2012). It has been found that treatment with Lenalidomide indirectly affects the stromal microenvironment that would otherwise support CLL cells' proliferation; it also promotes expression of CD154 on CLL cells and anti-ROR1 antibody production (Lapalombella et al., 2010). Moreover, this drug reverses the defective immunological synapse formation reported in CLL (Ramsay et al., 2008). Lately, as commented by (Seiffert, 2014), Lenalidomide was found to have a direct anti-proliferative effect on CLL cells *in vitro* by targeting cereblon, a protein involved in cell-cycle arrest.

Despite its relevant anti-proliferative activity, which resulted in encouraging results in the treatment of high-risk patients; the side effects of Lenalidomide are considerable. In 58% of patients, it caused tumour flare reactions (i.e. visible and painful increase in lymph nodes size, malaise and fever) and tumour lysis syndrome. Plus, the overall rate response when used as monotherapy ranged between 32-54% in different clinical trials (Hallek, 2013).

The combination of Lenalidomide with Rituximab and other drugs have more recently been explored. Improved response (ORR of 66%) has been reported in relapsed/refractory CLL in a phase II study when Lenalidomide was used in combination with Rituximab (Badoux et al., 2013). Furthermore, therapy with an anti-CD20 MAb 9 days before initiation of Lenalidomide therapy seemed to mitigate the risk for tumour flare reaction (Vitale et al., 2016).

Rituximab, a chimeric anti-human CD-20 monoclonal antibody, although vastly efficient when used in combination, it is less active as a single agent unless

very high doses are used (O'Brien et al., 2001). More recently, Ofatumumab – a fully humanised anti-CD20 antibody targeting a different epitope than the one recognized by Rituximab– has shown increased binding affinity and prolonged dissociation rate. When compared to Rituximab, higher levels of cell killing through cell-dependent cytotoxicity (CDC) (Pawluczkowycz et al., 2009) and antibody-dependent cellular cytotoxicity (ADCC) activity have been found (Hallek, 2013). Nevertheless, there has not been a formal clinical trial comparing both antibodies.

Obinutuzumab (GA 101) is the most recently developed anti-CD20 monoclonal antibody. It has been humanised and glyco-engineered in order to have a higher binding affinity and increased ADCC and direct cell death induction, although it does have a lower CDC activity when compared to Rituximab *in vitro* (Mossner et al., 2010). Updated results from a clinical trial (CLL11), where Obinutuzumab was used in combination with chemotherapy in elderly patients, showed significant reduction in disease progression or death. In combination with Chlorambucil (Goede et al., 2015), it has been approved for front-line treatment of frail or elderly patients (Emole et al., 2015).

Alemtuzumab, an anti-CD52 monoclonal antibody has also been widely used for the treatment of CLL. This is a recombinant, fully humanised antibody that has proven to be an effective therapeutic option for patients bearing high-risk genetic markers (Lozanski et al., 2004). Since Alemtuzumab can lead to severe immunosuppression, it is no longer commercially available for CLL and is reserved mainly for fit patients with high-risk disease through the Campath Distribution Program (Emole et al., 2015). A very recent study, however, has shown that subcutaneous administration of Alemtuzumab at low dosage has good tolerability and long-term efficacy in heavily pretreated CLL patients. The authors claim that low-dose Alemtuzumab represent an effective yet safe alternative for relapsed/refractory CLL and even for frail and elderly patients (Sciume et al., 2015). Further studies are needed in order to confirm these observations.

An important aspect to consider about monoclonal antibody therapy is that some CLL patients seem to easily develop resistance, particularly against anti-CD20 antibodies. Resistance mechanisms include downregulation of CD20 during therapy as well as decreased complement activity by the loss of component C2. Furthermore, it has been suggested that indirect resistance may be triggered by Lenalidomide treatment as it downregulates CD20 expression *in vitro* (Lapalombella et al., 2008).

As described in **section 1.1.4**, another form of immunotherapy is the CAR T-cell approach. The first trials investigating CAR T-cell therapy were performed on patients with CLL, where the first two out of three patients achieved a complete response (Porter et al., 2011). Updated results reported by researchers from University of Pennsylvania revealed that from 14 evaluable patients, 4 achieved a complete response and 4 other patients achieved a partial response (Porter et al., 2015). In contrast, studies carried out at the Memorial Sloan Kettering Cancer Centre (MSKCC), in which 9 patients were treated with or without conditioning therapy, resulted in no observable clinical benefit. Only one of the patients that received conditioning chemotherapy achieved a complete response (Park, 2012).

It has been suggested that CD19 CAR T-cells in CLL are not as successful as they are in B-ALL (Park, 2014) due to the inherent effector T-cell dysfunction observed in CLL (Riches et al., 2013). Also, immune suppression via PD-L1/2 (McClanahan et al., 2015), the presence of immunosuppressive cell types, such as Tregs, MDSCs or nurse-like cells, and the production of inhibitory cytokines (Boissard et al., 2015, Saulep-Easton et al., 2016, Burger et al., 2000) might influence CAR T-cell efficacy in patients with CLL. Further engineering of CAR T-cell therapy is needed in order to counteract the immunosuppressive TME existing in CLL.

Additionally, as reviewed by (Park and Brentjens, 2013), considerable toxicity of CAR-based cell therapies in the form of cytokine release syndrome, tumour

lysis syndrome and other adverse effects has been reported. Despite of this, adoptive cell transfer of CAR T-cells is currently amongst the most novel and promising type of treatments for CLL. Certainly, CD19 CARs can induce potent and sustained responses in some patients with advanced, refractory CLL and high-risk patients; the long-term efficacy and toxicity of this approach, however, needs to be further investigated.

Due to the key role that the TME plays in the success of immunotherapies, it is not surprising that the use of immune checkpoint inhibitors has been explored in CLL. The use of anti-PD-L1 blocking antibodies in preclinical *in vivo* models was shown to reactivate immune effector cells (McClanahan et al., 2015). More recently, Pembrolizumab, an anti-PD-1 antibody was used for treating patients with relapsed and Richter transformed (RT) CLL. Objective responses were observed in 4 out of 9 RT patients, whilst the median overall survival in this cohort was 10.7 months (Ding et al., 2017). Further clinical studies are needed to confirm the benefit of PD-1 blockade in CLL patients with RT observed in this trial.

In **Table 1. 1**, some of the most efficient and current therapies used for the treatment of chronic lymphocytic leukaemia are presented.

Table 1. 1. Efficient drugs in the treatment of Chronic Lymphocytic Leukaemia. Based on (Nabhan, 2014).

Alkylating agents (Cause DNA damage)	Purine analogues (Inhibit DNA repair)	B-Cell Receptor pathway and Tyrosine Kinase inhibitors	Immunotherapy		
			Monoclonal antibodies	Immuno-modulatory agents	CAR T-cells
Chlorambucil	Fludarabine	Ibrutinib (targets Bruton's tyrosine kinase)	Rituximab (aCD20)	Lenalidomide (multiple targets)	CD19 Chimeric Antigen Receptor (CAR) T-cells
Bendamustine	Pentostatin	Idelalisib (targets phosphoinositide-3'-kinase delta)	Ofatumumab (aCD20)		
Cyclophosphamide	Cladribine	Venetoclax (targets BCL-2)	Obinutuzumab (aCD20)		
		Fostamatinib (targets SYK)	Alemtuzumab (aCD52)		

Nevertheless, it is important to note that in the case of CD19 CAR therapy, the most successful CAR therapy so far, an additional form of cytotoxicity is introduced: on-target, off-tumour toxicity. As long-term persisting anti-CD19 CAR T-cells are infused into the patients, continuing elimination of both normal and malignant CD19-expressing cells will occur leading to profound and prolonged B-cell aplasia and ultimately, hypogammaglobulinemia (Dotti et al., 2014). Similarly, Rituximab, one of the first MAbs that revolutionised the treatment of B-cell malignancies, also causes on-target, off-tumour toxicity. Treatment with Rituximab and more advanced anti-CD20 antibodies also results in B-cell aplasia. Consequently, there is a pressing need to identify better tumour associated antigens (TAA) expressed, preferentially, by malignant cells. In this scenario, targeting of ROR1, a protein expressed on CLL cells but not healthy B cells, seems crucial if we are to improve the long-term toxicity profile and availability of this and other immunotherapies.

1.2.2 Pancreatic Cancer (PaCa)

According to (Ansari et al., 2016), the first known report on pancreatic cancer was authored by Giovanni Battista Morgagni in 1761. The lack of microscopic evaluation rendered the diagnosis of this disease uncertain. Almost 100 years later, Jacob Mendez Da Costa revisited Morgagni's work and produced the first microscopic diagnosis, describing PaCa as a true malignancy (Costa, 1858).

Similarly, the first reported attempt of pancreatic surgery took place in the last decade of the 19th century, but it was Allen Oldfather Whipple in 1935 who sparked the interest in pancreaticoduodenectomies (partial resection of duodenum and the head of the pancreas) (Whipple et al., 1935). Two years later, Alexander Brunschwig performed the first successful surgery for pancreatic adenocarcinoma (Brunschwig, 1937). Today, pancreatic surgery is a safe procedure with an operative mortality below 3% (Yoshioka et al., 2014).

Despite major advances in surgical management, long-term survival for PaCa patients is still extremely poor as only 10-15% of newly diagnosed patients are deemed eligible (Winter et al., 2012). The current understanding of this disease in terms of PaCa biology, TME and clinical management are briefly summarised below.

1.2.2.1 PaCa biology

According to (Warshaw and Fernandez-del Castillo, 1992), pancreatic cancer can be classified into two major categories according to the type of cells it originates from: exocrine and endocrine tumours. Of these, pancreatic ductal adenocarcinoma (PDAC), an exocrine tumour, is the most frequent type of pancreatic cancer (Wolfgang et al., 2013).

In PDAC, neoplastic cells of invasive ductal adenocarcinoma form glands and infiltrate into tissues (Hruban, 2007). In general, this type of tumour is solid and

firm probably because almost all invasive ductal adenocarcinoma cells invade nerves and spread along perineural spaces. Another feature of PDAC is its high invasiveness, which results in tumour spreading in lymph nodes and liver metastasis (Wolfgang et al., 2013). Not surprisingly, by the time most PDACs are diagnosed, the disease has spread beyond the gland and cannot be treated by surgical resection. Nevertheless, one of the major characteristics of PDAC is the intense desmoplastic reaction they elicit (Jacobetz et al., 2013). The latter consists of fibroblasts, inflammatory cells, endothelial cells and a complex extracellular matrix (ECM). The desmoplastic reaction reduces tumour tissue elasticity and increases tumour interstitial fluid pressure that represents a barrier for many therapeutic agents (Lohr et al., 1994, Heldin et al., 2004, Provenzano et al., 2012).

As reviewed by (Distler et al., 2014), PDAC originates from mainly three lesions: i) precursor lesions identified as intraductal papillary mucinous neoplasm (IPMN), ii) mucinous cystic neoplasm (MCN) or iii) pancreatic intraepithelial neoplasia (PanIN). The latter represent the most frequent pre-lesions in PDAC and are well characterised (Hruban et al., 2004). PanINs are classified into different grades based on their morphological characteristics and severity of the lesions: PanIN 1A (flat duct lesions) and PanIN 1B (papillary duct lesions), which are low-grade lesions with minimal atypia; PanIN 2 (intermediate-grade PanIN), which show mild/moderate dysplasia; and PanIN 3 (also known as carcinoma *in situ*), which present severe atypia. All PanIN lesions are non-invasive and are characterised by hypovascularity, immune cell infiltration and feature specific genetic alterations that increase in frequency and variety with the progression of PanIN stages. These biological alterations and somatic mutations are required for PanIN lesions to progress into invasive carcinoma and are also implicated in the rapid metastatic spread that characterises this malignant disease (Hezel et al., 2006).

In terms of molecular pathways and genetics in PDAC, there are currently no molecular signatures for staging or prognostication, as this disease is highly

heterogeneous (Yabar and Winter, 2016). Whole-exome sequencing performed in 124 PDAC genomes revealed that more than 1300 genes were mutated (Jones et al., 2008); of which *KRAS* was the only oncogene genetically activated in more than 95% of PDACs. Since targeted therapy against this gene has proved disappointing (Van Cutsem et al., 2004), researchers have focused instead on identifying core signalling pathways involved in PDAC initiation/progression (Jones et al., 2008, Biankin et al., 2012). Interestingly, (Waddell et al., 2015) found that approximately 25% of PDAC tumours harbour functional defects in DNA damage pathways; which suggests that these tumours might be sensitive to poly adenosine diphosphate ribose polymerase (PARP) inhibitors or platinum drugs.

Apart from *KRAS*, high-frequency mutations appear also in tumour suppressor genes, such as *CDKN2A, TP53* and *SMAD4* (Jones et al., 2008, Biankin et al., 2012). Inactivating alterations on these genes consist of mutations in one allele and genetic loss of the second allele due to chromosomal instability. Some of the most common gene mutations in PDAC are shown in **Table 1. 2**.

Table 1. 2. Significantly mutated pathways in pancreatic ductal adenocarcinoma. Based on (Yabar and Winter, 2016).

Core Pathway	Gene	Protein Function	Mutation Rate (%)*
KRAS signalling	*KRAS*	Oncogene; GTPase; activates MARK activity	100
	MAP2K4	Dual specificity mitogen-activated protein kinase 4; Toll-like receptor signalling pathway	
DNA damage control	*TP53*	Tumour suppressor p53	83
Control of G1/S phase transition	*CDKN2A*	Cyclin-dependent kinase inhibitor 2A; tumour suppressor	83–96
TGF-β signalling	*SMAD4*	Mothers against decapentaplegic homolog 4; BMP signalling pathway	63–100
	TGFBR2	TGF-β receptor type II; regulation of growth	

* Depending on which gene expressed in sample of tumor studied.
Abbreviations: BMP, bone morphogenetic protein; TGF, transforming growth factor.

It is worth mentioning that during PanIN 1, KRAS activation and telomere shortening are the first oncogenic events to occur. During PanIN 2, p16 loss is observed; whilst TP53, SMAD4 and BRCA2 inactivation takes place in the PanIN 3 stage (Distler et al., 2014). Epithelial-to-mesenchymal transition (EMT) is promoted by loss of E-cadherin, resulting in a highly lethal phenotype in advanced stages (Winter et al., 2008). Notably, (Yachida et al., 2010) have shown that this PanIN to PDAC transformation is a 10 to 20-year process.

1.2.2.2 Tumour microenvironment in PaCa

Histology studies evaluating patients with chronic pancreatitis have shown that epithelial wound healing response is particularly robust in the pancreas

(Ceyhan and Friess, 2015). Notably, relevant features associated with a wound healing response include fibroblast activation, immune suppression, remodelling of the extracellular matrix as well as trophic signals to promote re-epithelialisation (Dvorak, 1986).

It has been therefore hypothesised that the stromal response is hijacked during PDAC, as the stroma provides paracrine signals that seem to select certain tumour cells (Makohon-Moore and Iacobuzio-Donahue, 2016). These paracrine signals originate mostly from α-smooth muscle actin $(\alpha SMA)^+$ myofibroblasts, which in turn are derived from quiescent pancreatic stellate cells (qPSCs). Importantly, the characteristic desmoplastic reaction seen in PDAC is mediated by activation of qPSCs (Neesse et al., 2011). Upon activation, these cells: i) lose their cytoplasmic lipid, ii) transdifferentiate into αSMA^+ myofibroblasts with proliferative capacity, iii) secrete various growth factors and iv) promote ECM formation (Masamune and Shimosegawa, 2015).

In the PDAC context, PSCs and other stromal mesenchymal cells are continuously activated by the epithelium, through secretion of platelet-derived growth factor (PDGF), TGFβ and sonic hedgehog (SHH) (Bailey et al., 2008, Taeger et al., 2011). This notion was supported by an *in vivo* study where pharmacological inhibition of PSC activation led to stromal collapse, smaller tumours and improved chemotherapeutic delivery (Sherman et al., 2014).

The abundant extracellular matrix in PDAC is another part of its microenvironment and it effectively acts as a physical barrier to the neoplasm (Jacobetz et al., 2013). The hyaluronic acid contained in the ECM is a negatively charged glycosaminoglycan that binds to large amounts of water, resulting in high hydrostatic pressure and interstitial fluid pressure (IFP) (Stromnes et al., 2014). This is particularly problematic in terms of therapy delivery (Provenzano et al., 2012), and it has been shown it could also lead to hypoxia (Olive et al., 2009), a pervasive feature of cancer.

With regards to the immune system in PDAC, there is a large amount of data indicating that the pancreatic cancer microenvironment is immunosuppressed at multiple levels, as shown by (Clark et al., 2007) in a study where the immune response during tumour evolution was characterised using a mouse model of PaCa. More recently, (Ene-Obong et al., 2013) showed for the first time that activated PSCs appeared to reduce migration of $CD8^+$ T-cells to tumour-proximal stromal compartments, preventing therefore their access to cancer cells. As reviewed by (Makohon-Moore and Iacobuzio-Donahue, 2016), T-cell suppression in PDAC is promoted by several mechanisms: i) accumulation of Tregs, ii) M2 tumour-associated macrophages (TAMs), iii) MDSCs and iv)fibroblast activation protein $(FAP)^+$ fibroblasts, a type of stromal cell different from PSC-derived myofibroblasts. Interestingly, unlike CLL, endogenous cytotoxic T-cells do not seem to be dysfunctional, as latent immune responses and intratumoural accumulation of T-cells were observed when $(FAP)^+$ carcinoma-associated fibroblasts (CAFs) were removed and/or CXCR4 inhibitors were added to an *in vivo* model of human PDAC (Feig et al., 2013).

1.2.2.3 Standard therapy

In terms of clinical management and according to the American Joint Committee of Cancer and the Union for International Cancer Control (Cascinu et al., 2010), PDAC is divided into three categories: i) localised resectable tumours (stage I and II), ii) unresectable locally advanced tumours (stage III); and iii) metastatic tumours (stage IV). In the following paragraphs, the standard therapy approach provided to PDAC patients according to their staging is summarised.

Stages I and II, surgically resectable PDAC; if the tumour is restricted to the pancreas alone (stage I), then the treatment of choice is surgical removal of all recognisable tumour tissue. Unfortunately, relapse is observed in 60-70% of stage I patients due to micrometastases during or after surgery (Cid-Arregui and Juarez, 2015). To avoid this, systemic chemotherapy/chemoradiation

(also known as adjuvant therapy) is administered after surgery. As reviewed by (Goodman and Saif, 2014), treatment with Gemcitabine or 5-fluoruracil (5-FU) increased the 5-year survival rate from 10% to 20% compared to observation. Although there was no significant difference between Gemcitabine and 5-FU, PDAC patients treated with the former experienced significantly less toxicity. More recently, in a phase III study carried out in Japan, Gemcitabine was compared with S-1, an oral fluoropyrimidine prodrug that is enzymatically converted into 5-FU. The quality of life and 2-year overall survival was significantly higher (70%) for S-1 than for Gemcitabine (53%) (Ueno et al., 2013)). Further studies in other countries are needed in order to determine that the effect seen on Asian patients can be replicated in other populations.

The efficacy of chemoradiation after surgery is less clear due to mixed results from different clinical trials showing no added benefit (Klinkenbijl et al., 1999) or even detrimental effects (Neoptolemos et al., 2004). A recent retrospective study reviewing 955 patients however showed that 5-year overall survival for patients treated with chemoradiation was 41.2% compared to patients treated with adjuvant chemotherapy alone (25.7%) (Morganti et al., 2014).

Another approach to prevent micrometastases and relapse is the administration of neoadjuvant therapy (chemotherapy, chemoradiation or a combination of treatments) before surgery. Importantly, this type of therapy does not seem to be beneficial for patients with resectable tumour but for those diagnosed with borderline resectability or with locally advanced non-resectable tumours (Heinemann et al., 2013). This is consistent with a previous study by (Katz et al., 2008), who reported that out of 125 PDAC patients with borderline resectable tumours receiving neoadjuvant therapy and subsequent restaging, 66 (41%) underwent surgery. The median survival for the 66 patients who completed all therapy was 40 months compared to only 13 months for the 94 patients who did not undergo surgery.

Currently, no optimal protocol for neoadjuvant therapy has been reported, although multidrug therapy, such as Gemcitabine after Nab-paclitaxel (albumin bound paclitaxel) or the multiagent regimen FOLFIRINOX (Leucovorin, 5-FU, Irinotecan, Oxaliplatin) have shown promise. In a retrospective study, it has been shown that FOLFIRINOX was able to induce conversion to resectability in >20% of locally advanced PDAC patients (Faris et al., 2013). Moreover, there are at least two ongoing phase II trials using radiation therapy and FOLFIRINOX in borderline resectable PDAC patients (NCT01560949 and NCT01591733).

Stage III, locally advanced, unresectable PDAC; due to the poor response rates after different therapeutic strategies, the clinical management of these patients remains controversial. Chemotherapy with 2-3 cycles of Gemcitabine followed by restaging and, where possible, chemoradiation is the frequent treatment of choice (Cid-Arregui and Juarez, 2015).

Other options such as FOLFIRINOX or Gemcitabine/Nab-paclitaxel are being investigated (Faris et al., 2013). The efficacy and toxicity of these approaches remain to be determined.

Stage IV, metastatic PDAC; it can be classified as stage IVa, when metastasis is found adjacently, and in stage IVb, when the disease has spread to distant organs (usually, liver, stomach, spleen or lungs) (Cid-Arregui and Juarez, 2015). Gemcitabine is the first-line therapy for these patients since it was shown in 1997 that patients treated with this drug had a 12-month survival rate of 18% vs 2% achieved by 5-FU-treated PaCa patients (Burris et al., 1997). To date, different Gemcitabine-based combinations has been tested in randomised trials in comparison with Gemcitabine alone, of which three combinations have shown beneficial effects: Gemcitabine plus Erlotinib (an EGFR inhibitor) (Moore et al., 2007), Gemcitabine plus S-1 (Ueno et al., 2013), and Gemcitabine plus Nab-paclitaxel (Von Hoff et al., 2011).

Additionally, treatment with FOLFIRINOX has achieved a clear clinical benefit in metastatic PDAC (Conroy et al., 2011). In this clinical trial, 342 stage IV PDAC patients not previously treated with chemotherapy were assessed. The median overall survival in the FOLFIRINOX arm was 11.1 months compared to 6.8 months seen in the Gemcitabine group. Definitive deterioration in the quality of life at 6 months was 31% in FOLFIRINOX-treated patients and 66% in the Gemcitabine arm. One of the limitations of this approach however is the substantial toxicities. In an effort to counteract this, modified regimens of this drug (no bolus 5-FU and addition of haematopoietic growth factor) are being tested. In line with this, (Mahaseth et al., 2013) reported that modified FOLFIRINOX maintained efficacy whilst causing significantly less grade 3-4 toxicities. Further studies including additional refinement of these regimens will shed light on how to improve safety whilst maintaining/enhancing efficacy.

The relatively modest clinical benefit reached by the approaches mentioned above coupled with a better (although still limited) understanding of PDAC biology and its microenvironment has led scientists and clinicians to explore novel targeted therapies.

1.2.2.4 New therapies

In the past decade, several agents targeting the tumour or stroma have been developed. Although promising results were shown in preclinical studies, most of them have not achieved a significant improvement in overall survival in clinical trials when compared to Gemcitabine or other strategies.

1.2.2.4.1 Small molecule inhibitors

As indicated by (Cid-Arregui and Juarez, 2015) and (Adamska et al., 2017), inhibitors targeting various molecules have been developed, including PARP (DNA damage pathway), Matrix metalloproteinases (MMP; extracellular matrix), Vascular endothelial growth factor (VEGF; angiogenesis), Hedgehog, PI3K and KRAS pathways, amongst others. Of these, Everolimus and Sunitinib (mTOR inhibitors – PI3K signalling) have shown great promise as

progression-free survival time was increased from 5 to 11 months (Liu et al., 2013, Wiedmann and Mossner, 2012). In contrast, when Everolimus or Temsirolimus were used to inhibit PI3k/Akt/mTOR pathways in previous phase II studies, disappointing results were obtained (Javle et al., 2010). Nevertheless, differences in the study's design and patients' population make it difficult to draw further conclusions from these trials. Although no superiority over standard therapy has been shown with most of these inhibitors, clinical trials using different protocols are ongoing. For instance, PBI-05204, another mTOR inhibitor, is currently being tested in stage IV patients (NCT02329717).

1.2.2.4.2 Immunotherapies

Therapeutic vaccines; these are designed to stimulate the immune system to react against TSAs by induction of specific cytotoxic T-cells. In the PDAC context, several types of vaccines have been generated. A very good review on this can be found in (Amedei et al., 2014). Briefly, peptide-based vaccines, such as PANVAC-V (Bernhardt et al., 2006) and GV1001 (Middleton et al., 2014) failed to show significant clinical benefit over standard therapies in clinical trials. In contrast, whole-cell vaccines, such as Algenpentucel-L (NCT01072981, NCT01836432) and GVAX (NCT01896869) are now in phase II/III trials, where combinations with checkpoint blockade antibodies are being tested (Le et al., 2013).

MAbs; in PDAC, MAbs targeting EGFR or VEGF have shown disappointing results. In a phase III study, Cetuximab (an anti-EGFR MAb) was administered in combination with Gemcitabine to patients with advanced PDAC, yet no significant difference in median overall survival was observed when compared to Gemcitabine alone (6.3 vs 5.9 months, respectively) (Philip et al., 2010). A similar outcome was observed when Bevacizumab, an anti-VEGF MAb, was tested in phase II (Kindler et al., 2005) and phase III trials (Kindler et al., 2010).

Due to the immunosuppressive nature of the TME in PDAC, checkpoint blockade antibodies such as Nivolumab, an anti-PD-1 MAb, are being tested

alone (NCT02423954), or in combination with: i) Ipilimumab, an anti-CTL-4 MAb (NCT01928394) or ii) Gemcitabine (NCT01473940). Unfortunately, preliminary data was not encouraging, as there were no indications of significant improvement; nevertheless, official results are awaited. Interestingly, CD40 targeting has emerged as a novel strategy to block TME immunosuppression and increase anti-tumour activity (Loskog and Eliopoulos, 2009). Accordingly, a combination of Gemcitabine and an anti-CD40 antibody is being evaluated in clinical trials (Vonderheide et al., 2013). It is expected that this combination would enhance the accumulation of tumour-suppressive macrophages, thereby prompting tumour regression.

T-cell therapy; since the general number of tumour-specific T-cells in the PDAC population is too small, T-cells are taken from the patient, engineered and expanded *ex vivo* to then be transferred back to the patient. This can be done using the T-cell receptor (TCR) strategy, whereby T-cells from the patient are transduced to express a tumour-targeting TCR. This technology is currently being tested using the anti-MAGE-A3 protein (NCT02111850) and anti-NY-ESO-1 antigen (NCT01967823).

Another strategy is to use CAR T-cells. At the moment, CAR T-cells targeting mesothelin are in clinical trials for solid malignancies, including PDAC (NCT01583686) (Adamska et al., 2017).

1.2.2.4.3 Cancer stem-like cell therapy

Cancer stem cell-like cells (CSCs) in PDAC represent a small population of cells with the ability to prompt tumour initiation, disease progression and metastasis. It has been increasingly shown that these cells are highly resistant to conventional chemotherapy; furthermore, its presence may account for the rapid and virtually universal relapse seen in PDAC (Wolfgang et al., 2013, Qiu et al., 2015).

To date, no distinctive PDAC CSC biomarkers have been identified, yet markers, such as CD24, CD133 and ALDH1 are deemed as the most characteristic. Nevertheless, it is considered that various CSCs subtypes may express only one or two surface markers, which complicates the development of therapeutic strategies (Ansari et al., 2016). Furthermore, most of these markers are also expressed in healthy tissue. Recently, CSC targeting has been proposed to be carried out by disruption of signalling pathways involving Sonic hedgehog, Notch or PI3K (Raj et al., 2015), but none of these approaches are currently in clinical trials for PDAC.

Taken together, the complex genetic heterogeneity, desmoplastic nature of PDAC and immunosuppressive microenvironment make it a challenging disease to treat. Combinations of different targeted and immunotherapeutic strategies are now being actively evaluated in the clinic. It is envisaged that strategies that combine bypassing the immunosuppressive TME with CSC targeting will prove instrumental to PDAC therapy. Identification of druggable targets expressed on malignant cells, amongst them CSCs, but not healthy, critical organs is therefore required.

1.3 Need of a new therapeutic target: Receptor tyrosine kinase-like orphan receptor 1 (ROR1)

An example of better tumour-associated targets recently discovered is Receptor tyrosine kinase-like Orphan Receptor-1 (ROR-1). Considerable ROR1 expression has been found in a range of solid (Zhang et al., 2012b) and haematological malignancies (Daneshmanesh et al., 2013), including CLL (Baskar et al., 2008). Importantly, ROR1 is implicated in tumour cell survival and metastasis through the non-canonical Wnt signalling pathway (Fukuda et al., 2008).

Accordingly, ROR1 targeting with monoclonal antibodies induced apoptosis of CLL cells *in vitro* (Daneshmanesh et al., 2012), and inhibited cancer progression and reversed epithelial-mesenchymal transition (EMT) in breast cancer both *in vivo* and *in vitro* (Cui et al., 2013). More recently, ROR1 expression on cancer stem cell-like cells (CSC) has been reported in a glioblastoma cell line (Jung et al., 2016) and in ovarian cancer primary cells (Zhang et al., 2014). Remarkably, successful targeting of these CSCs following treatment with Cirmtuzumab, an anti-ROR1 antibody (UC-961 clone), was observed both *in vivo* and *in vitro* (Zhang et al., 2014).

In this context, the aim of my PhD project was to generate a novel anti-ROR1 monoclonal antibody-based therapy for ROR1^{+} malignancies. In keeping with this, a brief summary of ROR1 biology and underline its relevance as a target for cancer immunotherapy is provided.

1.3.1 ROR1 Structure

Receptor tyrosine kinase-like Orphan Receptor-1 (ROR-1) is a type I transmembrane protein consisting of 937 amino acid residues with intra and extracellular portions. The intracellular part contains a tyrosine kinase domain that might be phosphorylated by other cytoplasmic signalling proteins (Gentile et al., 2011). For immunotherapeutic purposes, however, the extracellular part is of special interest, and it is composed of an immunoglobulin-like (Ig) domain, followed by a cysteine-rich domain (CRD), also called the Frizzled (Fz) domain, and lastly, a Kringle (Kg) domain (**Fig. 1. 5**). Notably, its Fz module constitutes the

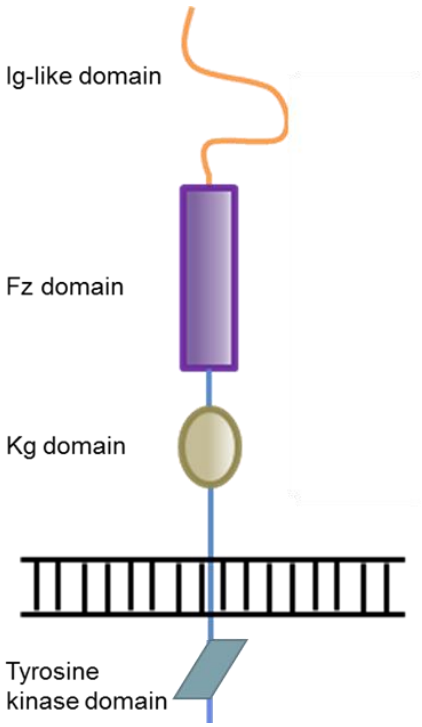

Fig. 1. 5. Receptor tyrosine kinase-like orphan receptor (ROR1)

extracellular ligand-binding region to Wnt5a (Roszmusz et al., 2001, Green et al., 2008, Fukuda et al., 2008).

Of note, both ROR1 and ROR2 –the other member of the ROR family– were originally isolated from a neuroblastoma cell line more than 20 years ago (Masiakowski and Carroll, 1992). Since their natural ligands were not identified, they received the ROR designation. Data from Oishi *et al*. (Oishi et al., 1999) indicated that ROR1 is expressed during embryonic development and is down regulated post-partum (Matsuda et al., 2001). Recent studies show that ROR1 is expressed at low levels in hematogones (a subset of B-cell precursors) and at very low levels on lungs, pancreas and adipocytes (Berger et al., 2015, Hudecek et al., 2010). Accordingly, ROR1-deficient mice do not exhibit any morphological abnormalities; but they die within the first 24h after birth, presumably due to respiratory failure (Broome et al., 2011).

1.3.2 Expression on normal and cancer tissues

Although ROR1 expression has not been fully investigated in humans, gene expression profiling of ROR1 in normal blood leukocytes showed that granulocytes, B-cells and T-cells of healthy donors are ROR1 negative (Dave et al., 2012, Shabani et al., 2015). In contrast, flow cytometry data indicated that ROR1 was present on the cell membrane of adipocytes and hematogones (Hudecek et al., 2010). More recently, investigation of ROR1 expression at a protein level using an intracellular anti-ROR1 MAb, revealed that critical tissues such as brain, heart, lung and liver had no ROR1 expression, yet considerable cell-surface staining was detected on normal parathyroid, pancreatic islet cells and some regions of the gastrointestinal tract, particularly in the stomach and gastric body (Balakrishnan et al., 2017).

With regards to malignant tissues, significant ROR1 expression has been found in CLL (Baskar et al., 2008) and other haematological malignancies, such as hairy cell leukaemia, mantle cell lymphoma, multiple myeloma, diffuse

large B-cell lymphoma, among others (Daneshmanesh et al., 2013). ROR1 was also found in solid cancers (Zhang et al., 2012b), including a subset of ovarian cancer, triple negative breast cancer and lung adenocarcinomas (Balakrishnan et al., 2017).

Importantly, ROR1 is implicated in tumour cell survival and metastasis through the non-canonical Wnt signalling (Fukuda et al., 2008). Recently, it has been suggested that Wnt5a autocrine signalling –through ROR1– allows CLL cells to overcome natural microenvironmental regulation and possibly enhance cell survival (Janovska et al., 2015). Furthermore, this biomarker has been associated with accelerated disease progression in CLL (Cui et al., 2016) and is considered as a prognostic marker in colorectal cancer (Zhou et al., 2017a), lung adenocarcinoma (Zheng et al., 2016) and triple negative breast cancer (Chien et al., 2016). Furthermore, silencing of ROR1 in breast cancer (Zhang et al., 2012a), ROR1 and ROR2 in ovarian cancer (Henry et al., 2016) or ROR1 and fibromodulin (FMOD)-a collagen-binding protein- in CLL cells (Choudhury et al., 2010) resulted in impaired cell migration and invasion in solid tumours as well as apoptosis of CLL cells. Remarkably, this would imply that resistance to therapy and tumour escape by downregulation of ROR1 would not be as viable as it indeed was the downregulation of CD19 or CD20 observed after CD19 CAR therapy or treatment with anti-CD20 antibodies.

1.3.3 ROR1 signalling and role in tumourigenesis

It has been shown that in the context of lung adenocarcinoma, the expression of ROR1 can be induced in the absence of Wnt5a by: i) Met phosphorylation of the proline-rich domain of ROR1; although the ROR1-Met interactions and their biological effect remain to be elucidated (Gentile et al., 2011, Gentile et al., 2014). And by ii) induction of thyroid transcription factor-1 (TTF-1), a lineage-survival oncogene in lung adenocarcinomas. TTF-1 prompts ROR1 expression, which in turn will activate c-Src in an EGFR-independent manner (Yamaguchi et al., 2012) (**Fig. 1. 6A**).

In other malignancies, such as breast cancer, ROR1 interacts with casein kinase 1ε and activates the PI3K/AKT/CREB pathway in order to prompt the activation of relevant genes involved in tumour cell growth and/or resistance to apoptosis (Zhang et al., 2012a, Shabani et al., 2015) (**Fig. 1. 6B**).

With regards to leukaemias, particularly CLL, it has been demonstrated that ROR1 is involved in the non-canonical, β-catenin independent, Wnt/planar cell polarity (PCP) pathway through Wnt5a binding (Janovska and Bryja, 2017). In mammals, Wnt factors such as Wnt5a activate this Wnt/PCP signalling branch through binding to Fz receptors (Fz family) and co-receptors (ROR1, ROR2). Crucially, it is this pathway the one that governs polarity and migration in CLL cells, as it controls chemotactic responses and cell homing (Kaucka et al., 2015, Kaucka et al., 2013).

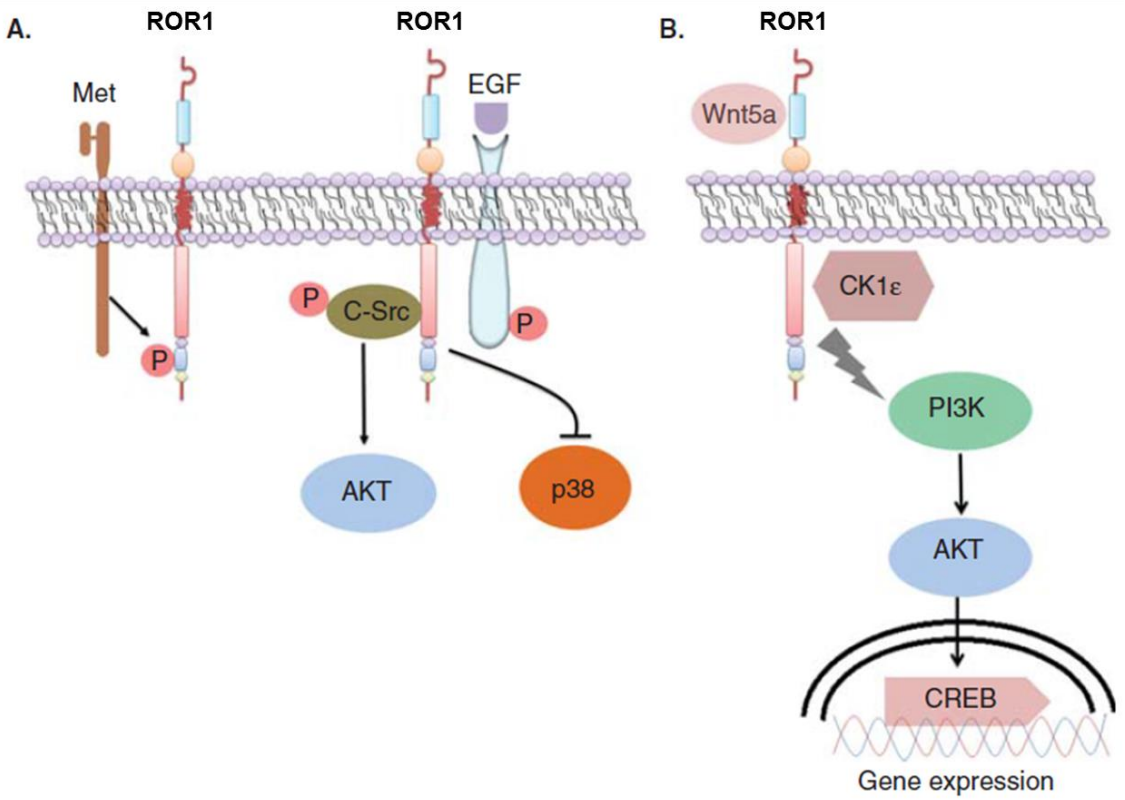

Fig. 1. 6. ROR1 signalling pathways in cancer. (A) In the absence of Wnt5a; ROR1 expression can be induced through phosphorylation of its proline-rich domain by Met oncogene. Alternatively, in lung adenocarcinoma for example, thyroid transcription factor (TTF-1) prompts ROR1-mediated c-Src-activation, which results in pro-survival AKT activation and inhibition of pro-apoptotic p38 signalling in an EGFR-independent manner. (B) In the presence of Wnt5a; ROR1 binding to Wnt5a triggers casein kinase 1 epsilon (CK1ε) signalling through PI3K, AKT and cAMP-response-element-binding (CREB) protein. This leads to expression of genes involved tumour cell growth and resistance to apoptosis. AKT= Protein kinase B, c-Src= cellular Src kinase, PI3K= Phosphatidylinositol 3-kinase. Modified from Shabani et al., 2015.

Interestingly, Yu *et al.* (Yu et al., 2016) reported for the first time that Wnt5a induces cellular motility and proliferation by enhancing hetero-oligomerisation of ROR1 with ROR2; which in turn recruits guanine nucleotide exchange factors (GEFs). The presence of GEFs activates downstream GTPases RhoA and Rac1 in CLL cells.

In the same study, researchers from this group suggested that the highly conserved Kg domain of ROR1 is involved in ROR1/ROR2 hetero-oligomerisation and that the Fz domain in the extracellular portion of ROR1, as well as the proline-rich intracellular domain are necessary for recruitment

of GEFs to ROR1/ROR2 complex (**Fig. 1. 7**). In line with this, the use of Cirmtuzumab, an anti-ROR1 monoclonal antibody, was able to block Wnt5a-ROR1 signalling; resulting in reduced migration and proliferation of a ROR1-expressing cell line (Yu et al., 2016). Nonetheless, further studies involving ROR1 biology and signalling in other malignancies are needed in order to determine whether the hetero-oligomerisation between ROR1 and ROR2 seen in CLL is cancer type specific or a common feature across ROR1^{+} tumours.

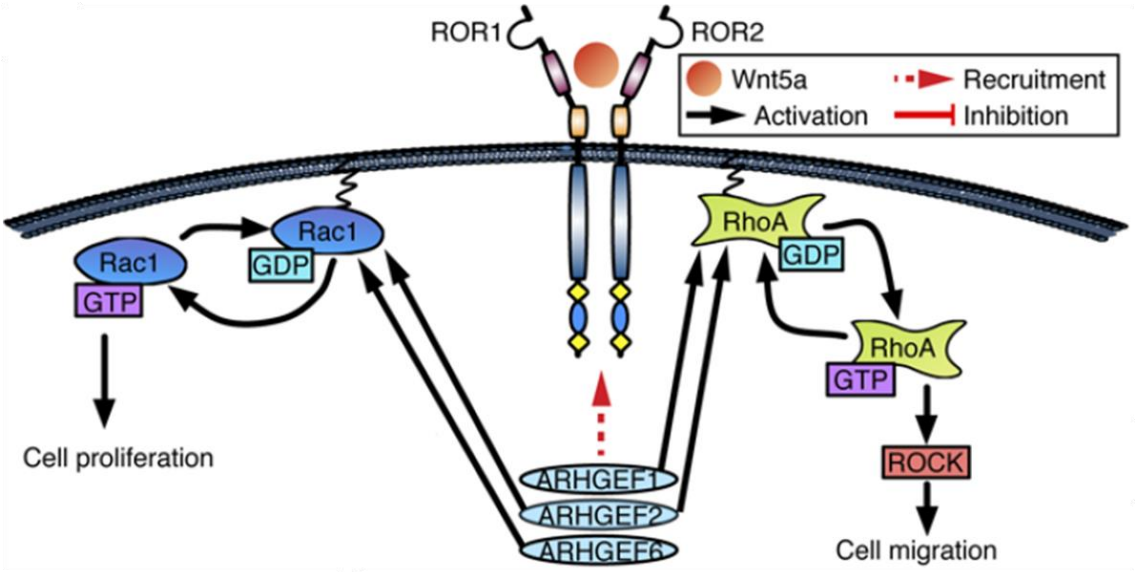

Fig. 1. 7. Schematic of Wnt5a-ROR1 signalling through hetero-oligomerisation with ROR2 in CLL. According to Yu et al., 2016, Wnt5a induces ROR1 and ROR2 hetero-oligomerisation that prompts recruitment of GEFs in order to promote both cell proliferation through Rac1 activation and cell migration through RhoA. Modified from Yu et al., 2016.

Additionally, it has been reported that Wnt activity is associated with increased stem cell potential and more aggressive cancers (de Sousa and Vermeulen, 2016); and Wnt5a signalling, in particular, is involved in the regulation of normal and cancer stem cell-like cells self-renewal, cancer cell proliferation, migration and invasion. Nevertheless, the role of Wnt5a in CSCs is varied and complex. It may suppress or promote tumour growth depending on receptor availability, which means that cellular context determines the effect of Wnt5a (Zhou et al., 2017b). All in all, evidence so far indicates that Wnt5a-ROR interactions sustain tumour progression but, as mentioned above, further

studies are required in order to increase our understanding of the complex cross-talk between Wnt5a and ROR1 and other cell membrane receptors expressed in CSCs.

1.3.4 Target for cancer immunotherapy

The preferential expression of ROR1 on solid and haematological cancers, and its absence on critical, healthy tissue, renders ROR1 as an attractive target for immunotherapy. Not surprisingly, due to its expression profile, preclinical safety has been demonstrated with Cirmtuzumab *in vitro* (Choi et al., 2015); and in non-human primates, where toxicity to normal organs was not detected after infusion with anti-ROR1 CAR T-cells (Berger et al., 2015). Moreover, recent reports indicate ROR1 is expressed on cancer stem cell-like cells in both ovarian cancer (Zhang et al., 2014) and glioblastoma (Jung et al., 2016). Crucially, this provides the ground-breaking possibility of eliminating CSC subpopulations by targeting ROR1, thereby drastically reducing the risk of relapse and metastasis.

In keeping with this, MAbs and antibody-derivatives such as CAR therapy are currently under pre-clinical and clinical investigation in a wide range of ROR1^{+} malignancies using a variety of anti-ROR1 clones (Hudecek et al., 2010), (Hudecek et al., 2013). See **Table 1. 3** for an overview of planned and/or on-going clinical trials evaluating the therapeutic effect of ROR1-based treatments:

Table 1. 3. Current and planned clinical trials using ROR1-based immunotherapies as per *Clinicaltrials.gov* (ClinicalTrials.gov, 2017)

CT No	Type of Therapy	Location	Malignancy	Status
NCT02222688	Cirmtuzumab (UC-961)	San Diego, CA, USA	Relapsed or refractory CLL	Recruiting
NCT02706392	ROR1 CAR (R12)	Seattle, WA, USA	ROR1^{+} solid and haematological malignancies	Recruiting
NCT02776917	Cirmtuzumab & Paclitaxel	San Diego, CA, USA	Breast cancer	Not yet recruiting
NCT02860676	Cirmtuzumab	San Diego, CA, USA	CLL patients previously treated with Cirmtuzumab	Enrolling by invitation
NCT03088878	Cirmtuzumab & Ibrutinib	San Diego, CA, USA	B-cell lymphomas	Not yet recruiting

Hence, based on the unique expression of ROR1 on malignant cells – particularly CSCs but not healthy, critical tissue– and due to its safety profile, the overriding aim of this project is to generate and test novel anti-ROR1 antibodies to ultimately produce therapeutic MAbs and/or antibody-derivatives against ROR1. A brief literature review on these topics is provided below.

1.4 Focus on: MAb-based therapies in cancer

In the past two decades, significant advancements in our understanding of monoclonal antibody biology have allowed the use of a variety of MAb-based approaches for cancer treatment (**Fig. 1. 8**).

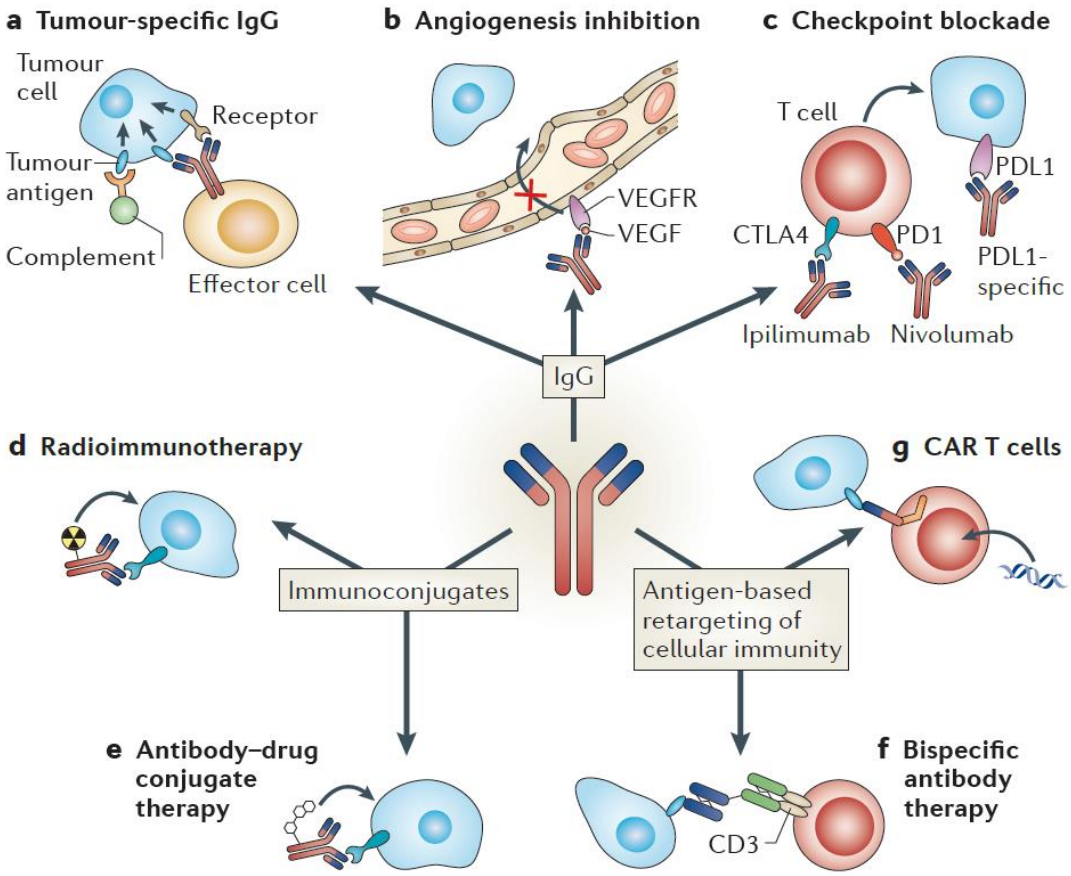

Fig. 1. 8. MAb-based therapeutics in oncology. From conventional naked antibodies specific for (a) TAA, (b) angiogenesis inhibition or (c) checkpoint blockade, to armed-antibodies with (d) radioisotopes or (e) drug payloads, to antibody-derivatives such as (f) bispecific antibodies and (g) CARs, MAb-based therapeutics represent a pivotal component of state-of-the-art cancer care. CD3= T cell surface glycoprotein CD3 ε-chain, CTLA-4= cytotoxic T lymphocyte-associated antigen 4, PD-1= programmed cell death protein 1, PD-L1= PD-1 ligand, TAA= Tumour-associated antigen, VEGF= vascular endothelial growth factor, VEGFR= VEGF receptor. Reproduced from Weiner, 2015.

One of the first steps in order to attain substantial clinical benefit in cancer patients without unwanted immunogenicity was the generation of chimeric antibodies in human isotypes derived from engineered murine MAbs (LoBuglio

et al., 1989, Maloney et al., 1997). Further modifications in order to produce humanised antibodies with greater cytotoxic potential have demonstrated significant utility in the clinic (Weiner, 2015). As a result, MAbs have become one of the largest classes of new agents for cancer therapy (Pillay et al., 2011). Thus, in the next few paragraphs, a brief introduction on therapeutic MAbs and antibody-derivatives, in terms of their biology, mechanism of action and current technology is presented.

1.4.1 Monoclonal antibody biology

Immunoglobulin G is one of the most abundant proteins in human serum and accounts for approximately 10-20% of plasma protein. It is the major class of five classes of immunoglobulins, namely IgM, IgD, IgG, IgA and IgE; and although IgG can be further divided in four subclasses: IgG1, IgG2, IgG3 and IgG4 (Schur, 1988); IgG1 is primarily employed as a therapeutic agent due to both its long half-life and effector functions.

IgG1 MAbs have a basic structure of approx. 150kDa, consisting of two identical 25kDa light chains and two identical 50kDa heavy chains. Each light chain consists of an N-terminal variable domain (V_L) and a constant domain (CL). Similarly, heavy chains consist of an N-terminal variable domain (V_H) and three constant domains (CH1, CH2 and CH3) (Natsume et al., 2009).

The association of the whole of the light chain with the V_H and CH1 domains forms a Fab arm (Fab= Fragment antigen binding), where the V regions interact with the antigen. Of note, this antigen binding region is formed by differential assembly of Variable, Diversity (V_H only) and Joining gene segments and inclusion of somatic mutations. The part of the antibody formed by the CH2 and CH3 domains is called Fc region (Fc= Fragment crystalline). The two Fabs and the Fc region are connected through a flexible linker, called hinge region (Vidarsson et al., 2014) (**Fig. 1. 9**).

Notably, the residues most proximal to the hinge region in the CH2 domain are involved in effector functions as it contains a binding site for C1q (complement activation) and for Fc-gamma receptors (FcγR) on effector cells of the innate immune system. Specifically, the glycoform of the oligosaccharide covalently attached to the CH2 at asparagine 297 (N297) is responsible for subtle but important changes of quaternary structure of the Fc. These glycans can also modulate the Fc-FcγR binding during specific immune responses in humans (Wuhrer et al., 2009). Not surprisingly, glyco-engineered afucosylated antibodies show enhanced Fc engagement with activatory FcγRIIIa and FcγRIIa, resulting in more potent ADCC and ADCP, respectively (Herter et al., 2014).

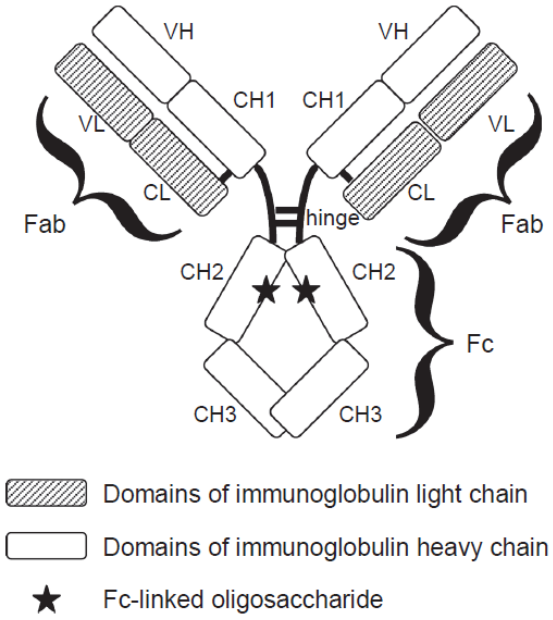

Fig. 1. 9. Structure of a human IgG1 MAb. MAbs in human IgG1 consist of two light and two heavy chains. Heavy chains are paired by disulfide bonds in the hinge regions, whilst heavy and light chains are connected by a disulfide bond between CH1 and CL. Both V_H and V_L form the antigen binding site. The CH2 domain within the Fc region contain an oligosaccharide. Importantly, the glycoform of the latter determines the interactions between the Fc and effector mechanisms. Reproduced from Natsume et al., 2009.

Interestingly, the V region of 10-15% of all antibodies is also glycosylated and it has been suggested that this glycosylation affect antigen-binding characteristics whilst allowing binding to regulatory lectins. This in turn can modulate the activation-threshold for B-cell stimulation (Vidarsson et al., 2014). Additionally, the interface between the CH2-CH3 domains contains the binding site for the neonatal Fc receptor (FcRn), responsible for the extended half-life of IgG, placental passage, and transport of IgG, to and from mucosal surfaces.

1.4.2 Mechanisms of action

Upon antibody engagement with its antigen, unconjugated antibodies targeting tumour-associated surface antigens exert their cytotoxicity by; i) direct transmembrane signalling to induce apoptosis, ii) complement-dependent cytotoxicity (CDC), iii) antibody-dependent cellular cytotoxicity (ADCC) and iv) antibody-dependent cellular phagocytosis (ADCP); depending on the nature of the antibody, target antigen and epitope. More recently, new evidence indicates that MAbs can also trigger a vaccinal effect. These mechanisms are briefly reviewed below as this thesis will focus on CDC activity only:

1.4.2.1 Direct cell death

Direct action of a monoclonal antibody can result in cell death in the absence of complement or immune effector cells. This is usually done through: i) receptor blockade, impeding an activating ligand to bind; ii) receptor dimerization inhibition, thereby blocking an activation signal or iii) by apoptosis induction through receptor agonist activity or receptor crosslinking (Scott et al., 2012, Weiner, 2015).

1.4.2.2 Complement-dependent cytotoxicity (CDC)

Complement activation results from the C1q binding to at least two cell-bound antibodies in close proximity –although hexameric conformation of antibody complexes has been demonstrated to be highly efficient (Diebolder et al., 2014). This in turn results in inflammation via C3 and activation of the cell-killing membrane attack complex (MAC) eliciting cell death.

Importantly, expression of CD46, CD55 molecules on target cells inhibits C3 convertase, thereby preventing CDC. Similarly, CD59 expression disrupts MAC formation. Also, evidence that CD55 can negatively regulate T-cell mediated immunity has been reported (Liu et al., 2005, Rogers et al., 2014). Expression of these antigens on various solid cancers might explain why CDC

evidence in *in vivo* models of these diseases is less clear compared to haematological malignancies.

While data from experiments carried out both *in vitro* (Golay et al., 2001, Bellosillo et al., 2001) and in some animal models (Golay et al., 2006) suggested CDC is a primary mechanism for Rituximab-mediated cytotoxicity, it is unclear to what degree CDC contributes to the clinical antitumour response and whether it occurs outside of the intravascular compartment.

A clinical observation suggestive for the role of CDC in patients relates to residual chronic lymphocytic leukaemia (CLL) cells present following Rituximab therapy, having been shown to express elevated levels of CD59 when compared against pre-therapy samples (Weiner, 2010). Crucially, the role of CDC-mediated deletion in Rituximab efficacy has been considered sufficiently substiantial as to merit generation of anti-CD20 antibodies engineered to enhance the complement fixation effect. Ofatumumab, a novel therapeutic anti-CD20 MAb which binds to the small membrane-proximal extracellular loop of CD20 was selected based on its enhanced CDC-mediated lysis (Barth et al., 2015).

Of note, some MAbs can induce complement dependent cytotoxicity depending on antigen density, orientation and antigen conformation on the cell membrane. The isotype of the antibody and the cell type that is being targeted can also affect CDC (Weiner, 2015).

1.4.2.3 Antibody-dependent cellular cytotoxicity (ADCC)

Fc gamma receptors expressed in immune effector cells, but particularly FcγRIIIa (CD16), expressed on natural killer (NK) cells, mediate this type of antibody cytotoxicity. The Fc region of antibodies bound to their target cells interact with Fc receptors, which then signal through immunoreceptor tyrosine-based activation motifs (ITAMs) and induce effector cell activation accompanied with the release of cytotoxic granules (perforin and granzymes),

which enter the targeted cell and results in cell death (Clynes et al., 1998, Bowles and Weiner, 2005).

The concomitant release of cytokines by activated effectors will in turn stimulate the activation of other immune effector cells in the microenvironment. In contrast, cells expressing immunoreceptor tyrosine-based inhibitory motifs (ITIMs) can inhibit ADCC activity.

1.4.2.4 Antibody-dependent cellular phagocytosis (ADCP)

Opsonisation leading to phagocytosis of cancer cells by macrophages (antibody-dependent cell-mediated phagocytosis, ADCP) is another form of cytotoxicity induced by MAbs in cancer therapy (Weiner, 2015). In ADCP, FcγR activation leads to cytoskeletal rearrangements, allowing the formation of a phagosome in the effector cell (Freeman et al., 2016). The MAb-coated target cell is then endocytosed and degraded by lysosomal enzymes.

1.4.2.5 Vaccine effect

A further potential role for Fc-FcγR interactions in anti-cancer MAb therapy is a so-called “vaccine effect” (DiLillo and Ravetch, 2015) (**Fig. 1. 10**). As mentioned above, during ADCP, anti-tumour MAbs opsonise tumour cells and elicit cell death through Fc-FcγR interactions. This process generates antibody-tumour antigen immune complexes which engage activating FcγRIIa expressed on CD11c+ APCs. This results in stimulation of DC maturation and presentation of tumour antigens to tumour-reactive $CD4^+$ and $CD8^+$ T-cells, thereby leading to long-term anti-tumour cellular memory formation (Arce Vargas and Quezada, 2015). This recent evidence underlines the crucial role that interactions between Fc and specific FcγRs can play in cancer therapy (Beers et al., 2016, Yu et al., 2017)

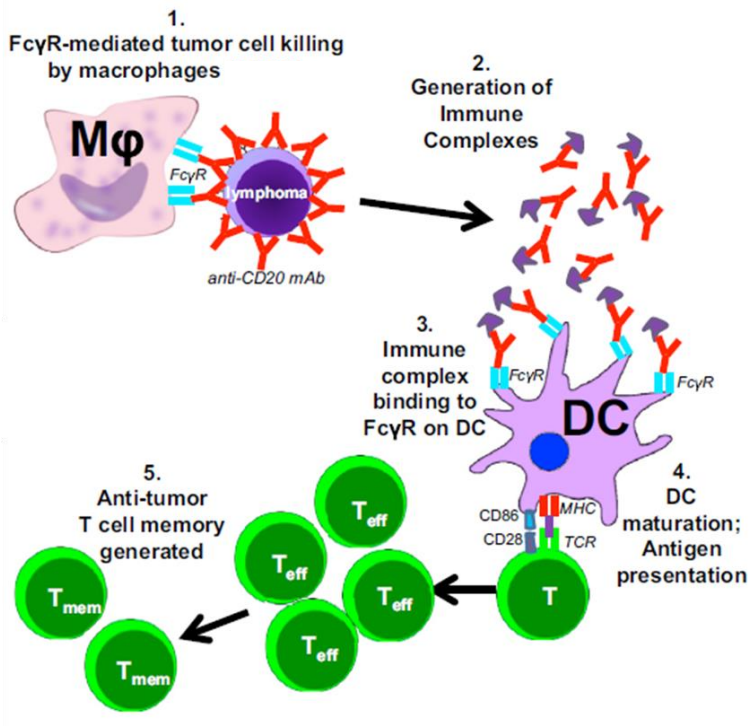

Fig. 1. 10. MAb anti-tumour vaccinal effect. Cytotoxic antibodies targeting cancer cells form tumour-antigen immune complexes which engage FcγRIIa expressed on DCs. In turn, they promote anti-tumour vaccinal effect through T-cell memory stimulation. Modified from DiLillo and Ravetch, 2015. DC= Dendritic cell.

As discussed earlier, other types of MAbs can elicit their anticancer activity by: i) inhibiting angiogenesis (eg. anti-VEGF MAbs), ii) blocking T-cell inhibitory pathways (anti-CTL4, anti-PD-1 MAbs), iii) delivering a radioisotope (radioimmunoconjugates) or drug/toxin payloads (antibody-drug conjugates, ADC), and by iv) re-directing T-cells towards malignant cells (bispecific T-cell engagers, BiTEs and chimeric antigen receptors, CARs).

1.4.3 Current technology in MAbs

Depending on the desired mechanism of action to be exploited, MAbs can be engineered in various different ways (**Fig. 1. 11**). Some of the most popular approaches currently used in the clinic –except for CAR therapy discussed earlier– are presented below.

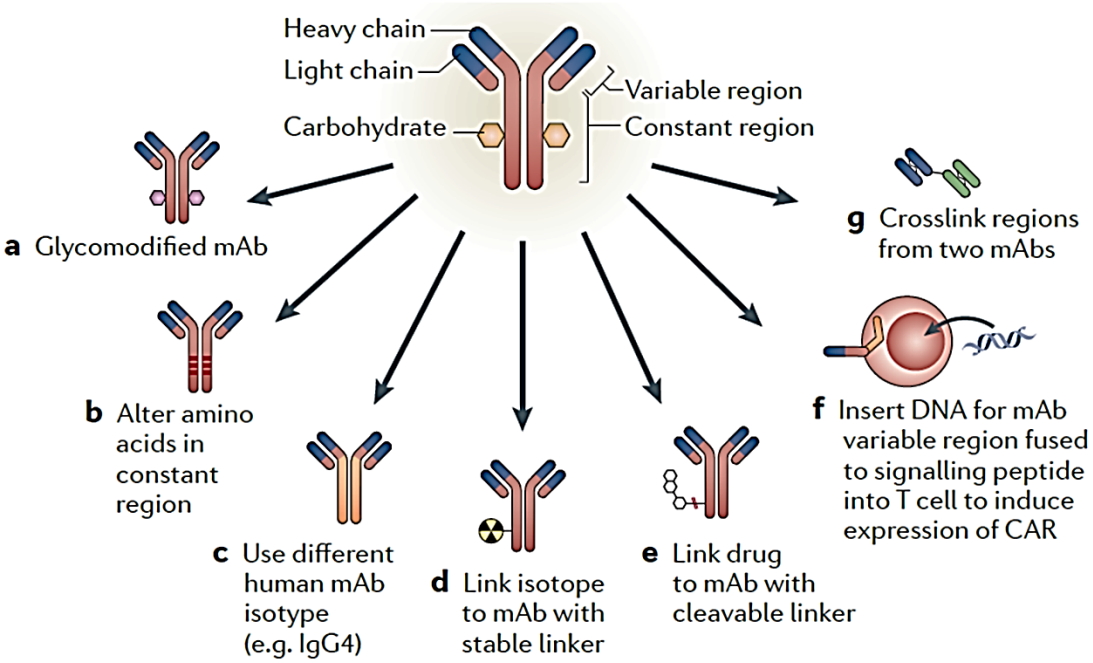

Fig. 1. 11. MAb modification for cancer therapy. Reproduced from Weiner, 2015.

1.4.3.1 Fc engineering

Most therapeutic antibodies contain the human constant IgG1 isotype, as it has been shown that it can induce potent ADCC and CDC activities when compared to other heavy chain isotypes (Natsume et al., 2008). As mentioned previously, cytotoxicity is mediated by the interaction of hIgG1 with C1q component of the complement system, and with Fc gamma receptors on immune effector cells; in particular FcγRIIIa (CD16) on NK cells (Clark, 1997, Natsume et al., 2009, Bowles and Weiner, 2005), macrophages, monocytes and granulocytes (Weiner, 2015). Moreover, hIgG1 isotype confer stability to

the MAb and a long half-life of approximately 21 days in the bloodstream through binding to the neonatal Fc receptor (FcRn) (Jefferis et al., 1998).

Due to the pivotal role of the Fc region in MAb therapeutics, a number of modifications have been attempted in order to enhance cytotoxicity (Yu et al., 2017). For instance, the amino acid sequence of the Fc region of Ocaratuzumab was modified using a directed evolution approach in order to produce an antibody with increased affinity for CD16 (Bowles et al., 2006). As a result, Ocaratuzumab showed a 3-fold improved ADCC activity on primary CLL cells compared to either Rituximab or Ofatumumab (Cheney et al., 2014).

A more common strategy is the afucosylation of the heavy chain constant region as it allows improved binding to Fc gamma receptors (Weiner, 2015). Stable production of non-fucosylated therapeutic antibodies is carried out by the utilisation of alpha-1,6-fucosyltransferase (FUT8) deficient Chinese hamster ovarian (CHO/FUT8$^{-/-}$) cells. Many MAbs currently in clinical development have been afucosylated (Naddafi and Davami, 2015). Such is the case for Obinutuzumab, a mAb with enhanced ADCC activity, already in use for the treatment of CLL patients.

As noted by (Weiner, 2015), however, a major ongoing research question in the field is whether IgGs with higher affinity for Fc receptors are clinically more effective than unaltered IgGs. In fact, when Obinutuzumab was compared with its non-glycoengineered version *in vivo*, similar anti-tumoural effect and tumour remission was observed (Herter et al., 2013). The authors of the study suggested that, in general, superior activity of GA101 is not related to glycoengineering but rather to direct effects. Nevertheless, more recent studies indicate that afucosylated antibodies do not only exhibit better ADCC through enhanced affinity to FcγRIIIa, but are also able to effectively bind to FcγRIIa, which warrants potential induction of a vaccinal effect (Arce Vargas and Quezada, 2015).

1.4.3.2 Antibody-drug conjugates (ADCs)

As mentioned above, monoclonal antibodies can also be used as a delivery system of a radioisotope (radioimmunoconjugates), or a toxin/drug (ADC) payload.

Antibody-drug conjugates possess a cleavable linker that connects the Fc portion of the monoclonal antibody to the drug or toxin it is carrying. The linker is usually pH-sensitive or enzymatically cleaved (Weiner, 2015), as it is desirable that ADCs are toxic only when they have got internalised by the cancer cell upon binding its target. Importantly, an outstanding advantage of ADCs is that this type of molecule exerts its cytotoxicity through the toxin it carries, unlike unarmed antibodies that rely on the immune system of patients (Baskar et al., 2012).

Of note, up until now, three anti-ROR1 antibody drug conjugates have been designed and tested *in vitro* (BT1, based on clone 2a2 (Baskar et al., 2012)) as well as *in vivo* (OSU-2S, based also on clone 2a2 anti-ROR1 antibody (Mani et al., 2015), and Cirmtuzumab Vedotin (Cui B., 2015)). All three molecules have shown cytotoxicity on B-cell lymphoma models. Although no follow-up studies have been reported. Additionally, there is a commercially available ROR1 ADC based on clone R11, reported by Yang *et al.* (Yang et al., 2011). This clone has been conjugated to a selenocysteine (Sec) residue, and is called R11-scFv-Fc-Sec (Biolabs, 2017). No cytotoxicity data has been yet reported in the literature.

1.4.3.3 Bispecific antibodies (BsAbs)

Bispecific antibodies are composed of fragments of two monoclonal antibodies binding different antigens or epitopes. These molecules can be classified in two main groups, those that possess an Fc region and those that don't (Kontermann and Brinkmann, 2015).

In cancer research, the most common format of BsAb is known as Bispecific T-cell engager (BiTE). These molecules contain the variable regions (scFv) of two MAbs, which are connected together via a peptide (linker). One arm of this bispecific antibody targets cancer cells whilst the other arm binds to activating receptors on immune effector cells (Kontermann and Brinkmann, 2015). This strategy allows retargeting immune effectors to cancer cells in the absence of an Fc region, an approach that has proved promising as more than 20 out of the 30 BsAbs in clinical development use this format (Fan et al., 2015). The main advantages of BiTEs are high tissue penetration due to their small size (55-60kDa) and potent anti-tumoural cytotoxicity using very low doses (approx. 10pg/ml in *in vitro* studies) (Kontermann and Brinkmann, 2015). Certainly, Blinatumomab, an anti-CD19/anti-CD3 BiTE, has been recently granted accelerated FDA-approval for its use as second-line treatment in acute lymphoblastic leukaemia (Przepiorka et al., 2015).

A different strategy in BsAbs therapeutics is to use the IgG-like format. Although large-scale production and purification may be more problematic, Fc-bispecific antibodies possess many advantages such as increased stability, longer half-life and cytotoxicity potential (through CDC, ADCC, ADCP and vaccinal effect) (Fan et al., 2015, Arce Vargas and Quezada, 2015). The main clinical application of this design is the efficient blocking of signalling pathways. Indeed, several BsAbs targeting EGFR pathway are now in clinical trials. More recently, this approach has also been tested on B-cell lymphomas *in vitro* using an anti-CD20/anti-HLA-DR bispecific antibody, achieving more specific cell death of malignant cells compared to Rituximab or anti-HLA-DR antibodies alone (Zeng et al., 2015).

A similar way to enhance anti-tumour activity, explored over the past decade, is targeting two antigens or epitopes at the same time with two monoclonal antibodies. Increasing amount of data suggest that co-administration of MAbs provides synergistic anti-tumour effects (Tebbutt et al., 2013). Symm004 and MM-151 are mixtures of EGFR-targeted antibodies which have been

developed to bind non-overlapping epitopes on EGFR and are currently in clinical trials for advanced solid malignancies (Machiels et al., 2015, Kearns et al., 2015). For haematological malignancies, anti-HLA-DR and anti-CD5 combined therapy has been successfully tested *in vitro* an *in vivo* using B-cell lymphoma models (Loisel et al., 2011).

As a whole, mixtures of monoclonal antibodies and bispecific antibodies targeting two antigens or two non-overlapping epitopes containing an IgG portion have provided promising results at a preclinical stage and some are already in clinical trials. Further research is needed in order to ascertain the effectiveness of these strategies in the clinic.

Intriguingly, no mixture of MAbs or bispecific antibody has been yet proposed for ROR1 using previously reported anti-ROR1 antibodies. In this study, I will focus on the investigation of monoclonal antibodies against ROR1 as potential therapeutic tools. Additionally, the cytotoxic potential of a humanised ROR1 BiTE on a CSC model *in vitro* will be explored.

1.5 Aim and objectives

The overriding aim of this project is to develop an innovative therapeutic approach that uses monoclonal antibodies and/or their derivatives against the receptor-tyrosine-kinase-like orphan receptor 1 (ROR1) –a protein present on the surface of malignant B-cells and other cancer cells but not on critical post-partum tissues. These new ROR1 therapy will specifically target and kill $CD19^{+}CD5^{+}ROR1^{+}$ malignant B-cells and other $ROR1^{+}$ solid malignancies.

The specific goals now are:

Aim 1: To generate new antibodies against human ROR1.

Objectives

1. To produce ROR1 hybridomas from rats immunised with the extracellular portion of ROR1 through collaboration with the specialised antibody company (Aldevron).
2. To generate single-cell clone hybridomas of ROR1 and extract their variable heavy (V_H) and variable light (V_L) regions, in collaboration with Dr Marco Della Peruta and Dr Satyen Gohil.
3. To produce chimeric rat-human antibodies by cloning the rat V_H and V_L sequences to human IgG1, kappa constant regions.
4. To assess binding of the new ROR1 chimeric antibodies on $ROR1^+$ and $ROR1^-$ cell lines.

Aim 2: To characterise the newly generated chimeric antibodies and assess their cytotoxicity on primary CLL cells.

Objectives

1. To identify the binding domain of our chimeric antibodies on the extracellular portion of ROR1 using flow cytometry.
2. To quantify the affinity of our antibodies to their target by determining their binding kinetics using Surface Plasmon Resonance (SPR) technology (Biacore).
3. To screen the cytotolytic activity of our ROR1 antibodies by Complement-Dependent Cytotoxicity (CDC) assay.
4. To assess internalisation of our antibodies into $ROR1^+$ cells by flow cytometry and pHAb amine dye labelling.

Aim 3: To further investigate potential therapeutic antibodies identified in previous studies.

Objectives

1. To perform a fine epitope mapping to ascertain the specific amino acids targeted by relevant clones.

2. To assess the complement-dependent cytotoxicity (CDC) *in vitro* of purified antibodies using cell lines and primary cells from CLL patients and healthy donors.
3. To generate humanised antibodies against ROR1 based on relevant clones' protein sequence (in collaboration with GenScript); assess their binding to ROR1 and evaluate their cytotoxicity on primary CLL and healthy donor cells by direct cell death, CDC, and ADCC assays.

Aim 4: To generate an *in vitro* model of tumourspheres containing cancer stem cell-like cells (CSCs) in order to assess the effects that BiTE therapy against ROR1 has on this cell population.

Objectives

1. To generate tumourspheres from a PDAC cancer cell line (PANC-1) by 3D spheroid formation assay, using ultra-low attachment plates.
2. To perform: i) gene, ii) protein and iii) functional characterisation of PANC-1-derived tumourspheres by qPCR, confocal microscopy and transwell migration assay, respectively.
3. To assess the effect of ROR1 BiTE therapy on the cell viability of tumourspheres and specific elimination of ROR1+ cell subpopulations.

Chapter 2 Materials and Methods

2.1 Cell culture

2.1.1 Propagation of cells

Tissue culture work was performed in Biological Safety Cabinet Class 2 hoods. All cell lines were obtained from ATCC or DSMZ; additionally, they were sent for cell line profile authentication (ATCC short tandem repeat DNA database). Cells were counted using an improved Neubauer haemocytometer (Abcam), where 10µl of cells were mixed with 10µl Trypan Blue (Life Technologies). Only cells that had not taken up the dye were counted as live cells under a light microscope.

In the next paragraphs, propagation of suspension and adherent cells, processing of primary cells and culture of hybridomas and pancreatic cancer cell line-derived tumourspheres is described.

2.1.1.1 Propagation of suspension cell lines

All suspension cell lines were kept at a density of 0.2-1x10^6c/ml. In general, a 1/10 split twice a week was enough to maintain all suspension cell lines used throughout this thesis at 0.6x10^6c/ml.

Human myeloid leukaemia K562 cells, obtained from ATCC, were cultured in Iscove's Modified Dulbecco's Media (IMDM, Sigma-Aldrich) supplemented with 10% heat-inactivated foetal bovine serum (HI-FBS, Gibco® Life Technologies) in a 5% CO_2 humidified atmosphere at 37°C.

MEC-1 cells (B-CLL in prolymphocytoid transformation to B-PLL), SUP-T1 (T-cell lymphoblastic lymphoma), SKW 6.4 cells (Epstein-Barr virus (EBV) transformed B cells), Jeko-1 (Mantle cell lymphoma B cells) and Jurkat (acute T-cell leukemia) were cultured in Roswell Park Memorial Institute 1640 (RPMI-

1640, Sigma-Aldrich) media supplemented with 10% HI-FBS in a 5% CO_2 humidified atmosphere at 37°C.

2.1.1.2 Propagation of adherent cell lines

Human Embryonic Kidney (HEK) 293T cells along with solid tumour cell lines from different cancer types such as: Pancreatic (PANC-1), breast (MCF-7), ovarian (SKOV3), were cultured in complete IMDM (HEK293T) and RPMI (solid cancer cell lines), according to ATCC guidelines.

Cells were passaged at ~80% confluence, typically every 3 days for all adherent cell lines mentioned above. Cell passaging was performed by washing the cells with 1x PBS, followed by a 5min incubation at 37°C with 5ml 1x trypsin/EDTA. After this, the reaction was stopped by adding complete media. Cells were transferred to a 15ml falcon, and centrifuged at 400g for 5min. After discarding the supernatant, cells were put in a single-cell suspension using fresh complete media and plated in T175cm^2 tissue culture-treated flasks at 37°C with a 5% CO_2 atmosphere.

2.1.1.3 Processing of primary cells from CLL patients and PBMCs from healthy donors

Whole blood was obtained from CLL patients after written consent or by venesection from consenting healthy donors. Blood from the latter was collected into 50ml syringes prepared with appropriate 0.5M EDTA solution to achieve a final concentration of 5mM EDTA to serve as an anti-coagulant.

Whole blood was diluted 1:1 with PBS; with each 30ml of blood solution layered onto 15ml Ficoll-Paque in 50ml falcon tubes. Tubes were centrifuged at 750g for 40 minutes at room temperature applying minimum acceleration and without brake. Following centrifugation, the buffy coat layer, localised to the Ficoll: plasma interface, was removed by aspiration with a Pasteur pipette. PBMCs were washed twice: once with unsupplemented PBS and once with complete RPMI prior to final resuspension into a volume of complete RPMI matching the volume of the initial blood donation.

From these PBMCs, CLL cells were isolated by CD2-negative selection (CD2 MicroBeads, human - Miltenyi Biotec). Briefly, a pellet of up to 10^7 primary cells resuspended in 80ul of sterile-filtered MACS buffer (PBS, 0.5% BSA, 2mM EDTA) was labelled with 20ul of CD2 microbeads, mixed and incubated for 15min at 4°C. Cells were then washed by adding 1ml of MACS buffer and centrifuged at 300g for 10min; supernatant was discarded. Pellet was resuspended in 500ul of MACS buffer and cells were separated from the CD2 MicroBeads using, typically, a LS column as per manufacturer's instruction. Unlabelled cells ($CD2^-$ cells) were collected. Alternatively, CLL cells were obtained by CLL isolation (CLL isolation kit, human - Miltenyi Biotec). The latter contained biotin-labelled antibodies against CD2, CD3, CD4, CD14, CD15, CD16, CD34, CD56, CD61, CD235a and FceRIa. Separation protocol was performed by incubating cells with the biotin-antibody cocktail. Immunoconjugated cells were then incubated with anti-biotin MicroBeads, and MACS column separation was continued as per manufacturer's protocol. Unlabelled cells were collected. CLL cells were then washed in complete RPMI and frozen down in freezing media (90% HI-FBS + 10% DMSO).

PBMCs obtained from healthy donors (HD) were also washed in complete RPMI and frozen down in freezing media. Alternatively, when used as effectors, PBMCs were cultured in 24-well, TC-treated plates at a density of $2x10^6$ cells/well. PBMCs were stimulated with 5ul/ml of PHA on the day of isolation. 24 hours later, 100U/ml of IL-2 was added with transductions performed 24 hours following IL-2 stimulation.

2.1.1.4 Propagation of tumourspheres: 3D culture

PANC-1 cells were diluted to a concentration of 10^4 cells/ml in either: i) MEBM supplemented with MEGM SingleQuots (Lonza) as per Zhang et al., 2014, or ii) Cancer Stem Cell (CSC) medium supplemented with CSC SuppMix (Promocell) as per Garikapati et al., 2017. A total of 4ml of cells at this

concentration were seeded in each well of ultra-low attachment 6-well plates (Greiner Bio-One). This methodology is based on

Tumourspheres were fed every 3-4 days with 1.5ml of complete CSC media and passaged every 7-9 days. Briefly, spheroids were transferred to 50ml falcon tubes (Corning®). After 20-30min, or once tumourspheres were at the bottom of the tube, supernatant was carefully aspirated. Spheroids were washed with 5ml of 1X PBS and the previous step was repeated. Tumourspheres were segregated into a single-cell suspension by gentle resuspension with 1ml of 1x trypsin/EDTA. The reaction was stopped by adding 1ml of complete CSC medium. Cells were then counted using trypan-blue and plated for continuous culture as described above, and/or for *in vitro* experiments. In **section 2.1.1.6,** a description on the generation of single-cell clone tumourspheres: CSC96 is provided.

Once spheroids were formed in high numbers and showed optimal viability, cell lysates were prepared in order to extract both mRNA and protein as described in the following sections.

2.1.1.5 ROR1 Hybridoma Culture (in collaboration with Aldervron, Dr Della Peruta and Dr Gohil)

Through collaboration with Aldevron Freiburg GmbH, a specialised company on generation of novel antibodies, a total of 3 Wistar rats were immunised using the company's proprietary DNA-based protocol: Briefly, publicly available human ROR1 coding sequence (GenBank) was cloned into Aldevron's immunisation plasmid. The latter was introduced into the rats, the target protein was expressed, and an immune response was generated. Four applications of DNA using a gene gun were initially performed. Rat serum was then analysed by flow cytometry, followed by 4 additional applications. After confirming that serum from all three challenged rats showed presence of anti-human ROR1 antibodies, animals were sacrificed after 102 days of immunisation. Lymph nodes were removed and pooled in order to produce

oligoclonal hybridoma cell lines according to the company's protocols. Our collaborators identified a total of 38 positive hybridomas by testing their binding ability to cells transfected with either pB1-ROR1-hum (Aldevron) or with an irrelevant construct. As before, this was assessed by flow cytometry.

Serum from the three immunised rats as well as all 38 hybridoma supernatants were sent to us by Aldevron, which were then tested on ROR1+ and ROR1- cells by flow cytometry. In parallel, Dr Marco Della Peruta was in charge of the culture of these hybridomas. Along with Dr Satyen Gohil, we passaged the polyclonal hybridomas in serum-free DMEM using 6-well plates (Corning®) at 37°C and 8% of CO_2. Enough cells were grown in order to then generate monoclonal hybridomas as described below.

2.1.1.6 Single-cell cloning by limiting dilution

In order to produce single-cell clones (for either hybridomas, new stable cell lines or CSCs), cells were diluted appropriately to ensure that, on average, one cell would be isolated into every second well of a 96-well plate (5 cells/ml, using 100ul/well). Plates were monitored at least twice a week, and cellular isolates were cultured until a clear population had been established. It it worth mentioning that, when available, cell sorting was also used for the generation of single cell clones from hybridomas and new stable cell lines. Briefly, cells were resuspended carefully but thoroughly in order to produce a single cell suspension (~$1x10^6$c/ml). In parallel, a 15ml falcon containing 1ml of HI-FBS was prepared in order to collect the sorted cells.

When applying this technique for tumoursphere formation assays, U-bottom 96-well suspension plates (Greiner Bio-One) were used. The resultant single-cell CSCs were called CSC96.

2.1.1.7 Transient transfection of HEK293T cells for protein expression

According to the number of constructs to be tested or proteins to be produced, transient transfection of HEK293T cells was performed in multiwell TC-treated plates or dishes as per **Table 2. 1.**

Table 2. 1. Transfection mixtures according to multiwell plate/dish size

Plate	Genejuice, µl	Media, µl	DNA, µg
15cm-dish	65	1,235	34
10cm-dish	30	470	12.5
6-well	5	95	2
12-well	2.5	47.5	1
24-well	1.25	23.75	0.5

For expression testing, a total of ~2.5x10^6 cells were seeded in a multiwell plate irrespective of the size. Therefore, for a 6-well plate, 2ml of cells per well were plated at a conc. of 0.20 x10^6 cells/ml. This was done 24h before transfection in order to attain around 60% confluence.

For protein production, HEK293T cells from T175 flasks were split 1/3 in 15cm-dishes (Greiner Bio-One), 24h prior transfection. An equivalent volume of Polyethylenimine (PEI – Sigma-Aldrich) was used as transfection reagent instead of Genejuice (Merck) when large amounts of 15cm-dishes were to be transfected (See **Table 2. 1**).

In either case, transfection mixtures where prepared by adding the transfection reagent to plain media (no FBS). After 5min of incubation at RT, DNA was added. Following a 15min incubation, the transfection mix was gently resuspended and added to the cells in a dropwise manner all around the well. Notably, Genejuice and PEI are lipid-base transfection reagents that complex with DNA in order to mediate transport into cells during transfection. The incubation times therefore allow the formation of micelles containing the DNA to be transfected.

Supernatants harvested after 72h were centrifuged at 1000g for 10min in order to remove any cell debris. Supernatant were then transferred to fresh tubes and immediately tested on relevant cells or stored at 4°C until use. In the meantime, transfected HEK293T cells were washed with 1X PBS, trypsinised and put in FACS tubes in order to check for transfection.

2.1.1.8 Cryopreservation and recovery of cells

Different cell types were harvested whilst in optimal growth conditions and viability in order to be cryopreserved. Typically, after centrifugation, 3-5x10^6 cells/ml were resuspended in ice-cold freezing media (10% DMSO in HI-FBS) and distributed in 1ml aliquots into 2ml cryovials (Corning®). Aliquoted cells were immediately placed in a Mr Frosty (Sigma-Aldrich) and kept at -80°C. The fresh isopropanol bath (up to 5 uses) in the Mr Frosty allows a controlled cooling rate of 1°C/min. Frozen cells were then transferred into liquid nitrogen for long-term storage.

In order to recover cells, frozen cryovials were promptly thawed in a 37°C water bath. Immediately after, thawed cells were resuspended in 10ml of suitable media. After centrifugation at 400g for 5min, the supernatant was discarded in order to rinse off the DMSO contained in the freezing media. Cells were then cultured as appropriate.

Thawed tumourspheres (frozen as single-cell suspensions) were washed with 8ml of complete CSC media and then plated in ultra-low attachment 6-well plates o/n. The next day, CSCs were split as per **section 2.1.1.4** and expanded in order to be used in subsequent experiments.

2.1.2 Retroviral work

2.1.2.1 Retroviral supernatant production

HEK293T cells (2.5x10^6) were plated in 10cm-dishes 24h before transfection. Cells were then transfected as described above, using a total amount of

12.5µg of DNA consisting of: 3.125µg/plate of envelope, 4.69µg/plate of gagpol and 4.69µg/plate of retroviral vector plasmid of interest.

After 48h, supernatants were collected and stored at 4°C, whilst fresh media was added to the cells. The 72h post-transfection harvest was then combined with the 48h time point supernatant. Supes were centrifuged at 1000g for 10min to remove cell debris and stored at -80°C in snap-frozen aliquots.

2.1.2.2 Retronectin coating of non-tissue culture treated 24-well plates

Non-tissue culture treated 24-well plates were coated with 500µl of PBS containing 8µl of retronectin/ml, using Pasteur pipettes. Plates were then stored at 4°C wrapped with parafilm until use (at least 24 hours prior to cell transduction). It is noteworthy that retronectin-supplemented PBS was re-used twice by direct transfer to fresh 24-well plates and kept in the fridge until required.

2.1.2.3 Retroviral transduction of suspension cell lines

A volume of 1.5ml of thawed retroviral supernatant was added to retronectin-coated plates. In the meantime, relevant cell lines were washed with appropriate complete media and resuspended at a concentration of $5x10^5$ cells/ml. Immediately after, 0.5ml of cells were added into wells containing the retroviral supernatant (2ml final volume). Cells were gently mixed and the plate was centrifuged at 1000g for 40min. Plates were then incubated at 37°C and 5% CO_2. Two days later, transduction was assessed by flow cytometry.

2.1.3 Flow cytometry

2.1.3.1 General staining protocol

Unless otherwise stated, $1x10^5$ cells were washed with PBS, stained with antibodies +/- viability dye, then washed and resuspended in PBS buffer and placed on ice until analysis.

Where multiple staining steps were required, samples were washed with PBS between individual staining steps. Isotype and/or non-transduced controls were included as required. All staining steps were performed at 4°C in the dark with 30min incubation per step unless indicated otherwise.

Flow cytometry was performed using Becton Dickinson (BD) FacsVerse or BD LSR Fortessa instruments.

2.1.3.2 Preparation of counting beads

To allow cellular enumeration within a sample, or to enable effective comparison between samples, the latter were supplemented with a pre-determined quantity of fluorescent 'counting beads' as an internal control. Beckman Coulter Flow-Check^{TM} fluorospheres are supplied at 1x10^{6} beads/ml in an aqueous solution containing preservative surfactant. To prevent toxicity to cellular samples, beads were washed once with PBS supplemented with 10%FBS prior to addition to samples. Following centrifugation (400g x 5min), beads were resuspended in an equal volume of FACS buffer with 10µl of beads added to each sample.

2.2 Molecular Biology

2.2.1 Molecular Cloning

2.2.1.1 Splicing DNA by overlap extension PCR

Expression plasmid transgene cassettes were generated using splicing by overlap extension PCR (SOE-PCR). Transgenes were generated in two or more fragments; with the N-terminal fragment containing 5' restriction site (typically NcoI in SFG plasmids) and the C-terminal fragment containing the 3' restriction site (typically MluI in SFG plasmid). Fusion and/or modification of fragments was achieved by designing overlapping internal oligonucleotide primers complimentary to both the flanking sequences and the desired modification.

The primary fragments were generated by PCR, using the following conditions: Melting temperature was 98°C for 2min, annealing temperature 65°C for 42s and extension temperature was 72°C. PCR was carried out for 35 cycles using Phusion polymerase (extension duration defined by amplicon length; approximately 70 seconds per 1000 base pairs of sequence to be amplified). Following PCR amplification, products were separated by gel electrophoresis and purified using the Wizard® SV Gel and PCR Clean-Up System (Promega). Primary PCR products were combined using a secondary fusion PCR reaction using appropriate numbers and the same conditions as above. Following PCR clean-up, PCR products were digested using suitable restriction enzymes and the insert was subcloned into appropriately digested destination plasmid.

2.2.1.2 Gene synthesis by overlapping oligo assembly

Where a novel sequence of DNA required to be generated, this was purchased from IDT (G-blocks Gene Fragments, <1000bp).

Gene fragments were designed with appropriate 5' and 3' restriction sites to enable subcloning. Commercially-sourced DNA was typically amplified by PCR before restriction digest.

2.2.1.3 Restriction endonuclease digestion

Restriction digests were performed according to manufacturer's instructions (NEB). Restriction enzymes able to generate "sticky ends" were preferred in order to facilitate DNA ligation. For inserts derived by PCR, the entire sample was digested.

To generate vector backbone, or vector-derived insert fragments, 5µg of plasmid vector DNA was used. In either case, the reaction volume was adjusted with nucleotide-free water such that the final reaction volume was 50µl. Buffer selection was defined by the manufacturer, with a final enzyme concentration of <5% of the final reaction volume.

2.2.1.4 DNA ligation

Following gel extraction of the digested vector and insert fragments, DNA ligations were performed using Quick Ligase (NEB) according to the manufacturer's instructions. A vector:insert molar ratio between 1:3 - 1:6 were used. Following 5min incubation at room temperature, 5ul of the resulting ligation mix was used for bacterial transformation of high efficiency C2987 (NEB) chemically competent *E. coli* bacteria (DH5α-derived).

2.2.1.5 Bacterial culture and heat-shock transformation

DH5α *E. coli* bacteria were grown in liquid Luria-Bertani (LB) for mini, midi or maxi-preps or terrific broth (TB) media for mega and giga-prep culture. Media was supplemented with appropriate antibiotic and cultured at 37°C with agitation at 220rpm. For bacterial growth on plates, LB-agar infused with appropriate antibiotic was used and bacteria was cultured overnight in a static 37°C incubator.

Bacterial transformation was performed by heat-shock. Briefly, 25µl of bacteria were thawed on ice, 5µl of ligation mix (from PCR based cloning into C2987 *E. coli*), or 1µl of mini-prep DNA (for retransformation) was added to the bacteria and incubated on ice for 30min. Bacteria were transiently heat-shocked by incubation in a 42°C water bath for 30-40s, followed by incubation on ice for 5min. Bacteria were transferred to 300µl of SOC media and allowed to recover for 30 minutes on a shaking incubator at 37°C, 220rpm (this step was omitted only if the primary resistance was ampicillin). Following recovery, bacteria were plated onto an LB-agar dishes infused with appropriate antibiotic and incubated at 37°C overnight.

2.2.1.6 DNA preparation: small and large-scale

Following bacterial transformation and for screening purposes, small-scale DNA preparation (miniprep) was performed by picking single colonies from an

agar plate. These colonies were then grown overnight in 3ml LB media supplemented with 100µg/ml carbenicillin (or other appropriate antibiotics).

The following morning, plasmid DNA was isolated using the Macherey-Nagel miniprep kit according to manufacturer's instructions. Constructs were verified by restriction digest and/or DNA sequencing.

Once the right constructs were obtained, large-scale generation of DNA (midiprep) for *in vitro* studies was prepared as follows: 200ml of LB were inoculated with the appropriate antibiotic and 250-500µl of bacterial culture and cultured for 16-18 hours in a bacterial shaking incubator; 220rpm at 37°C.

Macherey-Nagel midiprep kit was used to isolate plasmid DNA as per manufacturer's instructions. Midiprep DNA was verified by multiple separate restriction digests cutting in the vector backbone and transgene insert and by DNA sequencing. When even larger amounts of DNA were needed, megapreps using the Qiagen kit or gigapreps using the Invitrogen kit were performed according to manufacturer's instructions.

2.2.1.7 Measurement of DNA concentration

DNA concentration is based on its property to absorb light at a wavelength of 260nm, while the ratio of absorbances at 260:280nm and 260:230nm can be used to establish purity. If equal or higher than 1.8, these ratios indicate a high degree of DNA purity with little protein and solvent contamination, respectively. Purity and concentration of plasmid DNA was measure using a Nanodrop ND-1000 spectrophotometer.

2.2.1.8 Gel electrophoresis

Restriction digests and PCR products were assessed by DNA separation using agarose gel electrophoresis. Depending on the expected DNA band sizes, 1-1.7% agarose gels were prepared in 1x TBE buffer. Agarose solubilisation was achieved by microwave heating of the solution. Once solubilisation had been

achieved, the mix was cooled and infused with SybrSafe (Thermo Fisher Scientific) or GelStar (Lonza) –depending on experiment purposes- in order to enable UV visualisation of the DNA.

Samples were mixed with 6x loading buffer prior to loading into the gel in order to visualise sample progression within the gel. An appropriate DNA ladder was also used as reference for DNA band size, usually Hyperladder I, 1kb (Bioline). Typically, agarose gels were run at 130V in 1xTBE buffer for 1h or until appropriate separation was achieved. DNA was then visualised using a Dark Reader Transilluminator (dark reader blue light box, Clare Chemical Research).

2.2.1.9 Gel extraction and PCR clean-up

After agarose gel electrophoresis, bands were visualised using a dark reader blue light box to prevent UV-mediated mutagenesis. Relevant bands were excised from the gel with a clean scalpel, transferred into clean 2ml tubes and gel extracted using the ion of DNA was then accomplished using the Wizard® SV Gel and PCR Clean-Up System (Promega), according to manufacturer's instructions.

The latter Promega kit was also used on PCR reactions, in order to remove contaminants from the sample prior to downstream processing.

2.2.2 Preparation of nucleic acids from cells

2.2.2.1 RNA extraction (RNeasy mini kit)

Typically, 3-5x10^6 cells (human cancer cell lines, tumourspheres or rat lymph nodes/splenocytes) were resuspended in 350µl of buffer RLT supplemented with β-mercaptoethanol (Qiagen). To ensure effective cellular lysis, cells were vigorously vortexed before proceeding with the protocol enclosed in the RNeasy mini kit (Qiagen). For homogenisation purposes, QIAshredder columns were used, as suggested by the manufacturer. RNA was eluted in

35µl of nucleotide-free water and RNA concentration was determined by spectrophotometric measure using Nanodrop.

2.2.2.2 cDNA preparation

cDNA was generated from RNA through a two-step process: effective genomic DNA elimination and efficient reverse transcription. In the first step, a 28µl reaction mixture composed of 2µg of RNA, 4µl of gDNA wipeout buffer (7x) and nucleotide-free water was incubated at 42°C for 2min, followed by a 4°C incubation. In parallel, a reverse-transcription master mix for the second step was prepared, using 8µl of Quantiscript RT buffer (5x), which already includes Mg^{2+} and dNTPs, 2µl of Quantiscript Reverse Transcriptase and 2µl of RT Primer mix. This 12µl RT mix were then added to the first step reaction, resulting in a total volume of 40µl. Samples were incubated at 42°C for 30min followed by a 95°C incubation for 3min to inactivate the polymerase enzyme. To check for gDNA contamination and to confirm successful cDNA generation, a PCR reaction was set up using GAPDH as housekeeping gene. Forward and reverse primers for the human GAPDH sequence were 5'-ATTCCATGGCACCGTCAAGGCTG-3' and 5'-TTGGCAGCGCCAGTAGAGGCAGGGAT-3', respectively.

2.2.3 Evaluation of gene expression by RT-PCR and qPCR

Reverse transcription PCR (RT-qPCR) was performed with QuantiTect reverse transcriptase kit (Qiagen). The reaction was then followed by SYBR green PCR master mix (Qiagen) following the manufacturer's instructions. mRNA levels were determined by qPCR and normalized to β-actin (housekeeping gene). The list of human primers used in this thesis are presented in **Table 2. 2**.

Table 2. 2. List of human primers

Primers	
Description	**DNA Sequence 5' - 3'**
OL437.hActin_qPCR_Fw	ATTAAGGAGAAGCTGTGCTACGTC
OL438.hActin_qPCR_Rv	ATGATGGAGTTGAAGGTAGTTTCG
OL439.hROR1_paper-qPCR_Fw	GAGGCAACCAAAACACGTCAGAG
OL440.hROR1_paper-qPCR_Rv	GGCACACTCACCCAATTCTTCC
OL482.CD133_Fw	CAGAGTACAACGCCAAACCA
OL483.CD133_Rv	AAATCACGATGAGGGTCAGC
OL484.Notch-1_Fw	GTCAACGCCGTAGATGACC
OL485.Notch-1_Rv	TTGTTAGCCCCGTTCTTCAG
OL486.ALDH1-A1_Fw	TGTTAGCTGATGCCGACTTG
OL487.ALDH1-A1_Rv	TTCTTAGCCCGCTCAACACT
OL488.ALDH1-A2_Fw	TGATCCTGCAAACACTGCTC
OL489.ALDH1-A2_Rv	CTGGAGCTGGGTGGTAAGAG
OL490.ALDH1-A3_Fw	TCTCGACAAAGCCCTGAAGT
OL491.ALDH1-A3_Rv	TATTCGGCCAAAGCGTATTC
OL492.ALDH1-B1_Fw	CTGGAGCTGGGTGGTAAGAG
OL493.ALDH1-B1_Rv	CTTTCTCCACGGTTCTCTCG
OL494.ALDH1-L1_Fw	ATCTTTGCTGACTGTGACCT
OL495.ALDH1-L1_Rv	GCACCTCTTCTACCACTCTC
OL496.ALDH1-L2_Fw	GCCTGGTCTCGTTACCAAAA
OL497.ALDH1-L2_Rv	GCCACTTTCACCTCTTCAGC
OL498.Bmi-1_Fw	AATCCCCACCTGATGTGTGT
OL499.Bmi-1_Rv	GCTGGTCTCCAGGTAACGAA
OL500. CD24_Fw	TGCTCCTACCCACGCAGATT
OL501. CD24_Rv	GGCCAACCCAGAGTTGGAA
OL502.CXCR4_Fw	GATCAGCATCGACTCCTTCA
OL503.CXCR4_Rv	GGCTCCAAGGAAAGCATAGA
OL526.hSOX2-Saj_Fw	GGG AAA TGG GAG GGG TGC AAA AGA GG
OL527.hSOX2-Saj_Rv	TTG CGT GAG TGT GGA TGG GAT TGG TG
OL555.Vimentin-qPCR_Fw	CACCCTGCAGTCATTCAGACA
OL556.Vimentin-qPCR_Rv	GATTCCACTTTCCGTTCAAGGT
OL562.hROR2_qPCR_Fw	GGCAGAACCCATCCTCGTG
OL563.hROR2_qPCR_Rv	CGACTGCGAATCCAGGACC
OL584.hLgr4_qPCR_Fw	CAGTACCCAGTGAAGCCATTC
OL585.hLgr4_qPCR_Rv	TGTTGTCATCCAGCCACAGA
OL597.hABCA2_qPCR_Fw	AGATGGACAAGATGATCGAG
OL598.hABCA2_qPCR_Rv	GCTTGTACTTCAGGATGAGG
OL599.hABCB1_qPCR_Fw	GAGGAAGACATGACCAGGTA
OL600.hABCB1_qPCR_Rv	CTGTCGCATTATAGCATGAA
OL601.hABCC1_qPCR_Fw	ACCCTAATCCCTGCCCAGAG
OL602.hABCC1_qPCR_Rv	CGCATTCCTTCTTCCAGTTC
OL603.hABCG2_qPCR_Fw	GGTGGAGGCAAATCTTCGTTATTAGA
OL604.hABCG2_qPCR_Rv	GAGTGCCCATCACAACATCATCTT

2.2.4 Solving hybridomas by 5' RACE protocol: In collaboration with Dr Marco Della Peruta and Dr Satyen Gohil

The overall protocol for hybridoma solving by 5'RACE is summarised in **Fig. 2. 1.** 5'RACE PCR Strategy**.**

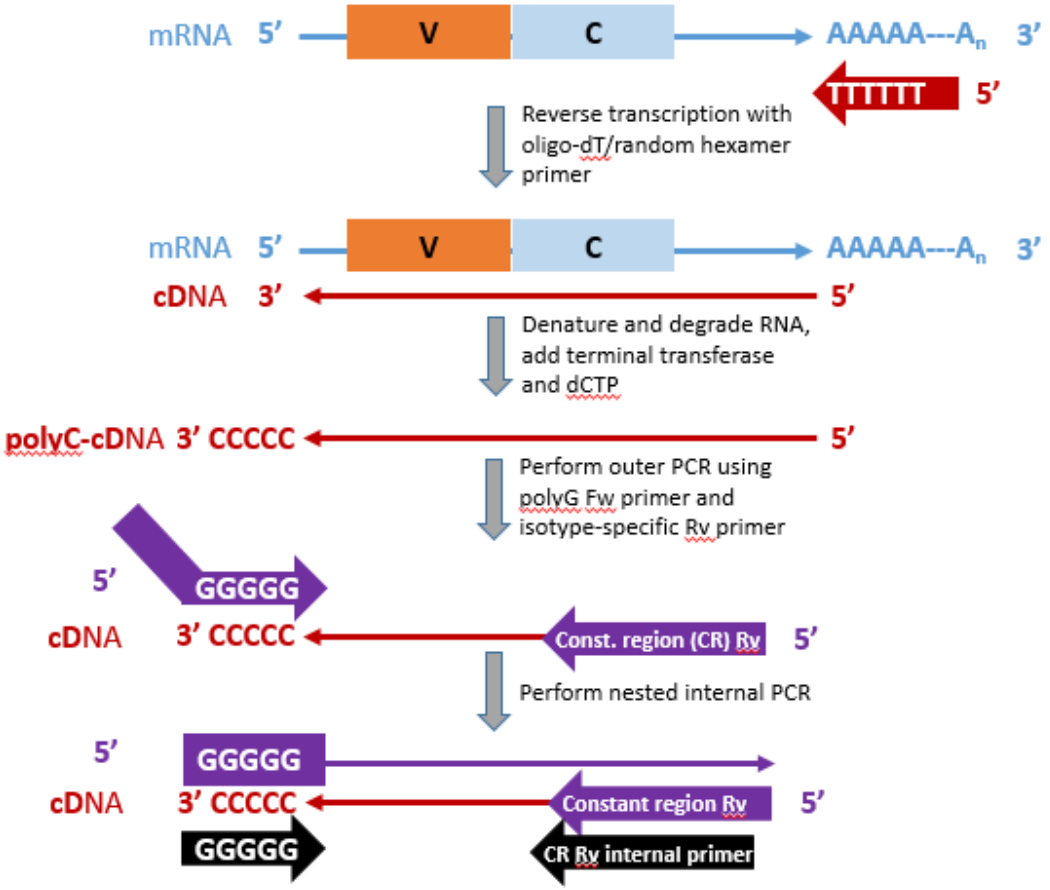

Fig. 2. 1. 5'RACE PCR Strategy

2.2.4.1 3'-polyC tailing

Following cDNA preparation, 3' polyC tailing of cDNA was performed by incubation of cDNA with terminal transferase and dCTPs, as follows: 10ul of cDNA was incubated at 95°C for 1min then immediately chilled on ice. 6uL of nuclease-free water, 2ul terminal transferase buffer, 1ul dCTPs (10mM) and 1ul terminal transferase were added and the mixture was incubated at 37°C

for 30mins, followed by 75°C for 30mins. Following this the poly-C tailed cDNA was concentrated using Microcon columns 100K NMWL (Millipore, Sigma) according to kit instructions.

2.2.4.2 Nested PCR for identification of heavy and light chain sequences

Outer PCR was performed separately for heavy and light chain using appropriate primers. 50ul master mix was made including 47ul Platinum PCR SuperMix high fidelity kit (Invitrogen) (which includes Taq polymerase for amplification, selected to facilitate subsequent TOPO-TA cloning), 1ul polyC-cDNA, 1ul forward primer, 1ul reverse primer. This was run on the thermocycler under the following conditions: 1) 94°C 2mins; 2)94°C for 30s; 3) 56°C for 30s; 4) 68°C for 30s; 5) Repeat step from 2, 25 cycles; 6) 68°C for 10mins. The PCR products were subsequently cleaned up using Qiagen QIAquick kit as per manufacturer's instructions, and used as template for subsequent inner PCRs.

Following outer PCR inner, 'nested' PCRs were performed separately for heavy and light chain. Of note, identical PCR conditions to the outer PCR were used for amplification.

Following amplification, the PCR products were run on 1% TBE gel. The resultant smear from 300-800bp for each chain were cut out and extracted using Qiagen QIAquick extraction kits, according to manufacturer's instructions. Subsequently these bands were subcloned into TOPO-TA vector.

2.2.4.3 Analysis of sequence data using the IMGT online database

To ensure that all sequences were at the correct 5' to 3' orientation of DNA sequence, the polyG sequence was used as reference. Sequence data was inputted into IMGT V-quest server, which is able to identify heavy and light chain sequences based on homology with germline sequences, and in addition will determine if sequences are in-frame.

2.2.5 Generation of chimeric antibodies: rat V_H and V_L in human IgG1, kappa constant regions

Following identification of productive heavy and light chain sequences these were cloned as full length heavy and light chains into SFG vector, by splicing by overlap extension PCR (**Fig. 2. 2**).

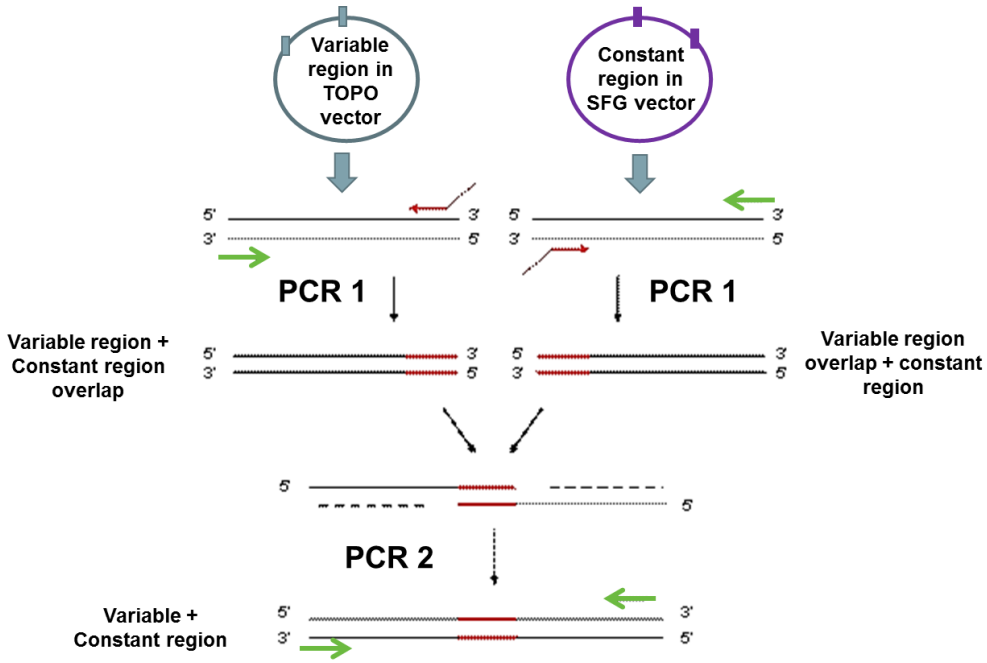

Fig. 2. 2. Generation of chimeric antibodies.

2.3 Protein work

2.3.1 Protein purification by FPLC (AKTA system) and dialysis

All purification runs were performed using an AKTA chromatography system (GE Healthcare). Importantly, before running the sample, filtered 20% ethanol was run through all lines of the AKTA system (PumpWashExplorer function). Then the machine was primed by running Binding buffer, pH 7 (68ml Buffer A [200mM $NaH_2PO_4.2H_2O$] + 32ml Buffer B [200mM Na_2HPO_4]) through lines A2 and A11. Elution buffer, pH 2-4 (0.1M Citric acid) was run through line B1. The 1ml-Protein A column (GE Healthcare) was later placed in the V3 position and

Binding buffer was also run at 1ml/min flowrate for 5-10min. After this set-up, line A2 was placed in our sample (concentrated supe+Binding buffer at a 1:1 ratio) and the appropriate “Protein A” programme run.

After a few steps of optimisation, the Protein A programme was modified by including a further wash right before the elution step, which was also extended, resulting in the new and final programme: “Protein A Long”.

To neutralise the pH of the fractions eluted in 0.1M citric acid, ~300ul of Tris-HCl buffer (pH 9) were distributed in all fractions tubes prior elution. Tris-HCl buffer volume was calculated by prior pH testing using pH paper strips. This was done everytime new buffers were prepared. Relevant fractions were then collected, pooled together and dialysed in PBS (Sigma-Aldrich®) at 4°C using Slide-A-LyzerTM 10k MWCO dialysis cassettes (Thermo ScientificTM, Life Technologies).

For AF488 conjugation, clone SA1 was dialysed in Borate buffer with EDTA (25mM Borate, 25mM NaCl, 1mM EDTA) at pH 8.

2.3.2 Quantification by Bicinchoninic acid (BCA) Assay

In order to quantify the dialysed protein, the PierceTM BCA Protein Assay kit (Thermo ScientificTM, Life Technologies) was used according to the manufacturer’s instructions. Briefly, diluted Bovine Serum Albumin (BSA) standards were prepared according to the Enhanced Protocol (5-250µg/ml) and for the microplate format. A volume of 25µl of either the standard or sample was pipetted into a 96-well plate, 200µl of the Working Reagent was then added, the plate mixed and incubated at 60°C for approx. 1h. The plate was later cooled down to RT and the absorbance was measured at 562nm on a plate-reader.

For analysis, the four-parameter (quadratic) curve was used for the standard curve as suggested on the kit's protocol.

2.3.3 Sample preparation for SDS-PAGE

Samples were prepared as follows: 5ul of sample, 2ul of 10x reducing buffer, 5ul of 4x loading dye and nuclease-free water made up to 20ul final volume with sample. The sample was then taken to 95°C for 5 minutes. Samples that were run under non-reducing conditions, were not exposed to reducing buffer or high temperatures.

Prepared sample were then loaded onto a premade 4-12% SDS-PAGE gel (LifeTechnologies-NuPage) at 200V, 500mA for 45 minutes on constant voltage mode. 10ul of protein ladder (Novex) was run as a size marker. Following run, gels were either used for Coomassie staining or Western blotting.

2.3.4 Coomassie staining

Post-separation, the gel was transferred to a staining tray, covered with 0.25% Coomassie R-250 stain solution and stained o/n assisted with gentle agitation supplied by a rotating plate shaker. Staining solution was decanted and the gel was destained with a Coomassie destaining solution (40% methanol and 10% glacial acetic acid in distilled water), again with gentle agitation. Further destaining solution was added as required until the protein bands became clearly visible. Finally, gels were documented using the G:BOX EF Imaging System (Syngene).

2.3.5 Western Blotting

Post separation, proteins were transferred to a Hybond nitrocellulose membrane (Amersham, GE Healthcare) using 200ml of Transfer buffer (10ml of 20x Transfer buffer [81.6g of Bicine, 104.6g of BisTris and 6g of EDTA in 1L

of distilled water], 40ml of methanol, 150ml of distilled water and 200ul of antioxidant). The program used was 25v, 125mA (constant) for 1h30min.

The membrane was then stained with Red Ponceau (Sigma-Aldrich) for 30s, which was then replaced with Wash buffer (1x TBS-Tween) and kept in rotation for 30-45min, changing the buffer every 10min. The membrane was then blocked with 10ml Veto solution (5% polyvinyl pyrolidine [PVP] in 1x TBS-Tween) + 0.5ml of HI-FBS in rotation. After 1h, the primary antibody incubation was performed by transferring the membrane to a 50ml falcon tube containing: 10ml Veto, 0.5ml HI-FBS, 100ul 10% azide and 5ul goat anti-human ROR1 antibody (R&D Systems™). The incubation was done overnight at RT in rotation. Of note, when Veto was not used, 5% milk in PBS-T was used as blocking buffer and for antibody staining.

On day 2, the membrane was washed for 30-45min, changing the buffer every 10min. After this, the membrane was transferred to a 50ml falcon tube containing 10ml veto, 0.5ml HI-FBS and 1ul of rabbit anti-goat IgG-HRP conjugated antibody (BioRad). For those membranes where the mIgG2a tag of our protein was assessed, 1ul of goat anti-mouse IgG-HRP conjugated antibody (Dako) was used directly. After 3h incubation in rotation, membranes were washed and treated with Pierce™ ECL Western Blotting Substrate kit (Thermo Scientific, Life Technologies) following manufacturer's guidelines. Films were developed using the SRX 101A Film Processor (Konica Minolta).

2.3.6 Evaluation of binding kinetics by surface plasmon resonance: Biacore system

Surface plasmon resonance evaluation was undertaken using a Biacore X100 instrument at the UCL Institute of Structural & Molecular Biology. ROR1 chimeric antibodies were immobilised using an anti-human IgG1 antibody capture kit and a CM5 sensor chip (GE Healthcare). All binding assays used 1x HBS-EP+ running buffer (GE Healthcare) and seven different

concentrations (100, 50, 25, 12.5, 6.25, 3.13 and 1.56nM) of the extracellular portion of ROR1 bearing a Histidine tag (and dialysed using the same buffer) were then injected. These concentrations were run at a random order, including the negative control (0nM). Data analysis was performed using Biacore X100 Evaluation Software, version 2.0 (GE Healthcare). The sensor chips were regenerated with glycine-HCl (pH 2.0) without any loss of binding capacity. Calculation of association (k_{on}) and dissociation (k_{off}) rate constants was based on a 1:1 Langmuir binding model. The equilibrium dissociation constant (K_D) was calculated from k_{off}/k_{on}.

2.4 *In vitro* work

2.4.1 Peptide-library ELISA

Mimotope's ROR1 peptide library contained more than ninety overlapping peptides. Each peptide was composed of biotin (at the N-terminal), followed by a linker that connected it to a sequence of 11 amino acids of eROR1, followed by an amide group (NH_2) at the C-terminal. Of note, each 11-amino acid peptide had 8 amino acids that overlapped the previous peptide whilst introducing 3 new amino acid to its sequence.

Lyophilised eROR1 peptides were solubilised in 50% Acetonitrile using a water bath sonicator. Peptides were then diluted in 0.1% Azide in PBS-Tween 20 (PBS-T). Control peptides (Mimotopes) were treated and processed in the same way. Control antibodies, also provided by Mimotopes were dissolved in purified water as per manufacturer's instructions. Briefly, 96-well plates were coated with NeutrAvidin, blocked with 1% sodium caseinate and washed thoroughly before incubation with the solubilised peptides. After 1h incubation, plates were washed again and incubated o/n with clones SA1 and F. On the next day, plates were washed and incubated for 1h with an anti-human IgG antibody conjugated to horseradish peroxidase (HRP). Plates were washed, and antibody signal detected with Tetramethylbenzidine (TMB); the reaction

was later stopped with H_2SO_4. Samples were then analysed at 450nm wavelength using a plate-reader.

2.4.2 Internalisation assays

ROR1$^+$ cell lines and/or primary cells from CLL patients were stained with relevant ROR1 MAbs on ice for 1h. After washing three times with ice-cold PBS to remove unbound antibody, the total number of cells was subdivided in different tubes, one per time point and two tubes for the 2h time point in order to include the endocytosis inhibitor control (phenylarsine oxide). Samples were either left on ice or incubated at 37°C for 15min, 30min, 1h, or 2h to facilitate internalization.

For the 2h time point, duplicate samples were incubated in the absence or presence of 10mM phenylarsine oxide (Sigma-Aldrich). Subsequently, the cells were washed once with ice-cold PBS buffer and incubated with an anti-human Fc secondary antibody on ice for 30 min. After three final washes with ice-cold PBS, the MFI of the cells was measured using a BD LSR Fortessa (5 laser) instrument and FlowJo analytical software. The percentage of MFI reduction was calculated for each mAb relative to the secondary antibody control (MFI background) and MAb maintained on ice (MFI max) by using the following formula, as per Yang et al., 2011:

[(MFI max-MFI background)-(MFI experimental-MFI background)] ***/***
(MFI max-MFI background)x100.

Samples used in internalisation assays with trypan blue were prepared as mentioned above, except that no double staining was performed since antibodies were conjugated to AlexaFluor488. Binding MFI was measured before and after addition of 500ul/sample of 0.4% Trypan blue (Gibco, Life Technologies).

Internalisation assays using pH-Amine reactive dye (Promega) were performed as per manufacturer's instructions and Nath et al., 2017. Briefly, purified antibodies at >2mg/ml were buffer exchanged from PBS to amine conjugation buffer (10mM sodium bicarbonate buffer, pH 8.5) using Zeba™ desalting columns (Pierce). In parallel, the pHAb amine reactive dye was dissolved at 10mg/ml in 25ul of 1:1 DMSO-water mix and vortexed for ~3min. A volume of 1.2ul of the freshly dissolved dye was added for 100ug of antibody, and incubated for 60min using an end-over-end mixer. Unreacted dye was removed by using desalting columns. Antibody concentration and fold increase in fluorescence response was calculated using the following equations:

$$\text{Antibody Concentration (mg/ml)} = \frac{A_{280} - (A_{532} \times 0.256)}{1.4}$$

$$\text{Fold increase} = \frac{\text{Fluorescence of antibody-pHAb (pH 4)} - \text{Fluorescence of blank wells (pH 4)}}{\text{Fluorescence of antibody-pHAb (pH 8)} - \text{Fluorescence of blank wells (pH 8)}}$$

Sample preparation was performed as mentioned above. In short, cells were incubated with pH-Amine labelled antibodies for 30min at 4°C. After this, cells were washed with ice-cold PBS and immediately after, fluorescence was read at Ex/Em: 532nm/562nm ("0h" time point) using a plate-reader. Cells were then incubated at 37°C and 5%CO_2 for 15min, 2, 5, 21 and 24h. After each time point, fluorescence was evaluated. Citrate buffer, pH 4 was used as positive control for fluorescence signal.

2.4.3 Complement-dependent cytotoxicity (CDC) assay

This assay was based on Yang et al., 2011 and the kind guidance provided by Dr Jenny Yeung (Prof Kerry Chester's research group, UCL Cancer Institute); and was carried out as follows: SKW 6.4 GFP, Jeko-1 cells, and primary cells from both CLL patients and healthy donors (target cells) were harvested, washed, counted and resuspended in R10 media. Cells were plated in 96-well

V-bottom plates (Corning) at a density of $4x10^4$ cells/well (100ul/well). Target cells were incubated for 10min at RT with 100ul of ROR1 MAbs, negative control (hIgG1, k isotype) and anti-CD20 antibodies: Rituximab (chimeric antibody) and GA-101 (Obinutuzumab – humanised antibody). Importantly, ROR1 MAbs contained in culture supernatants or FPLC-purified antibodies at a final concentration of 10ug/ml were used, depending on the nature of the experiment. In parallel, GA-101 was used at 0.5ug/ml whilst Rituximab was used at both 0.5 and 10ug/ml.

Immediately after, 20ul of ice-cold baby rabbit complement (BioRad) was added (10% complement, final concentration). Samples were incubated for 2h at 37°C in 5% CO_2. After this, cells were centrifuged at 500g for 5min and supernatant discarded. Samples were then washed using AnnexinV buffer (150ul/well) and centrifuged again. Cells were then co-stained with 1ul of AnnexinV-APC, 0.5ul of aCD5-APC Cy7 and 0.5ul of aCD19-FITC in 75ul of AnnexinV buffer. After 15min incubation in the dark, 2ul of PI in 75ul of AnnexinV buffer was added and incubated for approximately 10min.

Samples were then transferred to 2ml 96-well plates containing 150ul of washed counting beads in PBS (as per **section 2.1.3.2**). Live cells were detected by AnnexinV/PI exclusion using a BD LSR Fortessa instrument (Becton Dickinson) and FlowJo analytical software. Briefly, the Y586/15 and R670/30 filters were used in order to detect PI and AnnexinV-APC staining, respectively; and dot plots showing both channels were set up (**Fig. 2. 3**). Also, two gates were drawn. One corresponding to the counting beads (P1); which was used in order to acquire the same number of events/sample. The other gate included all events (P2), except for the beads. It was on P2 that the PI and APC fluorescence signals were applied.

Cells that showed APC staining in the plasma membrane were positive for Annexin V-APC and were considered as apoptotic cells. Target cells that lost membrane integrity showed PI positivity as the dye got inside the cells; therefore, cells that were double positive for PI and AnnexinV were considered necrotic cells. In contrast, double-negative cells were considered as live, healthy cells. Live cell counts were normalised to the number of beads per sample. These values were then normalised to the isotype control and expressed as % of live cells. Bar graphs and statistics were calculated in GraphPad Prism 7 as per **section 2.5**.

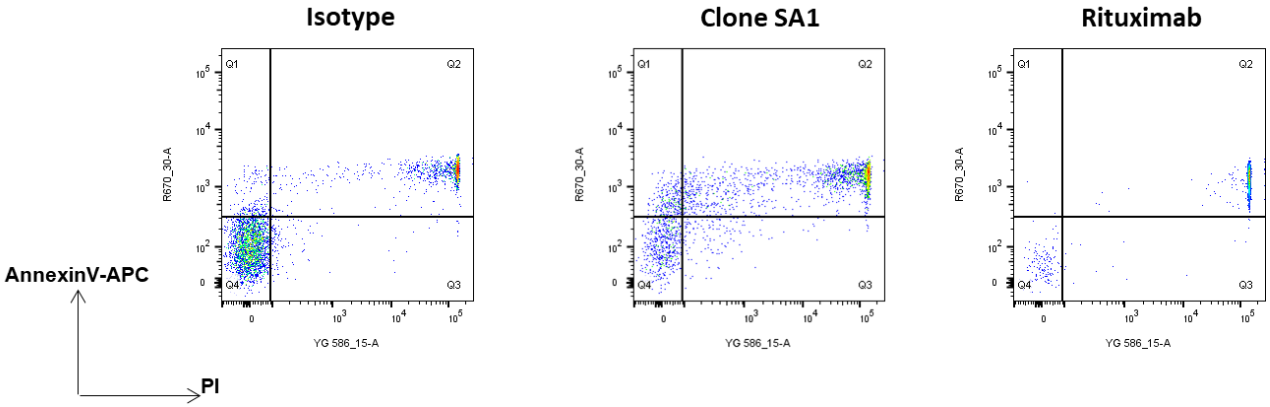

Fig. 2. 3. Representative AnnexinV/PI staining analyses by flow cytometry, following CDC assays on CLL cells.

2.4.4 Evaluation of cytokine release by ELISA

This was performed using a Biolegend IFNγ or IL-2 kits according to the manufacturer's instructions. Briefly, a 96-well strip plate was incubated with protein capture antibody overnight at 4°C. The plate was washed thoroughly 3x, blocked for 1h at room temperature with shaking and washed again 3x.

Samples for assay were added (at appropriate dilutions) and incubated for 2 hours at room temperature with shaking. The plate was washed 3x and IFNγ- or IL-2-detection antibodies (biotinylated) were added for a further 1 hour. The plate was washed 3x and avidin-horseradish peroxidase (HRP) was added.

After 30mins and following a further wash, detection substrate was added and after a further 15 minutes hydrogen peroxide stop solution was added.

Colorimetric changes corresponding to IFNγ or IL-2 were detected using a plate-reader measuring absorption at 450nm. Concentration of cytokines was determined according to a standard curve produced by simultaneously assaying serial dilutions of an IFNγ or IL-2 solution of known concentration.

2.4.5 WST1 Cell viability assay using tumourspheres

PANC-1 parental cells or CSCs ($5x10^3$ cells/well) were plated in 96-well TC-treated or suspension plates, respectively (100ul/well). The day after, cells were incubated with purified ROR1 BiTE (1ug/ml) or relevant controls for 10min at RT (50ul/well). Cells were then co-cultured with PBMCs from healthy donors (effectors) using a 1:1 E:T ratio (50ul/well) and incubated at 37°C with 5% CO_2, as per *in vitro* studies reported by Gohil et al., 2017.

After 72h, cell viability was measured by Cell Proliferation Reagent WST-1 (Roche Diagnostics) as per manufacturer's instructions. In short, 20ul/well of WST-1 reagent was added to all samples (1/10 final dilution), plates were incubated at 37°C with 5% CO_2 and were read after 1, 2 and 4h using a plate-reader at 440nm. Culture media was used as blank.

2.4.6 Migration assay using tumourspheres

Migration assays using a transwell system kit (96-well, 8um - PromoKine) were performed as manufacturer's instructions. Briefly, 150ul of either serum-free RPMI, serum-supplemented RPMI or conditional media (culture media of adherent PANC-1 cells taken at 48h post splitting) were added to the bottom chamber. Single-cell suspensions (10^4cells/well) resuspended in 50ul of non-supplemented CSC-media (tumourspheres) or serum-free RPMI (adherent

PANC-1) were added to the top chamber of the transwell system. Plates were incubated at 37°C and 5% CO_2 for 72h.

After incubation, the top chamber was removed, and the plate was taken to the microscope. Cells present in the bottom chamber only were photographed and documented using a microscope 4x objective.

2.4.7 Immunocytochemistry and confocal microscopy

The immunostaining protocol carried out in this study was based on (Goh et al., 2013) and on the kind guidance provided by Dr Sajjida Jaffer (ACN group – UCL Cancer Institute). Round coverslips (13mm) were ethanol-sterilised and dried under the hood overnight. The next day, they were placed in 24-well plates and coated with Matrigel resuspended in ice-cold DMEM (0.5ml/well). Plates were sealed with parafilm and left at 4°C overnight.

The following morning, untreated PANC-1 adherent cells and PANC-1 derived tumourspheres at a concentration of $3x10^4$c/well were seeded on Matrigel-coated coverslips and incubated at 37°C, 5% CO_2 for no less than 24h to ensure adherence.

The next day, media was removed, and cells were washed with PBS (0.5ml/well). Samples were then stained with a commercial ROR1 Ab (clone 2H6 - 1mg/ml) at a 1/200 dilution in Blocking solution (PBS + 0.1% BSA + 5% goat serum) for 1h. Cells were washed 3x with PBS and fixed with PFA 4% for 20min (0.5ml/well). Cells were washed again 3x with PBS (0.5ml) and permeabilised with ice-cold 100% methanol for 5 minutes prior to blocking (0.5ml/well).

Samples were blocked with Blocking solution for 30min at RT (0.5ml/well). Primary antibody 1/100 in blocking solution was added and cells were incubated o/n at 4˚C. For this study, Vimentin and ALDH1-A1 antibodies were

used as per Zhang et al., 2014. The following day, antibody staining solution was removed, and cells were washed 3x with PBS (0.5/well). Samples were then stained with appropriate secondary antibodies (Life Technologies) at a 1/400 dilution in Blocking solution for 1h at RT. This was followed by 3 washes with PBS (0.5ml/well) and DAPI staining (50ul/sample) for 5 min for nuclear stain. Cells were washed 3 times with PBS prior to slide mounting.

One drop of ProLong$^{(R)}$ Diamond (Thermo Fisher) was added onto the slide before putting the coverslip on top of the drop very carefully. Slides were then taken to 4°C for 1h, after which they were sealed using clear nail polish. Confocal images were obtained using a laser-scanning Zeiss LSM880 confocal microscope.

With regards to treated PANC-1 parental cells and CSCs, cells were co-cultured with ROR1 BiTE (1ug/ml) or relevant controls as per WST-1 cell viability assays described above (**section 2.4.5**), except that instead of $5x10^3$c/well, a concentration of 10^4c/well were seeded in appropriate 96-well plates. After 72h of incubation, cells were harvested and cells from replicate wells were pulled together in order to seed them in 13mm coverslips (previously coated with matrigel and placed in 24-well plates). Immunostaining was then carried out as described above. For quantification purposes, more than 500 cells per treatment and biomarker staining were counted. Cells were classified according to their single or double biomarker expression and conveyed as % of the total cell count.

2.5 Statistical analyses

Statistical analyses including t-tests and two-way ANOVA calculations were performed using GraphPad Prism 7 for Windows (Graph-Pad Software, USA). Differences were considered statistically significant when *p* values were <0.05. Significance was represented by $p<0.05$ (*), $p<0.01$ (**), $p<0.001$ (***), $p<0.0001$ (****).

Chapter 3 Generation of ROR1 antibodies

3.1 Introduction

Receptor tyrosine kinase-like orphan receptor 1 (ROR1) along with ROR2 represent one of 20 families of receptor tyrosine kinases (RTKs) (Daneshmanesh et al., 2012, Green et al., 2008). In the past few decades, a growing amount of data has shown that RTKs are typically involved in cell-cell interactions, differentiation, survival, proliferation, cell metabolism, migration and signalling (Zhang and Zhang, 2016). Hence, mutations or overexpression of RTKs have been described in many cancer types and are already being explored as potential targets for cancer therapy. Remarkably, ROR1 is selectively overexpressed in various haematological and solid malignancies but not in most normal adult tissue (Shabani et al., 2015).

Similar to other oncogenic RTKs, ROR1 overexpression may be targeted in cancer. According to (Zhang, 2012), there are two main strategies to do this: i) targeting the intracellular domain by tyrosine kinase inhibitors or ii) targeting the extracellular portion of the receptor by monoclonal antibodies (MAbs) and/or their derivatives. In this study, the latter approach will be explored; thus, a brief introduction on antibody generation is provided below.

3.1.1 Monoclonal antibody generation

As discussed in the Introduction section (**Chapter 1**), monoclonal antibodies are molecules of a single antigen specificity (i.e. bind to the same epitope) and are produced from a single B-lymphocyte clone (Liu, 2014). In general, there are two methods for generating monoclonal antibodies: i) phage display library and ii) hybridoma technology. The latter will be discussed in the next paragraphs.

3.1.1.1 Hybridoma technology

Hybridomas are generated by the fusion of B lymphocytes –derived from an immunised animal– with immortal myeloma cells that do not secrete any sort

of antibody themselves and that lack the hypoxanthine-guanine-phosphoribosyltransferase (HGPRT) gene. The latter will make the hybridoma sensitive to (hypoxanthine-aminopterin-thymidine) HAT medium, which will be used for positive selection of successful hybridomas (Zhang, 2012). As explained by (Little et al., 2000), cell fusions are grown in HAT medium in order to discriminate successful fusions from unfused cells: i) HPGRT-negative myeloma cells that have not acquired the natural resistance from the primary B-cells and ii) B-cells alone that would eventually die off as they would not have inherited immortality from myeloma cells.

Early cultures of fused cells contain a mixture of antibodies produced by a very diverse population of B-cells; these cultures are hence still polyclonal. At this stage, hybridomas can be screened against the target of interest by flow cytometry or ELISA. Once positive cultures are identified, single-cell cloning can be performed, and screening is again carried out. Positive hybridomas are then recloned and retested for activity (Liu, 2014, Li et al., 2010). See **Fig. 3. 1**.

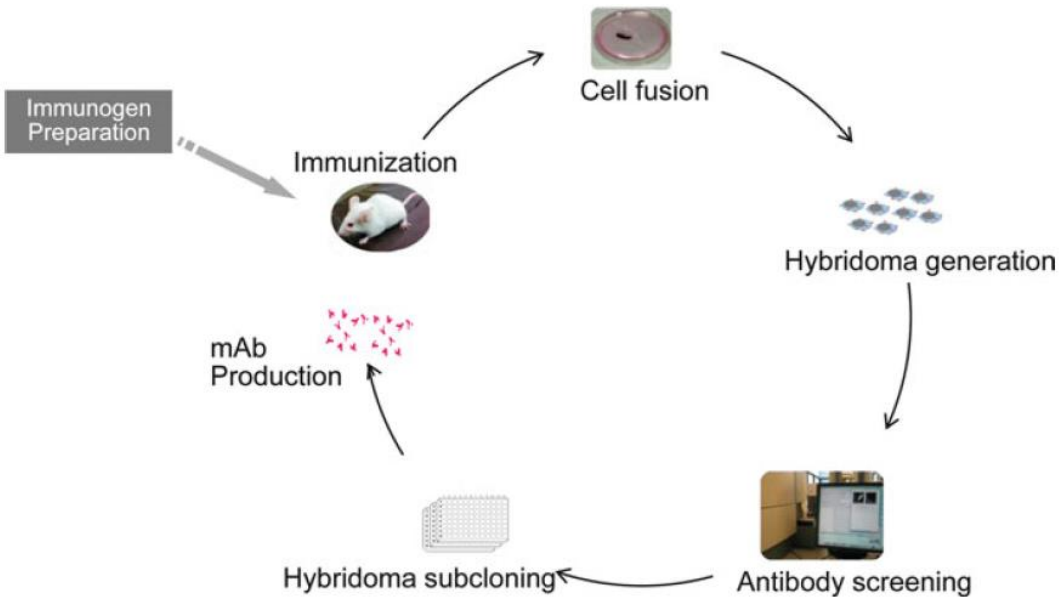

Fig. 3. 1. Hybridoma technology approach for the generation of monoclonal antibodies. Reproduced from Zhang, 2012

It is noteworthy that an advantage of hybridoma technology over phage display libraries is that the produced antibodies retain their native structure, including the Fab and Fc portions. It has been previously shown that the latter is pivotal in terms of cytotoxic function, as it mediates complement-dependent (CDC) and antibody-dependent cellular cytotoxicity (ADCC) (Kubota et al., 2009, Natsume et al., 2009). Alternatively, to increase cytotoxic potency, it has become common practice to isolate the variable regions from monoclonal antibodies (commonly as scFv) and link these molecules to a variety of toxic partners. Some of the most common derivatives are: radioconjugates, antibody-drug conjugates, immunotoxins, chimeric antigen receptors (CARs), and bispecific antibodies in various formats (Mackall, 2014).

The use of monoclonal antibodies and their derivatives was explored as possible routes for ROR1 therapy. In the first instance, and to reduce unwanted immunogenicity, rat-derived monoclonal antibodies in human constant regions will be generated and investigated; antibody molecules in this format are also known as chimeric antibodies.

3.1.2 Chimeric antibodies

Since the first monoclonal antibodies used in the clinic were mouse-derived, it was the first time that side effects caused by their murine origin were observed; these adverse effects are known as “human anti-murine antibody” (HAMA) response (Schroff et al., 1985). Repetitive dosing with murine monoclonal antibodies were therefore not advisable.

To overcome this issue, recombinant DNA approaches have been developed so that the binding portion of a monoclonal antibody could be merged with human constant regions. Constructs encoding for this chimeric DNA resulted in the expression of monoclonal antibodies that were partially murine and partially human.

In the context of therapeutic antibodies, the ability to elicit a cytotoxic immune response that does not stem from their organism of origin is desirable. MAbs efficacy relies on: i) their specificity, ii) bivalent binding to their target (for blockade/neutralisation of target and apoptosis induction) and iii) effector functions prompted by their Fc regions (CDC and ADCC). Therefore, the right Fc region (isotype) needs to be carefully chosen according to the therapeutic purpose of the antibody (Natsume et al., 2009).

3.1.2.1 Human IgG and therapeutic antibodies

Despite the fact that all four IgGs share more than 90% amino acid identity, each subclass possess a distinct profile in terms of antigen binding, immune complex formation, complement activation, triggering of effector cells, half-life and placental transport (Vidarsson et al., 2014). Consistent with this, it has been reported that human IgG1 and IgG3 are potent triggers of effector mechanisms, whilst IgG2 and IgG4 prompt more subtle responses (Bindon et al., 1988, Tao et al., 1993). Moreover, IgG1 has been the main isotype of choice in the clinic due to its half-life (approximately 21 days) and superior effector functions (Clark, 1997, Natsume et al., 2009).

To conclude, one of the best examples of a chimeric antibody used in clinic is Rituximab (Rtx), the anti-CD20 antibody that revolutionised the treatment of B-cell malignancies (Keating et al., 2005, Rai and Jain, 2015). As commented in previous sections, Rtx is a murine antibody in human IgG1, kappa constant regions. Below in **Table 3. 1**, selected next generation anti-CD20 antibodies that have IgG1 (engineered or not) as their isotype are presented.

Table 3. 1. Effector functions of selected anti-CD20 MAbs. Based on (Natsume A. et al., 2009)

MAb	Developer	Isotype	Effector functions compared to Rituximab (Rtx)
Ofatumumab	GSK/Genmab	IgG1	Potent CDC
Ocrelizumab	Genentech	IgG1	Potent ADCC and decreased CDC
Veltuzumab	Immunomedics	IgG1	Comparable to Rtx
AME-133	AME	Mutated IgG1	Potent ADCC
Obinutuzumab (GA101)	Roche/GlycArt	Glycoengineered IgG1	Potent ADCC/direct apoptosis, no CDC

In this chapter, data showing the generation of anti-ROR1 rat chimeric antibodies in human IgG1, kappa constants will be presented and discussed.

3.2 Aims

1. To produce ROR1 hybridomas, in collaboration with Aldevron, and evaluate their specificity by flow cytometry.
2. To generate single-cell clone hybridomas of ROR1 and extract their variable heavy (V_H) and variable light (V_L) regions, in collaboration with Dr Marco Della Peruta and Dr Satyen Gohil.
3. To produce chimeric rat-human antibodies by cloning the rat V_H and V_L sequences to human IgG1, kappa constant regions.
4. To assess binding of the new ROR1 chimeric antibodies on ROR1$^+$ and ROR1$^-$ cell lines.

3.3 Results

3.3.1 Aim 1: Production and evaluation of ROR1 hybridomas

3.3.1.1 Rat immunisation against the extracellular portion of ROR1: In collaboration with Aldevron

To successfully produce ROR1 hybridomas, our group set up a collaboration with Aldevron, a specialised company on generation of novel antibodies. Aldevron used a DNA-based protocol in order to immunise three Wistar rats with the extracellular portion of ROR1, as described in the Materials & Methods section (See **Chapter 2**).

After eight rounds of immunisation, our collaborators detected ROR1 antibodies in the rats' sera by flow cytometry analysis. These samples were then delivered to us for further confirmation. We first wanted to identify what dilution worked better for flow cytometry detection. As a result, rats' sera was tested by flow cytometry using different dilutions: neat, 1/10, 1/100, 1/1 000 and 1/10 000 on $ROR1^{+}$ cells (data not shown). It was identified that a 1/1 000 dilution of rat serum in PBS was the most informative in order to test for ROR1 binding.

Rat serum at the appropriate dilution was next incubated with MEC-1 GFP ($ROR1^{-}$), MEC-1 ROR1 ($ROR1^{high}$) and SKW GFP ($ROR1^{low}$) cell lines. Primary cells from Chronic Lymphocytic Leukaemia (CLL) patients, expressing different levels of ROR1, were also tested. An anti-rat IgG antibody conjugated to DyLight647 fluorophore was used as negative control (**Fig. 3. 2**).

In **Fig. 3. 2**, specific binding of "Rat 1" serum on $ROR1^{+}$ and $ROR1^{-}$ cells are shown. Presence of ROR1 antibodies was evidenced by positive binding to all $ROR1^{+}$ cells but not MEC-1 GFP cells ($ROR1^{-}$). Of note, the intensity of binding signal was proportional to level of ROR1 expression on the surface. Confirmation of ROR1 specific binding prompted the continuation of the

hybridoma protocol, whereby lymph nodes of all three immunised rats were removed and pooled together in order to fuse them with rat myeloma cells and generate rat hybridoma cell lines.

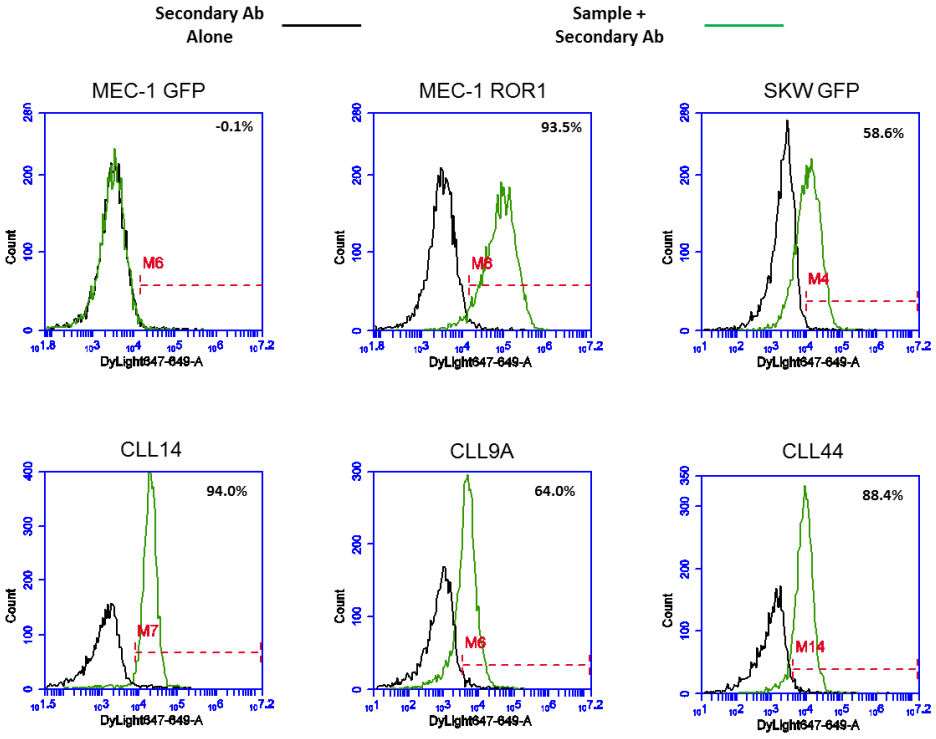

Fig. 3. 2. Flow cytometry evaluation of rat immunisation against ROR1. A 1/1000 dilution of rat serum (Rat 1) in PBS was tested on ROR1$^-$ and ROR1$^+$ cell lines as well as CLL primary cells. An anti-rat IgG-DyLight647 secondary antibody was used as negative control on each cell type. Percentage of frequency is shown in the top right corner of histograms. CLL=Chronic Lymphocytic Leukaemia.

3.3.1.2 Evaluation of ROR1 polyclonal hybridomas by flow cytometry

Aldevron reported successful generation of 38 hybridomas positive for ROR1 binding. In the first instance, supernatants from these cells were sent to us for further evaluation.

Hybridoma supernatant from all 38 samples were tested by flow cytometry on ROR1$^-$ (MEC-1 GFP) and ROR1$^+$ cell lines (MEC-1 GFP ROR1 and SKW GFP). In **Table 3. 2**, binding levels expressed as % of frequency and Median Fluorescence Intensity (MFI) of all 38 oligoclonal hybridomas on MEC-1 GFP and ROR1 are shown. With regards to primary cells from CLL patients, CLL

cells expressing different levels of ROR1 (CLL14, CLL9A and CLL44) were also included in these analyses.

Table 3. 2. ROR1 Binding of polyclonal hybridomas on MEC-1 GFP (ROR1$^-$) and MEC-1 ROR1 (ROR1$^+$) cell lines. Summary table showing the % of frequency and median fluorescence intensity (MFI). Overlay column represents the % of frequency when MEC-1 GFP and MEC-1 ROR1 are overlaid. Colours designate binding strength: >85% (bright green), 80-84.9% (light green), 50-79.9% (yellow), 10-49.9% (pink), <9.9% (red).

N	SAMPLE	MEC1 GFP		MEC1 ROR1		Overlay, %
		%	MFI	%	MFI	
19	5D7	1.6	61,273.61	90.6	72,069.55	89.0
14	8C1	2.2	38,027.23	90.5	70,359.24	88.3
1	8C3	1.1	44,784.75	89.2	70,287.21	88.1
7	3A8	1.5	62,007.26	89.6	70,705.81	88.1
5	10C4	0.8	40,340.41	88.8	67,938.10	88.0
20	6H4	2.1	70,080.39	90.1	72,341.44	88.0
22	9H11	1.9	41,694.26	89.1	68,376.60	87.2
31	7E9	2.2	55,798.64	89.3	70,055.74	87.1
10	7A7	2.1	56,637.60	88.9	69,210.26	86.8
12	1C3	1.5	61,097.83	88.2	68,257.54	86.7
38	5B2	1.5	101,735.52	87.3	69,060.04	85.8
8	8E6	1	46,668.86	86.7	64,454.33	85.7
4	8H3	1.3	62,990.46	86.8	64,431.04	85.5
26	3E2	2.1	78,780.02	87.1	66,515.54	85.0
37	5F4	2.2	47,417.44	87	68,029.30	84.8
3	8E2	0.7	75,997.27	85.3	56,603.20	84.6
34	4B10	3.4	51,606.93	87.9	69,907.79	84.5
2	9F3	0.9	42,978.79	85.3	61,784.14	84.4
16	1A4	3.4	28,657.66	87.4	67,447.81	84.0
23	9B10	2.3	44,533.09	86.1	64,289.96	83.8
32	2H6	4.6	44,151.68	85.5	64,368.22	80.9
21	7G10	2.4	42,935.96	72.7	50,513.58	70.3
24	9A6	1.7	107,224.78	69.8	45,481.58	68.1
18	4E7	1.8	60,146.05	66.9	46,576.86	65.1
13	1F4	1.3	40,476.32	63.5	35,745.56	62.2
29	10H3	1.3	60,210.35	62.5	33,269.10	61.2
30	5C8	1.7	49,382.46	62.4	33,259.51	60.7
36	9E4	1.9	58,055.64	58.3	33,418.63	56.4
11	10F6	2	77,666.22	35.3	27,581.53	33.3
17	5H9	2.1	84,958.41	13.6	30,323.60	11.5
15	4F4	1.8	77,181.62	5.7	41,269.05	3.9
27	10D2	1.5	46,042.65	4.4	49,702.23	2.9
25	5H5	1.6	55,046.38	3.2	44,205.06	1.6
35	1E8	1.6	60,535.81	3.2	27,483.88	1.6
33	4F9	1.3	60,403.03	2	67,109.79	0.7
9	6A2	1.5	37,682.61	2.1	63,234.04	0.6
6	9B4	1.5	35,846.83	1.8	64,576.07	0.3
28	7B11	2.8	46,798.21	1.8	45,046.18	-1.0

In **Fig. 3. 3**, histograms corresponding to four representative hybridoma supernatants show the ROR1 binding detected on the cell lines and primary CLL cells mentioned above. Similar to previous observations, signal intensity was proportional to ROR1 expression of the different targets. This was particularly evidenced by the difference of binding between MEC-1 ROR1 (high) and SKW GFP (ROR1 low). In the same way, this was observed on CLL cells expressing different levels of ROR1.

Since ROR1 expression on SKW GFP cells is comparable to CLL cells, we present, as an additional example, data obtained when testing all these supernatants on SKW GFP cells (**Fig. 3. 4**). Together, these results confirmed that successful generation of ROR1 polyclonal hybridomas was achieved. Thus, in order to produce monoclonal antibodies, the next step was to single-cell clone them.

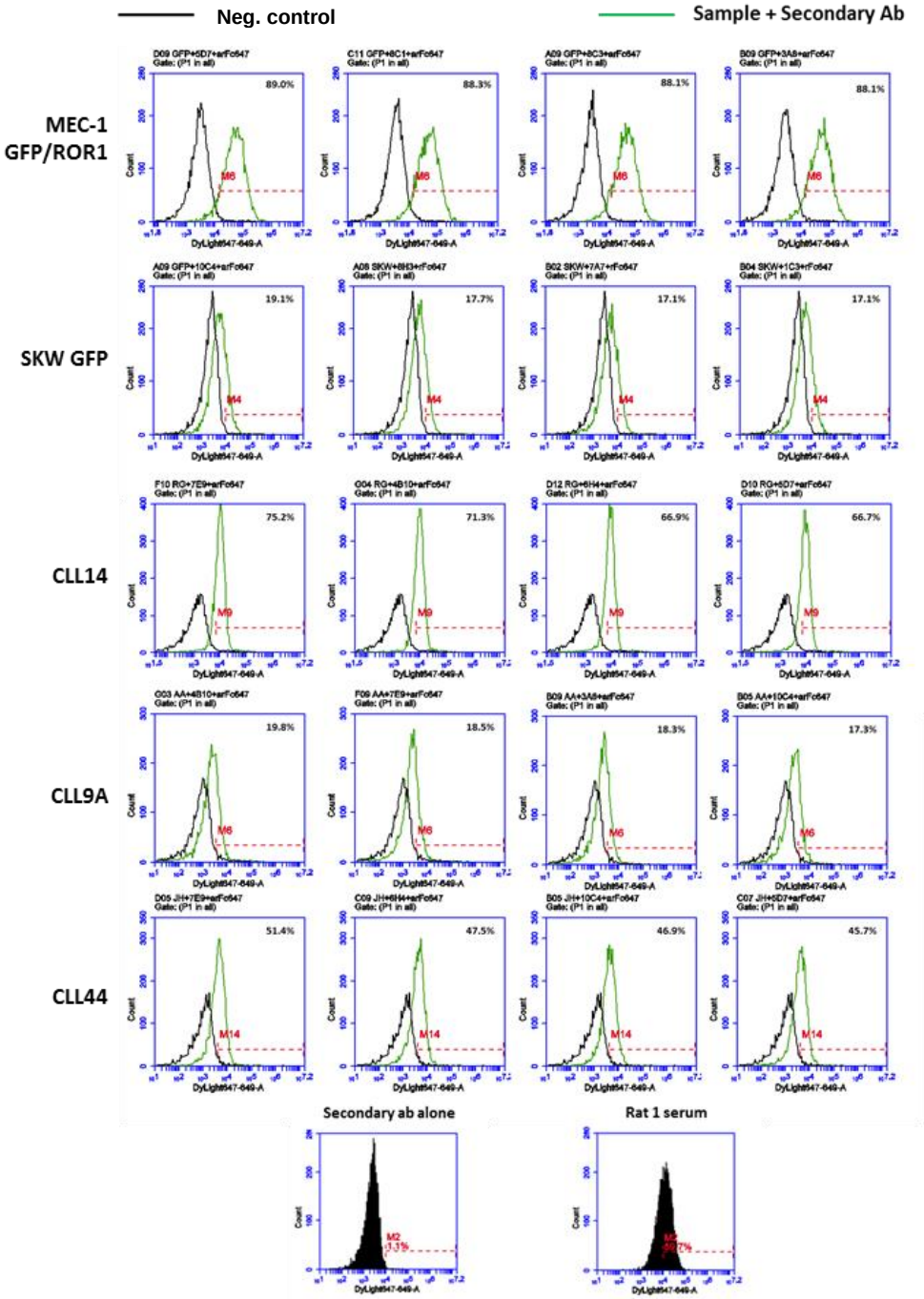

Fig. 3. 3. Binding of ROR1 polyclonal hybridomas assessed by flow cytometry. Supernatants from all 38 ROR1 polyclonal hybridomas were tested on different cell lines and primary CLL cells. Representative histograms from 4 polyclonal hybridomas are shown. The secondary ab (anti-rat IgG-DyLight647) alone and Rat 1 serum acted as negative and positive control, respectively. Black line= Negative cells or secondary ab alone, Green line= Supernatant+secondary ab. The % of frequency is displayed in the top right corner of each histogram.

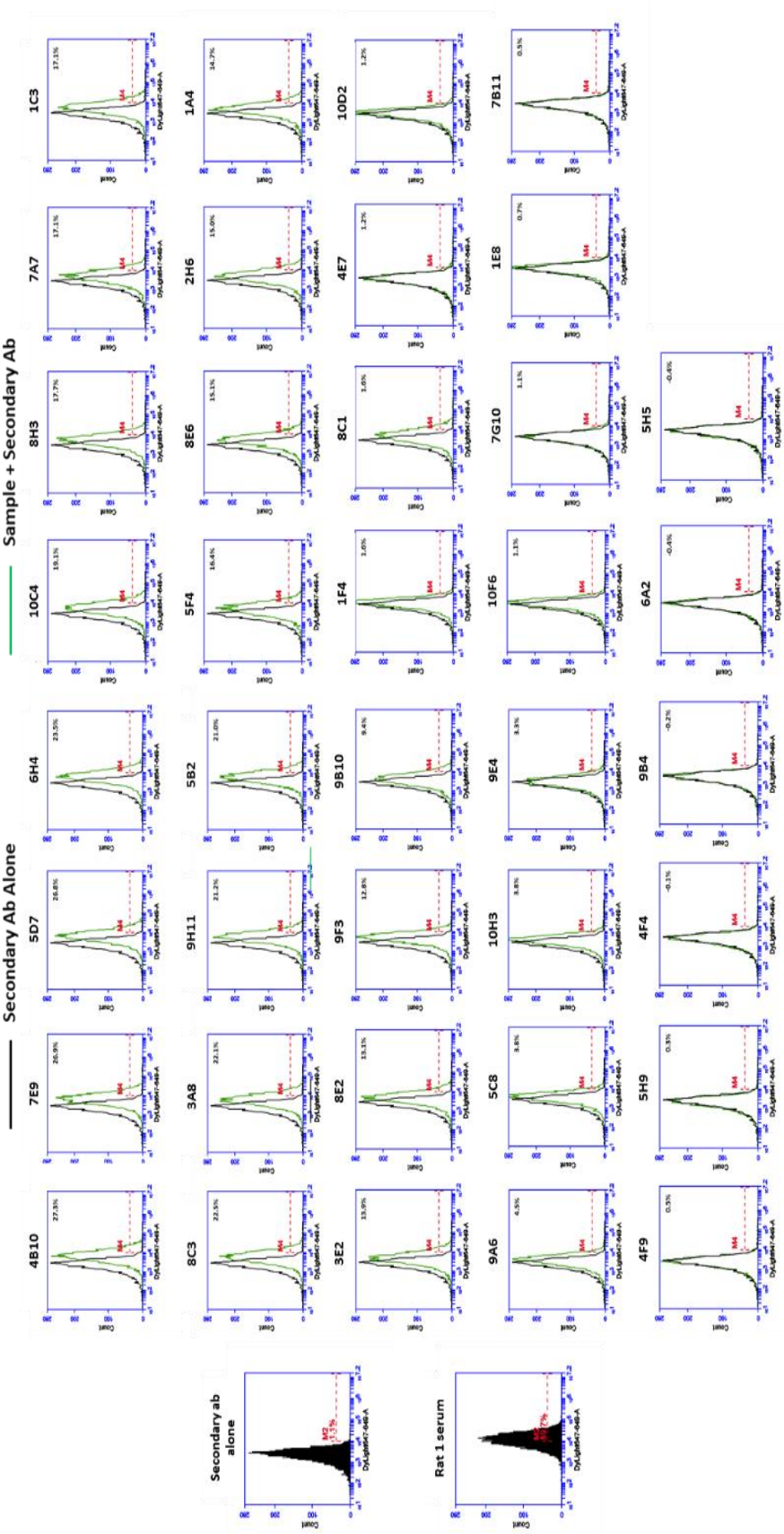

Fig. 3. 4. Binding of ROR1 polyclonal hybridomas on SKW GFP cells. Supernatants from all 38 ROR1 polyclonal hybridomas (at a 1/100 dilution) were tested on SKW GFP cells. The secondary ab (anti-rat IgG-DyLight647) alone and Rat 1 serum acted as negative and positive control, respectively. Black line= Negative cells or secondary ab alone, Green line= Supernatant+secondary ab. The % of frequency is displayed in the top right corner of each histogram.

3.3.2 Aim 2: Generation of ROR1 monoclonal hybridomas

3.3.2.1 Single-cell cloning by single-cell sorting/limiting dilution: In collaboration with Dr Marco Della Peruta and Dr Satyen Gohil

Having confirmed the specific ROR1 binding of our 38 polyclonal hybridomas, we set out to generate ROR1 single-cell clone hybridomas.

Single-cell cloning was performed by limiting dilution or single-cell sorting into 96-well plates. Colonies were grown until confluent (approximately 2 weeks) and a total of 178 single-cell clones were generated and tested on $GFP^{+}ROR1^{+}$ (SUP-T1 ROR1) and $GFP^{-}ROR1^{-}$ (SUP-T1 NT) cell lines.

In **Fig. 3. 5**, representative dot plots of supernatants screened for specific ROR1 binding are shown. Unlike MEC-1 cells used previously, SUP-T1 cell lines (NT and ROR1) could be clearly differentiated in a flow cytometry dot plot by their GFP expression. Therefore, in order to maximise efficiency, SUP-T1 NT (GFP^{-}) and SUP-T1 ROR1 (GFP^{+}) were mixed at a 1:1 ratio and incubated with supernatants from single cell clone hybridomas, followed by a washing step and secondary antibody staining (anti-rat IgG). Cells alone or in a mixture incubated with secondary antibody alone or non-stained were included as negative controls.

Additionally, and for illustrative purposes, data presenting the screening of all 178 single-cell clones can be found in **Fig. 3. 6.**

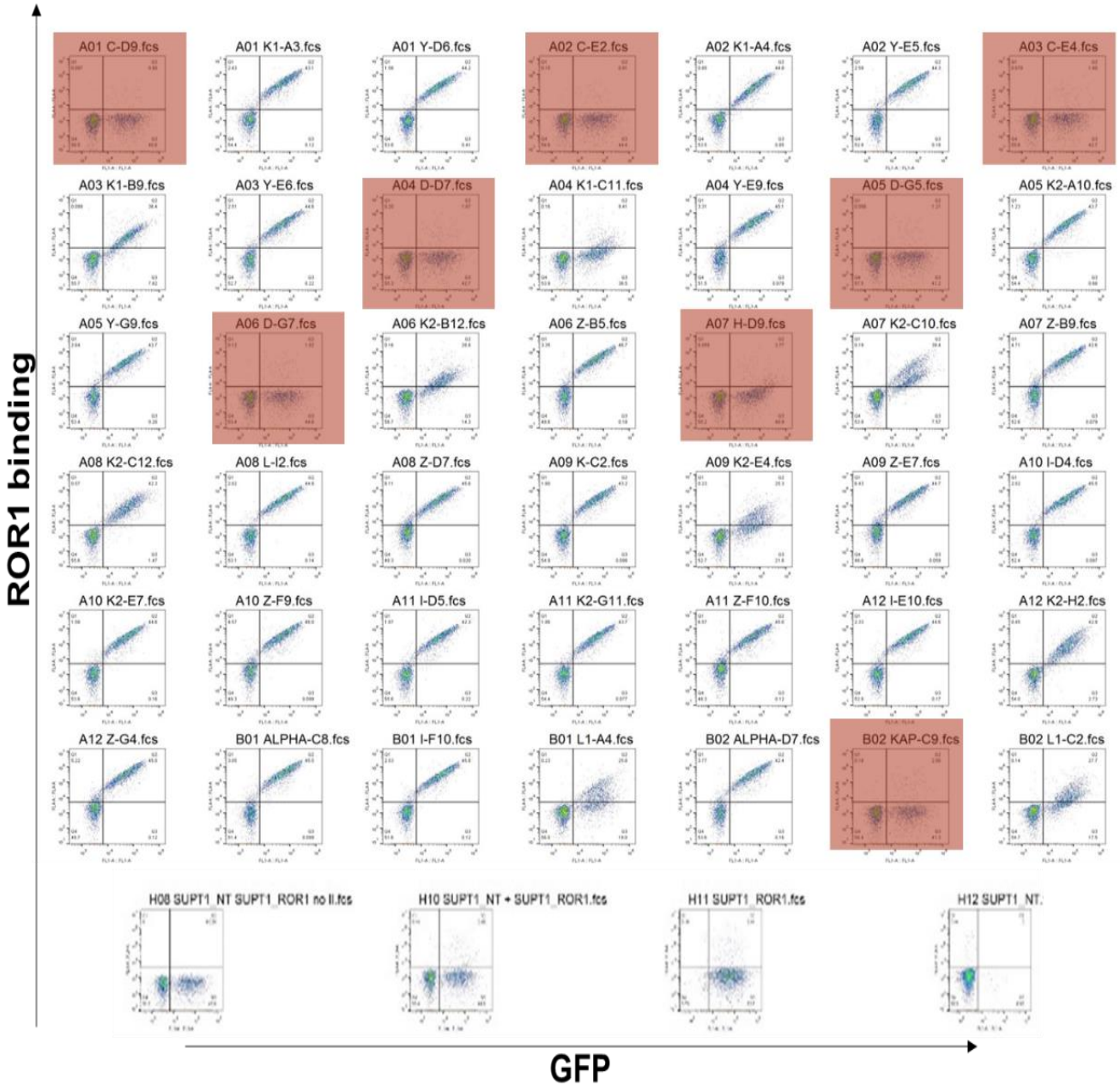

Fig. 3. 5. ROR1 binding by flow cytometry. A total of 178 single-cell clones were tested by double staining flow cytometry on a mixture of ROR1^{+}-GFP^{+} and ROR1^{-}-GFP^{-} cell lines. Representative dot plots are shown. Anti-rat IgG was used as secondary antibody and served as negative control for antibody staining. At the bottom, cells line alone or in a mixture are shown as controls. Negative single cell clones for ROR1 detection appear as shadowed in red.

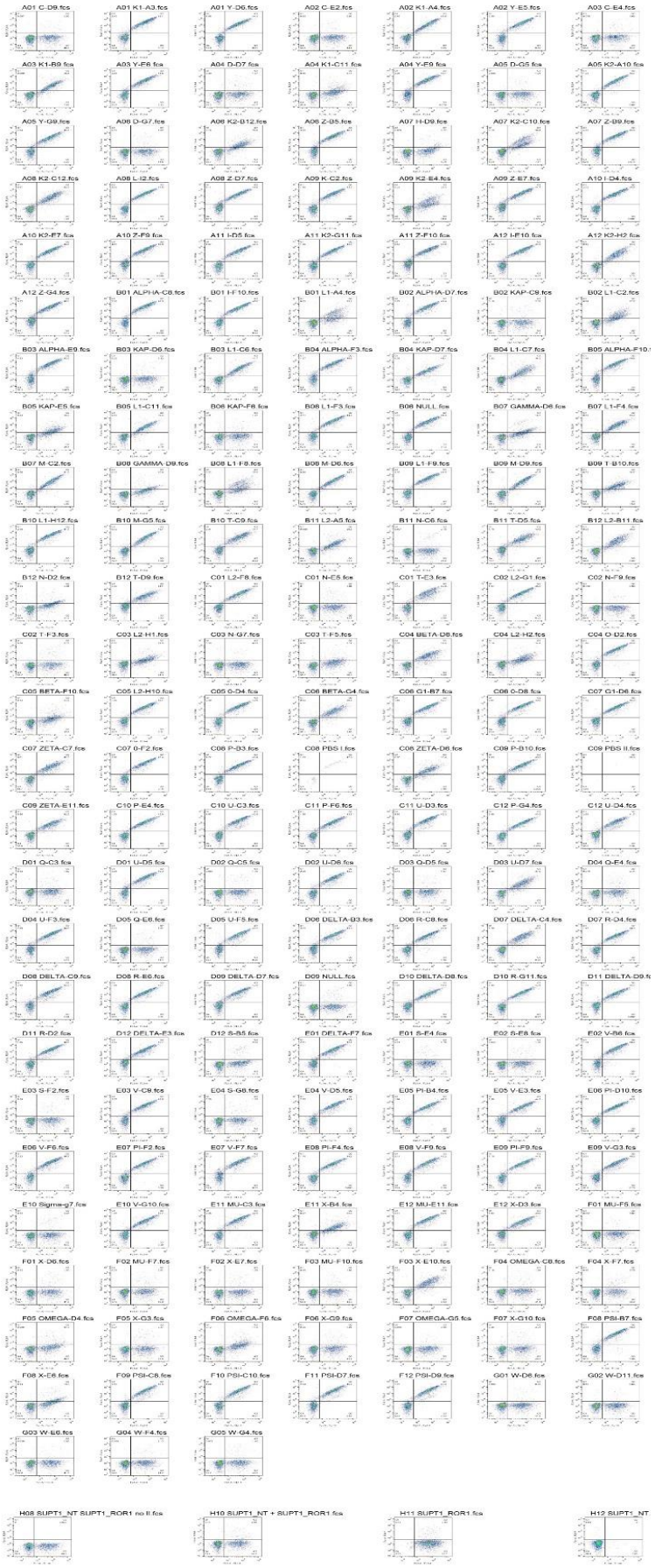

Fig. 3. 6. ROR1 binding by flow cytometry. In collaboration with Dr Marco Della Peruta and Dr Satyen Gohil, a total of 178 single-cell clones were tested by double staining flow cytometry on a mixture of ROR1^{+}-GFP^{+} and ROR1^{-}-GFP^{-} cell lines. Anti-rat IgG was used as secondary antibody and served as negative control for antibody staining. At the bottom, cells line alone or in a mixture as shown as cell counting controls.

3.3.2.2 5’ RACE PCR: In collaboration with Dr Marco Della Peruta and Dr Satyen Gohil

To ultimately isolate the variable heavy (V_H) and light (V_L) regions of our ROR1 antibodies, we needed to use the 5’ Rapid Amplification of cDNA Ends (RACE) PCR technique. This method allows amplification of a specific cDNA region starting with the knowledge of a small stretch of sequence from within an internal region of the cDNA (Frohman, 1993).

Applied to antibodies, this technique allows the isolation and cloning of the V_H and V_L regions by PCR using primers annealing to the 5’ and 3’ ends of the antibody sequence. Since the 3’ end of the variable regions corresponds to the immunoglobulin constant regions, specific primers for the isotype of each clone can be used. However, this is not the case for the 5’ end as there are many families of V-regions and it is unknown which one corresponds to what hybridoma.

Therefore, instead of performing multiple PCRs using a panel of forward primers designed to amplify all V-region families, a universal approach is adopted by which the cDNA is poly-C tailed by incubation with Terminal Transferase and dCTPs. PCR is then performed using a poly-G forward primer (including an anchor region) and a reverse primer specific to each constant region. Finally, a subsequent nested PCR is performed using an internal reverse primer and an external forward primer specific to the anchor region of the initial poly-G forward primer (See **Fig. 2.1** – Chapter 2).

Therefore, before starting processing cDNA from our single-cell clones, we first determined the isotype of all ROR1 positive single-cell clone hybridomas. To this end, we used an ELISA-based rat immunoglobulin isotyping kit (eBioscience), which allowed us to identify both the heavy and light chain constant regions (See **Fig. 3. 7**).

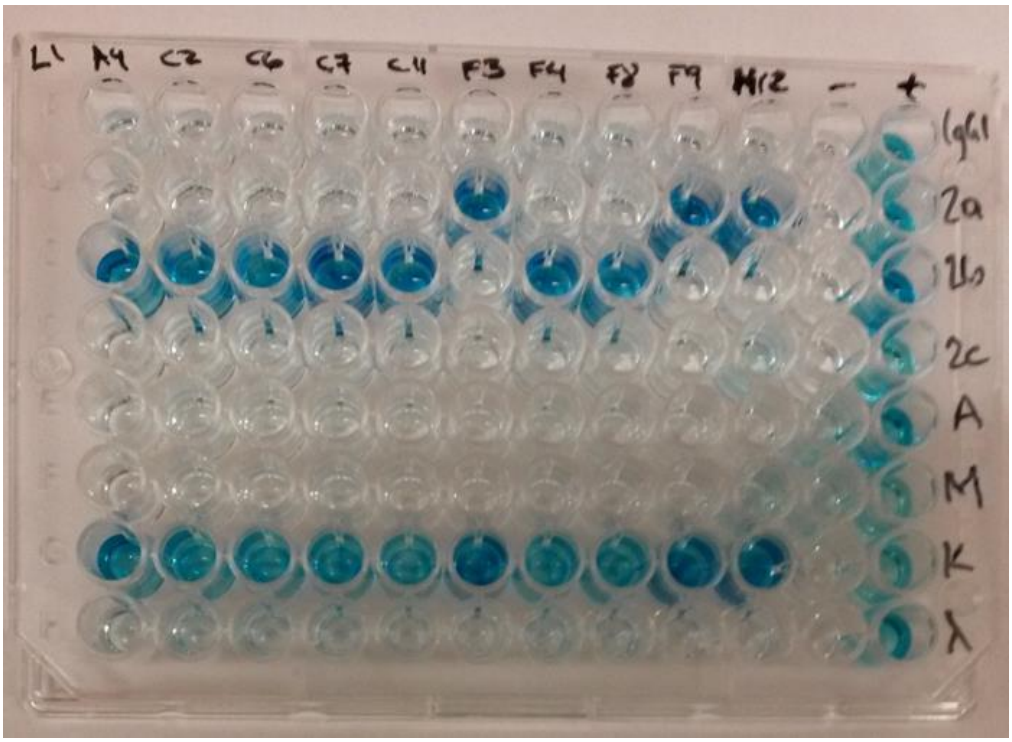

Fig. 3. 7. Single-cell clone hybridoma isotyping by ELISA. ELISA-based rat immunoglobulin isotyping kits from eBioscience or BD Bioscience were used to identify both the heavy and light constant regions of all ROR1 single-cell clone hybridomas.

Having identified the isotype of all ROR1 single-cell clone hybridomas, we grew the latter in 6-well plates or 10cm dishes in order to produce enough number of cells for RNA extractions. RNA was then reverse transcribed to cDNA.

To ensure quality of samples, cDNA was tested by using rat GAPDH primers able to differentiate between genomic DNA and cDNA. Briefly, rat GAPDH primers bound to two non-consecutive exons so that cDNA amplification would produce a 600bp band size, whilst genomic DNA would generate a 900bp PCR product (since intronic regions would also be amplified). An agarose gel showing a representative result after PCR amplification is shown in **Fig. 3. 8**.

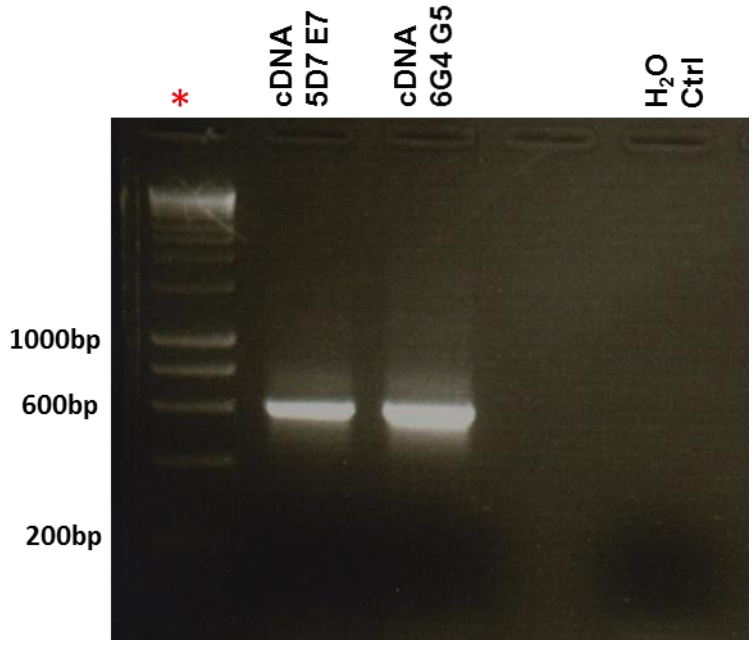

Fig. 3. 8. Evaluation of cDNA quality using GAPDH primers. cDNA was tested for genomic DNA contamination using rat GAPDH primers able to differentiate between the two. cDNA amplification resulted in a 600bp PCR product, whilst gDNA amplification was not detected (900bp). Water acted as negative control.

Following cDNA production and evaluation, 5'RACE PCR reactions were performed as described in the Materials & Methods section (**Chapter 2**). In short, cDNA was poly-C tailed and later amplified with a poly-G forward primer and an isotype-specific reverse primer. A nested PCR was then performed in order to maximise amplification of variable regions.

PCR products were run on a 1% agarose gel and stained with GelStar in order to maximise visibility. Of note, this method typically produces a smear of PCR products from 200-1000bp. However, when full length chains are successfully amplified, a defined band can be detected.

In **Fig. 3. 9**, we show representative gels displaying 5' RACE PCR products, before and after gel extraction. Amid the expected smear, clear and defined bands could be observed at approx. 600bp and 400bp corresponding to the variable heavy and light regions, respectively. PCR products using nuclease-free water were also run. Bands of the correct size were gel-extracted and sent for direct sequencing or inserted into TOPO cloning vectors for subsequent sequencing.

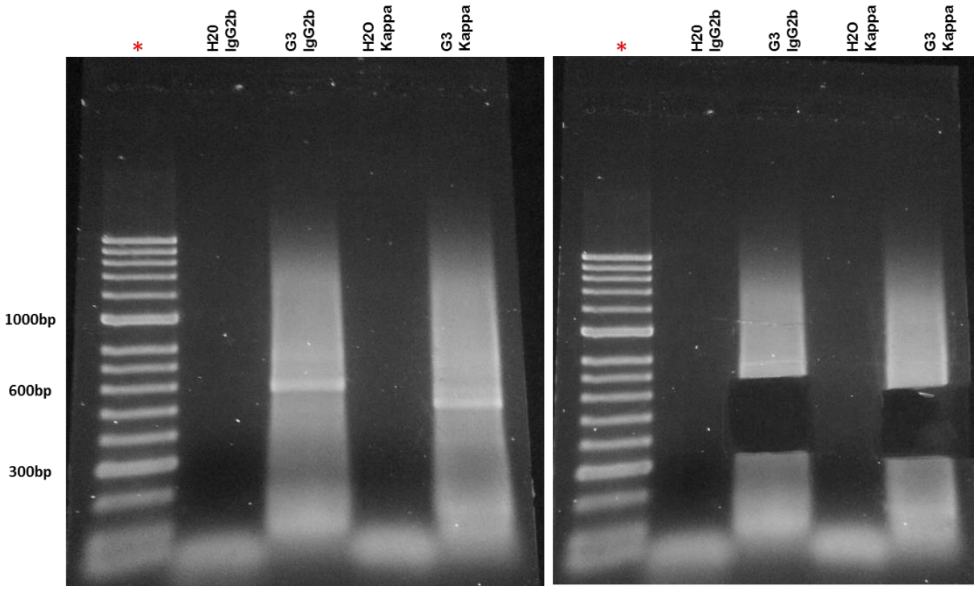

Fig. 3. 9. Isolation and amplification of V_H and V_L regions by 5' RACE PCR. cDNA from single-cell clone hybridomas were isolated by 5' RACE PCR. Amplified products were run in 1% agarose gels and stained with GelStar for maximum sensitivity. Representative gels before and after gel extraction of relevant bands are shown. Nuclease-free water for 5' RACE PCR amplification acted as negative control. 5' RACE= 5' Rapid Amplification of cDNA Ends.

Sequencing data was then analysed using the IMGT V-quest database of rat germline immunoglobulin and consensus gene and allele sequences (Brochet et al., 2008). IMGT V-quest, a bioinformatics tool developed by the international ImMunoGeneTics information system (IMGT), allows the identification of the variable (V), diversity (D) and joining (J) genes and alleles of any submitted antibody sequence to their platform.

In **Fig. 3. 10**, representative IMGT V-quest outputs for both V_H and V_L sequences are presented. The alignment for the V- (D-) and J-GENE included the alignment score and the identity percentage with the five closest genes and alleles. The software also evaluated the presence of a stop codon in the sequence and if it was in-frame. Full length chains with matching and in-frame V-, (D-) and J-sequences were classified as “productive”.

Heavy chain – IMGT identity

Result summary:	Productive IGH rearranged sequence (no stop codon and in-frame junction)		
V-GENE and allele	Ratnor IGHV11S1*01 F	score = 1336	identity = 96,18% (277/288 nt)
J-GENE and allele	Ratnor IGHJ3*01 F	score = 228	identity = 94,12% (48/51 nt)
D-GENE and allele by IMGT/JunctionAnalysis	Ratnor IGHD1-1*01 F	D-REGION is in reading frame 1	
FR-IMGT lengths, CDR-IMGT lengths and AA JUNCTION	[25.17.38.11]	[8.8.16]	CATEEMYTTDYYYGFAYW

Light chain – IMGT identity

Result summary:	Productive IGK rearranged sequence (no stop codon and in-frame junction)		
V-GENE and allele	Ratnor IGKV3S19*01 F	score = 1381	identity = 97,92% (282/288 nt)
J-GENE and allele	Ratnor IGKJ1*01 F	score = 180	identity = 100,00% (36/36 nt)
FR-IMGT lengths, CDR-IMGT lengths and AA JUNCTION	[25.17.36.10]	[10.3.9]	CQQNRESPRTF

Fig. 3. 10. IMGT V-quest identification of heavy and light chain sequences derived from ROR1 single-cell clone hybridomas. Shown is a representative result of heavy and light chain sequences that matched the rat germline immunoglobulin and consensus sequences (V, (D) and J genes) using the IMGT V-quest database. Matching clones that had an in-frame signal sequence were classified as “productive”. IMGT= The International ImMunoGeneTics information system.

From the single-cell clone hybridomas, a total of 32 V_H and V_L regions encoding for 16 unique antibody sequences came out as “productive”.

3.3.3 Aim 3: Cloning of rat scFv to hIgG1, k constant regions

Following verification of antibody sequences, 16 chimeric antibodies in full human IgG were generated using DNA splicing by overlap extension PCR. As indicated on Materials & Methods section (**Fig. 2. 2**), the variable chains (rat V_H and V_L) along with the constant regions (human IgG1 and human kappa) were PCR amplified using appropriate primers that would add both relevant restriction enzyme sites and an overlapping sequence.

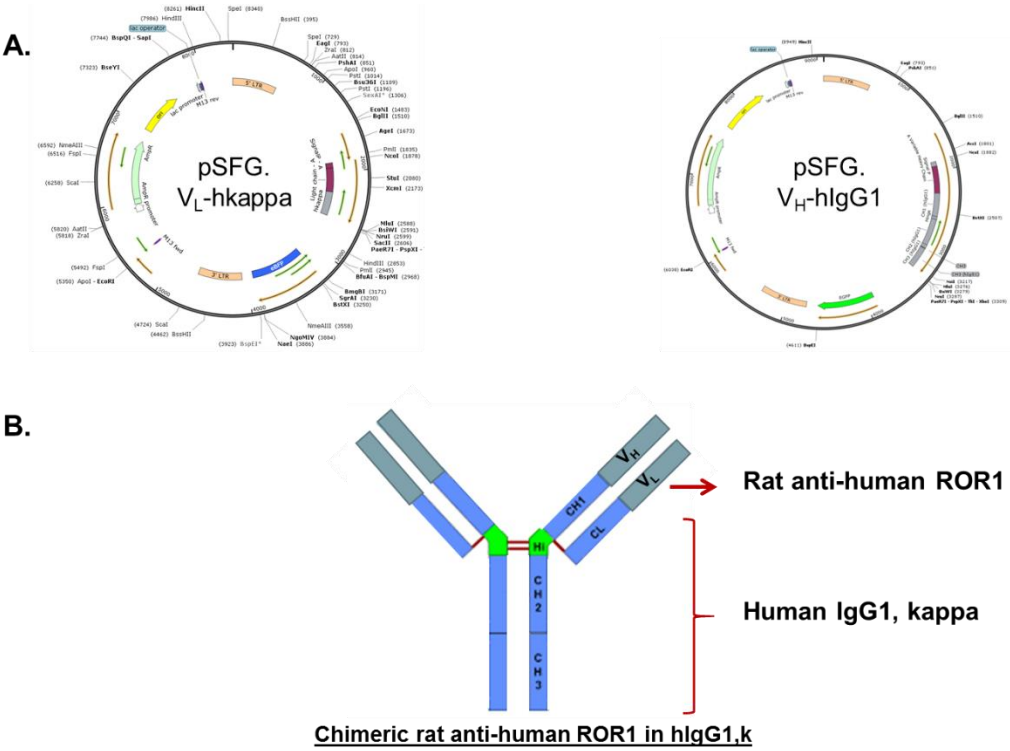

Fig. 3. 11. Cloning of rat scFv into human IgG1, k constant regions. (A) DNA splicing of variable and constant regions resulted in the generation of retroviral vectors coding for each: V_L-human kappa and V_H-human IgG1 chains. Each construct carried a reporter gene: eBFP and eGFP for the light and heavy chains, respectively. (B) Transfection of both plasmids was needed in order to produce rat-human chimeric antibodies comprised of rat anti-human ROR1 variable chains in human IgG1, k constants. eBFP= Enhanced blue fluorescent protein, eGFP= Enhanced green fluorescent protein.

A second PCR was then performed in order to splice the corresponding variable and constant regions together. The resulting inserts were subcloned into retroviral vectors carrying different reporter genes: eBFP (light chain) and eGFP (heavy chain) (**Fig. 3. 11**).

Correct cloning of all new constructs was evaluated by enzymatic digestion followed by agarose gel electrophoresis and sequencing analysis. These evaluations confirmed the successful subcloning of all 16 antibody sequences,

which resulted in the generation of 32 new constructs (16 for the light and 16 for the heavy chains).

3.3.4 Aim 4: Assessment of chimeric ROR1 antibodies by flow cytometry

We next sought to produce ROR1 chimeric antibodies by transient transfection of HEK 293T cells using two plasmids per antibody. In **Fig. 3. 12**, we show representative dot plots displaying transfection efficiency of 293T cells at 72h after co-transfection of light and heavy chains. We screened different clones encoding for the same antibody sequence (in this case, one for the light chain: L2 and three for the heavy chain: H2, H9 and H11).

Confirmation of successful transfection led me to evaluate the ROR1 binding ability of the chimeric antibodies contained in the culture supernatants. At 72h post-transfection, culture supernatants were tested on $GFP^{+}ROR1^{+}$ (SUP-T1 ROR1) and $GFP^{-}ROR1^{-}$ (SUP-T1 NT) cell lines. After 30min incubation, cells were washed and stained with an anti-human IgG-DyLight647. Culture media from non-transfected cells acted as negative control.

Both histograms and dot plots generated by flow cytometry showed specific detection of ROR1, which confirmed the correct expression of chimeric antibodies against ROR1.

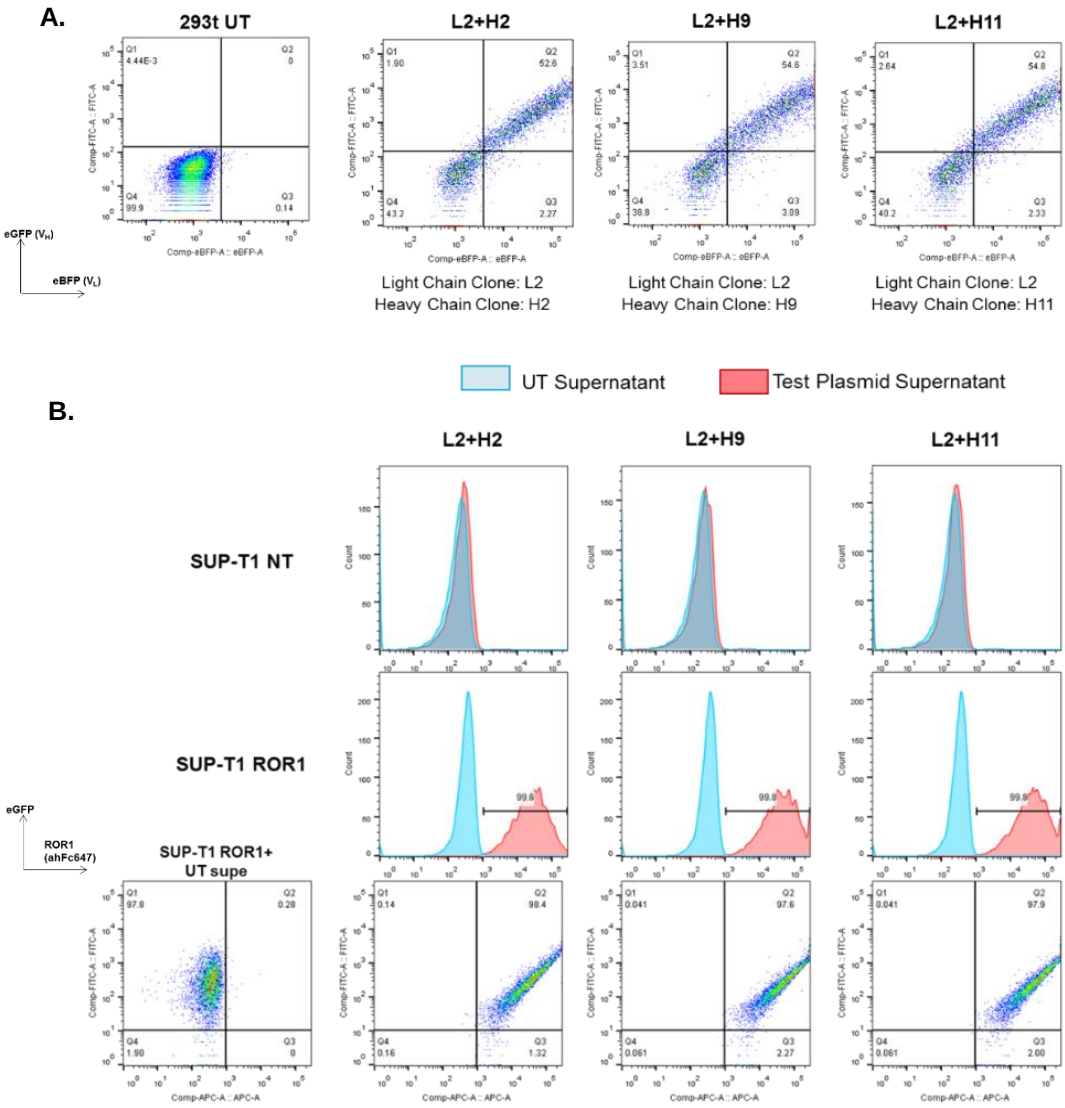

Fig. 3. 12. Generation of rat scFv into human IgG1, k constant regions. HEK 293T cells were transiently co-transfected with the light and heavy chain plasmids of chimeric ROR1 antibodies. Different clones coding for the same antibody sequence were tested each time. (A) Transfection Efficiency: Representative dot plots of 293T cells transfected using different clones (one for the light chain: L2 and three for the heavy chain: H2, H9 and H11) are shown. Both the GFP and BFP expression was evaluated for heavy and light chain transfection, respectively. Non-transfected 293T (293 UT) cells acted as negative control. (B) ROR1 Binding: Culture supernatants were collected at 72h post transfection. After centrifugation, supernatants were incubated with $GFP^{+}ROR1^{+}$ (SUP-T1 ROR1) and $GFP^{-}ROR1^{-}$ (SUP-T1 NT) cell lines. Supernatant from non-transfected 293T cells acted as negative control. After a wash step, all samples were stained with an anti-human IgG1-Dylight 647 antibody. Shown are representative histograms and dot plots obtained after assessment of ROR1 binding by flow cytometry.

Similarly, in **Fig. 3. 13**, we show the flow cytometry evaluation of ROR1 binding using all 16 chimeric antibodies. Of these, 12 clones presented specific detection of $GFP^{+}ROR1^{+}$ cells but not $GFP^{-}ROR1^{-}$ cells. It is noteworthy that additional to our chimeric antibodies, previously reported clones 4a5 (murine-derived) (Kipps, 2012) and R12 (rabbit) (Yang et al., 2011) were also cloned into hIgG1, kappa constants. These antibodies were also tested for ROR1 specificity and were included in these studies as reference. A summary of all ROR1 chimeric antibodies generated can be seen in **Table 3. 3**.

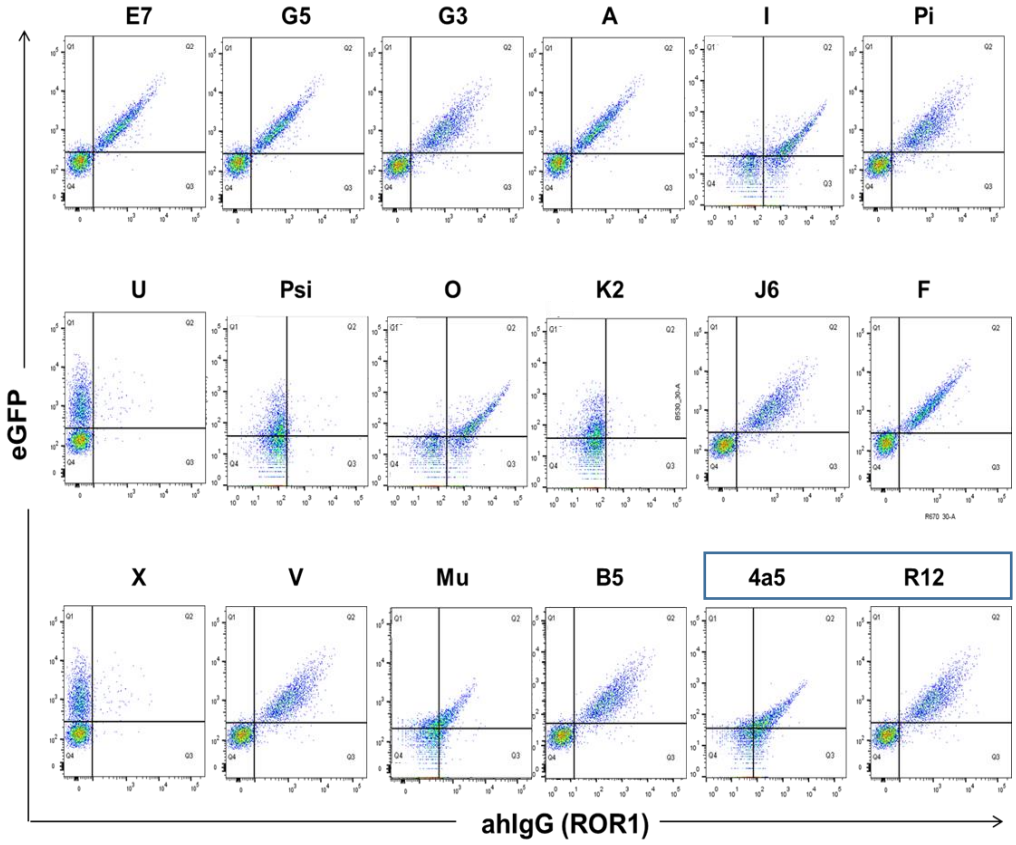

Fig. 3. 13. Specific binding of chimeric rat-human anti-ROR1 clones to $ROR1^{+}$ cells by flow cytometry. Sixteen rat hybridoma single-cell clones were fused to hIgG1, k regions. Of these, 12 showed specific binding to $ROR1^{+}$ cells. Ab supernatants from transfected 293T were tested by double staining flow cytometry on $ROR1^{+}GFP^{+}$ and $ROR1^{-}GFP^{-}$ cell lines. Previously published 4a5 (murine) and R12 (rabbit) clones were included as reference (blue square). Anti-human IgG was used as secondary antibody.

Table 3. 3. Summary of ROR1 Chimeric antibodies specific for ROR1. Previously reported clones 4a5 and R12 (in blue) were also cloned in hIgG1, k constants and were included in these studies as reference.

Antibody clone	Binds to ROR1
E7	Yes
G5	Yes
G3	Yes
A	Yes
I	Yes
Pi	Yes
U	No
Psi	No
O	Yes
K2	No
J6	Yes
F	Yes
X	No
V	Yes
Mu	Yes
B5	Yes
4a5	Yes
R12	Yes

As a whole, in this chapter it has been shown that although 32 retroviral constructs encoding for 16 chimeric ROR1 antibodies were generated, only 12 were able to specifically detect and bind to ROR1-expressing cells. The 12 new ROR1 antibodies will be further investigated in the next chapters.

3.4 Discussion

Fundamental to the aim of developing ROR1-based immunotherapies, was the generation of anti-ROR1 monoclonal antibodies. To this end, hybridomas derived from three immunised Wistar rats against the extracellular portion of ROR1 were produced.

It is noteworthy that rats and not mice were preferred as the ROR1 identity between human and the former was 90%, instead of the 97% identity found between human and mouse. Despite of this, our collaborator (Aldevron) had to perform eight rounds of immunisation in order to get ROR1 positivity in the

rats' sera. Arguably, this might have been of benefit as the effect of boosting enhances immunoglobulin class switching and the generation of higher affinity antibodies through somatic hypermutation (Nelson et al., 2000).

Flow cytometry evaluation of the rats' sera and subsequent 38 polyclonal hybridomas confirmed the presence of ROR1 antibodies as evidenced by specific binding to ROR1-expressing cell lines and primary CLL cells. Screening for ROR1 detection at the polyclonal stage was necessary in order to choose which hybridomas to take forward. However, no further assumptions could be made since their polyclonality and differences in concentration would not have allowed us to ascertain the most promising candidates.

Since all 38 hybridomas were positive for ROR1, they were all processed for single-cell cloning in order to generate monoclonal antibodies. This decision was driven by the knowledge that although antibodies derived from polyclonal hybridomas have the advantage of detecting multiple epitopes -whilst having a relatively simple and inexpensive production- batch to batch variation might be observed. This could include differences in antibody reactivity and titre (Nelson et al., 2000, Abcam, Wootla et al., 2014). In contrast, monoclonal antibodies target a single epitope and can be produced continuously. This is of particular importance for research and therapeutic purposes, as their reproducibility make them powerful tools for investigation of molecules and biological processes as well as clinical diagnosis and treatment.

Once single-cell clone hybridomas were produced, isotype determination was undertaken in order to facilitate isolation of the variable regions. Importantly, isotype determination also helps identify the presence of a single isotype, further confirming that the antibody under investigation is truly monoclonal.

V_H and V_L extraction was followed by the generation of chimeric antibodies. As discussed above, cloning of the variable regions into human constant chains was needed in order to avoid unwanted antibody immunogenicity (Schroff et

al., 1985). Furthermore, in terms of antibody derivatives such as Antibody-Drug Conjugates (ADCs), the use of human IgG could also be considerably beneficial. A study by (Ober et al., 2001), showed that whilst mouse neonatal Fc receptor (FcRn) binds IgGs from various species, human FcRn binds only human, guinea pig and rabbit IgG, but not mouse or rat IgG. Since the ADC-FcRn interaction is pivotal for preventing unwanted cell death and increasing the circulatory half-life of the ADC, these findings shed light on the importance of using a human isotype for ADC therapy (Peters and Brown, 2015, Hamblett et al., 2016, Sato et al., 2009).

Not surprisingly, most therapeutic antibodies contain the human IgG1, kappa isotype, as it has been shown that hIgG1 can induce potent ADCC and CDC activities when compared to other heavy chain isotypes (Natsume et al., 2008). Furthermore, Jefferis et al., showed that it confers stability and a half-life of approximately 21 days to the antibody molecule (Jefferis et al., 1998). As a result, it was decided to generate chimeric antibodies in hIgG1, k constants.

Using DNA splicing techniques, I produced 32 retroviral constructs encoding for 16 unique antibodies against ROR1. Additional to this, sequences from previously reported clones against ROR1 (4a5 (Kipps, 2012) and R12 (Yang et al., 2011)) were put in the same chimeric format.

After flow cytometry evaluation on $ROR1^{+}$ and $ROR1^{-}$ cells, it was found that 12 clones were still able to specifically bind to ROR1 as chimeric antibodies. Recently, observations that isotype does not only affect antibody activity but also specificity (Casadevall and Janda, 2012, Beers et al., 2016), structure (Janda et al., 2016) and affinity (Tudor et al., 2012) might explain the sudden lack of binding to ROR1 when clones U, Psi, K2 and X were put in the chimeric format.

Further characterisation of our 12 chimeric antibodies against ROR1 will be discussed in the next chapter.

3.4.1 Conclusions

- In collaboration with Aldevron, 38 rat polyclonal hybridomas against human ROR1 have been successfully produced.
- Our group generated more than 150 single-cell hybridomas and tested their ROR1 specificity by flow cytometry on both ROR1 positive and negative cells.
- The variable heavy (V_H) and variable light (V_L) regions of rat monoclonal antibodies were extracted, cloned, and sequenced.
- IMGT V-quest analysis allowed us to identify “productive” and in-frame sequences.
- A total of 32 constructs in retroviral vectors were generated. They encoded for 16 chimeric rat-human antibodies (rat V_H and V_L sequences in human IgG1, kappa constant regions).
- Transient co-transfection of these plasmids in HEK 293T cells allowed the production of all chimeric antibodies for further investigation.
- Flow cytometry analyses revealed that 12 out of 16 clones in the chimeric format were still able to specifically bind to ROR1-expressing cells.
- Previously reported clones 4a5 and R12 were produced as chimeric antibodies and included in these studies as reference. Specific binding to ROR1 was also assessed by flow cytometry.

3.4.2 Future work

It would be worth exploring whether the lack of binding seen in clones U, Psi, K2 and X is exclusive to their cloning into human IgG1, k constant regions. This would be of particular interest for clones U and Psi as analysis using their hybridoma supernatant revealed that they bind to the Frizzled domain of ROR1 (data not shown).

Chapter 4 Characterisation of chimeric ROR1 antibodies

4.1 Introduction

In the previous chapter, it was demonstrated that the variable heavy (V_H) and light (V_L) regions of 16 anti-ROR1 antibodies were successfully cloned into human IgG1, kappa constant regions. This resulted in the generation of 16 rat anti-human ROR1 antibodies; of which, 12 clones were able to specifically bind to ROR1-expressing cells.

The aims of the studies outlined in this chapter were to further characterise our chimeric antibodies in terms of: i) identification of their binding domain by flow cytometry, ii) binding kinetics determination by surface plasmon resonance, iii) cytolytic activity, and iii) ability to get internalised into $ROR1^+$ cells.

4.1.1 Epitope mapping

When an individual is exposed to an immunogen, a humoral response is provoked. As a result, a plethora of antibodies is produced against different regions of the foreign substance. These regions are called antigenic determinants, or epitopes, and they usually comprise 6-8 amino acids (Nelson et al., 2000).

Epitope mapping is therefore the process of identification of these molecular determinants. This is certainly a crucial step in the characterisation of monoclonal antibodies with therapeutic purposes as it enables the localisation of antigenic regions, and the effect that antibodies targeting them could have in cell function (Baerga-Ortiz et al., 2002).

Several methods have been developed in order to map binding epitopes of monoclonal antibodies. The biophysical and biochemical properties of this interaction have allowed the use of different techniques ranging from pepscan,

co-crystallisation of the antigen:antibody complex followed by x-ray diffraction, to nuclear magnetic resonance (NMR), Biacore technology, amino acid mutagenesis and other binding analyses. Recently, combinatorial approaches using phage display peptide libraries and computational algorithms such as Mapitope appear to be effective in mapping conformational epitopes (Gershoni et al., 2007).

In this study, an approach that is readily accessible yet able to map both linear and conformational epitopes was chosen, and it is presented in the first section of Results. There, binding analysis using cell lines expressing truncated domains of our protein of interest will be discussed.

4.1.2 Binding kinetics determination by surface plasmon resonance

Another important parameter in the characterisation of monoclonal antibodies is the measurement of the binding kinetics of antigen-antibody interactions, namely affinity. Biacore systems is the preferred approach as it is based on surface plasmon resonance (SPR) technology. SPR allows the investigation and quantitation of molecular interactions in real time, using a label-free technology, making it useful for a broad range of biological applications, including antigen-antibody complexes (Jason-Moller et al., 2006).

One major advantage of SPR biosensor-based assays is the option to separately determine association (k_{on}) and dissociation (k_{off}) rate constants. The knowledge of these distinct kinetic parameters provides detailed information that may be pivotal when screening for therapeutic antibodies. For instance, one demand could be that the antibody should bind fast (high k_{on}) and bind tightly (low k_{off}) (Hahnefeld et al., 2004).

Affinity can be determined in three independent ways using Biacore systems: i) calculation from kinetic constants, ii) measurement of steady-state binding levels and iii) determination of affinity in solution. For simple 1:1 binding

models, such as antigen-antibody interactions, affinity can be calculated from kinetic constants: k_{on} and k_{off} (Sciences, 2012).

Similarly, the equilibrium dissociation constant (K_D) can be determined by calculating the ratio of the k_{off} and k_{on} (k_{off}/k_{on}) between two molecules. It is used to evaluate the strength of the interaction between the antigen and the antibody, and it is expressed in terms of concentration (M).

K_D and affinity are inversely related. At equilibrium, the rate of antigen-antibody complex formation is equal to the rate of dissociation. Measurement of the reaction rate constants can be therefore used to define the affinity constant ($1/K_D$). Thus, the smaller the K_D value, the greater the affinity of the antibody for its target (Abcam, 2017).

Binding kinetics of the chimeric antibodies were investigated using the Biacore system. Data from these analyses is presented in the second section of Results.

4.1.3 Antibody cytotoxicity

4.1.3.1 Fc-mediated cytotoxicity: Unconjugated antibodies

As described in the Introduction (**Chapter 1**), naked or unconjugated antibodies can exert their cytotoxicity by five main mechanisms of action: i) antibody-directed cell death, ii) complement-dependent cytotoxicity (CDC), iii) antibody-dependent cellular cytotoxicity (ADCC), iv) antibody-dependent cellular phagocytosis (ADCP) and v) vaccinal effect. Of these, the last four involve Fc recognition by the immune system; namely complement system, NK cells and macrophages, respectively.

Most therapeutic antibodies currently used in the clinic trigger immune recognition and activation (Scott et al., 2012). Thus, cytotoxicity screening of our antibodies was performed through CDC activity evaluation.

4.1.3.2 Antibody internalisation: Potential for ADC therapy

Antibody-drug conjugates (ADCs) are armed antibodies with a cytotoxic payload. One of the key advantages of ADCs is that their therapeutic action is independent from the immune response, which can be considerably affected in cancer patients (Baskar et al., 2012).

ADCs combine the specificity of monoclonal antibodies with the cytotoxicity of toxins, chemotherapeutic agents or radioisotopes (Peters and Brown, 2015). ADCs rely on internalising antibodies in order to deliver their toxic payload. Antibody internalisation is in turn mediated by endocytosis. A short discussion of the mechanisms of endocytosis currently known as well as the inhibitors used in order to study antibody internalisation is presented below.

4.1.3.2.1 Mechanisms of endocytosis

Endocytosis is a cellular process by which extracellular material and plasma membrane is trafficked into the cell (Dutta and Donaldson, 2012). Endocytic mechanisms regulate the interactions of cells with their environment, and can be classified into two broad categories: phagocytosis (the uptake of large particles) and pinocytosis (the uptake of fluid and solutes) (Conner and Schmid, 2003). Phagocytosis, in this context, is restricted to specialised mammalian cells. Pinocytosis on the other hand occurs in all cells by at least three main mechanisms: clathrin-mediated endocytosis (CME), clathrin-independent endocytosis (CIE) and macropinocytosis (**Fig. 4. 1**).

Describes the isolation of highly purified coated vesicles from different sources and demonstrates that clathrin is the major coat protein, setting the stage for mechanistic

CME, previously known as receptor-mediated endocytosis, has been extensively investigated for the past four decades. The study of this mechanism was further developed ever since (Pearse, 1976) isolated coated vesicles and identified that clathrin was the major protein. Certainly, CME

requires adaptor proteins, amongst them clathrin and dynamin, in order to select and concentrate cargo into vesicles, and detach them from the cell membrane. In contrast, CIE occurs independently from adaptor proteins, and mostly does not require dynamin for vesicle scission (Damke et al., 1995). Although this mechanism is less understood, it is known that it is cholesterol-dependent and that there are certain forms that are caveolae- and RhoA-dependent (Mayor and Pagano, 2007). Lastly, macropinocytosis involves the actin-dependent formation of ruffled extensions of the cell membrane around an extracellular region followed by internalisation of said region (Doherty and McMahon, 2009, Dutta and Donaldson, 2012).

Recent studies have suggested that macropinocytosis might mediate endocytosis in cancer (Ha et al., 2016), and it can include internalisation of several cell receptors. Internalisation of receptor tyrosine kinases (RTKs) such as ROR1 however seems to occur preferentially, although not exclusively, by CME (Doherty and McMahon, 2009).

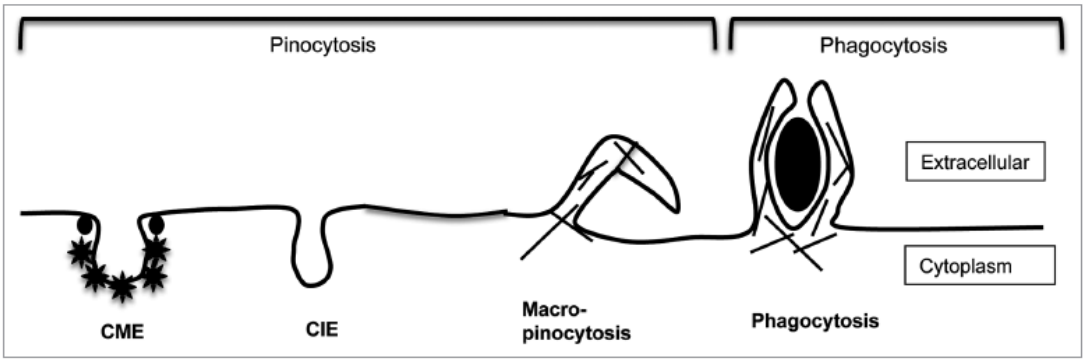

Fig. 4. 1. Different mechanisms of endocytosis. Phagocytosis and macropinocytosis are both driven by actin (hatched lines). Clathrin-mediated endocytosis (CME) is the main mechanisms whereby cell surface proteins are internalized by associating with adaptor proteins which in turn recruit clathrin (black stars). CME endosomes detach from the cell membrane by recruiting dynamin GTPase (black circles) to the bud neck. Clathrin-independent endocytosis (CIE) is depicted as one form, although several variations of CIE have been reported. Modified from Dutta & Donaldson, 2012.

4.1.3.2.2 Endocytosis inhibitors

In an effort to better understand the different types of endocytosis, scientists have used a range of non-specific chemical inhibitors. More recently, a new

generation of pharmacologic agents and genetic approaches have emerged in order to target and study a particular form of endocytosis.

One of the classical chemical endocytosis inhibitors is phenylarsine oxide (PAO), a trivalent arsenical compound. Unlike other chemical inhibitors, PAO does not significantly alter other cellular functions when used at concentrations <20uM (Gibson et al., 1989). Although its mode of action is not clearly known, it has been shown that CME, macropinocytosis and phagocytosis are all blocked by PAO (Dutta and Donaldson, 2012). In this study, evaluation of antibody internalisation by the use of PAO and other approaches will be discussed.

4.2 Aims

1. To identify the binding domain of our chimeric antibodies on the extracellular portion of ROR1 using flow cytometry.
2. To quantify the affinity of our antibodies to their target by determining their binding kinetics using Surface Plasmon Resonance (SPR) technology (Biacore).
3. To screen the cytotolytic activity of our ROR1 antibodies by Complement-Dependent Cytotoxicity (CDC) assay.
4. To assess internalisation of our antibodies into ROR1^{+} cells by flow cytometry and pHAb amine dye labelling.

4.3 Results

4.3.1 Aim 1: Identification of binding domain by flow cytometry

Having generated 16 of our own chimeric rat anti-human antibodies in human IgG1 and having shown that 12 of them bind specifically to ROR1 (Chapter 3), I aimed to identify their binding domain on the extracellular portion of ROR1. To do this, our lab generated stable cell lines that expressed either full-length extracellular ROR1 (eROR1) or varying regions of its extracellular domains: Ig-like alone, Ig-like+Frizzled (Fz), Fz alone, Fz+Kringle (Kg) and Kg alone **(Fig. 4. 2A**). Briefly, SUP-T1 cells, which are ROR1^{-}, were transduced with retroviral supernatants encoding for the ROR1 regions mentioned above.

Our antibodies were next evaluated on transduced SUP-T1 cells (**Fig. 4. 2B**), while non-transduced SUP-T1 (SUP-T1 NT) cells were used as negative control. The secondary antibody (anti-human Fc) served as negative control for antibody staining.

Fig. 4. 2 shows that 10 of our 12 antibodies bound to the Ig-like domain. In contrast, clone V (dark yellow) seems to bind to the intermediate portion between the Ig-like and the Fz domains -since no binding is detected when incubated with cells expressing either of those domains alone. Interestingly, clone F (dark green) is the only antibody that binds to the Frizzled domain. Of note, clone Mu (dark grey) is the only chimeric antibody that shows very low binding to eROR1, almost none to the Ig-like domain and a detectable but still very modest binding to the Ig-like+Fz domains. Thus, it is possible that Mu antibody binds to ROR1 in a similar way as clone V does.

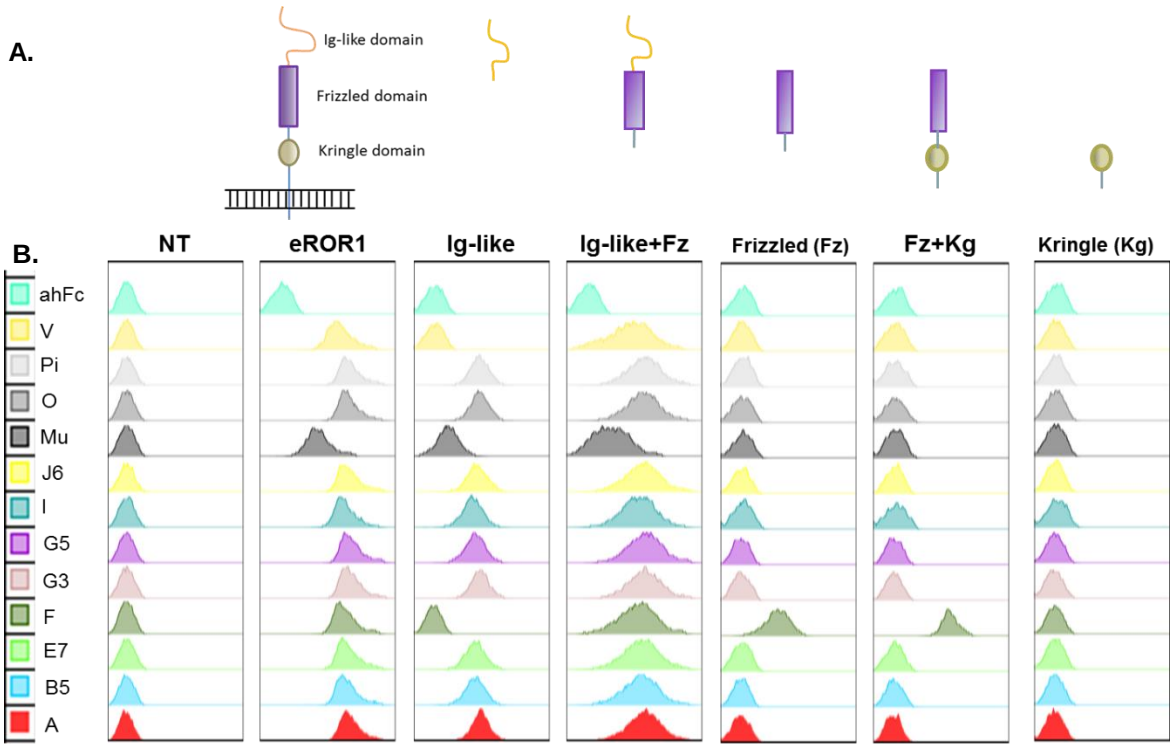

Fig. 4. 2. Epitope mapping of chimeric ROR1 MAb by flow cytometry. (A) SUP-T1 cells were transduced with retroviral vectors containing either the full extracellular portion of ROR1 or only one or two extracellular domains. Non-transduced SUP-T1 (SUP-T1 NT) cells served as negative control. (B) All 12 chimeric antibodies were incubated with SUP-T1 NT and the new stable cell lines at 4°C for 30min. Cells were washed and stained with a secondary antibody (anti-human Fc-Dylight647), which was used as negative control. eROR1= extracellular ROR1, Ig-like= Immunoglobulin-like domain, Fz= Frizzled domain, Kg= Kringle domain.

4.3.2 Aim 2: K_D determination by surface plasmon resonance (SPR) technology: Biacore

Having identified the binding domains of our chimeric ROR1 antibodies, I next explored their binding kinetics using surface plasmon resonance (SPR) technology (**Fig. 4. 3**). SPR evaluation using a Biacore X100 instrument was undertaken at the UCL Institute of Structural & Molecular Biology. As indicated in the Materials and Methods chapter, ROR1 chimeric antibodies were immobilised using an anti-human IgG1 antibody capture kit and a CM5 sensor chip. Seven different concentrations, ranging from 1.5-100nM, of the extracellular portion of ROR1 bearing a Histidine tag were then injected.

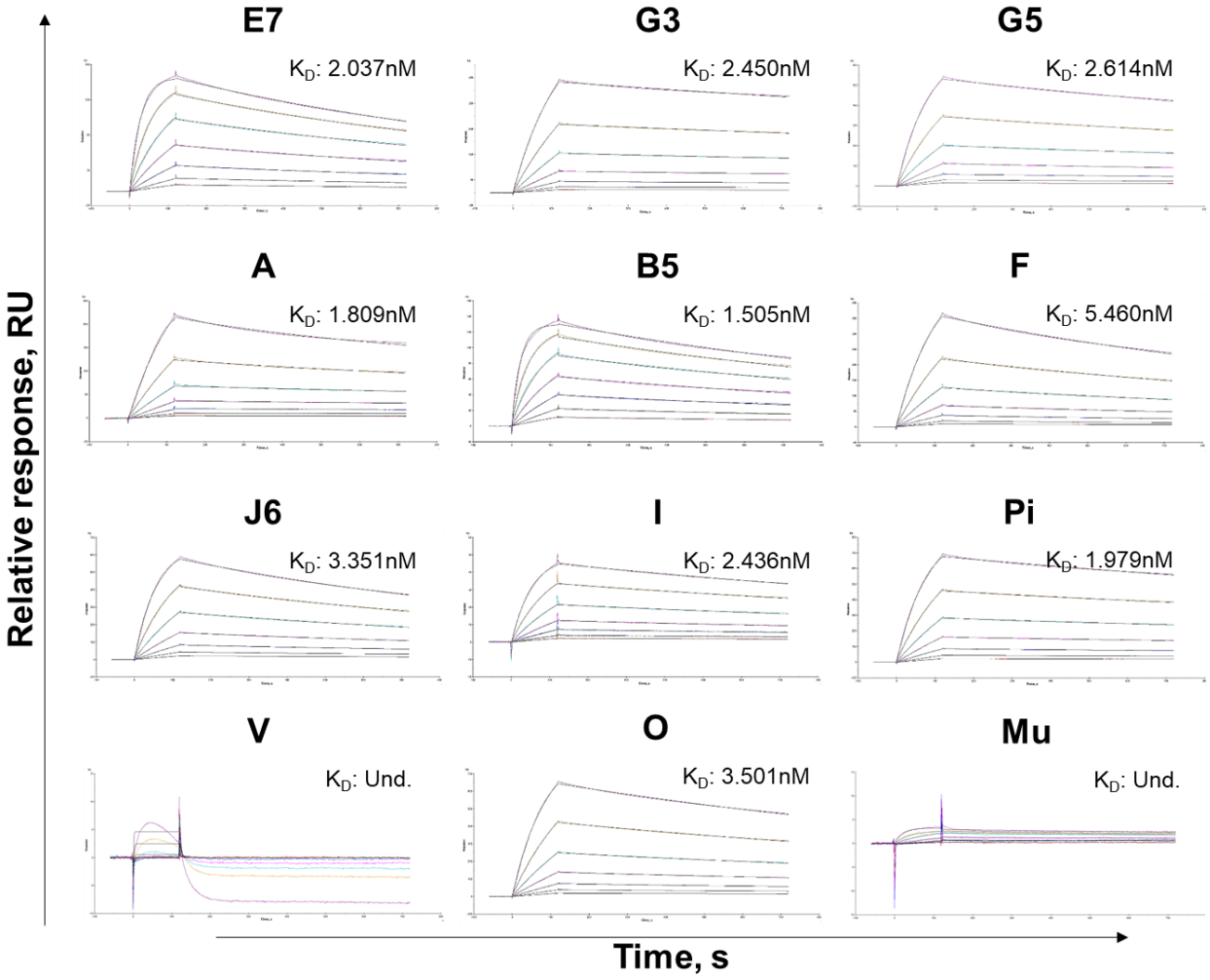

Fig. 4. 3. K_D determination by surface plasmon resonance. Sensorgrams obtained using a Biacore X100 instrument are shown. Briefly, ROR1 antibodies were immobilized using a CM5 chip and seven different concentrations of the Histidine-tagged ROR1 protein (extracellular region) were injected, (shown in different colours). Concentrations ranged from 1.5 to 100nm. Und= Undetermined K_D.

Surface plasmon resonance analysis showed that clones B5, A and Pi possessed the strongest affinities (1.51, 1.81 and 1.98nM, respectively), whilst clone F appeared to have the weakest binding affinity (5.46nM). Although all 12 of our chimeric antibodies were evaluated, K_D from clones V and Mu could not be calculated as the kinetic constants could not be determined. This correlates with flow cytometry data, where modest binding to ROR1 was observed. **Table 4. 1** further illustrates the binding kinetics of our ROR1 chimeric antibodies.

Table 4. 1. Affinity values (K_D) of chimeric ROR1 antibodies

ROR1 Antibody	K_{on}, $(10^5)M^{-1}s^{-1}$	K_{off}, $(10^{-4})s^{-1}$	K_D, $10^{-9}M$
E7	4.168	8.490	2.037
G3	1.086	2.660	2.450
G5	1.593	4.164	2.614
A	5.774	10.44	1.809
B5	4.639	6.980	1.505
F	1.531	8.362	5.460
J6	2.492	8.351	3.351
I	2.093	5.100	2.436
Pi	1.763	3.487	1.979
O	1.735	6.075	3.501
Mu	***	***	***
V	***	***	***

*** The K_D value could not be determined for these antibodies.

4.3.3 Aim 3: Screening of the cytolytic activity of our ROR1 antibodies by Complement-Dependent Cytotoxicity (CDC) assay

Essential to my ultimate goal to produce an effective immunotherapy against ROR1, was the identification of one or more cytotoxic antibodies. My previous results revealed that the affinity of our binders ranged in nanomolar concentrations. High affinity antibodies are indeed necessary to facilitate a

good antibody-target interaction which in turn results in a more efficient therapy (Scott et al., 2012). Therefore, we decided to screen the cytolytic activity of our antibodies on primary cells from Chronic Lymphocytic Leukaemia (CLL) patients and Peripheral Blood Mononuclear Cells (PBMCs) from a healthy donor.

This complement-dependent cytotoxicity (CDC) screening was performed using antibody supernatants prepared by transient cotransfection of the heavy and light chain plasmids using 293T cells. Previous experiments carried out in our lab showed that typical antibody concentration in 293T supernatants was approximately 0.5ug/ml (data not shown). The isotype and Rituximab (Rtx) controls were therefore used at this concentration. For Rituximab however an additional concentration of 10ug/ml was used; this was included in order to have a true positive control for the assay.

In **Fig. 4. 4A**, the CDC activity elicited by all 12 of our own ROR1 chimeric antibodies is shown. Clones R12 and 4a5 were again used as reference, whilst a human IgG1, kappa antibody and Rituximab (anti-CD20 antibody) acted as isotype and positive controls, respectively. Of all antibodies evaluated, clone A was the only one that showed significant cytotoxicity compared to the isotype (p<0.001). Remarkably, clone A was also better at killing CLL cells (<45% live cells) than R12 and 4a5 (>80% live cells) but was still not as CDC active as Rituximab (<10% live cells).
The expression levels of both CD20 and ROR1 antigens on the surface of CLL samples was also assessed (**Fig. 4. 4B**). Interestingly, clone A cytotoxicity seems to be ROR1 level dependent, although further experiments are required in order to conclusively claim this is the case. Also, the highest cytolytic activity is seen on CLL2 ($ROR1^{high}$), whilst the lowest cytotoxicity is detected on CLL1 ($ROR1^{low}$). Similarly, Rituximab is able to kill CD20 expressing cells very efficiently (CLL1 and 2), although this is not the case for CLL3, which is virtually negative for CD20.

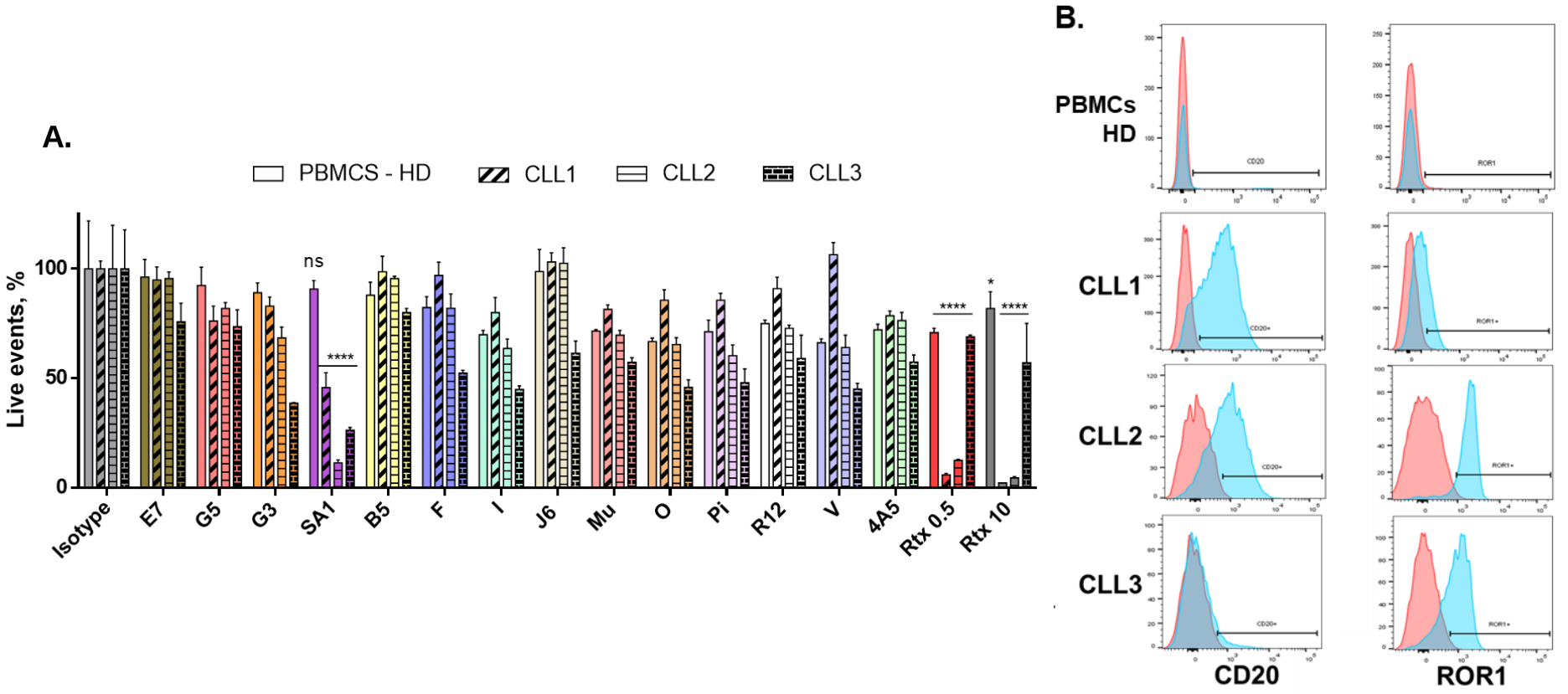

Fig. 4. 4. Complement-dependent cytotoxicity of ROR1 MAbs on CLL cells (n=3). (A) Chimeric ROR1 MAbs supernatants were tested at 0.5ug/ml on CLL cells or PBMCs from a healthy donor (HD). Only clone A showed a significant toxicity compared to the isotype (p<0.0001). Rituximab (Rtx) was used as positive control at 0.5ug/ml and 10ug/ml, and achieved significant cytotoxicity on CLL1 and CLL2 samples (p<0.0001). Cytotoxicity on CLL samples or PBMCs was normalized to the isotype control. (B) Cell surface staining for CD20 and ROR1 by flow cytometry. The red area represents the isotype control. Experiments were done in triplicates. Error bars in (A) represent SD. Statistical test: *2-way ANOVA with Dunnett's multiple comparison test*. ****$p \leq 0.0001$*, ns= not statistically significant. Statistical significance is shown on samples SA1, Rtx 0.5 and Rtx 10 compared to the isotype control.

4.3.4 Aim 4: Assessment of Internalisation

Antibody internalisation can have important implications as it could provide us with the opportunity to develop armed antibodies that could be conjugated to toxic payloads, such as toxins, radioisotopes or chemotherapeutic agents (Peters and Brown, 2015). This class of therapeutic antibodies are called Antibody-Drug Conjugates (ADCs). Interestingly, ADCs could have a therapeutic advantage over naked antibodies (unconjugated), in terms of potency and efficacy, as their cytotoxicity relies on the payload they carry rather than the immune system of patients (Baskar et al., 2012). Thus, I next investigated whether our antibodies were able to get internalised into ROR1^{+} cells by flow cytometry and pH-Amine dye labelling.

4.3.4.1 By flow cytometry

SKW 6.4 cells, Epstein-Barr virus-transformed B cells endogenously expressing comparable levels of ROR1 as CLL patients (See **Fig. 3. 3**), were incubated on ice with all 12 ROR1 chimeric antibodies. After 30min, cells were washed with ice-cold PBS, and either left on ice or incubated at 37°C for 1h. Subsequent staining with an anti-human Fc-Dylight 647 was used to detect any primary antibody that had remained on the cell surface. Previously reported clones R12 and 4a5 were also included in this assay as negative and positive[1] controls, respectively (**Fig. 4. 5**).

From all tested antibodies, clone V (green circle) showed almost complete MFI reduction. A modest but detectable decrease in MFI levels was observed in clones A and F (purple circles), similar to the one detected for clone 4a5. As previously reported, clone R12 did not show considerable MFI reduction after 1h incubation at 37°C.

[1] GF Widhopf II et al. 2014 have reported low although still detectable internalisation of 4a5 by flow cytometry. Due to lack of a better positive internalisation control, clone 4a5 use was referential.

MFI reduction could be caused by dissociation or internalisation or a combination of both (Yang et al., 2011). In order to further investigate what was triggering this drop in MFI for clones V, A and F, an endocytosis inhibitor was used in the next experiments.

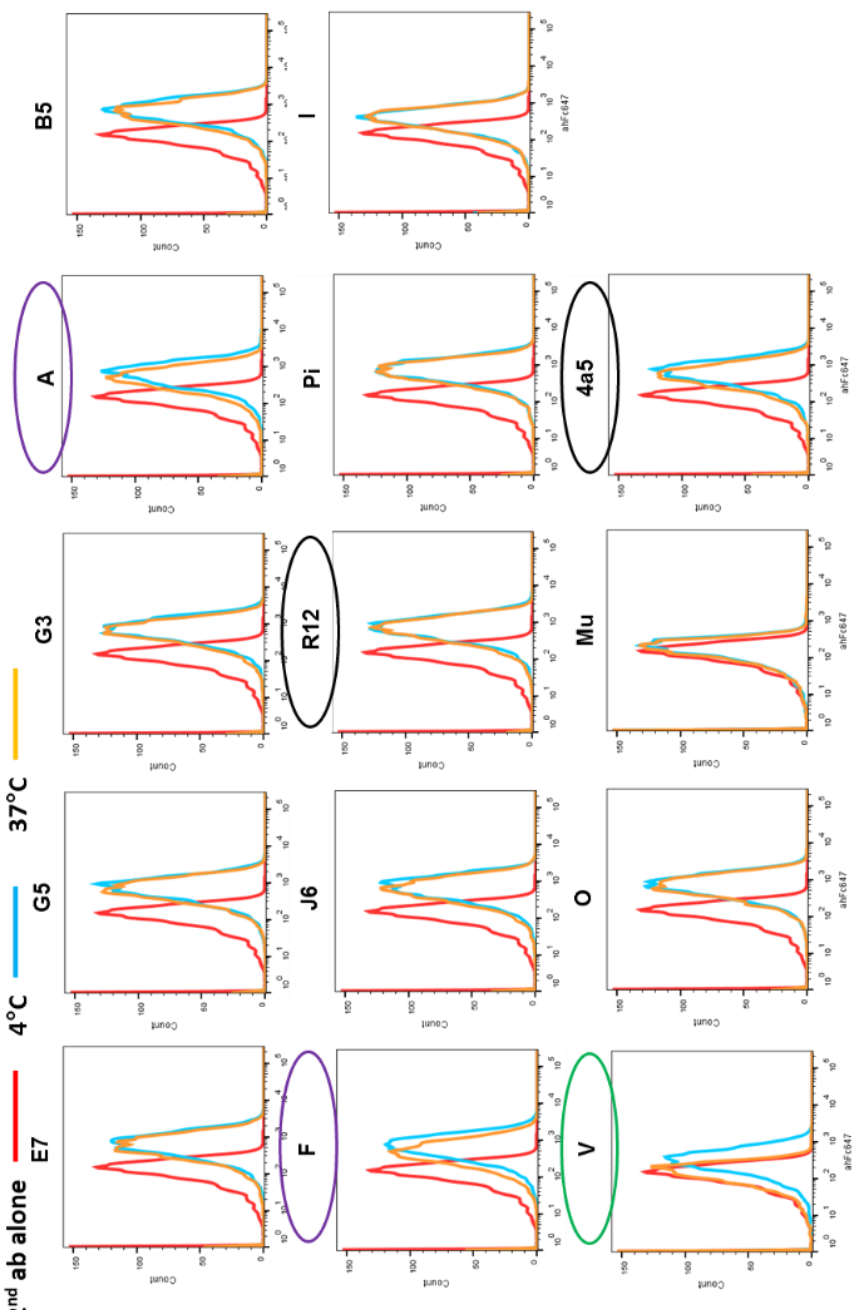

Fig. 4. 5. Internalisation of ROR1 antibodies on SKW 6.4 GFP cells by flow cytometry. SKW 6.4 GFP cells were stained at 4°C and either kept on ice (blue line) or incubated at 37°C (yellow line) for 1h. Of all tested MAbs, clone V showed a pronounced reduction in MFI (green circle). Clones A and F (purple circle) were selected for further investigation. Clones R12 and 4a5 (in black) served as negative and positive control, respectively. Anti-human Fc-Dylight 647 was used as secondary antibody and as staining control (red line). MFI= Median Fluorescence Intensity

4.3.4.1.1 Endocytosis inhibition

Phenylarsine oxide (PAO), a trivalent arsenical compound, is the typical chemical chosen to block Clathryn-mediated endocytosis (CME), although it can also inhibit macropinocytosis and phagocytosis. CME is the best studied mechanism of endocytosis, and it has been established that receptor tyrosine kinases (RTKs), such as ROR1, predominantly use this form of internalisation when engulfed by the cell membrane and drawn inside the cell (Doherty and McMahon, 2009).

To distinguish between dissociation and internalisation, SKW 6.4 cells were incubated on ice in the presence of the selected antibodies for 30min. Cells were then washed with ice-cold PBS and either left on ice or incubated at 37°C for 15min, 1h or 2h. Of note, additional time points were introduced in order to further assess and facilitate internalisation. For the 2h time point, a duplicate sample was incubated with PAO (10μM). Immediately after incubation, all samples were washed with ice-cold PBS and stained with an anti-human Fc-Dylight 647 for 30min (See **Fig. 4. 6**). Cells were analysed by flow cytometry and MFI reduction was calculated as described in **Chapter 2**.

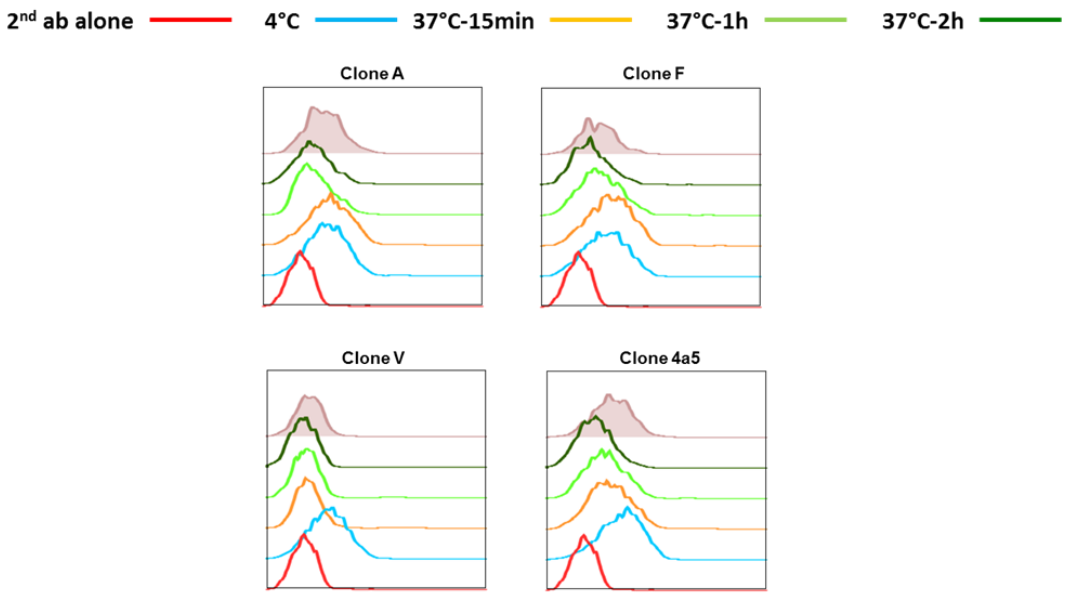

	37°C-15min		37°C-1h		37°C-2h		PAO: 37°C-2h	
	Δ %	Δ MFI	Δ %	Δ MFI	Δ %	Δ MFI	Δ %	Δ MFI
A	-12.98	-12.95	55.98	47.48	66.41	51.08	19.18	13.14
F	-17.54	-19.24	27.73	25.43	64.45	54.30	54.83	44.72
V	89.35	69.40	95.90	74.52	98.82	82.70	92.37	49.52
4a5	37.64	42.38	54.50	53.86	81.51	72.19	24.59	25.38

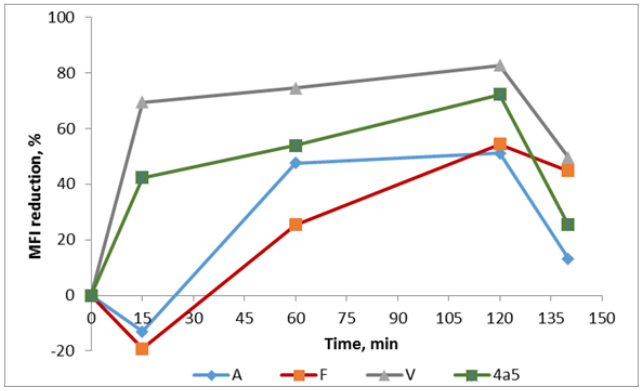

Fig. 4. 6. Internalisation assay of selected clones on SKW 6.4 GFP cells by flow cytometry. Cells were stained with selected clones at 4°C and either left on ice or incubated at 37°C for 15min, 1h and 2h. Cells were then analysed using an anti-human IgG as secondary antibody. (A) Histograms and (B) Trends over time showing the MFI reduction over time are presented. The % of MFI reduction was calculated as described in the Materials and Methods chapter. Phenylarsine oxide (PAO), an endocytosis inhibitor, acted as negative control (PAO-120).

Flow cytometry analysis showed that although clone V had an important MFI reduction, it was mainly due to dissociation as PAO did not considerably block the drop in MFI after 2h incubation at 37°C. A combination of internalisation and dissociation was more evident for the other 3 clones, being internalisation the dominating factor for clone 4a5. This was even more evident for clone A.

To verify these results, the experiment was repeated using SKW 6.4 cells and included 2 samples of primary cells from CLL patients, expressing either high or low levels of ROR1 (**Fig. 4. 7**). Samples were processed as mentioned above and analysed by flow cytometry. Interestingly, these data confirmed that whilst both dissociation and internalisation were involved in MFI reduction, for clone V, dissociation was the main reason for decrease in MFI. This was even clearer on CLL cells, where virtually no internalisation of clone V was detected.

The disappearance of clones F, 4a5 and A from the cell surface of CLL cells was very similar between samples and seemed to be independent of ROR1 levels. In contrast to clone V, internalisation of F, 4a5 and A appeared to be as the main contributing factor to MFI reduction. A similar observation was detected on SKW 6.4 cells; although on this cell model, clone A was the only antibody where MFI drop was almost completely blocked by PAO. Only partial blocking was detected for clones F and 4a5. These findings suggest that although clones F, 4a5 and A might get partially internalised, the latter might be the most promising one. Clone A was therefore further investigated.

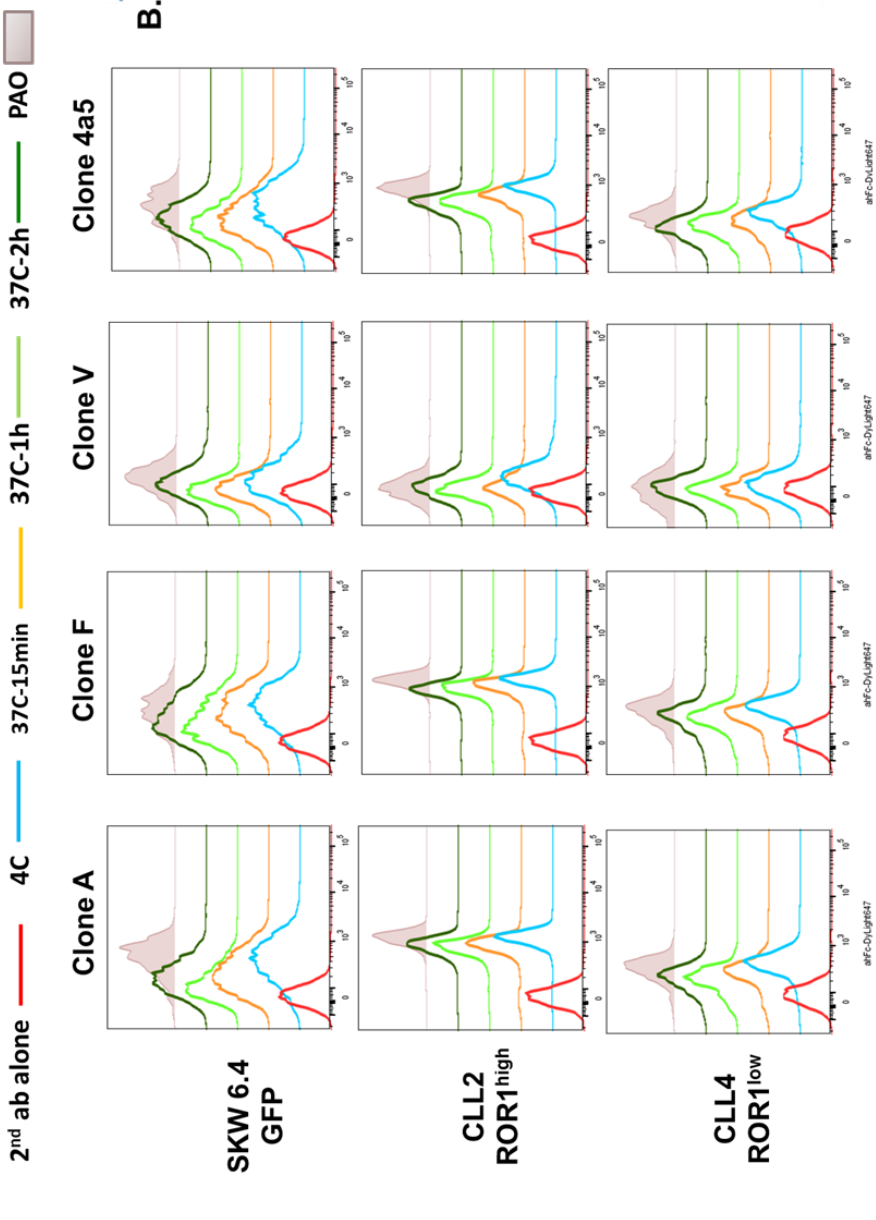

Fig. 4. 7. Internalisation of ROR1 MAbs on SKW 6.4 GFP and CLL cells by flow cytometry. Cells were stained at 4°C and either left on ice or incubated at 37°C for 15min, 1h and 2h. Cells were then analysed using an anti-human IgG as secondary antibody. (A) Histograms and (B) Trends over time showing the MFI reduction over time are presented. The % of MFI reduction was calculated as described in the Materials and Methods chapter. Phenylarsine oxide (PAO), an endocytosis inhibitor, acted as negative control (PAO-120).

4.3.4.1.2 Trypan blue (TB) quenching effect

To assess whether clone A was an internalising antibody with potential to be developed as an antibody-drug conjugate (ADC), it was conjugated to the AlexaFluor488 fluorophore so that direct analysis of the antibody could be performed.

To this end, our group set up a collaboration with Dr Vijay Chudasama's research group at the UCL Dept. of Chemistry. Dr Chudasama's group has developed a novel site-selective technique that incorporates a serum-stable linker bearing a strained alkyne, a functional group that can be reacted cleanly in the presence of all amino acids in a so-called "click" reaction. Importantly, this reaction does not negatively affect antibody properties, including their specificity (Chudasama et al., 2016, Nunes et al., 2015).

Therefore, I produced a large amount of clone A in-house and purified it by FPLC, using the AKTA system as detailed in the Materials & Methods section. Elution fractions were run on SDS-PAGE and stained with Coomassie dye in order to select those fractions containing the antibody (See **Fig. 4. 8**). Clone A, henceforth called clone SA1, was then dialysed in Borate buffer with EDTA, pH 8.0. Antibody was then concentrated in order to attain a 3-6mg/ml concentration, a requirement that needed to be met in order to ensure successful conjugation of clone SA1 to AlexaFluor 488, using the "click" technology developed by our collaborators.

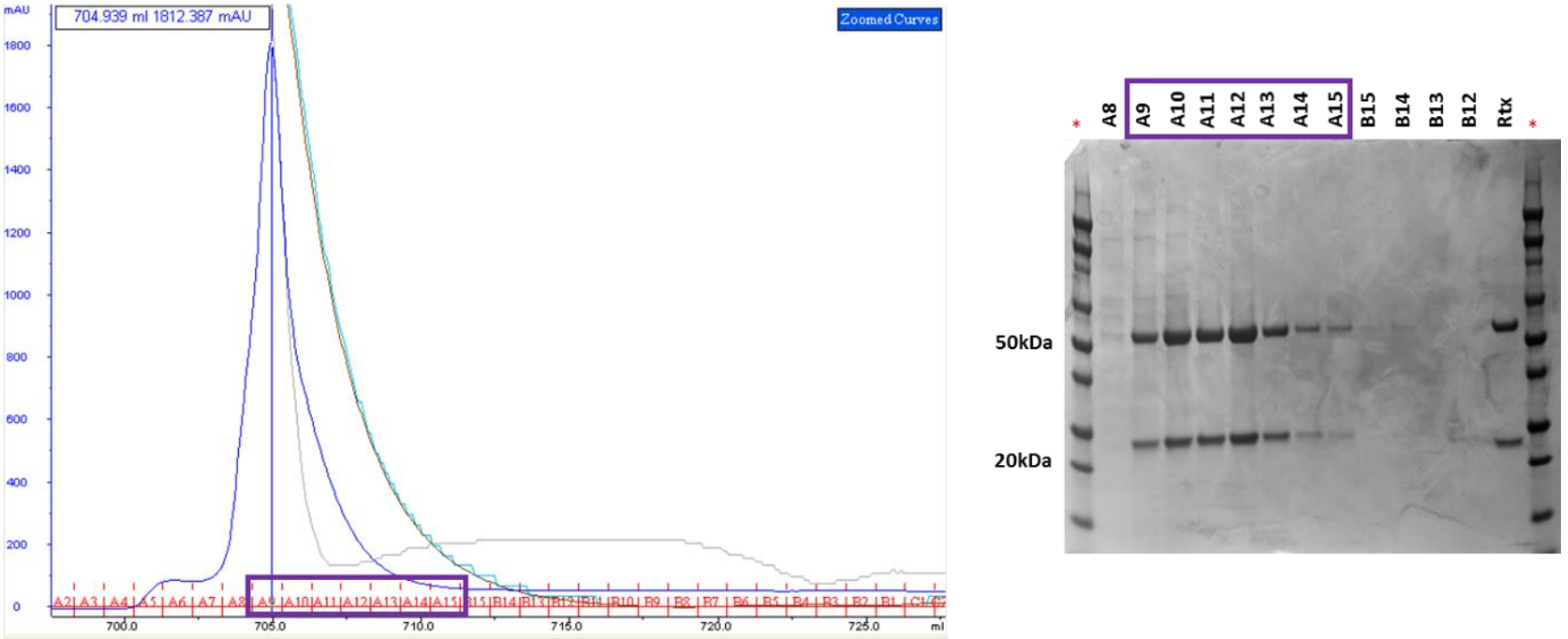

Fig. 4. 8. AKTA purification of clone A antibody using a 5ml Protein A column. A total volume of 300ml of supernatant from transiently transfected 293T were harvested 72h post-transfection. 293T were cultured in FBS supplemented IMDM until transfection. 12h after cell media was replaced with fresh phenol-red free IMDM supplemented with ultra-low IgG HI-FBS. Supernatant was centrifuged, filtered and dilute with Protein A Binding buffer in a 1:1 ratio, in order to be then purified by FPLC. Elution fractions A8-B12 were run in a SDS-PAGE and stained with Coomassie dye. Fractions A9-A15 (purple square) were pooled together and dialysed in Borate buffer with EDTA, pH 8.0.

Dr Antoine Maruani, a postdoctoral researcher at Dr Chudasama's group was in charge of the antibody labelling. Using the same "click" technology applied to ADCs, Dr Maruani successfully conjugated clone SA1 to the fluorophore in a clean and homogeneous manner, as evidenced by an SDS-PAGE stained with Coomassie dye and exposed to UV light in order to show an efficient conjugation (See **Fig. 4. 9**).

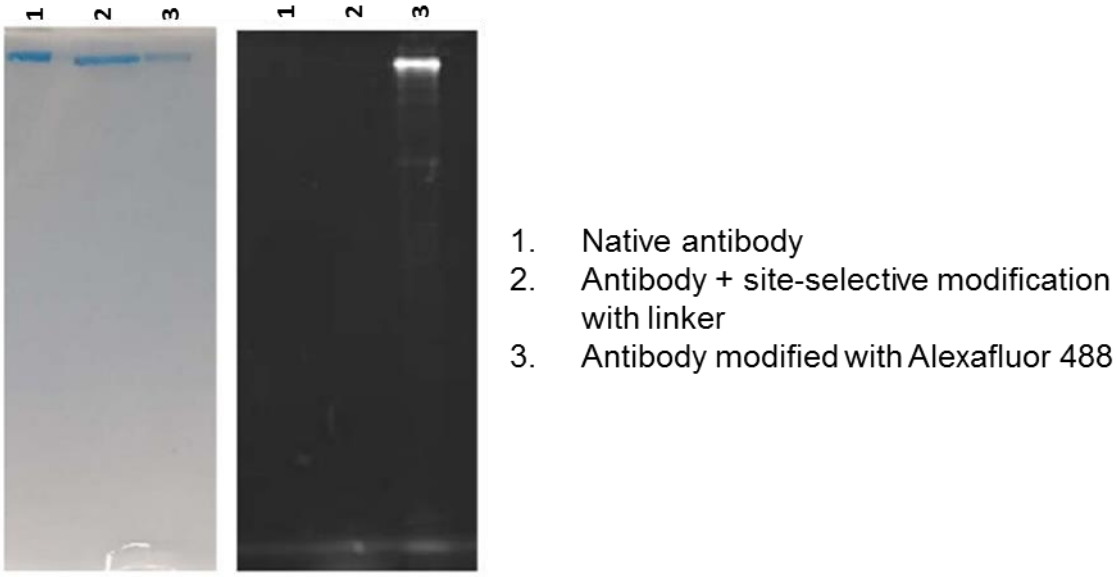

Fig. 4. 9. SDS-PAGE stained with Coomassie blue/under UV lamp. SA1 dialysed in Borate buffer with EDTA, pH 8.0 (native antibody) along with SA1 coupled with a linker after site-selective modification, and SA1 conjugated to Alexafluor488 using the same site-selective linker were run in a SDS-PAGE. The gel was stained with Coomassie dye and exposed to UV lamp in order to detect a fluorescence signal.

Before proceeding with the internalisation assay, I decided to test and compare the binding of the following antibodies: i) Clone SA1, produced and purified in-house and dialysed in PBS as per usual (SA1 Ctrl), ii) Clone SA1, produced and purified in-house and dialysed in Borate buffer with EDTA, pH 8.0 (SA1 Unconjugated), and iii) Clone SA1, dialysed in Borate buffer with EDTA, pH 8.0 and conjugated to AlexaFluor488 (SA1 AF488). These antibodies were incubated with either non-transduced or eGFP-ROR1 transduced SUP-T1

cells (SUP-T1 NT and SUP-T1 61, respectively). Incubation was done for 30min at 4°C. After this, cells were washed and stained with an anti-human Fab-DyLight647 secondary antibody (**Fig. 4. 10**). Importantly, an anti-Fab and not an anti-human Fc antibody was used for this experiment. The rationale for this was that the site-selective conjugation of the fluorophore involved the Fc region of the SA1 antibody, potentially blocking the anti-Fc antibody binding to SA1.

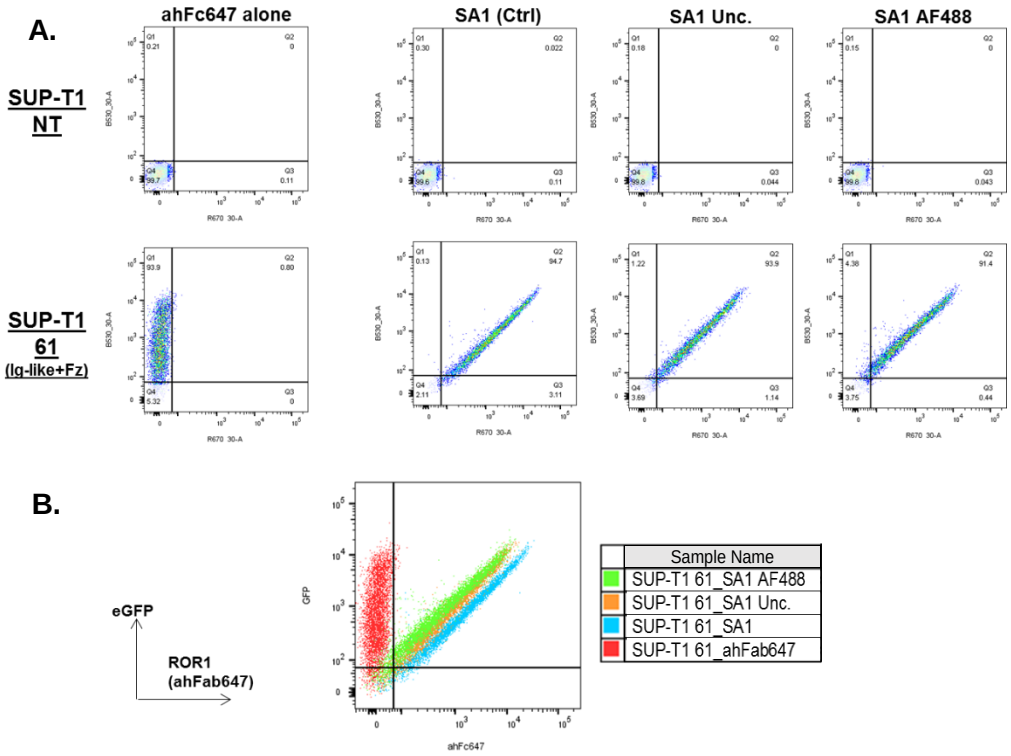

Fig. 4. 10. Binding evaluation of unconjugated and conjugated clone SA1 on ROR1$^-$ and ROR1$^+$ cell lines. Clone SA1 dialysed in PBS (SA1 Ctrl), SA1 dialysed in Borate buffer with EDTA, pH 8.0 (SA1 Unconjugated), and SA1 dialysed in Borate buffer and conjugated to AlexaFluor 488 (SA1 AF488) were incubated with eGFP$^-$ROR1$^-$ (SUP-T1 NT) and eGFP$^+$ROR1$^+$ cells (SUP-T1 61). After the first staining, cells were washed and stained with an anti-human Fab-Dylight647 secondary antibody. (A) Individual dot plots of eGFP against ahFab647 of all 3 antibodies tested against SUP-T1 NT and SUP-T1 61 are shown. (B) The overlap of antibodies tested on eGFP$^+$ROR1$^+$ cells is shown for comparison. eGFP= enhanced green fluorescent protein, ahFab= anti-human Fab-Dylight647 antibody.

Fig. 4. 10A shows the specific binding of all versions of clone SA1 antibody to SUP-T1 61 cells (GFP$^+$ROR1$^+$), presenting all 3 antibodies very similar % of

frequency. It is in **Fig. 4. 10B** however where the difference in binding can be detected. The overlap dot plot indicates that the binding of clone SA1 dialysed in PBS (in blue) have the best binding to SUP-T1 61 cells compared to the other two versions of SA1 dialysed in borate buffer. Importantly, there seems to be no major difference between SA1 Unc. (in yellow) and SA1-AF488 (in green), suggesting that the addition of the fluorophore via the site-selective linker might not be responsible for the decrease of binding; a phenomenon that rather might be explained by the change of dialysis buffer.

Having confirmed that SA1-AF488 ab was still able to bind to ROR1^{+} cells, I proceeded to test its ability to get internalised into ROR1-expressing cells. For this experiment, the Trypan blue (TB) quenching effect was used to distinguish antibody molecules internalised from those attached to the cell membrane (Thiele et al., 2001, Patino et al., 2015). Briefly, SA1-AF488 was incubated with Jeko-1 cells, a Mantle cell lymphoma cell line that endogenously express high levels of ROR1. After 30min incubation, cells were washed with ice-cold PBS and either left on ice or incubated for 15min or 2h at 37°C. AlexaFluor488 fluorescence was then analysed before and after addition of TB (**Fig. 4. 11**).

In **Fig. 4. 11A**, at time point “0h”, fluorescence was completely eliminated after TB addition, validating the quenching effect of this reagent. At time points “15min” and “2h”, it is observed that -before TB addition- AlexaFluor488 signal is partially reduced compared to time “0h”; suggesting that the disappearance of fluorescence is due to dissociation of the antibody from the cell surface. This is consistent with my previous results, where a combination of dissociation and internalisation were responsible for MFI reduction.

For the remaining signal detected at the “15min” time point, it was observed that it was caused by both antibody bound to the cell membrane and antibody molecules present inside the cell, as evidenced by signal detection even after addition of TB. At the “2h” time point however the main factor contributing to AlexaFluor488 detection was internalisation. **Fig. 4. 11B** provides with a bar graph representation of the MFI ratio (MFIR) calculated by dividing the MFI of Jeko-1 cells stained with SA1-AF488 (in the absence or presence of TB) and the negative control.

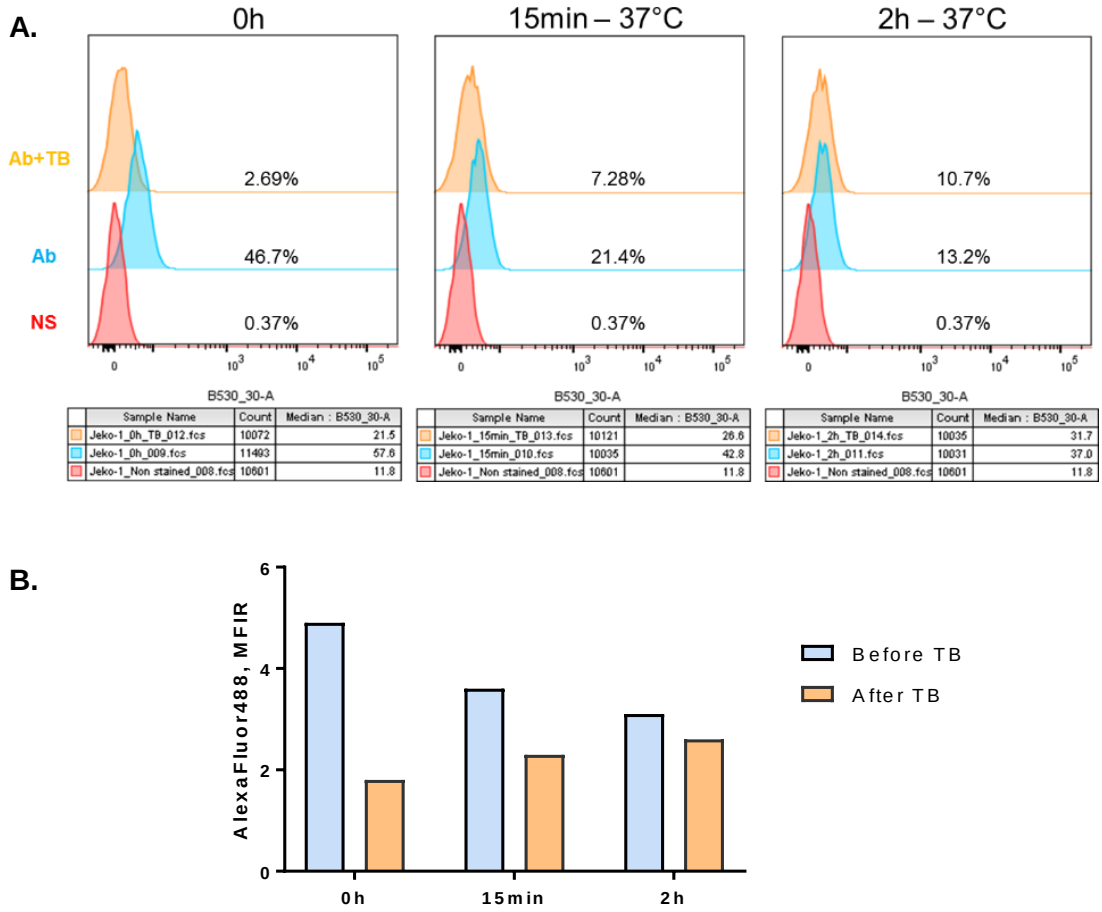

Fig. 4. 11. Binding evaluation of clone SA1-AF488 on Jeko-1 cells using the quenching effect of Trypan Blue (TB). Jeko-1 cells were stained with SA1-AF488 antibody for 30min at 4°C. Cells were then washed with ice-cold PBS and either left on ice or incubated at 37°C for 15min or 2h. Samples were analysed by flow cytometry in the absence or presence of TB. (A)Histograms of the fluorescence intensity of AlexaFluor488 before addition of TB (in blue) and after (in yellow) are shown. Non-stained cells acted as negative control (red histogram). Both % of frequency and MFI values are included within the histograms and in tables, respectively. (B) Bars represent the MFI ratio between samples stained with SA1-AF488 ab and negative control. MFIR= Median fluorescence intensity ratio.

4.3.4.2 pHAb-Amine dye labelling

pHAb-Amine dyes are pH sensor dyes that have very low fluorescence at pH≥7. However, a dramatic increase in fluorescent signal is detected at pH<6; when they internalise into the cells and traffic into acidic pH vesicles like the endosome or lysosome (Nath et al., 2016).

The key advantage of this reagent is that antibodies labelled with pHAb dyes will not fluoresce upon binding to the cell membrane due to the neutral pH of the media. After receptor-mediated internalisation however antibodies will get transported into early endosomes and lysosomes, where the dye will fluoresce due to the acidic pH of said vesicles. This detectable and significant increase in fluorescence at low pH makes this approach suitable for monitoring antibody internalisation.

Therefore, to validate previous observations, clones SA1 and F were labelled with a pHAb Amine dye kit (Promega). This time, based on studies by Nath et al., 2016, internalisation over a 24h period was assessed. To this end, SKW 6.4 and Jeko-1 cells, both expressing endogenous ROR1, were incubated with pHAb Amine-labelled SA1 and F. As before, cells were incubated with these antibodies for 30min at 4°C. After this, cells were washed with ice-cold PBS and immediately read at Ex/Em: 532nm/562nm (“0h” time point). Cells were then incubated at 37°C and 5%CO_2 for 15min, 2, 5, 21 and 24h. After each time point, fluorescence was evaluated using a plate-reader. Of note, citrate buffer pH 4 was used as positive control for fluorescence signal (**Fig. 4. 12**).

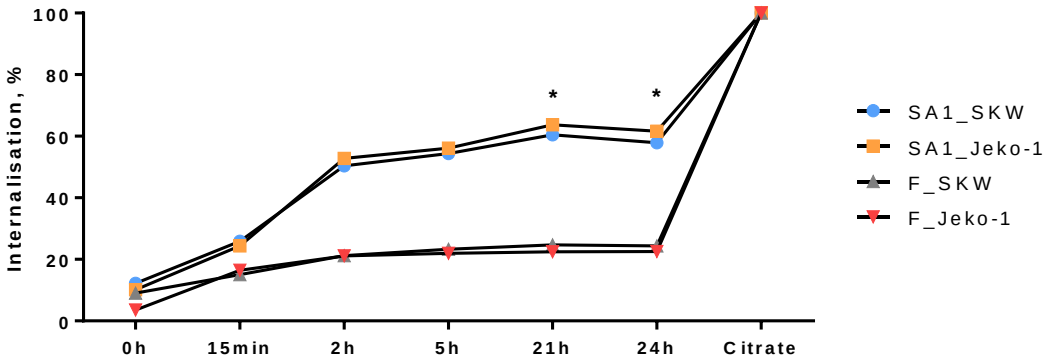

Fig. 4. 12. pH-dependent fluorescence using pHAb Amine reactive labelled clones F and SA1 ROR1 MAbs on ROR1^{+} cell lines. SKW 6.4 and Jeko-1 cells were incubated with pHAb Amine-labelled SA1 and F antibodies for 30min on ice. After a thorough wash, fluorescence was read at Ex/Em: 532nm/562nm for the "0h" time point. Cells were then incubated at 37C for 15min, 2, 5, 21 and 24h. Fluorescence was read after each time point. Citrate buffer, pH 4.0 acted as positive control for fluorescence signal. Data from all time points was normalised to positive control fluorescence values. * indicates statistical significance of the differences between SA1 and F groups at those time points, as calculated using two-way ANOVA analysis ($p<0.05$).

An increasing difference in fluorescence levels between clone F and clone SA1 labelled with pHAb amine dye was observed throughout all time points. The inclusion of Citrate buffer, pH 4.0 served to test for the successful conjugation of both antibodies to the pHAb amine dye, as fluorescence would only be detectable at low pH. A calculation of the fold increase in fluorescence can be seen in **Table 4. 2**.

Table 4. 2. Measure of pHAb amine-labelled antibody response to pH, using the "Fold increase" formula shown in the Materials & Methods section (Chapter 2)

Antibody	SKW 6.4	Jeko-1
SA1	8.22	9.92
F	11.10	28.51

Fluorescence readouts from all time points were normalised to those from the positive control. Data confirms that internalisation can be detected even after 15min and that it intensifies over time, becoming significantly higher than the one caused, on both cell lines, by F antibody at both 21 and 24h time points. Remarkably, this approach confirms that not all antibody gets internalised, as evidenced by the level of fluorescence detected. As seen in previous results, data from this experiment also suggest that a combination of both dissociation and internalisation take place for both antibodies. Of which, dissociation is the main factor for clone F as it is internalisation for clone SA1.

4.4 Discussion

In this chapter, data have shown that, out of 12 ROR1-binding antibodies, 10 recognise the Ig-like extracellular domain of ROR1. This is likely due to the fact that this domain represents the most immunogenic portion of ROR1. An interesting observation was that clones V and Mu might possess a conformational epitope that requires the presence of both the Ig-like and the Fz domain. Alternatively, they could bind to a stretch of amino acids or continuous epitope located at the junction of these two domains. This could be further investigated by other methods of epitope mapping, such as peptide library ELISA.

Clone F stands out as the only chimeric antibody able to bind the Fz domain alone; which is a notable feature as it has been shown that it is through the Fz domain that Wnt5a mediate its signalling (Fukuda et al., 2008). Furthermore, none of our antibodies targeted the Kg domain of ROR1. This is not surprising as human and rat have a sequence identity of 99% for these two domains, as revealed by UniProt alignment (data not shown).

Although the gold standard for epitope mapping is x-ray analyses of antigen:antibody complexes, this technique requires a high degree of instrumentalisation and expertise. Plus, it is not readily applicable to many

antigens and antibodies (Gershoni et al., 2007). Hence, the identification of binding domains by the use of cell lines expressing truncated domains of ROR1 was particularly suitable; with the additional advantage that it allows the study of both discontinuous (conformational) and continuous (linear) epitopes.

I then investigated the binding kinetics of our chimeric antibodies by surface plasmon resonance (Biacore systems), and found that all tested clones had nanomolar affinities. Unfortunately, K_D values for clones V and Mu could not be calculated as their binding kinetics were not able to be determined. A possible explanation for this might be the complex interaction of these clones with ROR1. This is consistent with flow cytometry data which showed both modest and difficult binding to ROR1, possibly caused by a discontinuous epitope.

Out of the 10 clones successfully analysed by SPR, clones B5, A and Pi possessed the strongest affinities: 1.51, 1.81 and 1.98nM, respectively. Interestingly, the only antibody targeting the Fz domain (clone F) showed the lowest K_D value (5.46nM).

Since the overriding goal of this thesis is to develop an anti ROR1-based approach for cancer immunotherapy, the next step was to evaluate the cytolytic activity of our antibodies by CDC. ROR1 antibodies have been first shown to elicit cytotoxicity on samples from patients with chronic lymphocytic leukaemia (CLL) (Borcherding et al., 2014, Choi et al., 2015, Daneshmanesh et al., 2012, Lapalombella et al., 2010, Widhopf et al., 2014). Accordingly, all 12 of our chimeric antibodies on CLL samples were tested and it was found that clone A was the only antibody able to produce significant CDC activity after 2h. Rituximab however showed a more potent cytotoxicity under the same conditions. It is hypothesised that the low CDC activity exerted by all the other clones might be due to low ROR1 antigen density on target cells coupled with low antibody affinity.

Naked antibodies exert their cytotoxic activity mainly through the activation of the immune system via their Fc region (Scott et al., 2012). Antibody-drug conjugates (ADCs), on the other hand, combine the specificity of monoclonal antibodies and the toxicity of, predominantly, chemotherapeutic drugs (Peters and Brown, 2015). This feature may be particularly advantageous as its therapeutic effect do not rely on the immune system of cancer patients. I therefore set out to explore if any of our clones was an internalising antibody.

Internalisation was first studied by flow cytometry. Data showed that out of all tested antibodies, clones V, F and A showed MFI reduction after 1h incubation at 37°C, using cells that express endogenous ROR1 (SKW 6.4). In this context, MFI reduction could be explained by either dissociation or internalisation (Yang et al., 2011); as a result, these clones were evaluated further.

To distinguish between dissociation and internalisation, Phenylarsine oxide (PAO), an endocytosis inhibitor, was included in these studies. The key advantage of PAO is that it blocks the main types of endocytosis by which RTKs get engulfed into the cells, namely CME and macropinocytosis (Doherty and McMahon, 2009). Furthermore, when used at concentrations <20μM, it does not significantly interfere with other cells functions (Gibson et al., 1989). In my experiments, PAO was used at 10μM as it has been shown that this concentration is enough to inhibit endocytosis (Gibson et al., 1989, Yang et al., 2011).

PAO inclusion revealed that both dissociation and internalisation were responsible for the MFI reduction seen in all three antibodies. Experiments performed on both SKW 6.4 and CLL cells showed more clearly that despite this combination of factors, dissociation was the main feature for clone V. Also, dissociation partially explained the drop in MFI levels for clone F and, to a lesser extent, clone A. Consequently, internalisation was the main contributing factor for the latter, as evidenced by almost complete blocking of MFI reduction at the 2h time point, particularly on SKW 6.4 cells.

To validate these observations, clone A (aka SA1) was conjugated to AlexaFluor488 using a novel site-selective linker developed by Dr Chudasama's research group. This so-called "click" reaction is particularly useful in ADC technology, as it significantly reduces the levels of heterogeneity usually responsible for the lack of efficiency seen in some ADC preparations, without negatively affecting antibody properties (Maruani et al., 2016, Nunes et al., 2015, Maruani et al., 2015). Through this collaboration, clone SA1-AF488 was produced, and subsequently tested on Jeko-1 cells, which also express endogenous ROR1.

Prior to internalisation experiments, I sought to verify that conjugation of SA1 -using the same "click" reaction applied to ADCs- did not affect its binding to ROR1. To this end, a head-to-head comparison of: i) SA1 antibody dialysed in PBS, ii) SA1 antibody dialysed in Borate buffer, pH 8.0 and iii) SA1-AF488 dialysed in the latter buffer was performed. Flow cytometry data showed that conjugation of AlexaFluor488 to SA1 did not alter antibody binding. However, the change in dialysis buffer, from PBS to Borate buffer, pH 8.0 seemed to visibly affect the efficiency of antibody-antigen recognition.

Internalisation was then investigated by exploiting the quenching effect that Trypan blue (TB) has on extracellular compounds labelled with a fluorophore detectable in the FITC channel, such as AlexaFluor488 (Sahlin et al., 1983, Thiele et al., 2001). Although the precise mechanism of quenching remains unclear, it is known that TB is able to absorb light in the range of FITC when bound to proteins (Thiele et al., 2001). Due to its physico-chemical properties, TB cannot pass intact membranes of live cells. Thus, the recorded fluorescence strictly originates from internalised antibody in viable cells (Thiele et al., 2003, Patino et al., 2015)

Flow cytometry data after TB addition confirmed previous observations, whereby a combination of both dissociation and internalisation were detected.

Internalisation however was again identified as the main contributing factor for clone SA1-AF488, as evidenced by signal detection in the presence of TB.

Lastly, a third approach was used to validate internalisation of clone SA1: pHAb dye labelling. This method uses pH sensor dyes that have virtually no fluorescence at neutral pH but become highly fluorescent at acidic pH, such as that found inside cellular vesicles (Nath et al., 2016). Clones F and SA1 were labelled with these pHAb dyes, and internalisation was assessed on both SKW 6.4 and Jeko-1 cells over a 24h period. Data confirmed that both dissociation and internalisation take place for both antibodies; being dissociation the main explanation for clone F and internalisation for SA1 antibody.

It is worth mentioning that using a visual approach such as confocal microscopy would have been more informative and would have probably provided conclusive data. Unfortunately, this methodology was not readily available in our lab at that stage of this thesis. Nonetheless, taken together, these data suggest that: i) clone F, due to its binding to the Fz domain, and ii) clone SA1, due to its CDC activity and internalisation profile might have therapeutic potential and merit further investigation.

4.4.1 Conclusions

- A total of 10 ROR1 chimeric antibodies specifically recognise the Ig-like extracellular domain of ROR1.
- Clone F is the only ROR1 antibody that binds to the Fz domain.
- Clones V and Mu seem to either recognise the portion between the Ig-like and the Fz domains, or a conformational epitope formed only when both domains are present.
- All tested clones presented nanomolar affinities. Of these, clones B5, A and Pi possessed the highest K_D values, unlike clone F, which had the weakest affinity.

- Further optimisation of Biacore analyses for clones V and Mu is needed in order to successfully determine their binding kinetics.
- Clone A was the only chimeric antibody to elicit significant CDC activity on CLL primary cells, although it was not as potent as the one produced by Rituximab.
- Dissociation was found to be the main cause for MFI reduction of clone V, and partially for clones F and A. Accordingly, internalisation was the main contributing factor on the disappearance of clone A from the cell surface.
- The latter observations were further confirmed by direct conjugation of clone A (aka SA1) to AlexaFluor488 fluorophore, and by labelling of clones F and SA1 using pHAb amine dyes.
- Clones F and SA1 will be investigated further in the next chapters.

4.4.2 Future work

More extensive characterisation of our ROR1 antibodies is needed in order to identify relevant tools for investigative research or for diagnostic applications. A key step in this process is to perform antibody profiling using different assay systems (Nelson et al., 2000). This is of particular importance as some antibodies may perform well in some systems but not in others. Briefly, this relates to how an antibody binds its target epitope in the context of the system used, a phenomenon known as assay restriction (Jefferis et al., 1985).

With regards to internalisation assays, confocal microscopy would be a preferable approach over flow cytometry as it would not only allow the investigator to visually assess antibody internalisation, but -depending on the staining strategy- it would potentially provide with information of antibody trafficking inside the cell.

Chapter 5 Further analysis of clones F and SA1

5.1 Introduction

Flow cytometry data presented in **Chapter 4** showed that clones SA1 and F bound to the Ig-like and Frizzled (Fz) domains of ROR1, respectively. Here, the first aim was to further investigate the uniqueness of binding of these two clones by four different methods: i) peptide library ELISA, ii) Western blot, iii) single amino acid mutations, and iv) flow cytometry-based competition assays.

Based on previous CDC screening data, the second aim was to focus cytotoxicity studies on clone SA1. To this end, its CDC activity on cell lines and primary cells from both CLL patients and healthy donors was assessed. Importantly, for these evaluations, purified SA1 antibody at standard concentrations previously reported in pre-clinical studies (Barth et al., 2015, Herter et al., 2013) was used.

Lastly, in order to enhance its therapeutic potential, the third aim involved humanisation of the variable regions of clone SA1 through collaboration with GenScript. In the following sections, findings obtained from: i) fusion of humanised variable domains to human constant regions (IgG1, k), ii) binding analyses of humanised antibodies to ROR1-expressing cells by flow cytometry, and iii) cytotoxicity assays of the novel humanised clones on primary cells from CLL patients and healthy donors will be discussed. Cytotoxicity potential was again evaluated through a CDC assay; where clone SA1 and two clinically approved anti-CD20 antibodies were used for comparison.

Of note, clone F was also chosen for humanisation. Unlike SA1, and based on its cytotoxicity as a full IgG antibody, the therapeutic potential of clone F was

explored using solely antibody derivatives, such as chimeric antigen receptors (CARs) and bispecific T-cell engagers (BiTEs) by other members of our group.

Since humanisation is a pivotal step in the development of therapeutic antibodies, and considering that the majority of approved monoclonal antibodies used in cancer therapy are humanised antibodies (Pillay et al., 2011), a brief introduction on this subject is provided below.

5.1.1 Humanisation of monoclonal antibodies

As discussed in **Chapter 3**, the first attempt to reduce unwanted immunogenicity of mouse-derived antibodies involved genetic engineering techniques that resulted in the generation of chimeric mouse-human antibodies (Boulianne et al., 1984). Nevertheless, it has been reported that, in some cases, chimeric antibodies were still able to prompt a human anti-chimeric antibody (HACA) response (Hwang and Foote, 2005). Therefore, the next logical step was to further engineer chimeric antibodies in order to produce humanised binders.

In general, humanised antibodies possess a protein sequence that is essentially identical to that of a human variant, except for the non-human origin of its complementarity determining region (CDR) segments. The latter are essential for antibody recognition and subsequent binding to the epitope of its target antigen (Wootla et al., 2014).

So far, researchers have developed several rational approaches in order to produce humanised monoclonal antibodies (Safdari et al., 2013), among them: CDR-grafting, framework (FR) shuffling (Dall'Acqua et al., 2005), resurfacing (Padlan, 1991), and super-humanisation (CDR homology) (Tan et al., 2002).

I will focus the rest of this brief introduction to CDR-grafting, as this was the first method developed for humanisation purposes (Jones et al., 1986); and,

to date, remains widely-used in the field. Notably, CDR-grafting has been used to generate most of the humanised antibodies currently available in the clinic (Safdari et al., 2013).

5.1.1.1 CDR-grafting

CDRs are the segments within the variable regions of an antibody responsible for antigen recognition. The CDR-grafting approach therefore involves insertion of the appropriate non-human CDRs into a human antibody “scaffold” (human framework sequences). As a result, this humanisation method may have some structural consequences that can potentially produce conformational changes, ultimately affecting antigen binding affinity (Dall'Acqua et al., 2005). Importantly, an approach that is regularly used to circumvent this issue is the identification of human FRs with the highest homology to the FR regions of the non-human antibody. By the use of these potential FR acceptors, CDR conformation and V domain orientation is likely to remain unaffected. (Safdari et al., 2013, Cheung et al., 2012).

One of the most relevant examples of humanised antibodies produced using this approach is Alemtuzumab, an anti-CD52 antibody, originally used in the treatment of CLL patients (Lozanski et al., 2004). In line with this and other monoclonal antibodies used in cancer therapy, CDR-grafting was the method of choice for humanisation of our own ROR1 antibodies.

In **Fig. 5. 1**, a schematic representation of the humanisation process of a rat monoclonal antibody is presented.

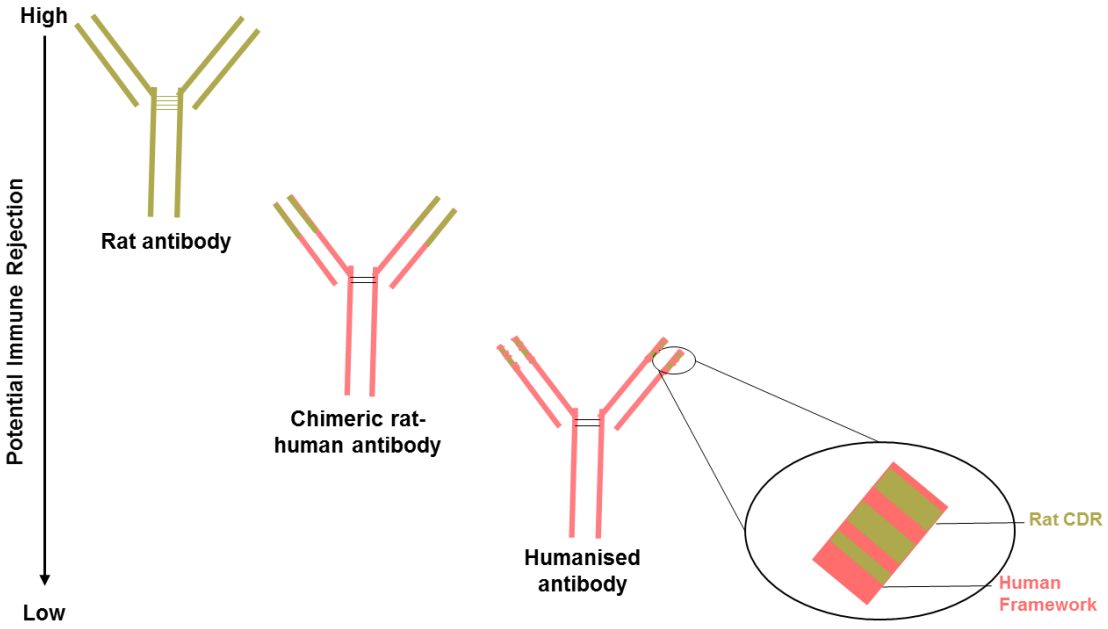

Fig. 5. 1. Schematic humanisation process of chimeric rat-human MAbs by CDR-grafting. Humanised antibodies derived from rat-human chimeric versions still possess rat CDRs that have been grafted in human framework acceptor sequences, thereby significantly reducing unwanted immunogenicity. CDR= Complementarity determining region.

5.2 Aims

1. To perform a fine epitope mapping in order to ascertain the specific amino acids targeted by clones SA1 and F.
2. To assess the complement-dependent cytotoxicity (CDC) *in vitro* of purified SA1 antibody using cell lines and primary cells from CLL patients and healthy donors.
3. To generate humanised antibodies against ROR1 based on SA1's protein sequence (in collaboration with GenScript); and to assess their binding to ROR1 and evaluate their cytotoxicity on primary CLL and healthy donor cells by direct cell death, CDC, and ADCC assays.

5.3 Results

5.3.1 Aim 1: Fine epitope mapping: Clones F and SA1

To further investigate whether clones SA1 and F were able to detect a unique epitope (i.e. distinct from the ones recognised by clones previously reported in the literature), four different approaches were undertaken:

5.3.1.1 By overlapping peptide-library ELISA: In collaboration with Mimotopes Ltd

Monoclonal antibodies can detect continuous (linear) or discontinuous (conformational) epitopes (Nelson et al., 2000). In order to investigate the former, an overlapping peptide library based on the extracellular portion of ROR1 (**Fig. 5. 2**) was synthesised in collaboration with Mimotopes Ltd.

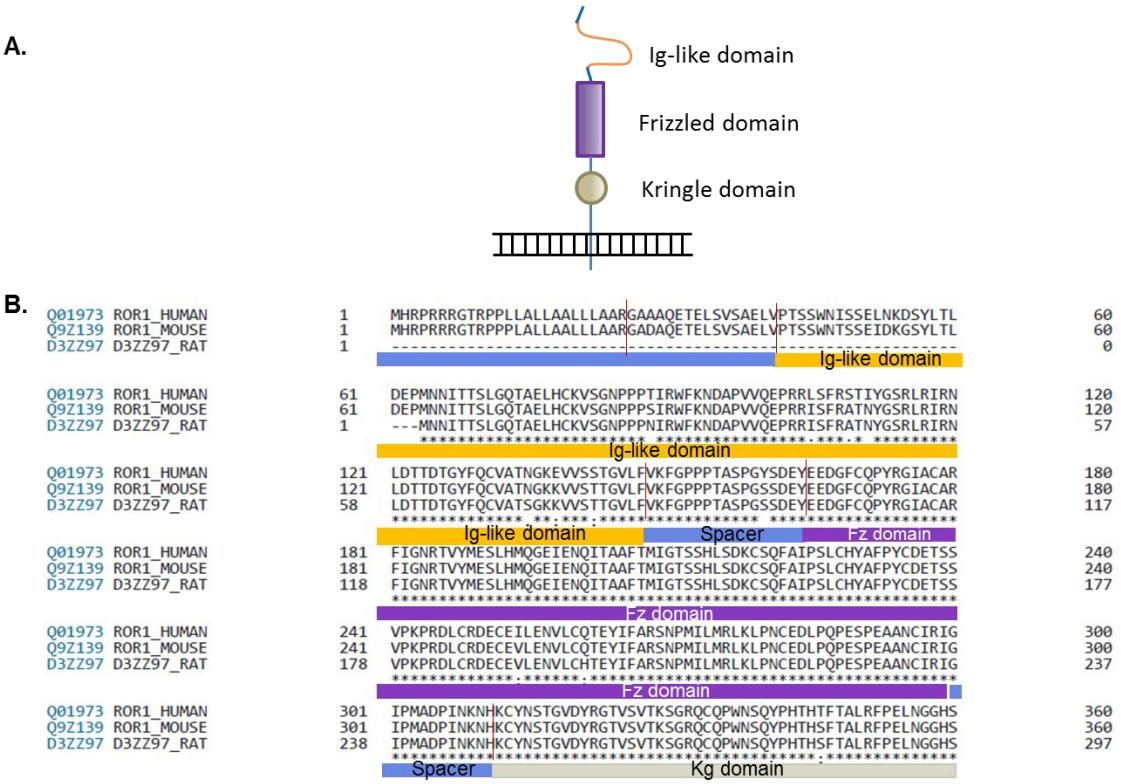

Fig. 5. 2. Extracellular ROR1 (eROR1). (A) Schematic of the extracellular portion of ROR1, indicating its three domains. (B) Alignment of human, mouse and rat amino acid sequences of eROR1. The regions encoded by these sequences are annotated. Ig-like= Immunoglobulin-like, Fz= Frizzled, Kg= Kringle.

Mimotope's ROR1 peptide library contained more than ninety overlapping peptides. Each peptide was composed of biotin (at the N-terminal), followed by a linker that connected it to a sequence of 11 amino acids (aa) of eROR1, followed by an amide group (NH_2) at the C-terminal (See **Fig. 5. 3A**). Of note, each 11-aa peptide had 8 amino acids that overlapped the previous peptide whilst introducing 3 new aa to its sequence.

Lyophilised eROR1 peptides were solubilised in 50% Acetonitrile and processed for ELISA evaluation as described in the Materials & Methods section (**Chapter 2**). Briefly, 96-well plates were coated with NeutrAvidin, blocked with 1% sodium caseinate and washed thoroughly before incubation with the solubilised peptides. After 1h incubation, plates were washed again and incubated o/n with clones SA1 and F. On the next day, plates were washed and incubated for 1h with an anti-human IgG antibody conjugated to horseradish peroxidase (HRP). Plates were washed, and antibody signal detected with Tetramethylbenzidine (TMB); the reaction was then stopped with H_2SO_4. A graphic representation of this sandwich ELISA can be found in **Fig. 5. 3B**.

In **Fig. 5. 3C**, the reactivity of clones SA1 and F to the overlapping peptides by ELISA are shown. As expected, clone SA1 produced a clear and defined peak in peptides 13-17, which corresponded to the apical portion of the Ig-like domain. This data is consistent with previous observations obtained by flow cytometry (**Chapter 4**). Peaks below an absorbance (Abs) value of 0.5 were considered background as even the negative control (peptide and antibody provided by Mimotopes) had an absorbance value of approximately 0.4. In contrast, the absorbance produced by the positive control (also provided by Mimotopes) reached a peak value of 1.0 as did SA1 with peptides 13-17.

Clone F, on the other hand, did not produce any relevant peaks above background, although positive and negative controls worked accordingly.

Independent repeats of this experiment confirmed this observation, which led me to hypothesise that clone F might not have a continuous epitope.

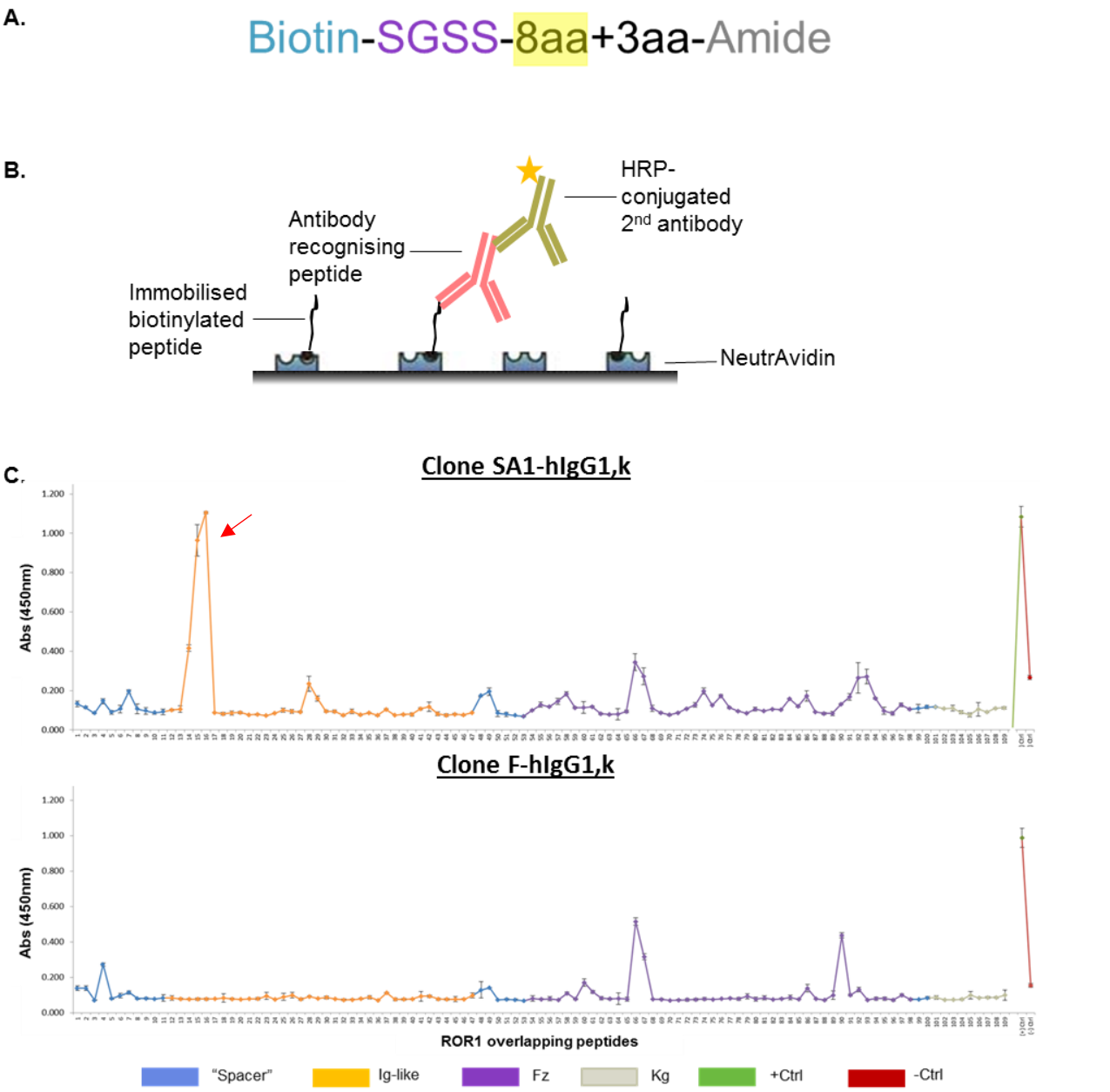

Fig. 5. 3. Epitope mapping of ROR1 clones SA1 and F by peptide-library ELISA. (A) Structure of biotinylated ROR1 peptides. Each one was composed of: Biotin (at the N-terminal), linker (SGSS), 11 amino acids, and an amide group (NH_2) at the C-terminal. The position of overlapping amino acids are highlighted in yellow. (B) Schematic of the sandwich ELISA approach used for epitope mapping. (C) Reactivity of clones SA1 and F with ROR1-derived overlapping peptides. Different colours indicate the domain the peptides encoded for. Positive (green) and negative (red) control peptides and antibodies were provided by Mimotopes. Experiments were done in triplicates. One out of three independent experiments is shown. Red arrow indicates binding to relevant peptides. Peaks below 0.5 Abs were considered background. Error bars represent SD.

Although clone F produced two detectable peaks in the Fz domain (**Fig. 5. 3C**), they were considered irrelevant as they appeared around peptides number 65-68 and 90-93 (already identified as background in clone SA1 analysis). Also, their Abs value was near or below the 0.5 criterion. This dataset suggested that whilst clone SA1 had a linear epitope in the apical region of the Ig-like domain, clone F had potentially a discontinuous epitope, making it undetectable by peptide library ELISA.

5.3.1.2 By Western Blotting

Previous results obtained by peptide library ELISA led me to investigate whether clones SA1 and F had conformational epitopes. To this end, soluble extracellular ROR1 protein was run in SDS-PAGEs under reducing and non-reducing conditions for Western blot analysis. Clones SA1 and F were then used to detect soluble ROR1 followed by incubation with a relevant secondary antibody conjugated to HRP (**Fig. 5. 4**).

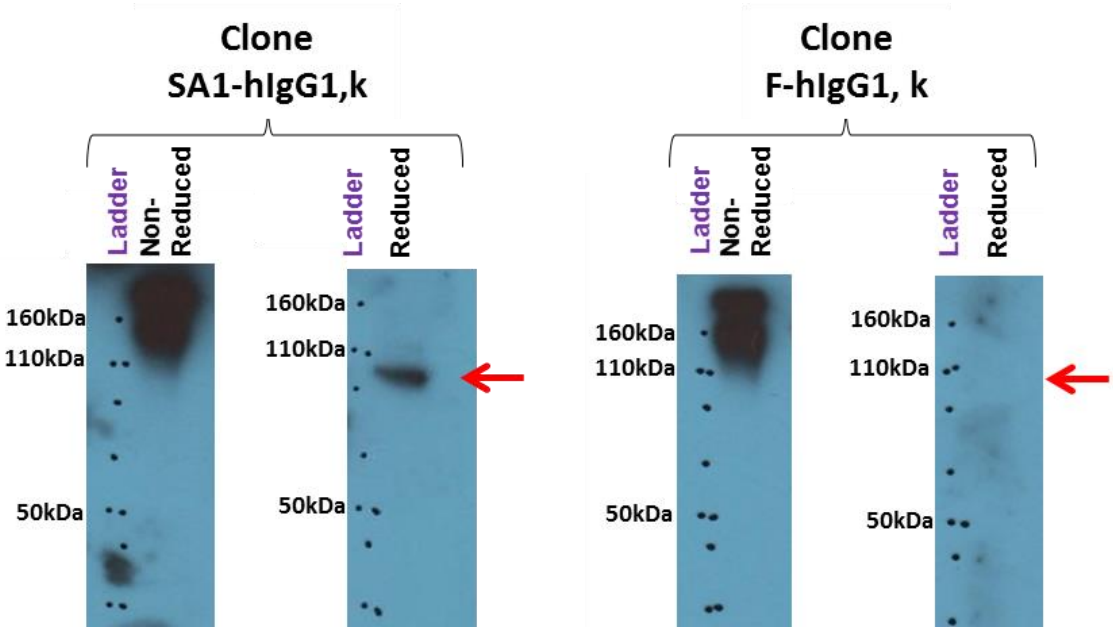

Fig. 5. 4. Investigation of conformational epitopes by Western Blot. SDS-PAGE was carried out using soluble extracellular ROR1 protein under reducing (80-110kDa) and non-reducing (>110kDa) conditions. After protein transfer, membranes were incubated with clones SA1 and F, and binding was detected by anti-human IgG conjugated to HRP. kDa values are included for protein size reference. Red arrows indicate the expected size of ROR1 detected under reducing conditions. HRP= Horseradish peroxidase

In **Fig. 5. 4**, strong detection of eROR1 run under non-reducing conditions (>110kDa) could be seen when either SA1 or F were used. However, under reducing conditions (i.e. when the disulphide bridges were disrupted leaving ROR1 in its primary/secondary structure), only SA1 was still able to detect the protein. Consistent with previous data, clone F did not bind to reduced ROR1, as evidenced by the absence of a ROR1 band at 80-110kDa (red arrows).

Similarly, when cell lysates from $ROR1^-$ and $ROR1^+$ cell lines (expressing full length or truncated extracellular domains of ROR1) were assessed by Western Blot, clone F was able to detect ROR1 only when samples were run in non-reducing conditions. Clone SA1, in contrast, bound to reduced and non-reduced samples with the same efficiency (See **Fig. 5. 5**).

Taken together, peptide library ELISA and Western blot data indicated that clone SA1 binds to a continuous (linear) epitope in the Ig-like domain of ROR1, whereas clone F detected a discontinuous (conformational) epitope in the Frizzled domain. However, the essential amino acids needed for ROR1 recognition still needed to be identified.

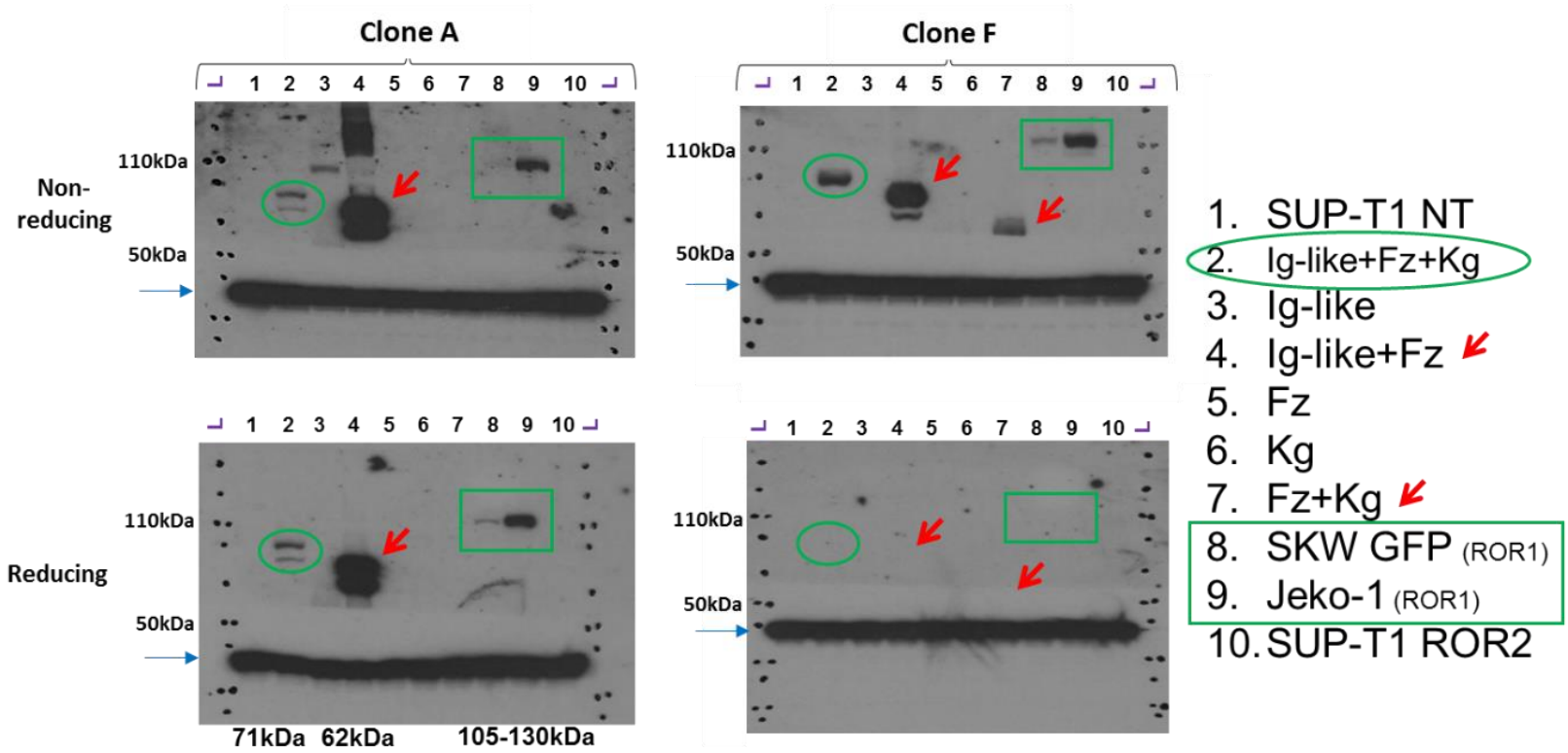

Fig. 5. 5. Investigation of conformational epitopes by Western Blot using cell lysates. Cell lysates were obtained from ROR1^{-} (SUP-T1 NT and SUP-T1 ROR2) and ROR1^{+} cells expressing full length ROR1 (SKW 6.4 GFP and Jeko-1 (105-130kDa)) or its extracellular domains (Ig-like+Fz+Kg (71kDa), Ig-like, Fz, Ig-like+Fz (62kDa), Kg, Fz+Kg (55kDa)). Samples were run in non-reducing (top) and reducing conditions (bottom). The loading order is shown at the right-hand side of the figure, and the kDa values are included for protein size reference (at the left-hand size of the gels and at the bottom). Green circles indicate bands for the Ig-like+Fz+Kg expressing cells. Red arrows point to bands corresponding to Ig-like+Fz and Fz+Kg cell lines. Green rectangles indicate expected bands from SKW 6.4 GFP and Jeko-1 (which express endogenous ROR1). GAPDH was used as loading control (blue arrow). Protein from cells expressing individual domains could not be detected due to experiment limitations (i.e. due to their low size they were contained in the part of the membrane used for GAPDH detection).

5.3.1.3 By single amino acid point mutations

To ascertain the critical amino acids required for clones SA1 and F recognition of ROR1, the next experiments were planned based on data previously obtained by flow cytometry, peptide library ELISA and Western blot.

Since clone SA1 bound to the Ig-like domain, specifically to peptides 13-17, I analysed their sequences and identified the top 3 amino acids most likely to be involved in ROR1 recognition (within a 5aa region contained in the 13-17 peptides). By DNA splicing techniques, primers were designed in order to introduce each of the three single amino acid mutations or all five together. Mutated sequences were cloned by Phusion PCR into retroviral plasmids already present in the lab (See **Chapter 2**). This cloning strategy allowed the generation of four new constructs: “Point mutation 1”, 2 and 3, and “5aa mutation”. All constructs carried a GFP reporter gene. Correct cloning was verified by restriction enzyme digestion and sequencing.

Once the correct sequences were obtained, retroviral supernatants were prepared by transient transfection of HEK293T cells. 72h post transfection, supernatants were harvested and used for transduction of SUP-T1 NT cells on RetroNectin-coated plates. Similarly, 72h later, GFP expression was assessed by flow cytometry in order to confirm successful transduction (**Fig. 5. 6A**).

Fig. 5. 6B, shows the binding of clone SA1 to the newly generated stable cell lines expressing different mutations in the Ig-like domain of ROR1. Also, since Jeko-1 (Mantle-cell lymphoma - MCL) and PCL-12 (Chronic lymphocytic leukaemia - CLL) cell lines expressed high and low levels of endogenous ROR1, respectively, they were included in this analysis as reference. Additionally, clones 4a5 and R12 (anti-ROR1 antibodies previously reported in the literature) were also included in order to evaluate whether they shared epitopes with clone SA1. Furthermore, the patent of clone D10, the prototype of Cirmtuzumab (the ROR1 MAb currently in the clinic) became available at this point of the project. Therefore, I cloned its sequence into hIgG1, kappa

retroviral vectors in order to put it in the same chimeric format as our ROR1 antibodies. Binding of chimeric D10 to the cell lines mentioned above was also assessed.

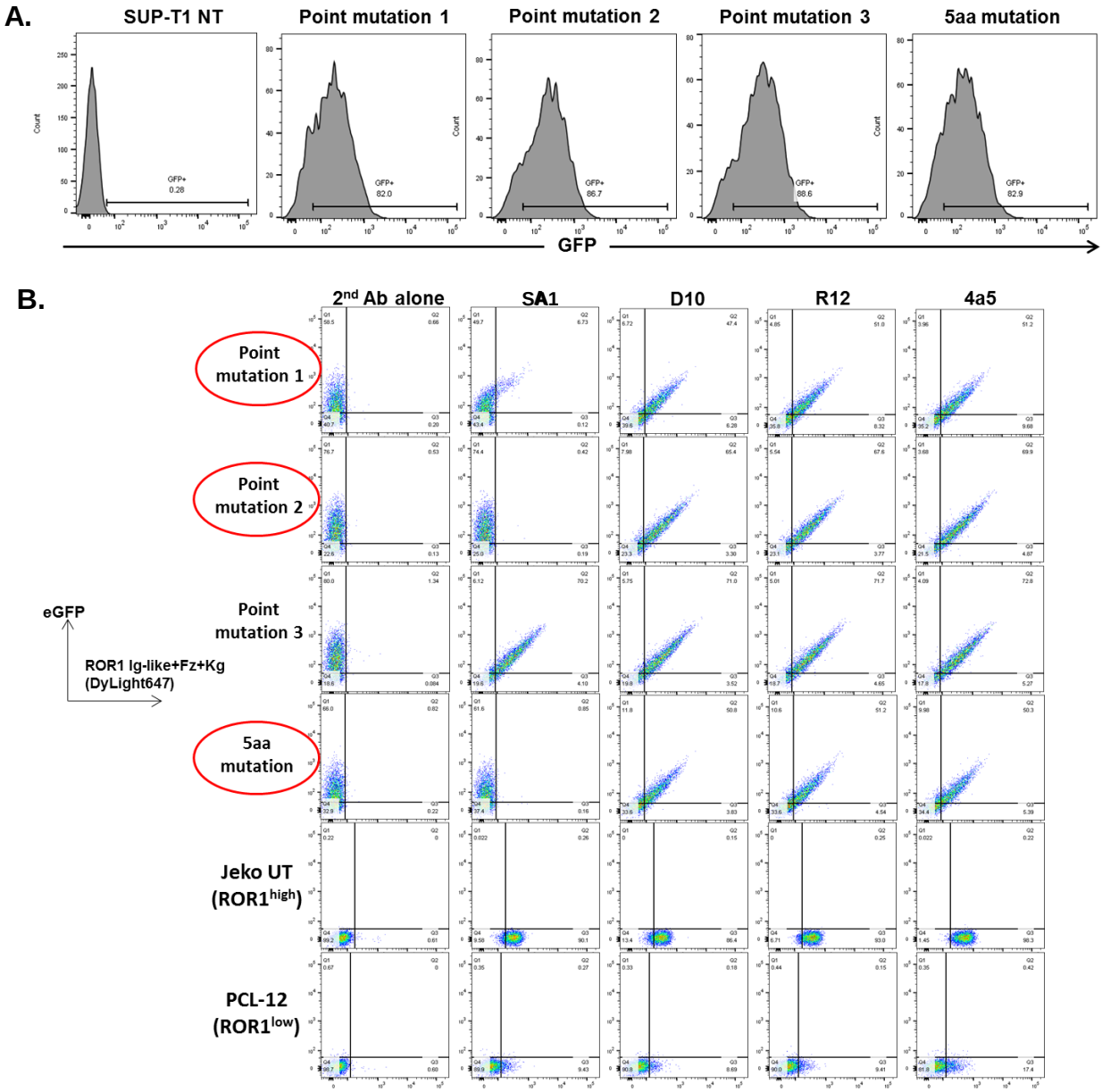

Fig. 5. 6. Epitope mapping of SA1 MAb by single amino acid mutations using flow cytometry. (A) Stable cell lines expressing relevant mutations in the Ig-like domain were generated by retroviral transduction of SUP-T1 NT cells. GFP expression was evaluated in order to assess transduction levels. (B) Clone SA1 binding was tested on all four new stable cell lines expressing different mutations in the Ig-like domain. Jeko-1 UT and PCL-12, which endogenously express high and low levels of ROR1 respectively, were included in our studies as reference. The secondary antibody alone (anti-human IgG-DyLight647) acted as negative control. Also, previously reported clones R12, 4a5 and the newly available D10 were also included for comparison. Red circles indicate cell lines expressing crucial mutations disrupting SA1 binding to ROR1.

Flow cytometry data shows that “Point mutation 1” critically affected the binding of SA1 to the Ig-like domain, although weak ROR1 binding was still detectable. In contrast, no binding was observed on cells expressing “Point mutation 2”. There was also no binding to the “5aa mutation” cell line as it contained “Point mutation 2”. Importantly, binding of 4a5, R12 and D10 to ROR1 was not affected by any of the mutations. Thus, this data indicated that clone SA1 binds to a unique epitope in ROR1 that is not shared with other anti-ROR1 antibodies.

With regards to clone F, previous results indicated that it bound to the Fz domain of ROR1 and that it recognised a conformational epitope. Having no further information on potential binding regions within this domain, I aligned the amino acid sequences encoding for rat, mouse and human Fz in order to identify probable relevant amino acids (**Fig. 5. 2**).

Two non-conserved amino acids were found, which were therefore potentially involved in clone F binding. Thus, as with clone SA1, I used DNA splicing and cloning techniques to generate three new retroviral constructs: “Point mutation F1”, F2, and “Mutation F1+F2”. Restriction enzyme digestions and sequencing were used to confirm correct cloning. As mentioned above, retroviral supernatants were produced and used to transduce SUP-T1 NT cells. These constructs also carried GFP as reporter gene, therefore transduction levels were assessed by GFP expression (**Fig. 5. 7A**).

Having confirmed good levels of transduction, clone F was tested on the three new stable cell lines by flow cytometry (**Fig. 5. 7B**). SUP-T1 cells expressing wild-type Fz were also tested and included in these studies as positive control, whilst staining with the secondary antibody alone acted as negative control.

Flow cytometry data showed that “Point mutation F1” did not affect F detection of ROR1. However, this clone was not able to recognise cells expressing either “Point mutation F2” and, consequently, “Mutations F1+F2”. These results

confirm that clone F binds to the Fz domain of ROR1 and that “Point mutation F2” but not F1 is critical for the formation of its discontinuous epitope. Of note, binding to ROR1 by clone F was not compared to other reported clones, as all anti-ROR1 antibodies and/or their derivatives that are currently in clinical trials bind to the Ig-like domain; making clone F a unique tool for ROR1 immunotherapy

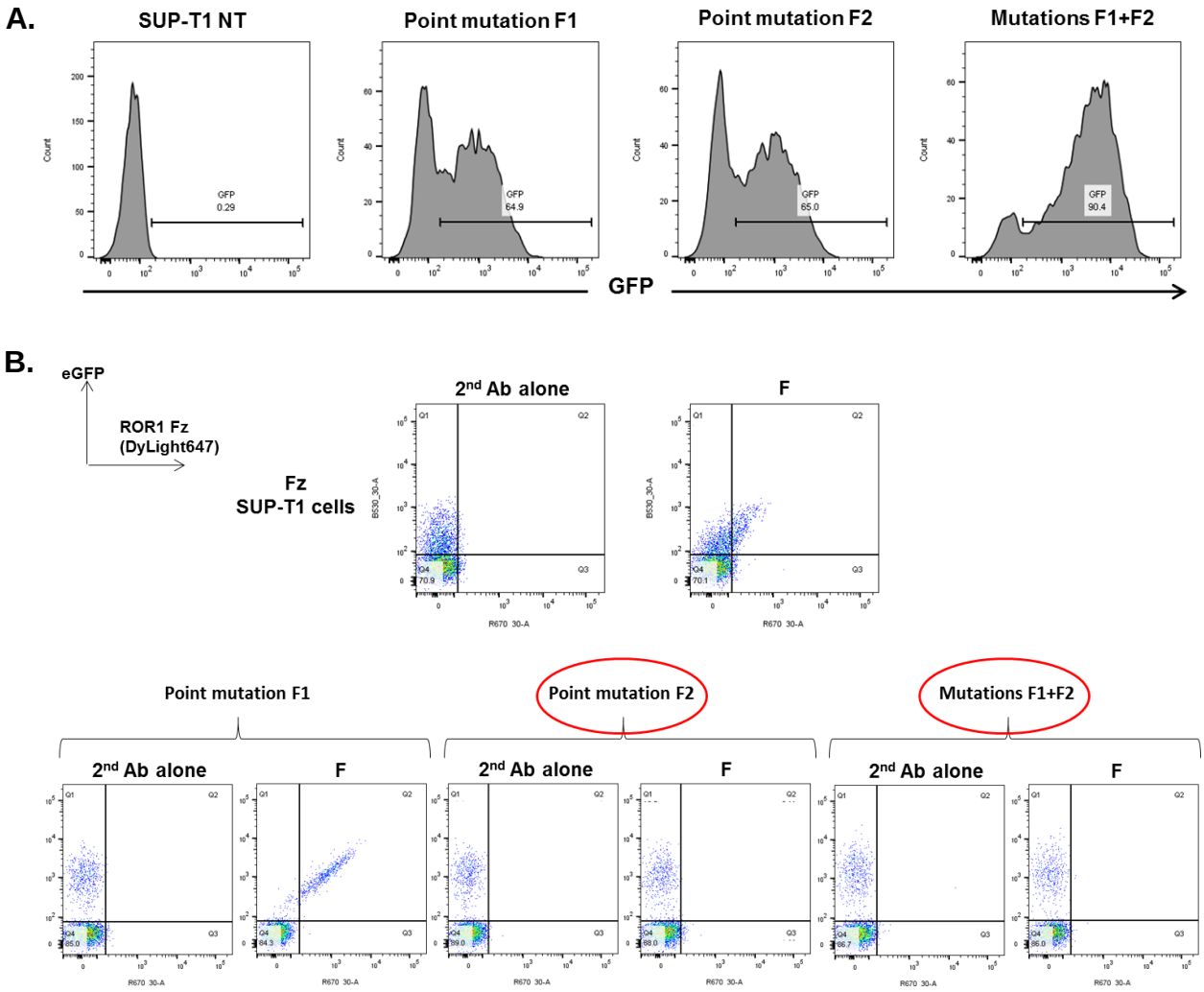

Fig. 5. 7. Epitope mapping of F MAb by single amino acid mutations. (A) Stable cell lines expressing relevant mutations in the Fz domain were generated by retroviral transduction of SUP-T1 NT cells. GFP expression served to assess transduction levels. (B) Clone F binding was tested on all three new stable cell lines. The secondary antibody alone (anti-human IgG-DyLight647) acted as negative control. Cell expressing wild-type Fz (Fz SUP-T1) were included as positive control. Red circles indicate cell lines expressing crucial mutations disrupting F binding to ROR1. Fz= Frizzled.

5.3.1.4 Competition assay by flow cytometry

To further confirm whether clone SA1 had a distinct epitope that was not shared with other anti-ROR1 antibodies, the binding of SA1 to ROR1 with other relevant clones through a flow cytometry-based competition assay was performed.

Based on previous studies (de Jong et al., 2005), it was hypothesised that consecutive- and/or simultaneous-staining of $ROR1^+$ cells, using clone SA1 in combination with other anti-ROR1 antibodies, would allow the identification of any overlapping epitopes by flow cytometry analysis.

To this end, the variable region of clone SA1 was fused to a mouse IgG2a, kappa constants following the same protocols discussed in previous chapters. All other chimeric antibodies were kept in their existing rat-human format. This was required as it enabled simultaneous detection of the SA1 rat-mouse IgG2a antibody and the other anti-ROR1 rat-human IgG1 antibodies using different secondary antibodies. Also, for ease of analysis, $ROR1^+GFP^+$ cells were used.

Fig. 5. 8A shows strong ROR1 binding when antibodies were used as single agents, which confirmed their correct expression and specificity for ROR1. Since SA1 and F antibodies detected different extracellular domains, this combination was included in these studies as negative control for overlapping epitopes.

In **Fig. 5. 8B**, three different columns are presented. Dot plots on the first column correspond to ROR1 binding assessed when SUP-T1 ROR1 cells were stained with clone SA1 (mIgG) in the first instance. After a washing step, cells were stained with a competitor antibody (hIgG), followed by another washing step. Both antibodies were then detected by a third staining step using the appropriate secondary antibodies. In the second column, a similar approach was taken when staining these cells, except that this time it was the

antibody in hIgG1, k format the one used for the first staining step, followed by SA1 staining. On the third column, both antibodies were used at the same time.

In all cases, a clear and defined shift of all events was observed; indicating that, independent of the order in which cells were stained, antibodies used in the first staining step did not impede binding of the antibodies used in the second step. This was further confirmed when both antibodies were assessed at the same time. Hence, these results confirm that clone SA1 binds to a unique epitope within the Ig-like domain, which is not shared (not even partially) with any of the other clones tested.

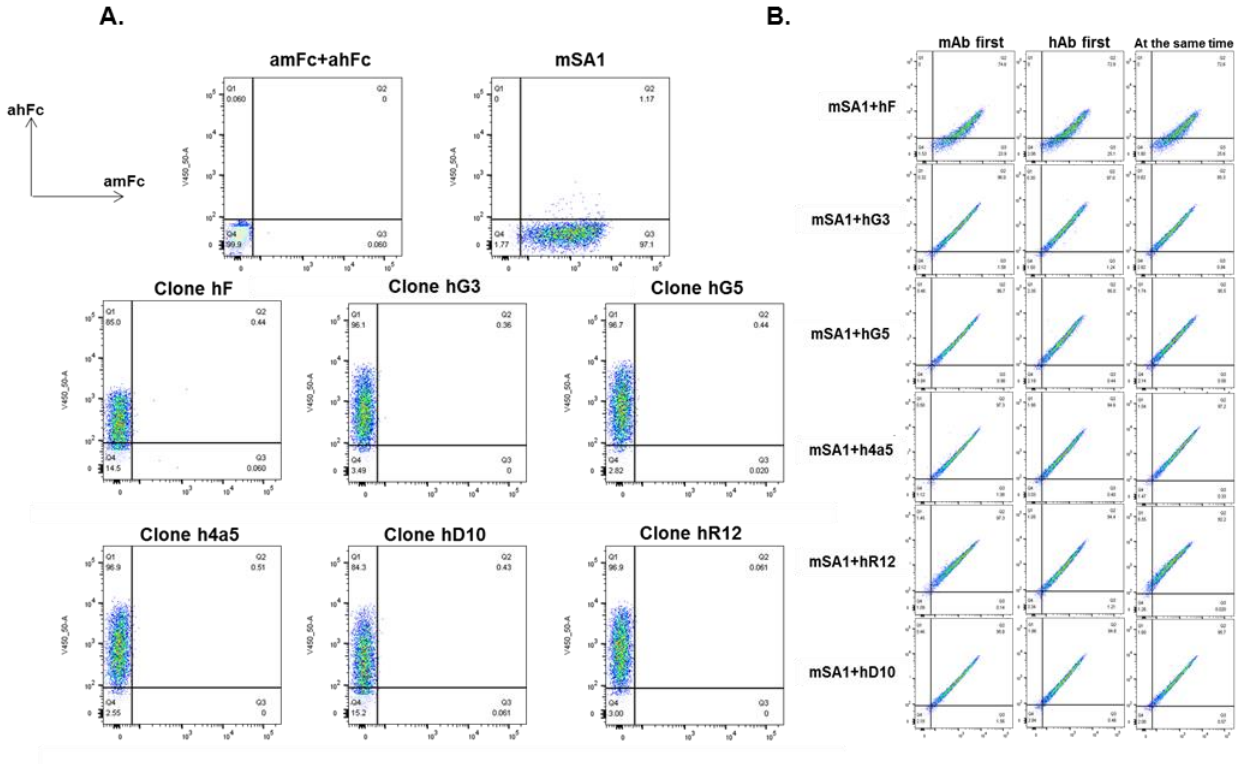

Fig. 5. 8. Competition assay by flow cytometry. Clone SA1 in murine IgG2a, k (mSA1) along with other ROR1 MAbs in human IgG1, k were used for staining ROR1-transduced cells. MAb staining was done as (A) single agents or (B) in combination with clone mSA1. Anti-human IgG (eFluor450) and anti-mouse IgG (DyLight649) were used as secondary antibodies. Combined staining using clones F and mSA1 acted as negative control for overlapping epitopes.

5.3.2 Aim 2: CDC activity of FPLC-purified SA1 antibody

It has been shown that clone F binds to the Fz domain of ROR1, making it a unique tool for ROR1 immunotherapy; however, previous data revealed that its cytolytic potential in the antibody format was not significant when compared to the isotype control. Therefore, other members of our group explored its immunotherapy efficacy in other formats (antibody derivatives).

In parallel, cytotoxicity studies focused on clone SA1, as previous screening of CDC activity (**Chapter 4**) revealed that this chimeric antibody elicited superior cytolysis compared to other ROR1 binders, including clones 4a5 and R12. Thus, in the following paragraphs, the CDC activity of SA1 on cell lines and primary cells from CLL patients and healthy donors (HD) will be discussed. Unlike previous experiments -where culture supernatants were used- a 10ug/ml dose of purified antibody by Fast Protein Liquid Chromatography (FPLC) (**Fig. 5. 9**) was employed, as per preclinical studies of anti-CD20 monoclonal antibodies (Herter et al., 2013, Barth et al., 2015).

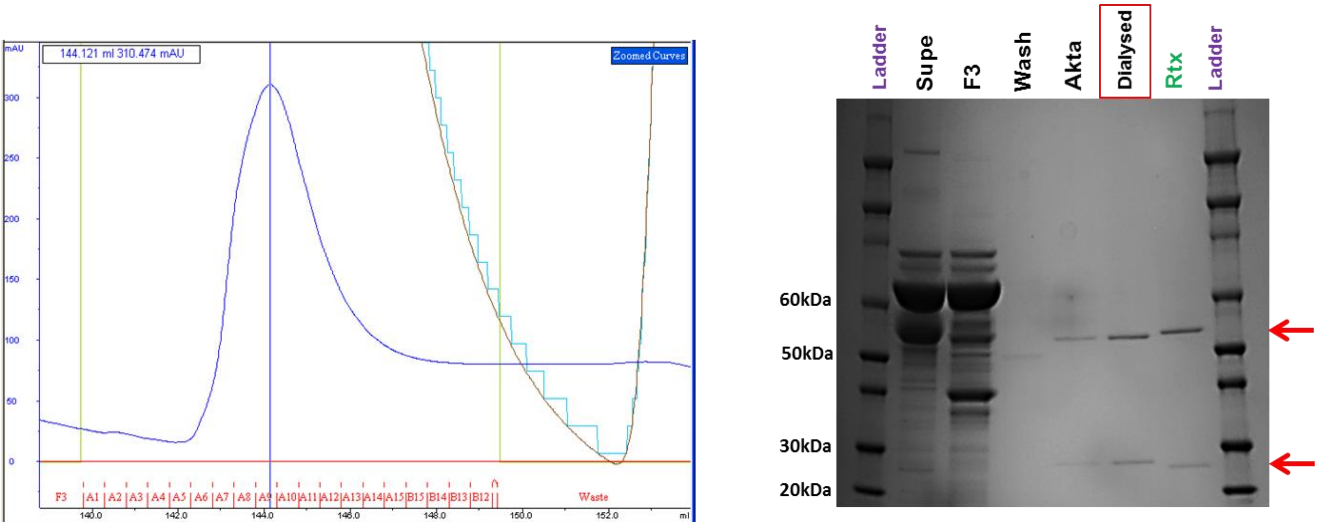

Fig. 5. 9. FPLC purification (AKTA) of clone SA1 using a 1ml Protein A column. 293T cells were cultured in FBS supplemented IMDM until transfection. 12h after later, co-transfection media was replaced with fresh phenol-red free IMDM, supplemented with ultra-low IgG HI-FBS. Prior to FPLC purification, supernatant was centrifuged, filtered and dilute with Protein A Binding buffer in a 1:1 ratio. Aliquots taken at every step of the purification process were run in a SDS-PAGE and stained with Coomassie dye. Rituximab (Rtx) was used as reference. Red arrows indicate heavy and light chain bands. Red square points out the final version of clone SA1 (i.e. purified antibody after dialysis).

CDC activity of clone SA1 was first assessed on B-cell lymphoma cell lines expressing high (Jeko-1) or low (SKW 6.4 GFP) levels of ROR1 (**Fig. 5. 10A**). An isotype control and a chimeric anti-CD20 antibody (Rituximab: Rtx) were used as negative and positive controls, respectively.

In **Fig. 5. 10A**, AnnexinV/PI staining data from cells treated with SA1 (10ug/ml) in presence of 10% rabbit complement for 2h, showed that SA1 was able to elicit significant cytotoxicity on both cell lines compared to the isotype ($p \leq 0.0001$). Furthermore, when ROR1 expression was high, similar levels of cell killing induced by both SA1 and Rtx (>95% cell death). As expected, for $ROR1^{low}$ cells, SA1 cytotoxicity was not as potent (80%) as the one produced by Rtx (>95%).

Next, clone SA1 was tested on PBMCs from healthy donors (**Fig. 5. 10B**). Positive and negative controls were the same as above. As expected, no significant cell death was observed for clone SA1. In contrast, a significant although small reduction (20%) on anti-CD20-treated PBMCs was detected.

Finally, SA1 was tested on primary cells from 8 untreated CLL patients, expressing different levels of ROR1 (**Fig. 5. 10C** and **Table 5. 1**). Significant cell death compared to the isotype was observed when CLL cells were treated with either clone SA1 (75-98% cell death, $p \leq 0.0001$) or Rtx (>98%, $p \leq 0.0001$). An interesting observation was that correlation between ROR1 density on target cells and cytotoxicity was not evident; suggesting that a larger number of CLL samples might need to be investigated.

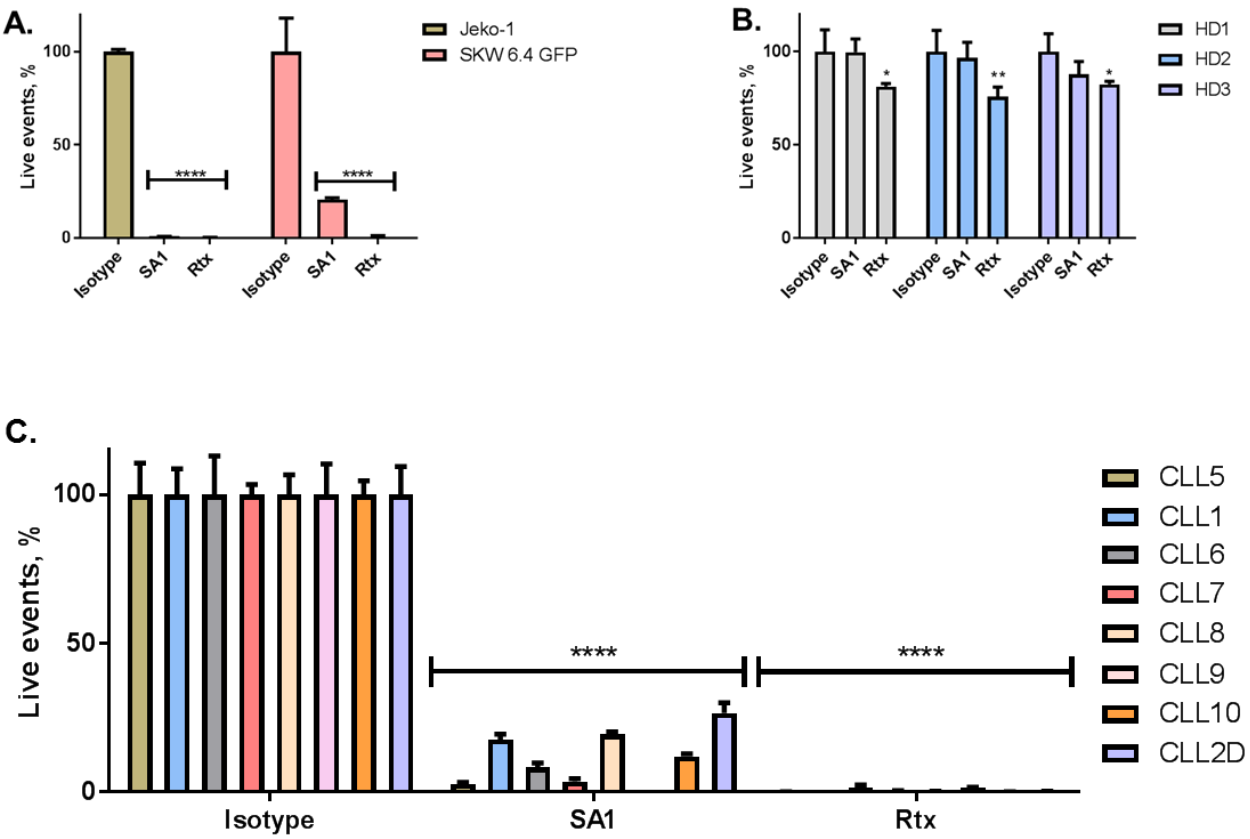

Fig. 5. 10. Complement-dependent cytotoxicity of clone SA1 ROR1 MAb on (A) Jeko-1 (Mantle-cell lymphoma) and SKW 6.4 GFP (EBV-B cells), (B) PBMCs from healthy donors (n=3) and (C) CLL cells (n=8). Clone SA1 chimeric MAb was tested at 10ug/ml in the presence of 10% baby rabbit complement. CDC was measured by AnnexinV/PI staining. Significant and specific toxicity was achieved on ROR1 cell lines and CLL cells, compared to the isotype ($p \leq 0.0001$). Rituximab (Rtx) was used as positive control ($p \leq 0.0001$). Datasets from all 3 panels were normalised and compared to the isotype control for statistical calculations. All experiments were done in triplicates. Error bars represent SD. Statistical test: *2-way ANOVA with Dunnett's multiple comparison test*. *$p \leq 0.05$, **$p \leq 0.01$, ****$p \leq 0.0001$. HD= Healthy donor. PI= Propidium iodide.

Table 5. 1. List of samples from CLL patients. Treatment, ROR1 expression and percentage of live events remaining after SA1 antibody therapy are presented.

Sample	Treatment	ROR1, MFI	Live events (after SA1 CDC therapy), %
CLL5	Untreated	198.01	2.85
CLL1	Untreated	84.9	17.69
CLL6	Untreated	224.42	8.31
CLL7	Untreated	144	3.57
CLL8	Untreated	150.01	19.47
CLL9	Untreated	164.91	0.13
CLL10	Untreated	58.22	11.98
CLL2D	Untreated	276.4	26.57

So far, the findings of this study indicate that, although less potent than Rituximab, clone SA1 was able to elicit significant CDC activity on primary CLL cells. However, a further factor to consider is that –although all samples expressed the CD20 antigen– cytotoxicity prompted by Rtx (>98%) was higher than the one reported by others (60-80% cell death (Kennedy et al., 2004, Pawluczkowycz et al., 2009)). Nevertheless, cautiously encouraged by these results, a humanisation program for clone SA1 was set up.

5.3.3 Aim 3: SA1 humanisation (in collaboration with GenScript)

Our research group set up a collaboration with GenScript for the humanisation of clone SA1. In the following paragraphs, i) the cloning of humanised variable regions into hIgG1, k constants, ii) their binding to ROR1$^+$ cells and iii) their cytotoxicity assessed by CDC assay will be discussed.

5.3.3.1 Cloning

By using the complementarity determining regions (CDR) grafting method, GenScript provided us with 5 V_H and 5 V_L humanised regions. SA1 rat-derived variable domain sequences were searched against the human IgG germline database. The top 5 human framework sequences with the highest homology to SA1 were chosen as human acceptors for each light and heavy variable chains. Amino acid sequences of 5 humanised V_H and 5 humanised V_L were obtained after grafting the CDRs of SA1 to the human acceptor frameworks.

DNA sequences encoding each humanised region were synthesised (G-blocks® Gene Fragments <1000bp), whilst primers introducing relevant restriction enzyme sites and overlapping sequences were designed in order to fuse the humanised variable domains to human constants. As before, DNA splicing methods and retroviral vectors already present in the lab were used for cloning. This technique allowed the successful generation of 10 constructs (i.e. 5 retroviral vectors encoding for each the light (V_{L1}-V_{L5}) and heavy (V_{H1}-V_{H5}) chains). Correct cloning of all 10 constructs was verified by sequencing.

Of note, F antibody was also selected for humanisation. Cloning was performed by other members of our group in order to produce clone F in the single chain variable fragment (scFv) format but not as a full IgG antibody.

5.3.3.2 Binding

To identify the best combination of humanised V_L and V_H sequences, all 25 possible combinations of these 10 sequences were used for transfection of HEK293T. After 72h, antibodies contained in culture supernatants were incubated with SUP-T1 ROR1 cells (GFP^+ROR1^+).

To account for differences in transfection levels that could confound these analyses, GFP (V_H) and BFP (V_L) expression of HEK293T cells were also evaluated. Flow cytometry data showed that co-transfection levels of all constructs were comparable as they ranged between 50-60% (**Fig. 5. 11**).

Antibody binding was then detected by flow cytometry using a secondary antibody, which also acted as negative control (**Fig. 5. 12**).

Fig. 5. 12 illustrates how most of the combinations of humanised constructs presented poor or moderate binding to ROR1. Remarkably, all pairings involving construct V_L1 showed good binding, of which V_H1-V_L1 and V_H3-V_L1 were identified as the best combinations. The latter will be referred to as HuA1 and HuA3, respectively.

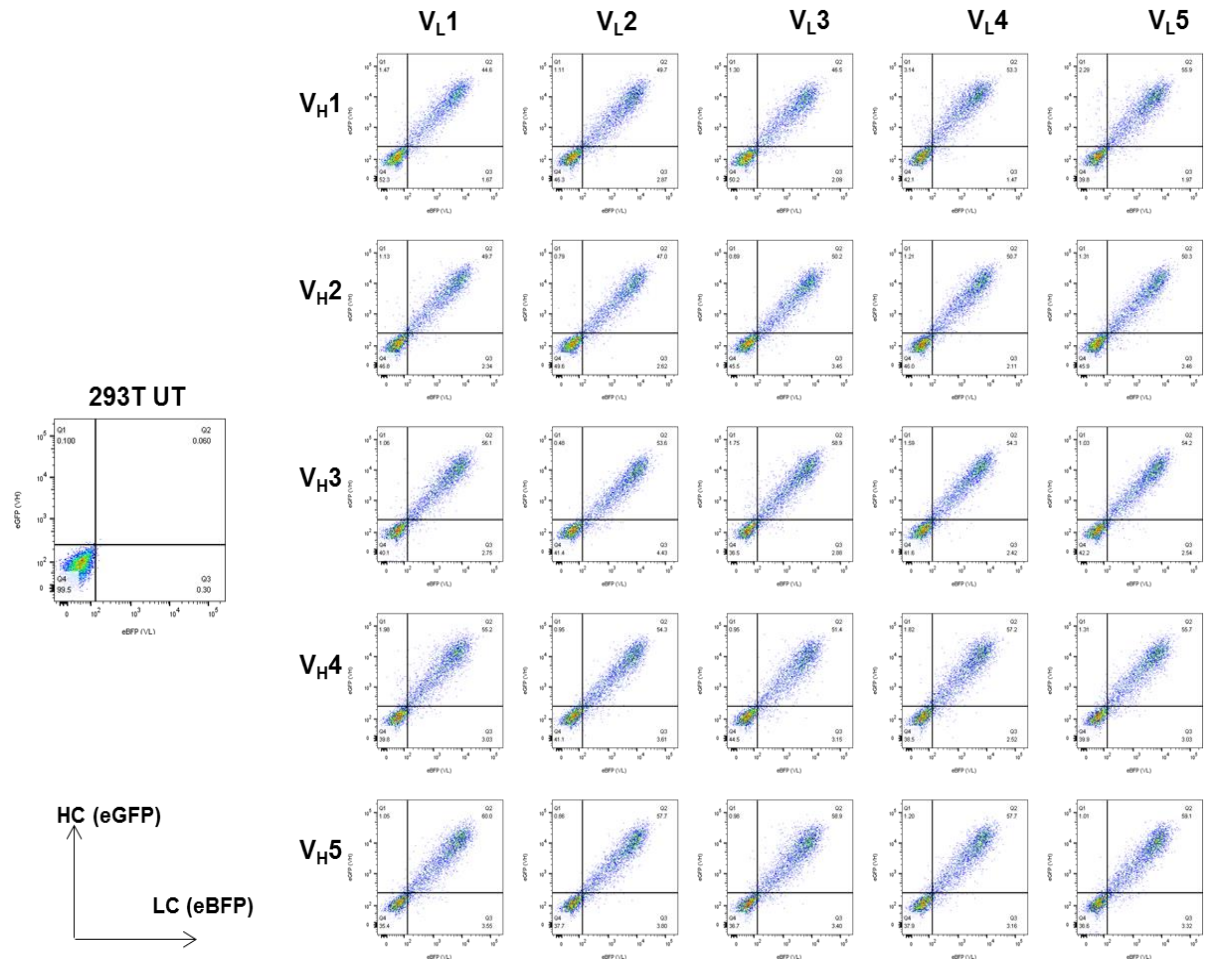

Fig. 5. 11. Transfection evaluation of HEK293T co-transfected with humanised SA1 candidates by flow cytometry. HEK293T cells were co-transfected with 5 different V_L (BFP^+) and 5 V_H (GFP^+) constructs, which resulted in 25 different combinations. 72h post transfection, the GFP and BFP expression of HEK293T cells were assessed by flow cytometry. Transfection levels of all pairing ranged between 50-60%.

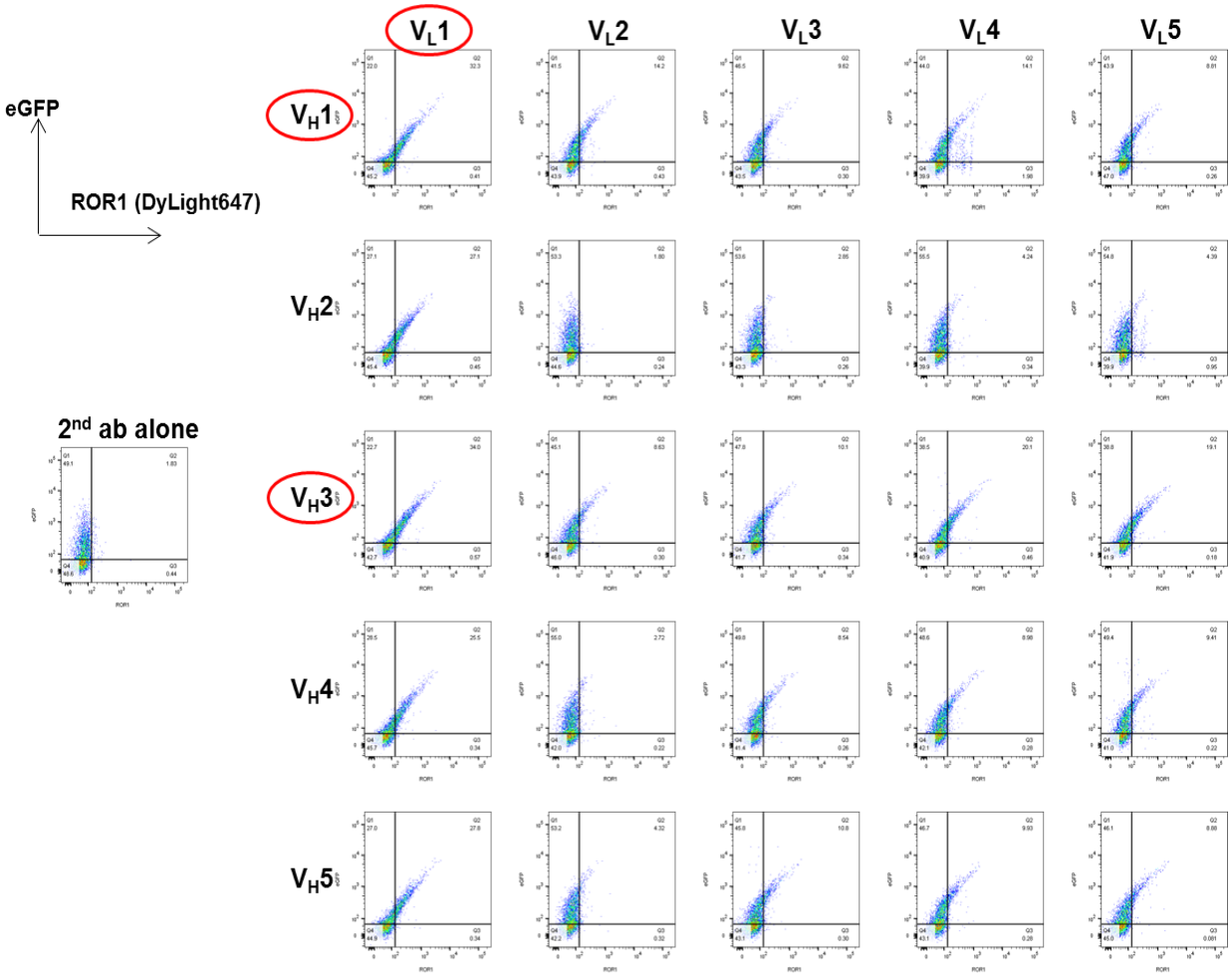

Fig. 5. 12. ROR1 binding of humanised SA1 candidates. HEK293T cells were co-transfected with 5 different V_L and 5 V_H constructs, which resulted in 25 different combinations. 72h post transfection, supernatants were harvested and incubated with SUP-T1 ROR1 cells (GFP^+ROR1^+). The anti-human IgG-Dylight647 secondary antibody served as negative control. Red circles point to those combinations that showed superior binding to ROR1.

Having identified the top two binders, ROR1 detection by flow cytometry was compared to the one produced by chimeric rat-hIgG1 clone SA1. Again, the secondary antibody served as negative control (**Fig. 5. 13**).

Differences in ROR1 binding between clones HuA1 (41%) and HuA3 (43.5%) were not observed. However, it was evident that both of them presented decreased levels compared to clone SA1, which showed 49.4% binding to ROR1^{+} cells.

Although flow cytometry data indicated that the humanised candidates presented a slight reduction in ROR1 binding, investigation of their cytotoxic properties was undertaken.

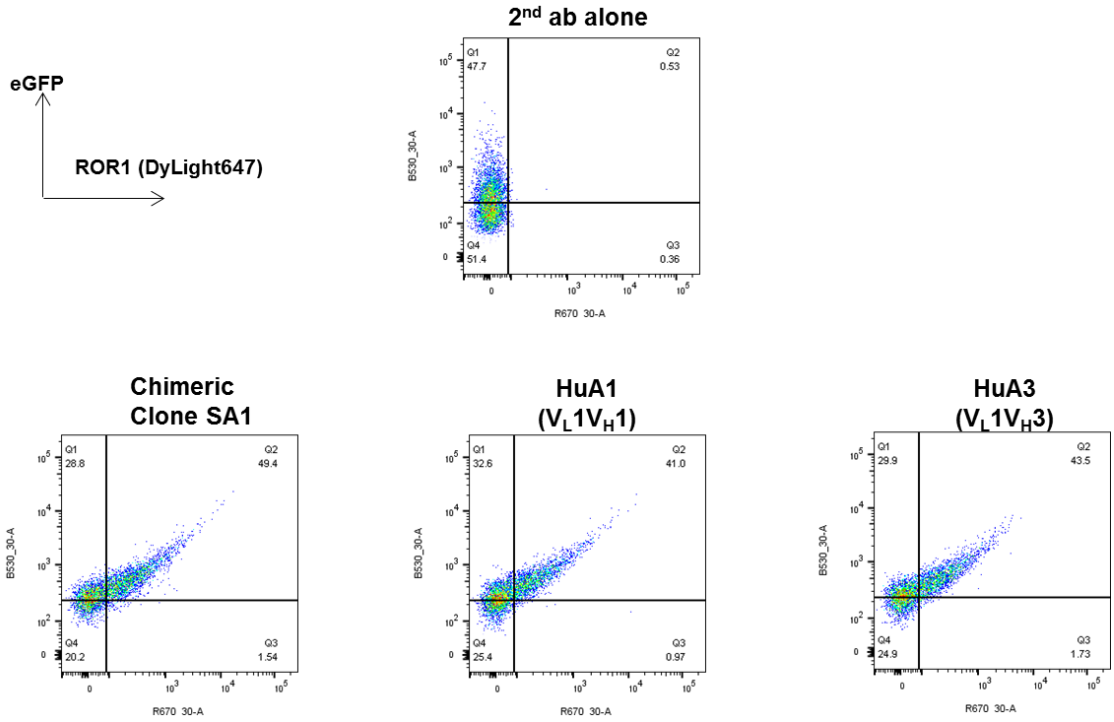

Fig. 5. 13. Flow cytometry comparison of ROR1 binding of HuA1 and HuA3 candidates against clone SA1. Chimeric clone SA1 and humanised clones HuA1 and HuA3 were incubated with SUP-T1 ROR1 cells (GFP^{+}ROR1^{+}) for comparison. The anti-human IgG-Dylight647 secondary antibody served as negative control.

5.3.3.3 Complement-dependent cytotoxicity (CDC)

In terms of cytotoxicity, the first step was to assess the CDC activity of the humanised clones and compare it to chimeric SA1. To this end, antibodies contained in culture supernatants from HEK293T cells were used. These cells were transfected at the same time with SA1, HuA1 and HuA3 constructs. Also, a hIgG1, k isotype (negative control) and two clinically approved anti-CD20 antibodies (Rtx= chimeric Rituximab and GA-101= humanised Obinutuzumab) were included in these studies for comparison.

MAbs supernatants from SA1-, HuA1- and HuA3-transfected cells along with controls at 0.5ug/ml were incubated with primary cells from 3 CLL patients and a healthy donor. An additional control at 10ug/ml (Rtx) was also included (as per **Chapter 4 – Fig. 4.4**). Incubation of MAbs and target cells was performed in the presence of 10% rabbit complement for 2h at 37°C and 5% CO_2. After incubation, cell death was detected by AnnexinV/PI staining using flow cytometry. All datasets were normalised and compared to the isotype control for statistical tests (**Fig. 5. 14A**).

Data shown in **Fig. 5. 14A** indicate that both chimeric and humanised clones produced statistically significant cell death compared to the isotype control; albeit SA1 still presented superior CDC activity than both HuA1 and HuA3 clones.

Similarly, Rtx (at both concentrations) and GA-101 elicited significant cytotoxicity compared to the isotype. As expected, Rtx exhibited a more potent cytotoxicity than GA-101 as the latter is known to possess a weak CDC (Herter et al., 2013). In both cases, however, reduced cell killing was observed when these MAbs were tested on “CLL3”. The latter observation is consistent with the poor CD20 expression found on “CLL 3” cells (**Fig. 5. 14B**).

Also, since the samples, method and assay illustrated in **Fig. 5. 14A** were the same as the one presented previously in **Fig. 4.4** -where the CDC activity of

all chimeric antibodies was assessed- data showing those results have been included for illustrative purposes (**Fig. 5. 14C**).

Although all ROR1 antibodies evaluated in this experiment displayed significant cytotoxicity, there was a noticeable difference between the CDC activity of SA1 and the humanised clones, particularly with clone HuA1. This might be explained by the reduced binding of HuA1 and HuA3 to ROR1, seen in **Fig. 5. 13**.

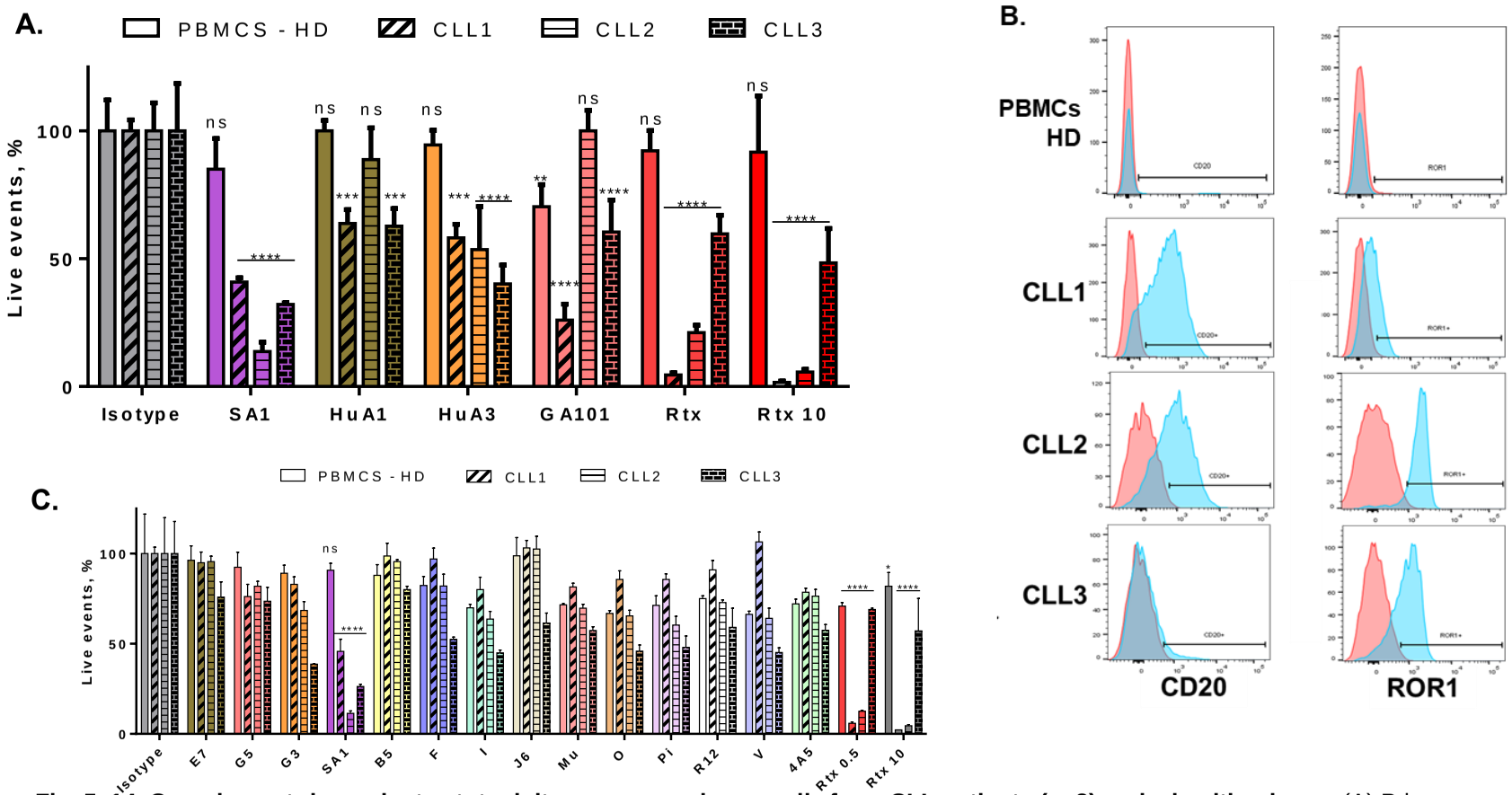

Fig. 5. 14. Complement-dependent cytotoxicity assay on primary cells from CLL patients (n=3) and a healthy donor. (A) Primary cells were incubated with the following antibodies' supernatants: chimeric SA1 and humanised clones HuA1 and HuA3. hIgG1, k isotype (negative control) was used at 0.5ug/ml; whereas Rtx (at 0.5ug/ml and 10ug/ml) along with GA-101 (at 0.5ug/ml) were used for comparison. After 10min incubation, 10% rabbit complement was added. After 2h incubation at 37°C, cell death was quantified by flow cytometry using AnnexinV/PI staining and counting beads. (B) Cell surface staining for CD20 and ROR1 by flow cytometry. The red area represents the isotype control. (C) CDC screening of all chimeric antibodies (as per Fig. 4.4) was included as reference. All datasets were normalised and compared to the isotype control for statistical calculations. Experiment was done in triplicates. Error bars represent SD. Statistical test: *2-way ANOVA with Dunnett's multiple comparison test*. ***p≤0.01*, ****p≤0.001*, *****p≤0.0001*, ns= not statistically significant. Rtx= Rituximab (chimeric), GA-101= Obinutuzumab (humanised), PI= Propidium iodide.

As a whole, these data suggest that after the humanisation program, SA1-derived clones HuA1 and HuA3 had a decreased binding to ROR1. Not surprisingly, the significant CDC activity seen previously with chimeric SA1 was reduced in its humanised versions.

In an effort to counteract this lack of cytotoxicity, bispecific antibodies in full IgG targeting either ROR1 and CD3 or ROR1 and PD-1 format were generated (Kim et al., 2016b) (See **Fig. 5. 15A**). These constructs were tested on three solid cancer cell lines by co-culturing them with effector cells (PBMCs from healthy donors) (**Fig. Fig. 5. 15B**). Unfortunately, MTS assay data suggested non-specific binding of clone SA1 to ROR1^{-} cells (MCF-7, breast cancer), which led to non-specific cytotoxicity. These results were confirmed by independent experiments and ELISA quantification of interferon-gamma (IFN-γ) and interleukin 2 (IL-2) cytokines (**Fig. Fig. 5. 15C**).

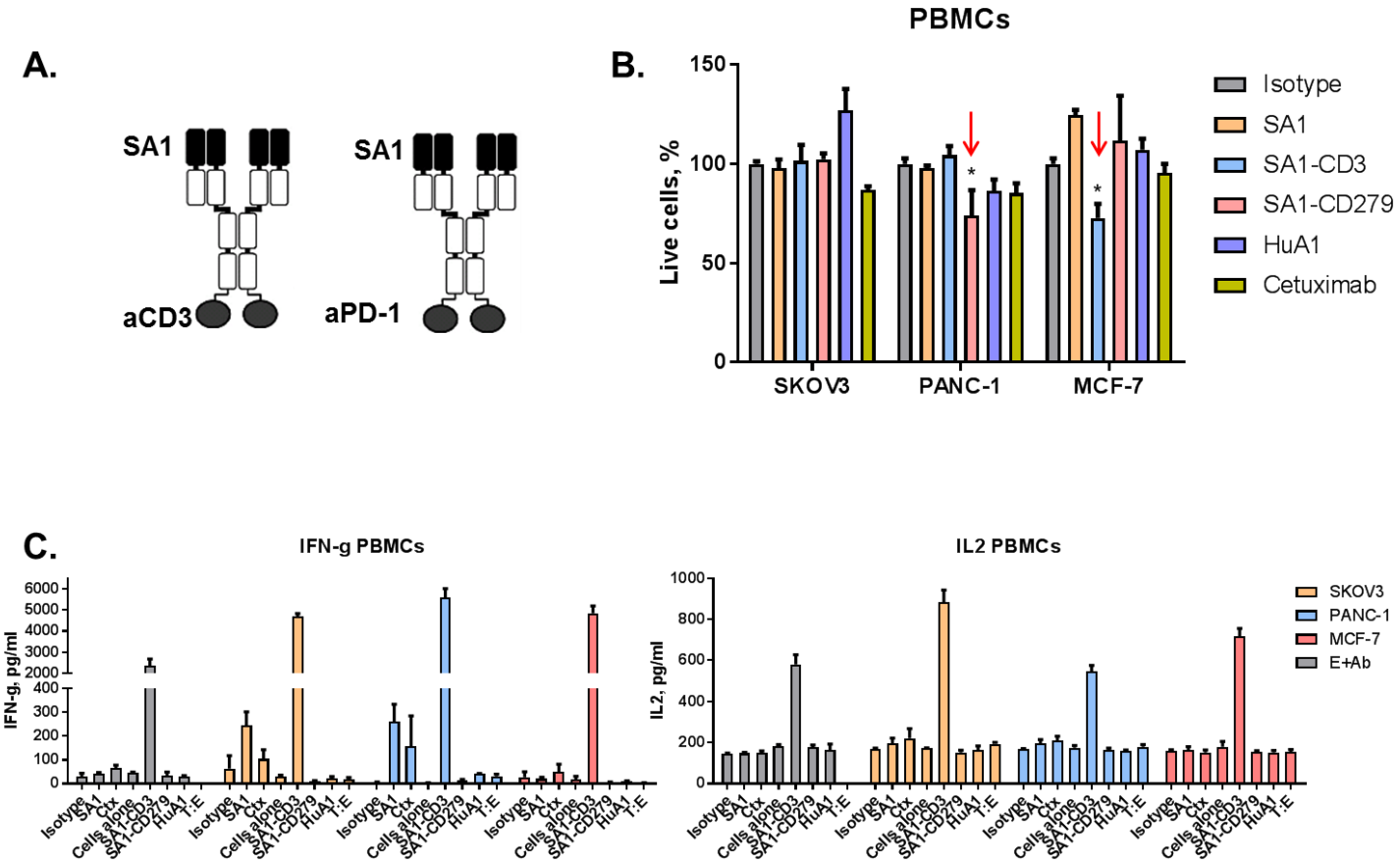

Fig. 5. 15. Co-culture of solid cancer cell lines and PBMCs in the presence of clone SA1 bispecific antibodies. (A) SA1-antiCD3 and SA1-antiPD-1 bispecific antibodies (in full IgG-scFv format) were designed, cloned and expressed in HEK293T cells. (B) ROR1^{+} (SKOV3, PANC-1) and ROR1^{-} (MCF-7) target cells were incubated with each bispecific antibody followed by addition of PBMCs (effectors) at a 25:1 (E:T) ratio. The hIgG1, k isotype was used as negative control. Cetuximab Rtx and GA-101 were used as referential therapeutic antibodies. After 24h incubation, live cells were quantified by MTS (colorimetric) assay. Red arrows indicate significant cytotoxicity prompted by ROR1 bispecific antibodies in full IgG. All datasets were normalised and compared to the isotype control. (C) ELISA quantification of IFN-γ and IL-2 are shown. Experiments were done in triplicates. Error bars represent SD. Statistical test: *2-way ANOVA with Dunnett's multiple comparison test*. *$p \leq 0.05$. SKOV3= Ovarian cancer cell line, PANC-1= Pancreatic cancer cell line, MCF-7= Breast cancer cell line, IFN-γ= Interferon gamma, IL-2= Interleukin 2.

To test for non-specific binding to MCF-7, both clones SA1 and F were incubated with these cells, and binding was evaluated by flow cytometry (**Fig. 5. 16**). Also, gene and protein analyses performed on these cells showed no presence of ROR1, confirming non-specific binding of SA1 but not clone F to MCF-7 cells. These findings were unexpected as non-specific binding was not detected previously when suspension cell lines or PBMCs from healthy donors were assessed.

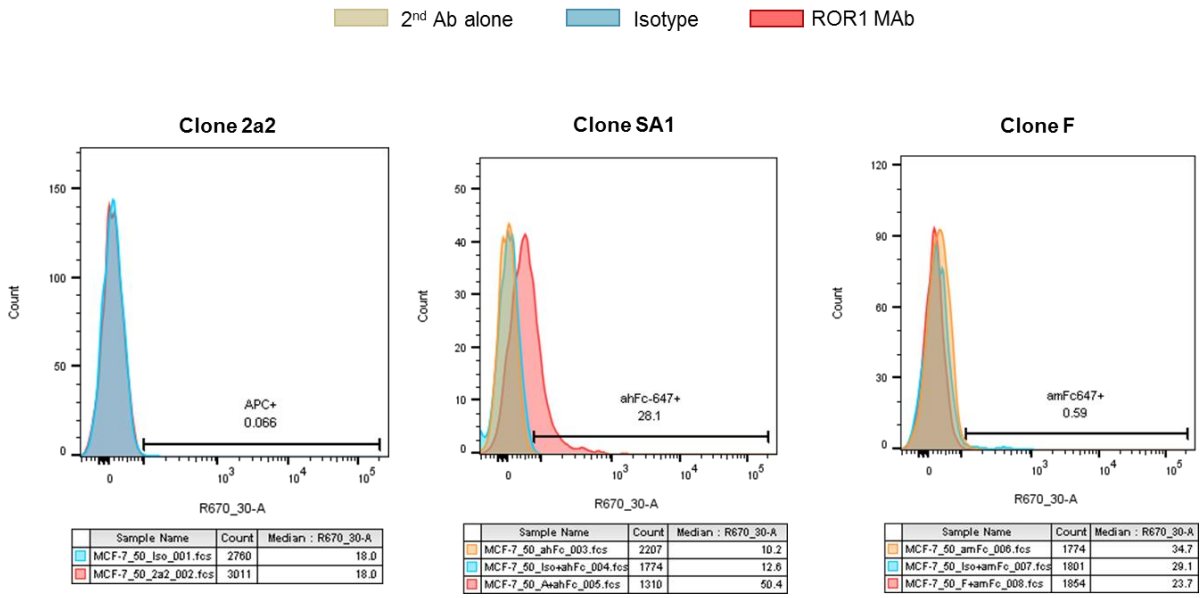

Fig. 5. 16. ROR1 MAbs binding to MCF-7 cells (ROR1$^-$) assessed by flow cytometry. MCF-7, a ROR1$^-$ breast cancer cell line, was stained with SA1 or F antibodies. Commercial ROR1 antibody, clone 2a2 conjugated to APC, was also used for comparison. Relevant isotype controls, and the secondary antibody (anti-hIgGDyLight647) used to detect binding of unlabeled clones, served as negative controls. Binding was quantified by flow cytometry. Negative controls were used for gating. Independent repetitions of this experiment were performed.

All in all, no further studies with this reagent were pursued and instead my investigation focused on an antibody derivative generated by using clone F scFv.

5.4 Discussion

Based on data from this and previous chapters, it has been established that clone SA1 binds to the Ig-like segment of ROR1, whereas clone F binds to its Fz domain. However, the specific epitopes of both antibodies still needed to be identified.

In collaboration with Mimotopes Ltd, the first approach was to generate a library of biotinylated and overlapping peptides covering the extracellular portion of ROR1. One of the main advantages of this method is that it allows high throughput and quantitative analysis for identification of linear epitopes. Moreover, the presence of a linker between the biotin end and the actual peptide minimises steric hindrance to binding (Ltd). These features proved particularly useful for clone SA1, as data obtained from this approach narrowed down the search of SA1's epitope to three peptides within the Ig-like domain.

In contrast, when clone F was evaluated using the same platform, no binding was detected. Consistent results after independent repetitions of this experiment led to the hypothesis that clone F did not have a continuous but a conformational epitope. Intrigued by this possibility, soluble ROR1 protein was run under reducing (R) and non-reducing (NR) conditions on a Western blot (SDS-PAGEs). The presence of SDS in the polyacrylamide gels implied that although run under non-reducing conditions, soluble ROR1 protein was not in its native form. The absence of a reducing agent (such as β-Mercaptoethanol), however, meant that no disulphide bridges were disrupted. This explains the appearance of a higher molecular weight for ROR1 in the NR gels, since these conditions conveyed some 3D structure to the protein, although still minimal compared to native gels.

Consistent with this, the 3D structure still present in soluble ROR1 allowed the binding of clone F to its conformational epitope. In contrast, when ROR1 was

run under reducing conditions, F binding was not detected. These results were further confirmed when cell lysates expressing full-length ROR1 or its truncated domains were run in SDS-PAGEs using the same methodology. Together, Western blot analyses confirmed clone F detected a discontinuous epitope in the Fz domain of ROR1.

I next investigated the specific amino acids required for ROR1 binding. Data obtained from different approaches was collated in order to identify the most likely binding regions within the Ig-like and the Fz domains. Using this rational approach, retroviral vectors bearing single aa mutations within selected regions were generated. Importantly, amino acid substitutions were carried out using non-conservative mutations, whereby substituting amino acids were chosen based on the dissimilarity between them and the wild-type aa in terms of structure and the chemical characteristics of their side chains (R groups) (Yampolsky and Stoltzfus, 2005). As a result, this approach allowed the exact identification of those aa that were essential for the binding of clones SA1 and F to ROR1.

Currently, there are other research groups working on ROR1 antibody-based immunotherapies, and some of their binders have resulted in the development of: i) a therapeutic antibody (Cirmtuzumab) (Choi et al., 2015) or ii) antibody derivatives such as CARs (Deniger et al., 2015, Berger et al., 2015). Clinical trials are now on-going or about to start in order to assess whether these products are able to achieve a significant clinical benefit on cancer patients, particularly those affected by CLL. With this in mind, one of the aims of this study was to differentiate our own ROR1 antibodies from the binders developed elsewhere.

Clone D10, the prototype of clone UC-961 (Cirmtuzumab), and the scFv of clones 4a5 and R12 (used for CAR therapy) bind to the Ig-like domain of ROR1, as does clone SA1. Therefore, to verify that the epitope of SA1 was not shared with any other reported clone, competition assays were performed by

flow cytometry; where the combination of SA1 and F antibodies were used as negative control for overlapping epitopes.

Consistent with previous findings, no reduced binding was observed when different pairings of reported antibodies and SA1 were used. This data indicated no epitope overlap, confirming the uniqueness of SA1 antibody. Another interesting observation was the shift produced when clones F and SA1 were used together. Approximately 20% of the live events did not shift to the double positive quadrant. A likely explanation is the lower affinity of clone F towards ROR1, discussed in the previous chapter.

Having established the uniqueness of both of our antibodies, I sought to determine the CDC activity of SA1. Based on pre-clinical *in vitro* studies of other monoclonal antibodies used in cancer therapy (Barth et al., 2015, Bowles et al., 2006, Cheney et al., 2014, Herter et al., 2013), purified SA1 was tested on CLL cells at 10ug/ml; and its cytotoxicity was compared to the one produced by another chimeric binder, Rituximab, a clinically approved anti-CD20 antibody. Significant CDC activity elicited by both antibodies was observed, although the cytotoxicity of SA1 was not as high as Rtx's. It is considered this might be due to the difference in expression between ROR1 and CD20, as high antigen density seems to contribute to potent cytotoxicity (Prang et al., 2005, Velders et al., 1998).

The next step was to humanise clones SA1 and F in order to increase their therapeutic potential. To this end, our collaborators, GenScript, used a CDR-grafting approach. Certainly, this is a well-established humanisation method that has generated many of the therapeutic antibodies currently used in the clinic (Safdari et al., 2013). However, one of the major pitfalls of this strategy is the potential changes it can cause to CDR conformation, thereby causing loss of affinity (Safdari et al., 2013, Dall'Acqua et al., 2005). In line with this, a slight decrease of binding and subsequent CDC activity of our humanised antibodies compared to SA1 was observed.

Albeit reduced, it appears that both humanised clones HuA1 and HuA3 were still able to prompt significant CDC of CLL cells. However, as discussed in the Introduction section (**Chapter 1**), other mechanisms of action in terms of antibody cytotoxicity exist, such as those provoked by direct antibody binding in the absence (direct cell death) or presence of effector cells (ADCC). Assays evaluating these two mechanisms remain to be assessed.

Up to date, these two mechanisms of killing using ROR1 MAbs have been reported before with mixed results. A study by (Yang et al., 2011) showed that no significant cytotoxicity was elicited by rabbit-raised ROR1 MAbs, suggesting that naked antibodies against ROR1 were not viable as therapeutic MAbs. The only publication where ROR1 binders were able to produce direct apoptosis on CLL cells was performed on FPLC-purified IgG and IgM murine antibodies (Daneshmanesh et al., 2012). However no follow up study on these antibodies has been reported.

Moreover, except for a human tissue cross-reactivity study (Choi et al., 2015), the preclinical evaluation of Cirmtuzumab was not based on classicak *in vitro* or *ex vivo* data, but on *in vivo* models, amongst them: immunodeficient mice (for breast cancer (Cui et al., 2013)), Eμ-TCL1 transgenic mice (CLL (Widhopf et al., 2014)) and rodent and non-human primates for off-target or non-ROR1-specific activity (Choi et al., 2015).

Being aware of the potential that antibodies with dual specificity offer to the advancement of cancer immunotherapy, I developed bispecific antibodies that could combine simultaneous targeting of ROR1 and CD3 or ROR1 and PD-1. Since other members of our group were developing a similar concept in a BiTE format, I decided to design bispecific antibodies in full IgG. The main two advantages of this strategy are the extended half-life of the molecule and the extra cytotoxic potential this format offers due to Fc-Fc gamma receptor (FcγR) interactions (Kim et al., 2016b); providing this molecule with a potential three-fold cytotoxicity.

After successful cloning and expression of these new bispecific antibodies, their cytotoxicity was assessed by co-culture of ROR1^{+} and ROR1^{-} solid cancer cell lines and PBMCs from healthy donors. Unfortunately, non-specific binding and cytotoxicity of a ROR1^{-} breast cancer cell line (MCF-7) was detected. Independent experiments and cytokine data confirmed non-specificity of SA1.

It is hypothesised this might be due to a number of reasons. In some cases, although a single B-cell produces a monoclonal antibody with exquisite specificity, this antibody can crossreact with other antigens or exhibit dual specificity. This could be caused by similarity in shape or chemical composition of the epitope (Nelson et al., 2000). Also, the fact that the epitope of an antibody is a short linear peptide, does not mean it is not part of a particular conformation (Gershoni et al., 2007). Furthermore, SA1 antibody detects the apical region of the Ig-like portion of ROR1. Genomic analyses have shown that membrane proteins with Ig-like domains (immunoglobulin superfamily) are extremely abundant (Barclay, 2003). Moreover, this domain has evolved to be particularly good at being recognised as it is involved in many different kinds of protein interactions.

Taken these data as a whole, studies using clone SA1 or its humanised versions were stopped. Research focused instead on the investigation of the therapeutic potential of a BiTE antibody based on humanised F and anti-CD3. Data from these studies will be explored in the next chapter.

5.4.1 Conclusions

- Peptide library ELISA indicated that clone SA1 detected a continuous epitope located in the apical region of the Ig-like domain of ROR1.
- Single amino acid mutations in said domain, and flow cytometry-based competition assays confirmed that SA1 recognised a particular epitope

that is not shared with other anti-ROR1 antibodies reported in the literature.

- In turn, I found that clone F did not possess a linear but a discontinuous epitope, as revealed by both peptide library ELISA, and Western Blot run under reducing and non-reducing conditions.
- Single amino acids mutations allowed me to identify the amino acid within the Fz domain that is crucial for F binding to ROR1.
- The latter confirmed that clone F is a unique antibody, able to detect a different domain in ROR1 compared to all the ROR1 antibodies (and/or their derivatives) currently used in the clinic.
- CDC activity of clone SA1 assessed at 10ug/ml concentration revealed potent *in vitro* cytotoxicity of $ROR1^{+}$ cell lines and primary cells from CLL patients but not PBMCs from healthy donors. However, it was not as strong as the one prompted by Rituximab (Rtx).
- To increase the therapeutic potential of clones SA1 and F, their variable domains were humanised using the CDR-grafting method through collaboration with GenScript.
- Humanised F was developed as antibody derivatives (CARs and BiTEs) by other members of the lab.
- HEK293T cells were co-transfected with all 25 possible combinations of humanised V_H and V_L sequences derived from SA1.
- Flow cytometry data allowed the identification of the best two possible combinations: HuA1 and HuA3 clones.
- No considerable difference was found between them in terms of ROR1 binding (41% and 43%, respectively). However, these values were lower than SA1's (49.4%).
- The CDC of HuA1 and HuA3 was compared to SA1, Rtx and GA-101 (Obinutuzumab). Although still significant, cytotoxicity elicited by humanised clones on CLL cells was not as potent as the one prompted by SA1.

- To circumvent reduced CDC activity, bispecific antibodies in full IgG combining SA1 and anti-CD3 or SA1 and anti-PD-1 were designed.
- When two ROR1^{+} and one ROR1^{-} solid cancer cell lines were treated with these bispecific molecules, non-specific binding and cytotoxicity was revealed.
- Independent experiments and quantification of IFN-γ and IL-2 cytokines confirmed non-specific killing of ROR1^{-} cells.
- As a whole, it was decided not to pursue further studies with clone SA1 and focus instead on the investigation of the therapeutic potential of a clone F derivative developed alongside in our lab: F-aCD3 BiTE.

5.4.2 Future work

Although the *in vitro* studies reported in this chapter suggest that -except for clone SA1- our ROR1 antibodies might not elicit potent cytotoxicity, other methods such as direct cells death and ADCC assays need to be performed. Furthermore, it is considered that data from *in vivo* studies will ultimately reveal their cytotoxicity potential. As discussed above, the only example of a successful ROR1 antibody currently in clinical trials is Cirmtuzumab. It is believed the *in vivo* studies performed using this antibody were fundamental to its development as a therapeutic alternative, as no classical *in vitro* evaluations have been reported.

Importantly, apart from the classical antibody mechanisms of action (direct cell death, CDC, ADCC and ADCP), recent studies have reported an additional vaccinal or autoimmunisation effect (**Chapter 1**); which was identified solely by *in vivo* evaluations. In brief, the vaccinal effect is prompted by the ability of antibodies to trigger an adaptive immune response that results in the activation of tumour-reactive CD4^{+} and CD8^{+} T-cells. This property is essential for the efficacy of antibody therapy as it promises anti-tumour long-term protection after cessation of MAbs treatment (Arce Vargas and Quezada, 2015).

Furthermore, in order to induce a T-cell dependent vaccinal effect, DiLillo *et al*. demonstrated that monoclonal antibodies need to engage FcγRIIA, the only activating FcR expressed on dendritic cells (DiLillo and Ravetch, 2015).

Intriguingly, these Fc-FcR interactions can be further enhanced by glycoengineering of the Fc portion of monoclonal antibodies (Yu et al., 2017, Beers et al., 2016). I propose that a first step towards this would be the production of afucosylated antibodies. Certainly, afucosylation of the heavy chain constant has proved to enhance Fc-Fc gamma receptor interactions (Weiner, 2015). This can be achieved by production of monoclonal antibodies using alpha-1,6-fucosyltransferase (FUT8) deficient Chinese hamster ovarian (CHO/FUT8$^{-/-}$) cells. A relevant example of this approach is Obinutuzumab, a humanised anti-CD20 antibody with superior ADCC activity.

Chapter 6 ROR1 therapy on PANC-1-derived tumourspheres

6.1 Introduction

Cytotoxicity data discussed in the previous chapter revealed that clone SA1 bound non-specifically to MCF-7 cells, a ROR1$^-$ breast cancer cell line. Further confirmation of those results led me to focus instead on the study of a humanised ROR1 bispecific T-cell engager (BiTE). The latter was engineered to target both the Fz domain of ROR1 (through clone F scFv) and the CD3 molecules on T-cell membranes (through an anti-CD3 scFv).

Our group has already established the potent and specific killing that our ROR1 BiTE therapy has on a range of ROR1$^+$ solid cancer cell lines both *in vitro* and *in vivo*, including pancreatic cancer cells (Gohil et al., 2017). To date, pancreatic cancer (PaCa) is one of the most aggressive malignancies, where metastasis and therapeutic resistance are hallmarks of the disease. The difficulties in curing PaCa are attributed to the presence of cancer stem-cell like cells (CSC) (Sergeant et al., 2009). Importantly, some reports indicate that ROR1 is also present on the cell surface of CSCs (Jung et al., 2016, Zhang et al., 2014). Thus, in this chapter, the ability of our ROR1 BiTE to target and eliminate ROR1$^+$ pancreatic CSC was investigated.

In the following sections, I will describe the generation of tumourspheres from a pancreatic cancer cell line by spheroid formation assay. Also, to corroborate the presence of an enriched CSC population within the generated tumourspheres, data from gene, protein and functional characterisation will be discussed. Finally, the efficacy of the ROR1 BiTE therapy on general cell viability and on specific ROR1$^+$ compartments within the tumourspheres will be explored. Additionally, below it is provided a brief introduction on relevant research concepts involved in this study: i) BiTE therapy, ii) Pancreatic cancer, iii) CSC and iv) Spheroid formation assay.

6.1.1 BiTE Therapy

BiTEs, a subclass of bispecific antibodies, are constructed by genetically linking the scFv portions of two different MAbs. In this format, one arm binds to the CD3ε subunit of the TCR complex expressed on T-cells, whilst the second targets a tumour-associated antigen (TAA) expressed on cancer cells. Both scFvs are connected by a short flexible glycine-serine linker which facilitates antigen-scFv interactions (Wolf et al., 2005).

BiTEs induce the formation of immunological synapses by bringing T-cells closer to tumour cells (**Fig. 6. 1**). As a result, cytotoxicity is elicited by the release of perforin and granzymes from granules in the cytotoxic T-cell, which in turn induces apoptosis and lysis of the malignant cell (Suryadevara et al., 2015). Notably, it has been shown that T-cells exposed to Blinatumomab, the first-in-class clinically approved CD19-CD3 BiTE, remain activated and continue to produce and store perforin and granzymes in order to serially attack additional $CD19^{+}$ cells (Nagorsen and Baeuerle, 2011, Hoffmann et al., 2005). On top of that, inflammatory cytokines are released, and T-cell proliferation is promoted (Newman and Benani, 2016).

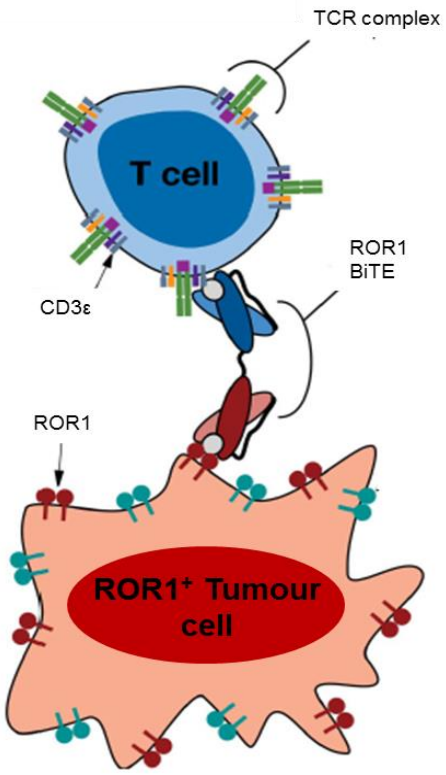

Fig. 6. 1. Schematic representation of immunological synapse between a T-cell and a ROR1⁺ cancer cell mediated by ROR1 BiTE binding. Modified from Suryadevara CM et al., 2015.

It is noteworthy that a major advantage of BiTEs over other T-cell immunotherapies such as CARs is that these bispecific antibodies are able to exploit the resident polyclonal T-cell population and do not rely on a particular

subset. Data from several studies indicate that, in addition to $CD8^+$ cytotoxic T-cells, $CD4^+$ helper T-cells are also able to upregulate production of perforin and granzyme B upon BiTE-mediated binding to target cells (Brischwein et al., 2006, Haas et al., 2009, Suryadevara et al., 2015). Furthermore, this type of therapy does not require *ex vivo* manipulation.

Due to their small size (55-60kDa), BiTEs may have a better chance to penetrate deep into solid tumours and re-activate local tumour-infiltrating lymphocytes (TILs) or even co-opt T_{REGs} (Suryadevara et al., 2015). Plus, the short half-life of these bispecific binders offers a reduced clinical risk in the scenario of adverse events caused by BiTE therapy.

In terms of clinical benefit, a long-term survival analysis of patients with minimal residual disease after chemotherapy showed 61% haematologic relapse-free survival at a median of 33 months after Blinatumomab (Newman and Benani, 2016). Despite these encouraging results, better strategies for managing concomitant major adverse events such as cytokine release syndrome (CRS), seen in both BiTE therapy and CD19 CARs, are required. Furthermore, although infrequent, the loss of CD19 expression has been reported as a mechanism of resistance after acute lymphoblastic leukaemia (ALL) patients treated with Blinatumomab in a phase II trial relapsed with CD19-negative B-cell ALL disease (Portell et al., 2013, Topp et al., 2012). More recently, adaptive resistance to BiTEs was described when (Kohnke et al., 2015) reported for the first time increased PD-L1 positivity in a 32-year-old male patient with refractory B-precursor ALL resistant to Blinatumomab. Also, high frequency of Tregs (defined with a cutoff of 8.525%) in B-precursor ALL patients had a 100% failure rate to Blinatumomab (Duell et al., 2017). Nevertheless, researchers suggested that therapeutic removal of Tregs by the use of cyclophosphamide and fludarabine (as per CAR therapy) could convert Blinatumomab non-responders to responders.

All in all, BiTEs represent a major advancement in cancer immunotherapy, with the added possibility of stepwise dose escalation and rapid cessation of treatment should toxicity occur. Further improvement in the management of toxicities coupled with better targets, such as ROR1, and long-term survival benefits will enhance the great promise that BiTE technology offers for patients, particularly those suffering from cancers where survival rates are dismal, such as pancreatic cancer.

6.1.2 Pancreatic cancer (PaCa)

According to the American Cancer Society (Society, 2015), PaCa is currently the third most common cause of cancer-related death in the US and the 7th worldwide. It has an extremely poor prognosis, which has shown little improvement over the last 40 years (Muniraj et al., 2013). Even with currently available therapies, a median survival of less than 6 months and overall 5-year survival rates of 1-5% are obtained (Ercan et al., 2017). For a more detailed description of PaCa biology, TME and current therapies, please see **section 1.2.2** (**Chapter 1**).

Early detection of the disease is impaired by absence of symptoms and lack of specific diagnostic markers (Costello et al., 2012). Hence, the majority of patients (80-90%) are diagnosed when local metastasis has already occurred. Standard therapy at this stage is gemcitabine-based chemotherapy. However, the long-term efficacy and prognosis of this approach varies and is widely unsatisfactory for most PaCa patients (Ciliberto et al., 2013, Nakai et al., 2012). Of note, even patients diagnosed at early stages of the disease and therefore able to benefit from surgical resection -currently the only curative option- have poor prognosis and more than 80% of patients relapse within 2 years after surgery (Zhou et al., 2013).

Pancreatic ductal carcinoma (PDAC) is a major histological subtype and represents more than 90% of all PaCas (Society, 2015). The high mortality

seen in pancreatic cancer in general, and PDAC in particular, is often associated to the highly dense fibrotic tissue (constituting 90% of the tumour volume) as it acts as a physical barrier to effective drug delivery. In addition, PDAC shows minimal response to chemotherapy, often attributed to the presence of cancer stem cell-like cells (Ercan et al., 2017, Wolfgang et al., 2013), as they have been associated to tumourigenesis, metastasis, chemotherapy resistance and poor clinical outcome (Qiu et al., 2015).

6.1.3 Cancer stem cell-like cells (CSC)

For several decades, the heterogeneity seen in malignant tumours has been a source of continuous debate amongst scientists. Thereof, two main models have been proposed: i) the clonal evolution hypothesis (stochastic model), and ii) the hierarchical hypothesis (CSC model) (Reya et al., 2001).

The first model proposes that a distinct population of tumour cells acquires relevant somatic mutations and stochastically self-renew/differentiate, allowing selection of more aggressive subclones. This would ultimately result in metastasis and therapy resistance. The CSC hypothesis, in contrast, suggest that only a small subset of tumour cells (CSC) has the ability to self-renew and give rise to heterogeneous progenitor cells with limited proliferation and tumourigenic potential (Reya et al., 2001, Cabrera et al., 2015, Odoux et al., 2008).

More recently, however, data from several studies indicate that both models are not mutually exclusive (Cabrera et al., 2015, Gasch et al., 2017, Nakata et al., 2014), but rather it would appear as if a single cancer tumour may comprise several CSC subclones that have a common ancestor. These CSC subsets would have persisted over time and accumulated genetic and epigenetic changes necessary for cancer initiation and progression. Each CSC subclone would then generate different progenitor cells, which would also accumulate genetic changes. In time, some of them would acquire self-renewal capabilities

modulated by microenvironmental stimuli. Remarkably, this unified model highlights the existence of different CSC subpopulations, tumour cells plasticity and suggests bidirectional conversion between non-CSC to CSC states (**Fig. 6. 2**).

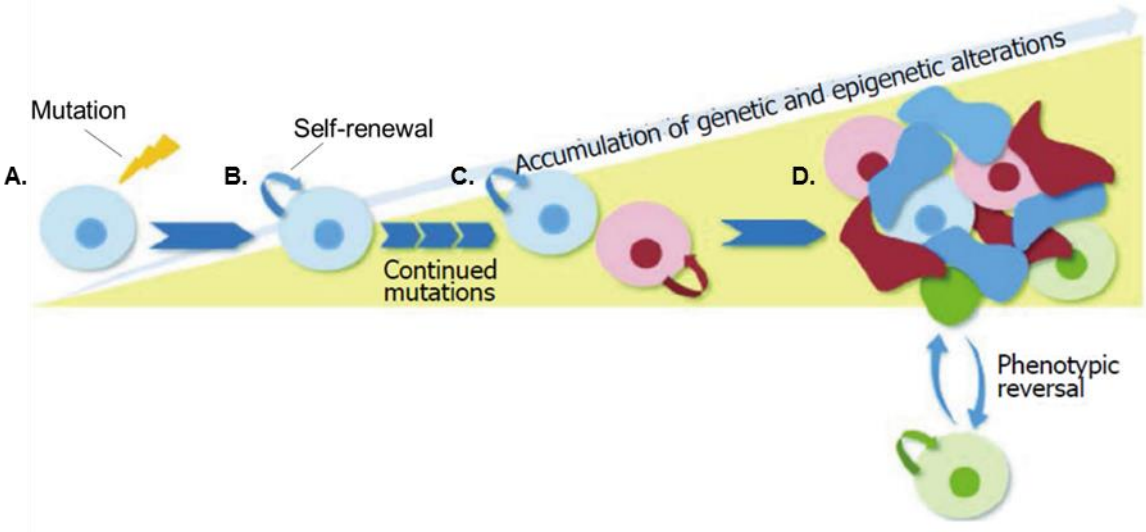

Fig. 6. 2. Schematic representation of unified model of clonal evolution and cancer stem cell-like cells. (A) The originating CSC, exposed to oncogenic mutations, (B) gives rise to subclones with self-renewal capacity. (C) Over time, these CSC accumulate genetic and epigenetic changes. Each different CSC subclone will go through asymmetrical division, generating more CSC and progenitors. (D) Progenitors in turn will proliferate, and fully differentiated cancer cells will emerge. Shown also is a subset of these progenitors (green) depicting tumour cell plasticity and bidirectional conversion between non-CSC and CSC, modulated by microenvironmental stimuli. Modified from Cabrera MC et al., 2015.

According to a report produced by CSC specialists at a workshop convened by the American Association of Cancer Research (AACR) in 2006, the consensus definition of a cancer stem cell is a cell within a tumour that possess self-renewal capacity and the ability to generate heterogeneous lineages of cancer cells. Researchers emphasised that a frequent error in defining stem cells is to extrapolate expression of biomarkers from CSC studies obtained in one organ to different organs, as they can differ significantly from one another (Clarke et al., 2006). To avoid misleading results, Clarke et al. indicated that

CSCs need to be tested first for their potential to show both self-renewal and tumour propagation and then for biomarker expression. The gold standard assay for this is serial transplantation in animal models. The feasibility, cost and time that this assay requires, however, rise the necessity of developing alternative *in vitro* models, such as tumourspheres generated by 3D sphere formation assay (Qureshi-Baig et al., 2016).

6.1.4 Sphere formation assay: Tumourspheres

Isolation of CSC relies on a number of functional features, such as anoikis-resistance (evidenced by anchorage-independent growth), self-renewal, pluripotency, asymmetric division and chemoresistance (Qureshi-Baig et al., 2016). The spheroid formation assay utilises the anchorage-independent growth properties of cancer stem cells-like cells and it has shown to better preserve the characteristics of original tumours in terms of: gene expression profile, tumour heterogeneity and morphology, compared to adherent cultures (Lee et al., 2015, Weiswald et al., 2015, Lee et al., 2006).

The exact extent to which tumourspheres favour CSC enrichment, however, has not been fully described. Furthermore, contrasting results on CSC enrichment have been found depending on the cancer subtype studied and whether spheroids were obtained from primary tumour cells or cell lines – where not all cell lines derived from the same cancer subtype possessed the same sphere formation capability (Bowles and Weiner, 2005, Collura et al., 2013).

Nonetheless, using a sphere formation system, (Hansford et al., 2007) showed for the first time successful expansion of tumourspheres derived from aggressive neuroblastoma, able to form metastatic tumours in a murine xenograft model with as few as 10 passaged cells. Furthermore, several reports have used tumoursphere culture as a means to isolate, enrich, maintain and expand CSC subpopulations from various types of cancer (Lee

et al., 2006, Ponti et al., 2005), including pancreatic cancer cell lines (Dalla Pozza et al., 2015, Gaviraghi et al., 2011). In this chapter, 3D culture of tumourspheres will be used for the study of the therapeutic effect of ROR1 BiTE on pancreatic CSCs.

6.2 Aims

1. To generate tumourspheres from a PDAC cancer cell line (PANC-1) by 3D spheroid formation assay, using ultra-low attachment plates.
2. To perform: i) gene, ii) protein and iii) functional characterisation of PANC-1-derived tumourspheres by qPCR, confocal microscopy and transwell migration assay, respectively.
3. To assess the effect of ROR1 BiTE therapy on the cell viability of tumourspheres and specific elimination of $ROR1^{+}$ cell subpopulations.

6.3 Results

6.3.1 Aim 1: Generation of PANC-1-derived tumourspheres

To evaluate the efficacy of ROR1 BiTE therapy on PaCa CSCs, I first needed to establish tumourspheres from PANC-1, a pancreatic ductal adenocarcinoma cell line. For this, ultra-low attachment plate-3D culture approach was used (See Materials & Methods section – **Chapter 2**).

As reported by others (2016, Cao et al., 2011, Qureshi-Baig et al., 2016), stemness and pluripotency of cancer cells can be assessed *in vitro* by inducing anchorage-independent growth of tumourspheres in the absence of serum. In line with this, single-cell suspensions of adherent PANC-1 cells (Parental) were cultured in ultra-low attachment 6-well plates. With regards to the cell culture media used, two different types were tested: i) MEBM + MEGM SingleQuots supplements (as per (Zhang et al., 2014)) and ii) CSC + Supplement Mix (as per (Garikapati et al., 2017)).

Tumourspheres were fed every 3-4 days and passaged every 7-9 days. Of note, most cells died within the first 5 days of culture, indicating that ultra-low attachment plates selected for anoikis-resistant cells, a feature of CSC. During the second week, some small spheroids were detected. Moreover, cell viability increased over consecutive passages, which resulted in more and bigger spheroids over time.

In **Fig. 6. 3**, images of PANC-1 Parental cells and tumourspheres generated using the different types of media aforementioned are shown. Although spheroids from both methods presented high cell viability after 7 passages; it became evident that cells grown with CSC media displayed a higher count of live cells and formed bigger tumourspheres than those cultured with MEBM. As a result, the subsequent experiments were performed using only tumourspheres generated with CSC media.

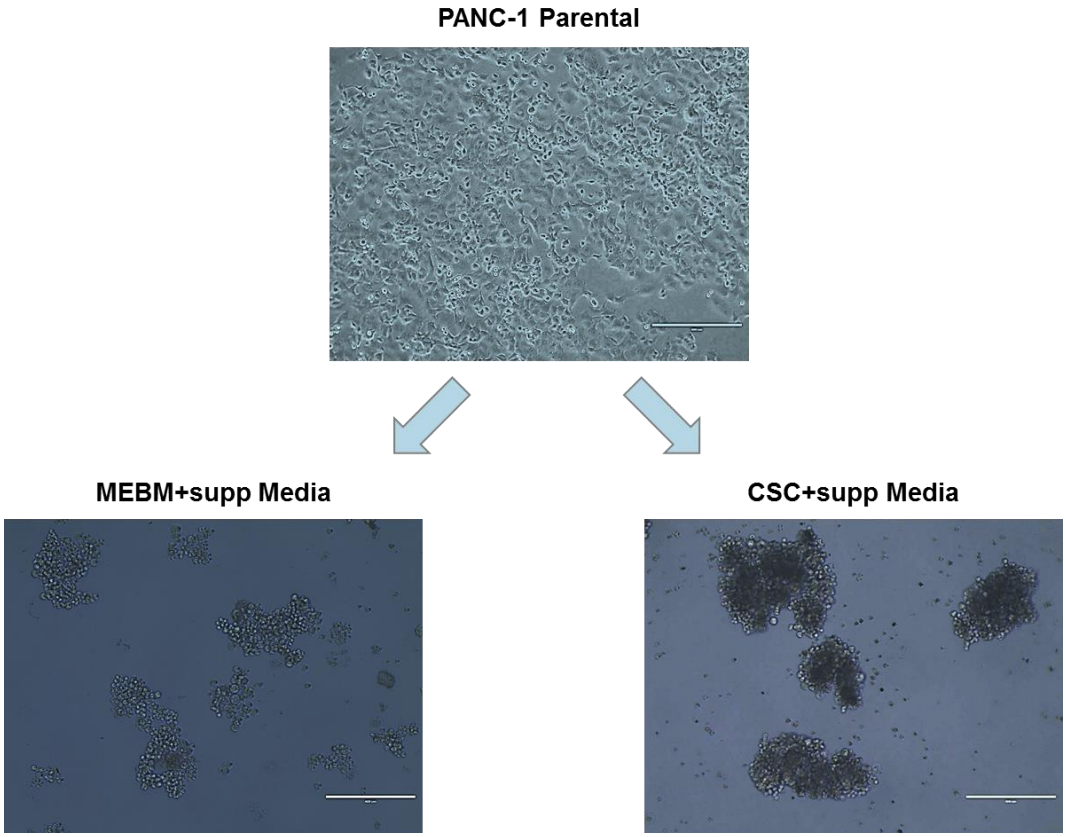

Fig. 6. 3. Tumoursphere formation assay on PANC-1 cells. Single-cell suspensions of PANC-1 adherent cells (Parental) were cultured in ultra-low attachment 6-well plates, using either: i) MEBM+supplements or ii) CSC+supplements media. Shown are images of PANC-1 parental cells and tumourspheres (P7) generated using the culture media mentioned above. Images were taken with a 4x microscope objective lens. Scale represents 400um. P7= Passage 7.

As mentioned in the Introduction section of this chapter, specialists on CSC indicated more than a decade ago that relying solely on a marker expression profile for isolation of CSC, has proved to be equivocal as marker expression can vary from organ to organ (Clarke et al., 2006). Instead, there seems to be a consensus that CSC should be defined by their potential to show key properties of cancer stem cell-like cells: anchorage-independent growth (anoikis resistance) and the ability to self-renew. Having tested the former, I sought to evaluate their self-renewal capacity by performing a tumoursphere formation assay by limiting dilution.

In brief, tumourspheres (“CSC”) -directly obtained from PANC-1 parental cells- were segregated and carefully trypsinised in order to produce a single-cell suspension. Single cells were seeded in ultra-low attachment 96-well plates at a density of 0.5cells/well. CSC were fed every 4-6 days and their growth assessed under the microscope. Spheroids were detected after approximately 10-12 days. CSC which possessed the capacity to form spheroids from a single cell were called “CSC96” (**Fig. 6. 4**).

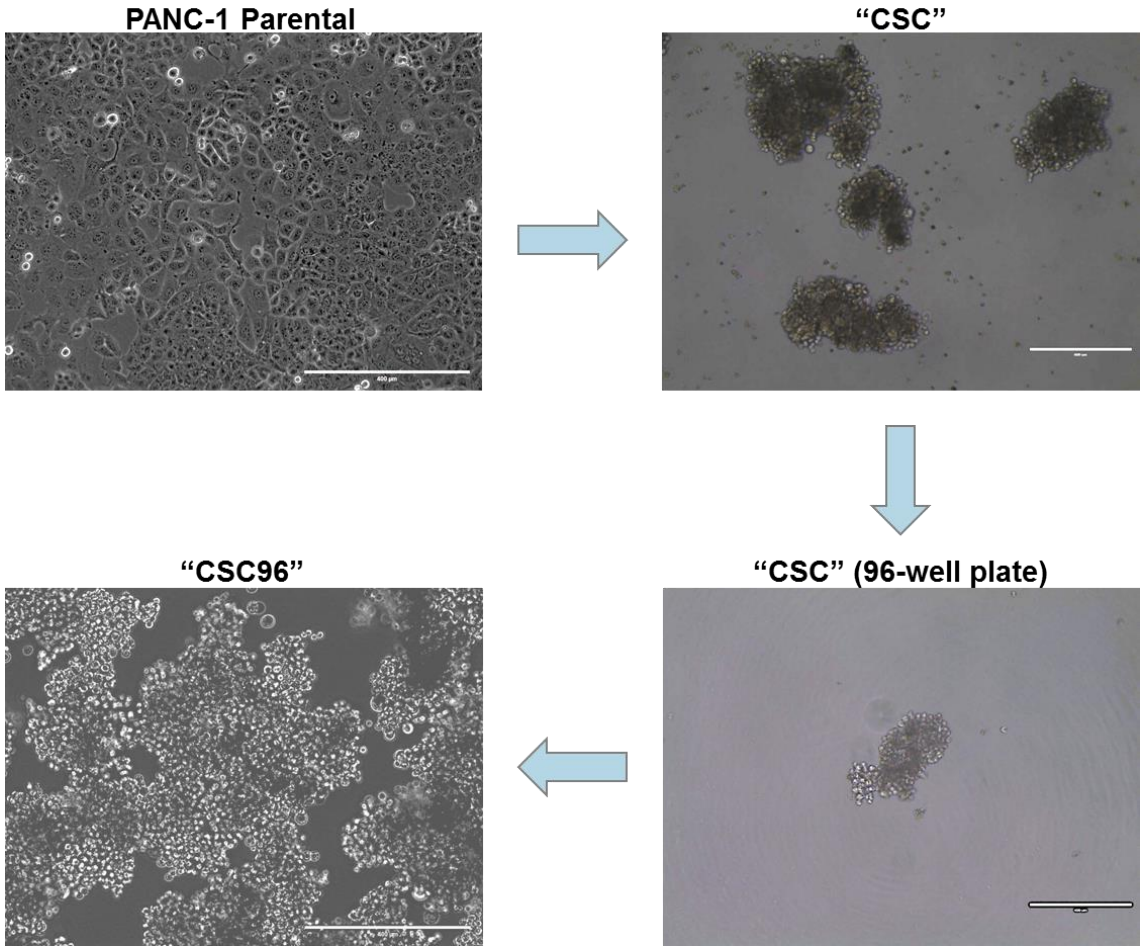

Fig. 6. 4. Evaluation of tumoursphere formation by limiting dilution. Shown are images of PANC-1 Parental cells, from which “CSC” were generated. After a few passages, CSC were prepared as a single-cell suspension by enzymatic dissociation in order to be plated by limiting dilution (0.5 cells per well) on ultra-low attachment 96-well plates. After 10-12 days, spheroids were observed (“CSC” 96-well plate). Cells able to form tumourspheres from a single cell were called “CSC96”. Newly generated “CSC96” were then transferred to ultra-low attachment 6-well plates for serial passage and expansion. Images were taken with a 4x microscope objective lens. Scale represents 400um.

Fig. 6. 4 shows the generation of anoikis-resistant tumourspheres with self-renewal capacity (“CSC96”); a process that started with PANC-1 Parental cells and involved cell culture in serum-free media under anchorage-independent growth conditions. This was then followed by limiting dilution, and resulted in the production of CSC96 cells. Images of PANC-1 Parental cells, the spheroids they originated (“CSC”) and a picture of a tumoursphere in a 96-well plate generated from a single CSC are presented. These new spheroids (“CSC96”) were transferred to 6-well plates in order to be expanded for further investigation.

It is noteworthy to mention that apart from “CSC” and “CSC96” cells, a third type of spheroids were generated: “CSC Conf”. The latter were obtained by serial passage of CSC spheroids using a higher concentration of cells/ml (i.e. Once CSC were passaged at a 10^4 cells/ml conc., all the remnant cells were cultured together, typically at a $5x10^4$ cells/ml). Morphologically, “CSC Conf” were bigger than regular “CSC” but not “CSC96” (data not shown).

6.3.2 Aim 2: Characterisation of PANC-1 tumourspheres

As mentioned above, identification and subsequent isolation of CSC based only on a marker expression profile might lead to error. However, if performed on established anokis-resistant tumourspheres with self-renewal capacity, the stemness of these cells can be ascertained in a more reliable manner, especially if markers at both gene and protein levels are coupled with functional characterisation.

In this section, gene and protein expression will be assessed by qPCR and confocal microscopy, respectively. Additionally, the migration ability of CSC96 compared to PANC-1 Parental cells will be evaluated using a transwell system.

6.3.2.1 Gene expression by qPCR

The mRNA of all three versions of PANC-1 tumourspheres (namely, CSC, CSC Conf and CSC96), along with PANC-1 Parental cells were isolated in order to obtain cDNA. The absence of contaminant genomic DNA was verified by PCR using purposely-designed GAPDH primers (See **Chapter 3**). Having tested the cDNA quality of all the samples, gene expression of different biomarkers was then evaluated.

In **Fig. 6. 5A**, the expression of stemness markers such as CD133, SOX2 and Nestin is shown. qPCR data indicates significant upregulation of both CD133 and SOX2 in all three types of tumourspheres compared to Parental cells. Nestin expression, however, was downregulated.

In terms of typical CSC-related markers, I evaluated genes encoding for antigens, molecules and signalling pathways involved in self-renewal (Notch1, Bmi1), as well as high invasiveness and metastatic potential (ROR1, ALDH1, CD24, Vimentin and CXCR4).

As expected, data shown in **Fig. 6. 5B** indicates significant upregulation of Notch1, Bmi1, two isoforms of ALDH1, CD24 and CXCR4. Although slightly elevated, one isoform of ALDH1 (ALDH1-B1) and Vimentin gene expression on tumourspheres was not significantly different from the one observed on Parental cells. Surprisingly, however, ROR1 levels were significantly reduced.

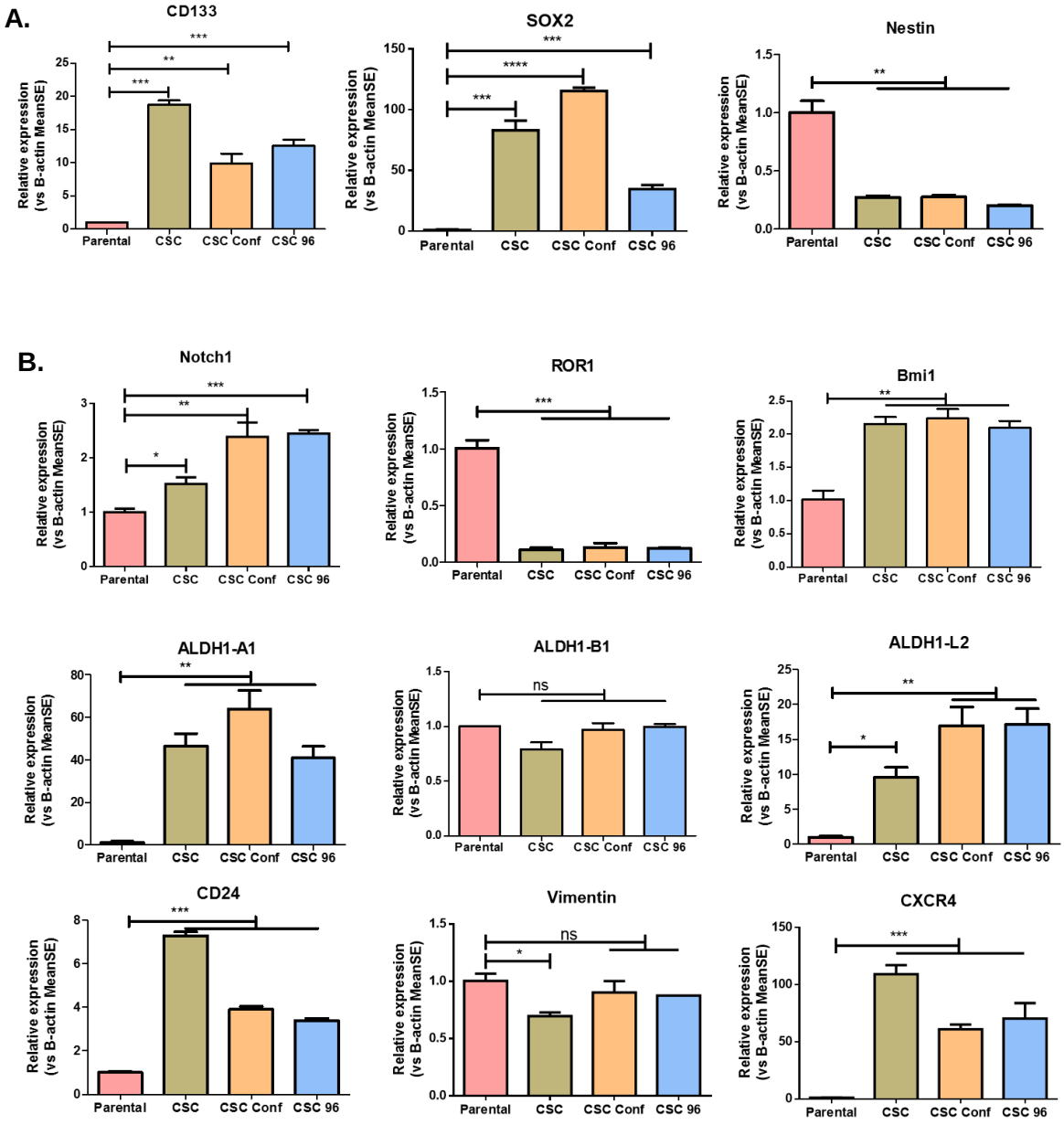

Fig. 6. 5. Biomarker gene expression by qPCR. cDNA from PANC-1 Parental cells and all three versions of tumourspheres were evaluated by qPCR. (A) Typical stemness and (B) CSC-related genes were investigated. Gene expression was normalized to B-actin and compared to PANC-1 Parental. Experiments were performed in triplicates. Error bars represent SEM. Statistical test: *Unpaired t-tests*. **p*≤0.05, ***p*≤0.01, ****p*≤0.001, ns= not statistically significant.

To further investigate the latter, several repetitions of this experiment were carried out and the resulting qPCR products were run in an agarose gel. In **Fig. 6. 6A**, typical results showing the significant difference in ROR1 gene expression between PANC-1 Parental and tumourspheres are presented.

Fig. 6. 6B shows those qPCR products run in an agarose gel after 40 cycles of amplification. These results suggest that although ROR1 is significantly downregulated in all versions of tumourspheres, its presence is still detectable on all samples.

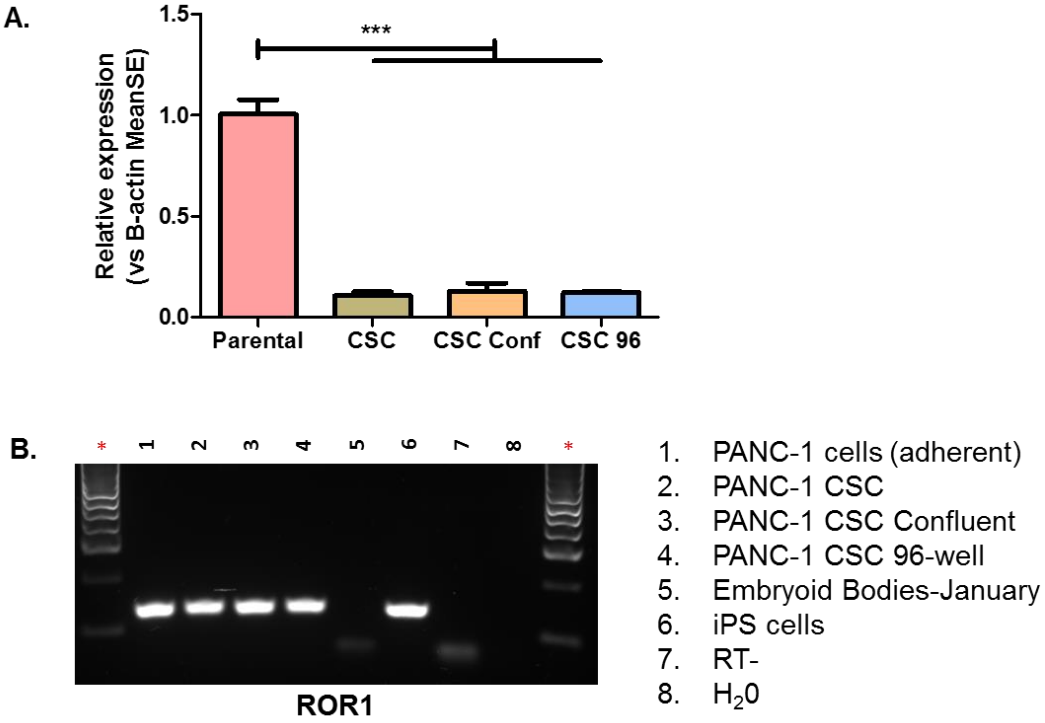

Fig. 6. 6. ROR1 gene expression on PANC-1 Parental and tumourspheres. (A) ROR1 gene expression evaluated by qPCR. (B) qPCR products run in a 1.7% agarose gel and stained with GelStar™. cDNA from iPS was used as positive control, whilst nucleotide-free water, RT negative and cDNA from embryoid bodies acted as negative control. Gene expression was normalized to B-actin and compared to PANC-1 Parental expression. Experiments were performed in triplicates. Error bars represent SEM. Statistical test: *Unpaired t-test.* ***$p \leq 0.001$. RT= Retro-transcriptase control. Ladder: Hyperladder 100bp.

In an effort to explain this apparent incongruence between qPCR and agarose gel data, qPCR experiments using 25, 30, 35 and 40 cycles of amplification were performed. qPCR products were subsequently run in agarose gels (See **Fig. 6. 7**).

At 25 cycles, no quantifiable amplification was detected although faint bands corresponding to Parental and iPS samples were observed. After 30 cycles,

however, qPCR data showed ROR1 amplification on Parental cDNA only, whilst products run in agarose gel revealed a clear difference in band intensity between Parental and all CSC versions. As expected, after 35 and 40 cycles, ROR1 gene expression was able to be quantified on all samples and agarose gels showed bands with similar intensity throughout, as ROR1 amplification reached saturation levels. Taken together, these data suggest that the discrepancy between qPCR and agarose gel data is explained by the fact that qPCR measured the difference in Ct values (i.e. gene expression in real time), whereas agarose gels showed the total accumulated product after qPCR amplification.

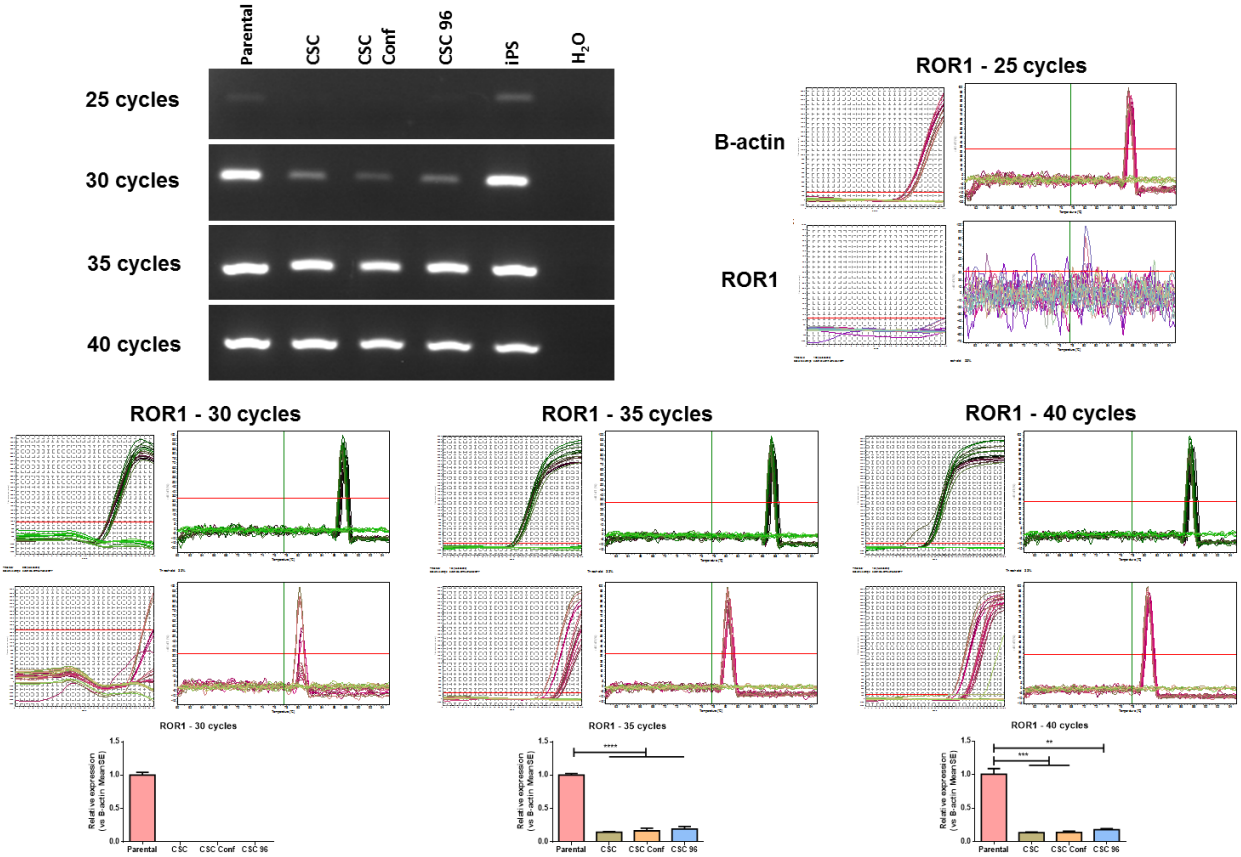

Fig. 6. 7. Investigation of ROR1 gene expression by qPCR. Several qPCRs were performed using 25, 30, 35 and 40 cycles of amplification. qPCR data was analysed, whilst amplicons were run in a 1.7% agarose gel, followed by staining with GelStar™. cDNA from iPS and nucleotide-free water were used as positive and negative control, respectively. Gene expression was normalized to B-actin and compared to PANC-1 Parental expression. Ct and Melting curve graphs are shown for illustrative purposes. Experiments were performed in triplicates. Error bars represent SEM. Statistical test: *Unpaired t-test.* ***p*≤0.01, ****p*≤0.001.

Additionally, to verify that the qPCR products being tested corresponded to the ROR1 gene, amplicons were sent for sequencing and aligned with full-length ROR1 nucleotide sequence (**Fig. 6. 8**). These results confirmed that the qPCR products matched the cytoplasmic region of ROR1. In turn, this further validated the observation that, whilst ROR1 was downregulated on PANC-1-derived tumourspheres, its expression was still detectable.

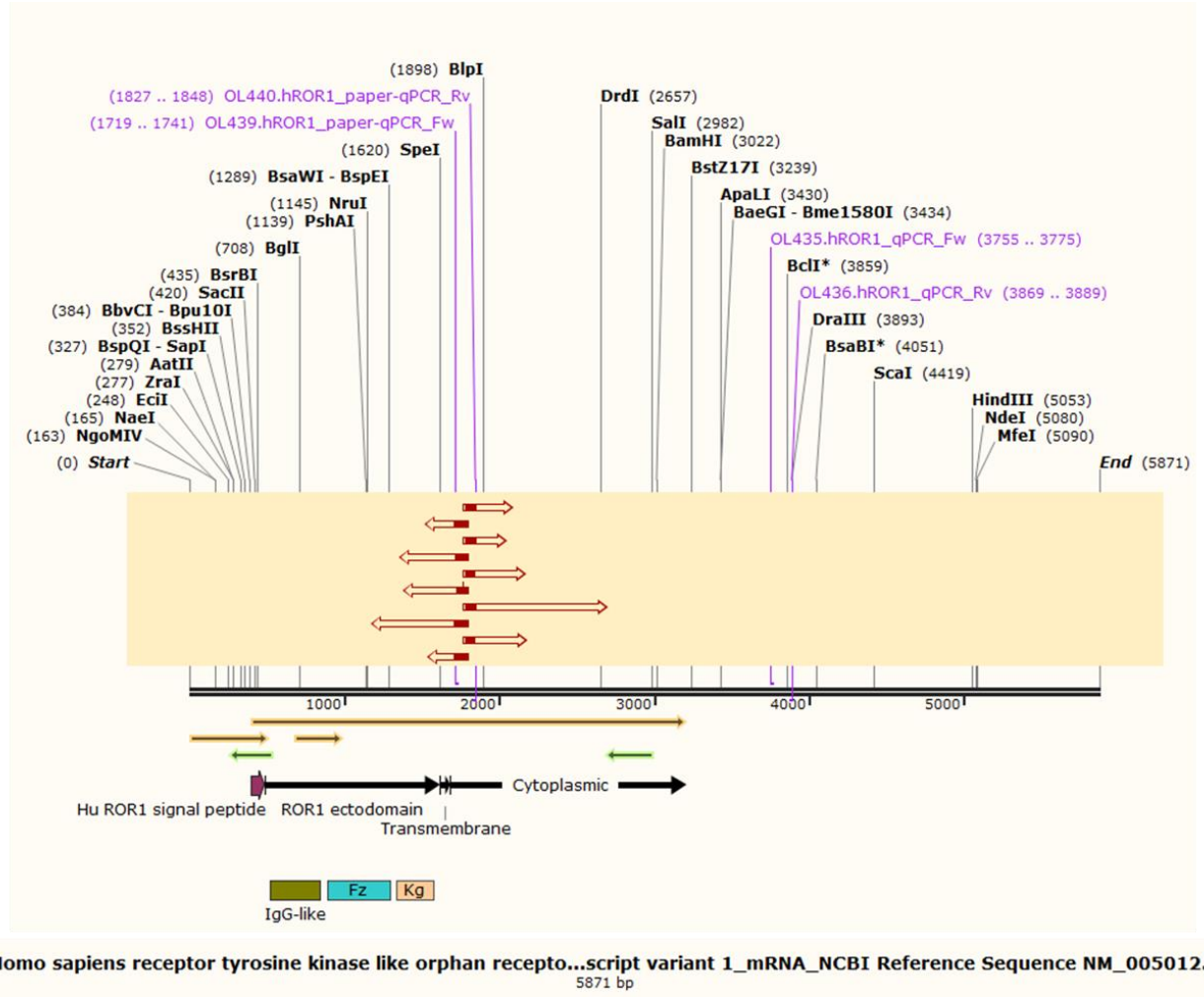

Fig. 6. 8. Sequencing alignments of ROR1 qPCR products. Amplicons from qPCR reactions were sent for sequencing and the resulting data was aligned with full-length ROR1 mRNA sequence. Amplicons showed correct alignment to the cytoplasmic region of ROR1. Red arrows represent location and matching sequence of qPCR products within the ROR1 nucleotide sequence.

In light of these results, my studies focused on CSC96 tumourspheres only and sought to further confirm their identity by testing five additional genes: i) Lgr4, a member of the leucine-rich repeat-containing GPCR (G-coupled protein cell receptor) family, which has increasingly been suggested to play critical roles in maintaining stem cell functions (Hsu et al., 2014, Nakata et al., 2014); ii) ABCA2, ABCC1 and ABCG2, members of the ATP-binding cassette (ABC) transporters, involved in drug efflux and chemo-resistance (Calcagno and Ambudkar, 2010, Li et al., 2015, Mack et al., 2008), and iii) ROR2 (Huang et al., 2015, Many and Brown, 2014). I hypothesised that, if expression of ROR1 was truly downregulated on CSC96, another member of the ROR family could be overtaking ROR1's role in promoting increased invasiveness and metastasis potential.

Fig. 6. 9 shows significant upregulation of Lgr4 and ROR2 gene expression on CSC96 compared to PANC-1 Parental cells. An unexpected finding was the significant reduction of ABCG2 gene expression on tumourspheres; albeit both ABCA2 and ABCC1 showed significant upregulation compared to PANC-1 adherent cells. Together, these findings confirm the enriched presence of cancer stem cell-like cells within CSC96 tumourspheres.

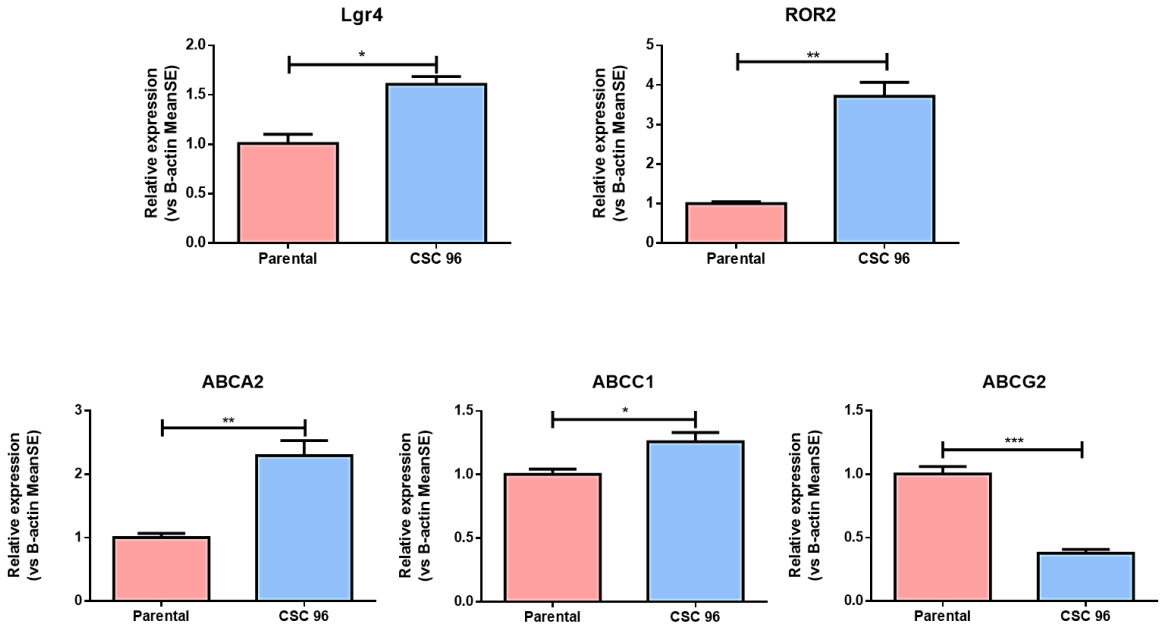

Fig. 6. 9. Further investigation of CSC biomarkers gene expression by qPCR. The gene expression of Lgr4, ROR2, and ABC transporters A2, C1 and G2 on CSC96 was compared to PANC-1 Parental cDNA amplification. Gene expression was normalized to B-actin. Experiments were performed in triplicates. Error bars represent SEM. Statistical test: *Unpaired t-test.* **p*≤0.05, ***p*≤0.01, ****p*≤0.001.

6.3.2.2 Protein expression by confocal microscopy

As per (Zhang et al., 2014), the protein expression studies were performed on ROR1 and the following biomarkers: i) ALDH1, an enzyme suggested to be involved in the detoxification of intracellular aldehydes and/or several cytotoxic drugs (Martinez-Cruzado et al., 2016, Nakahata et al., 2015, Alison et al., 2011); and ii) Vimentin, a protein associated with epithelial-mesenchymal transition (EMT) that provides traits required for invasion and metastasis (Cui et al., 2013, Mitra et al., 2015, Scheel and Weinberg, 2012).

In **Fig. 6. 10A**, high expression of Vimentin on both Parental and CSC96 tumourspheres was observed. Conversely, whilst ROR1 could be detected on all Parental cells, its expression was clearly reduced on the cell surface of the tumourspheres; which was consistent with gene expression data discussed above.

As expected, **Fig. 6. 10B** shows similar results to **Fig. 6. 10A** in terms of ROR1 protein levels. For ALDH1, however, its expression was detectable on tumourspheres but not Parental cells. These findings were also in line with gene expression results. Notably, confocal microscopy allowed the identification of a mixture of cell populations that expressed each biomarker alone: cells with single positivity ($ROR1^+$, Vim^+, $ALDH1^+$), double positives ($ROR1^+Vim^+$, $ROR1^+ALDH1^+$) or double negatives ($ROR1^-Vim^-$, $ROR1^-ALDH1^-$).

As per qPCR data, co-expression of ROR2 and Vimentin or ALDH1 was also investigated (**Fig. 6. 11**). Consistent with previous findings, the protein levels of ROR2 were clearly upregulated on tumourspheres compared to Parental cells.

An interesting observation was the heterogeneity of ROR1, ROR2, Vimentin and ALDH1 expression throughout the cells comprised within CSC96 tumourspheres. Importantly, the presence of mixed populations within our tumourspheres is congruent with the notion that a single CSC from a primary tumour is able to generate a novel tumour replicating comparable levels of heterogeneity. Moreover, based on previous reports and both gene and protein expression, it is considered that in this particular model, $ALDH1^+$ and $ALDH1^+ROR1^+$ cells may account for different CSC populations, whilst other cell subsets, such as cells with single ROR1 positivity or double-negative cells, could be the ones comprising the bulk of the tumour. Since Vimentin expression is not exclusive to CSCs, it was not possible to classify Vim^+ cells as a CSC subpopulation.

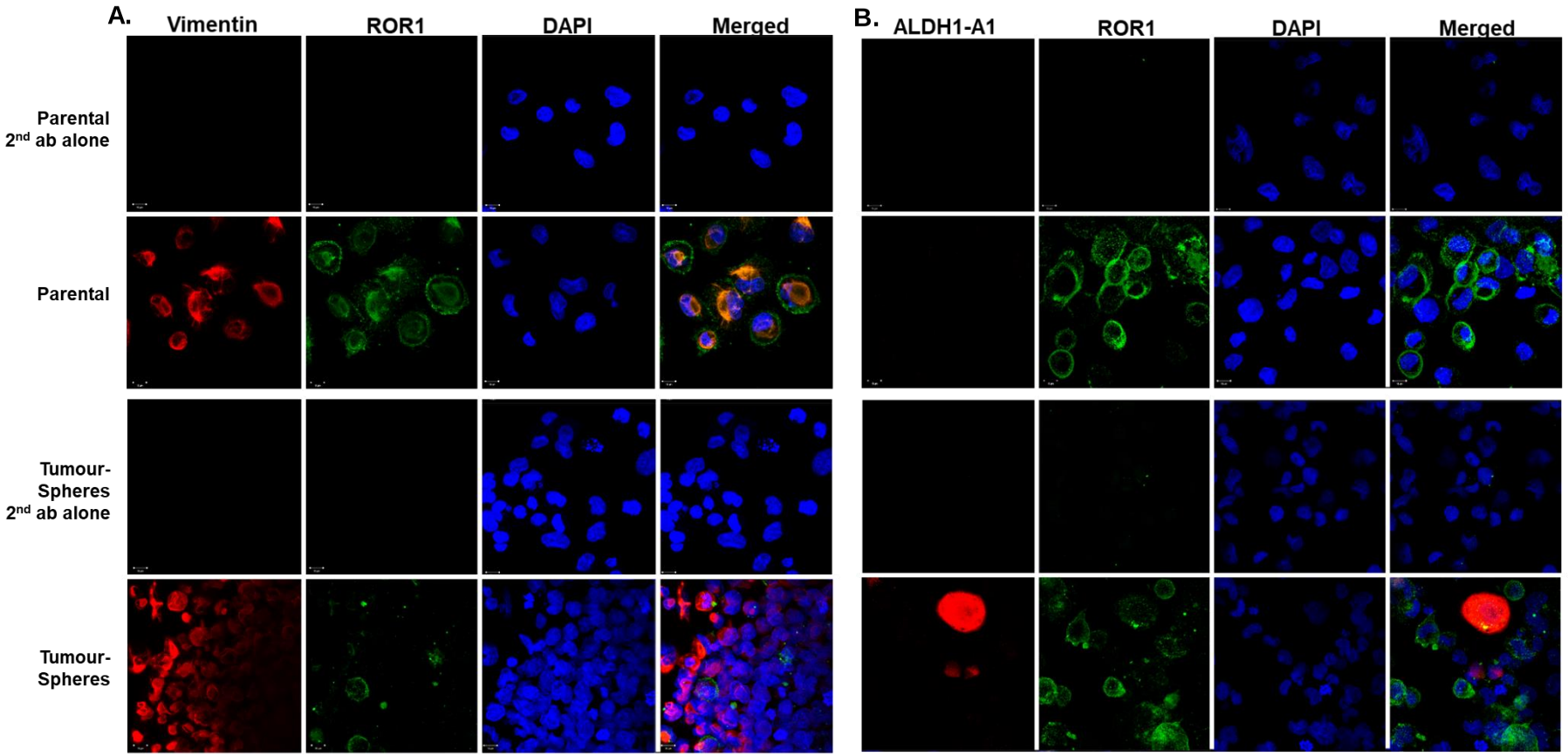

Fig. 6. 10. Co-expression levels of ROR1 and stem cell markers in PANC-1 Parental and CSC96 tumourspheres. Protein expression levels were detected by confocal microscopy. Cells were stained with a commercial antibody against ROR1 (green) and either (A) Vimentin (red) or (B) ALDH1-A1 (red). Nuclei was counterstained with DAPI (blue). Images were taken with a 63x microscope objective lens. Scale represents 10um. DAPI= 4',6-diamidino-2-phenylindole.

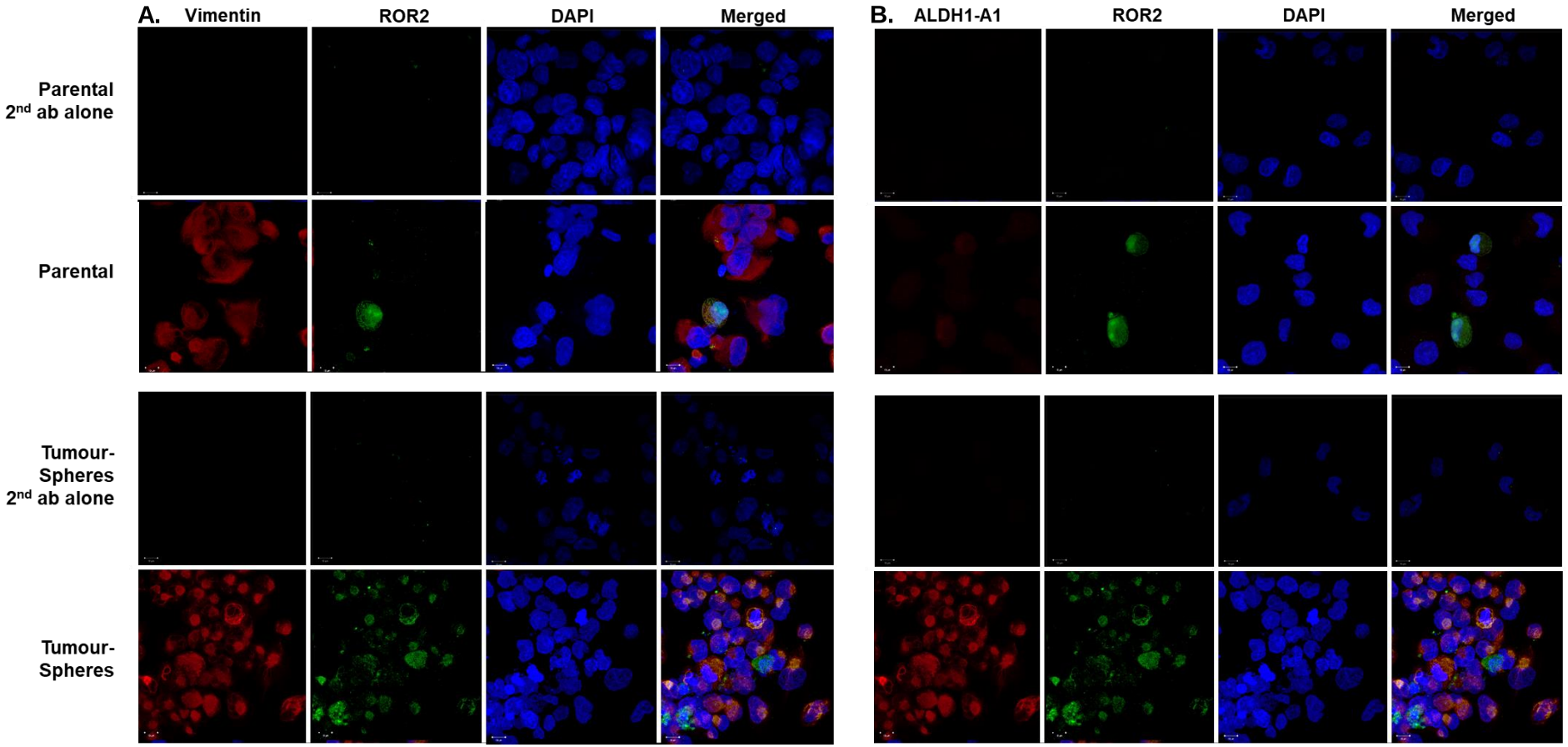

Fig. 6. 11. Co-expression levels of ROR2 and stem cell markers in PANC-1 Parental and CSC96 tumourspheres. Protein expression levels were detected by confocal microscopy. Cells were stained with a commercial antibody against ROR2 (green) and either (A) Vimentin (red) or (B) ALDH1-A1 (red). Nuclei was counterstained with DAPI (blue). Images were taken with a 63x microscope objective lens. Scale represents 10um. DAPI= 4',6-diamidino-2-phenylindole.

6.3.2.3 Transwell migration assay

Having assessed the gene and protein expression of distinctive CSC biomarkers on CSC96 tumourspheres, their functional properties were characterised through a transwell migration assay.

Based on Jung *et al.* (Jung et al., 2016), PANC-1 Parental cells and tumourspheres prepared as single-cell suspensions were seeded in an 8um pore size transwell 96-well plate. The lower wells were filled with either: i) serum-free RPMI (R0), ii) serum-supplemented RPMI (R10) and iii) conditioned media (Cond). For the latter, PANC-1 Parental culture media was used. After 72h, cells contained in the lower chambers were documented using a microscope to be then counted for quantitative analysis.

Fig. 6. 12 illustrates the clear difference between PANC-1 Parental cells and tumourspheres in terms of migration capacity when exposed to R0. Specifically, **Fig. 6. 12A** shows representative images of lower chambers from both monolayer and CSC96 cells exposed to different types of stimuli. The quantitative analysis represented in a histogram graph is displayed in **Fig. 6. 12B**.

A significantly higher tumoursphere cell count compared to Parental cells located in the lower chambers was observed when both cell types were exposed to R0, but not R10 or conditioned media. These findings are in line with the enhanced gene expression of Notch1, CD24, CXCR4 and ROR2 observed on PANC-1-derived CSC96 but not adherent cells. It is hypothesised that the reduced migration of tumourspheres on R10 and conditioned media is likely due to extended exposure to serum (72h). The presence of the latter could have trigger differentiation of CSCs, reducing their migration ability to almost that of adherent cells.

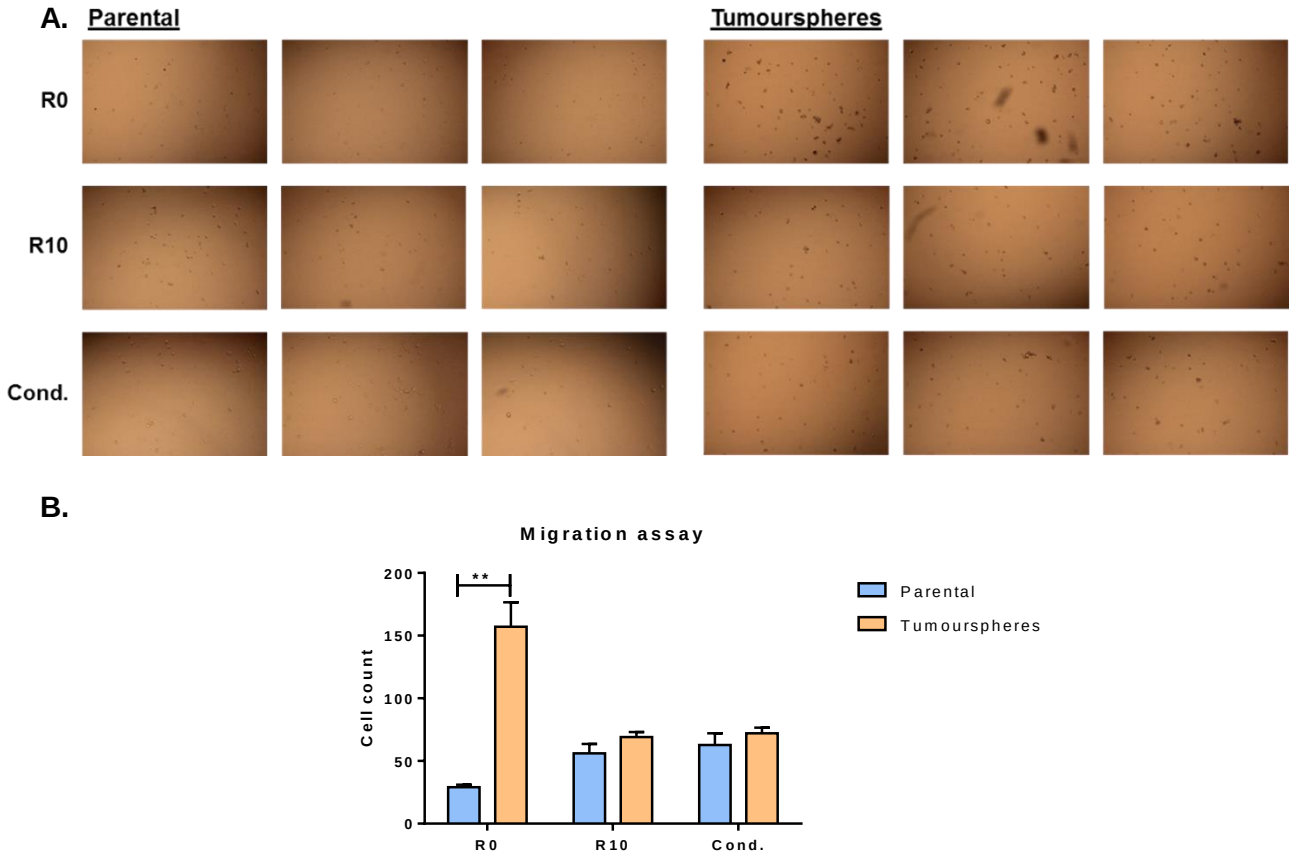

Fig. 6. 12. Transwell migration assay. Single-cell suspensions in serum-free media were prepared from PANC-1 Parental cells and tumourspheres in order to be seeded in the upper chamber of a transwell 96-well plate. The lower wells were filled with either: i) serum-free RPMI media (R0), ii) complete media (R10) or iii) Condition media (Cond). Shown are (A) images of cells contained in the lower chamber after 72h of incubation. (B) Cells were counted for analysis and compared for calculation of statistical differences. Images were taken with a 4x microscope objective lens. Experiments were performed in triplicates. Error bars represent SD. Statistical test: *Multiple t-tests.* $**p \leq 0.01$. Unless indicated, other comparisons were not statistically significant. SD= Standard deviation.

6.3.3 Aim 3: Evaluation of ROR1 BiTE therapy on CSC96

One of the ROR1 antibody-based therapies we have developed in our group is a humanised anti-ROR1 BiTE; which combines the unique binding of clone F to the Fz domain of ROR1, and an anti-CD3 scFv.

We have previously shown the specific and potent cytotoxic effect that our ROR1 BiTE has on a range of ROR1^{+} solid cancer malignancies, both *in vitro* and *in vivo* (Gohil et al., 2017). Therefore, I set out to evaluate the efficacy of

this approach on PANC-1 derived cancer stem-cell like cells by two approaches: i) WST1 cell viability assay and ii) specific cytotoxicity evaluation of $ROR1^+$ CSCs and $ROR1^+$ bulk cells by immunocytochemistry and confocal microscopy.

6.3.3.1 WST1 cell viability assay

Single-cell suspensions from both PANC-1 Parental and CSC96 tumourspheres were seeded in appropriate TC-treated and suspension 96-well plates, respectively. On the following day, cells were treated with 1ug/ml ROR1 BiTE and co-cultured with PBMCs at a 1:1 (E:T) ratio. After 72h, cell viability was assessed by cell proliferation reagent WST1 (**Fig. 6. 13**).

Fig. 6. 13A display representative images of both Parental and CSC96 co-cultures 72h post-ROR1 BiTE treatment. As expected, no morphological changes were observed on those cells treated with either “PBMCs alone” or “ROR1 BiTE alone” controls. Conversely, PANC-1 Parental cells exposed to ROR1 BiTE therapy (BiTE+PBMCs) were obliterated, whilst T-cells on those wells proliferated and formed clusters, a trait associated with potent cytotoxicity. Although less evident, CSC96 exposed to ROR1 BiTE therapy presented a different morphology compared to those treated with controls. Specifically, they were less sparse and seemed to present a fewer number of cells. Thus, these observations needed to be verified through a cell viability assay.

Results of cell viability quantified with WST1 reagent are presented in **Fig. 6. 13B**. Significant reduction of live PANC-1 Parental cells and CSC96 tumourspheres was detected when these targets were treated with ROR1 BiTE therapy compared to negative controls. A surprising finding was the unexpectedly high absorbance seen on Parental cells, as previous analysis of these wells under the microscope showed almost complete elimination of the target population. It is presumed that this observation could be explained by

the presence of various clusters of proliferating T-cells. In contrast, since CSC96 tumourspheres expressed lower levels of ROR1, it is likely that the cell viability signal on those wells was generated by a combination of both targets and proliferating effectors. Importantly, these findings show significant reduction on cell viability levels of CSC96 tumourspheres after ROR1 BiTE therapy.

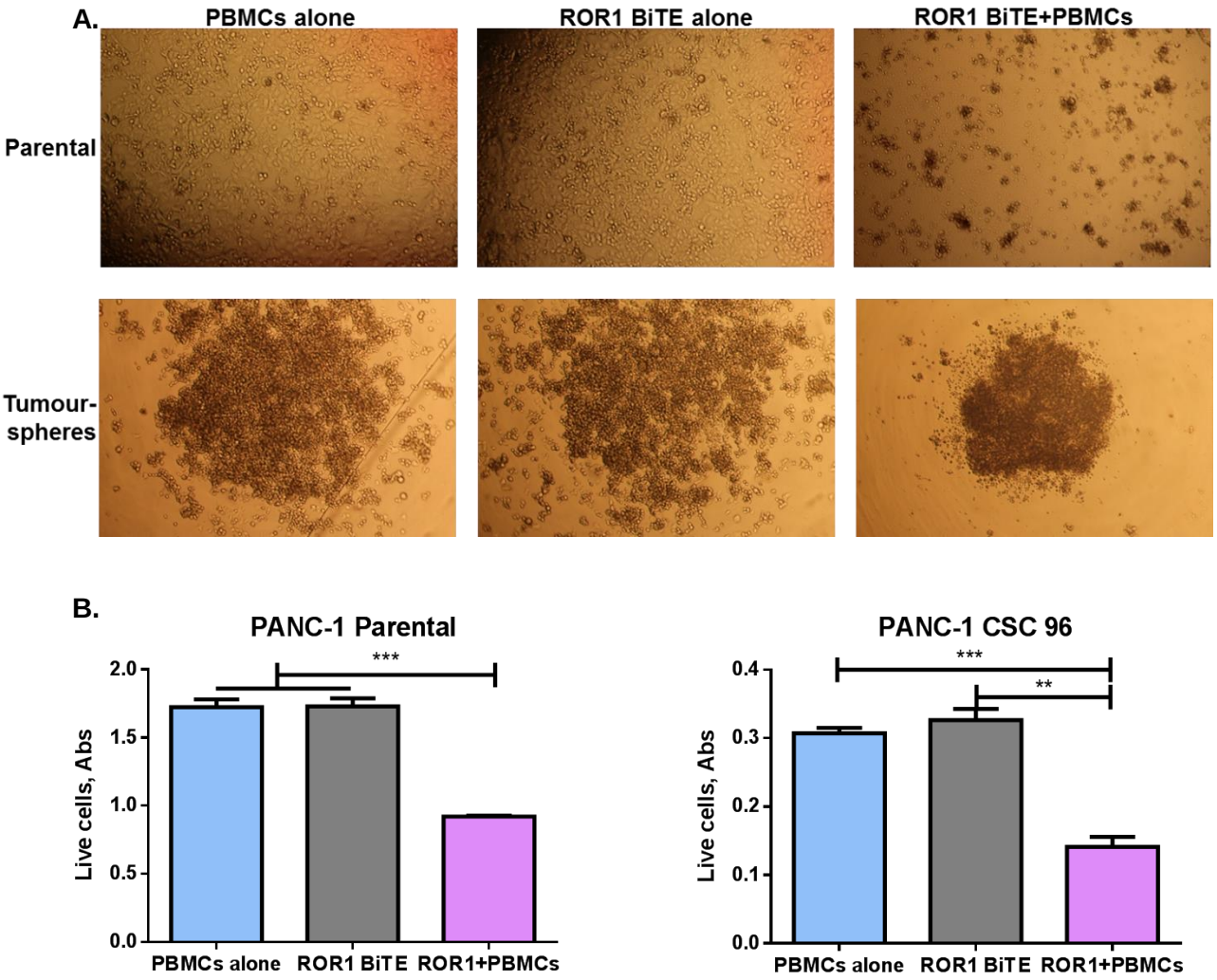

Fig. 6. 13. WST1 cell viability assay on PANC-1 Parental and CSC96 cells after ROR1 BiTE therapy. (A) PANC-1 Parental cells and CSC96 tumourspheres were seeded in appropriate 96-well plates. On the next day, cells were treated with 1ug/ml ROR1 BiTE, followed by addition of effector cells (activated PBMCs) at a 1:1 ratio. After 72h, WST1 was added in order to measure cell viability (Abs). (B) Abs values were compared to both PBMCs and ROR1 BiTE controls for statistical calculations. PANC-1 Parental cells were used as positive control. Images were taken with a 4x microscope objective lens. Experiments were performed in triplicates. Error bars represent SD. Statistical test: *Unpaired t-test.* $^{**}p \leq 0.01$, $^{***}p \leq 0.001$. SD= Standard deviation.

6.3.3.2 Cytotoxicity evaluation of ROR1$^+$ CSC and ROR1$^+$ bulk cells

In an effort to ascertain true elimination of ROR1$^+$ cells amongst the mixed cell populations detected within the tumourspheres, a cytotoxicity assay followed by immunocytochemistry and confocal microscopy was performed.

CSC96 tumourspheres were treated with ROR1 BiTE and co-cultured with PBMCs as described above. After 72h, the assay plate was inspected under the microscope and images from representative wells were taken (**Fig. 6. 14**).

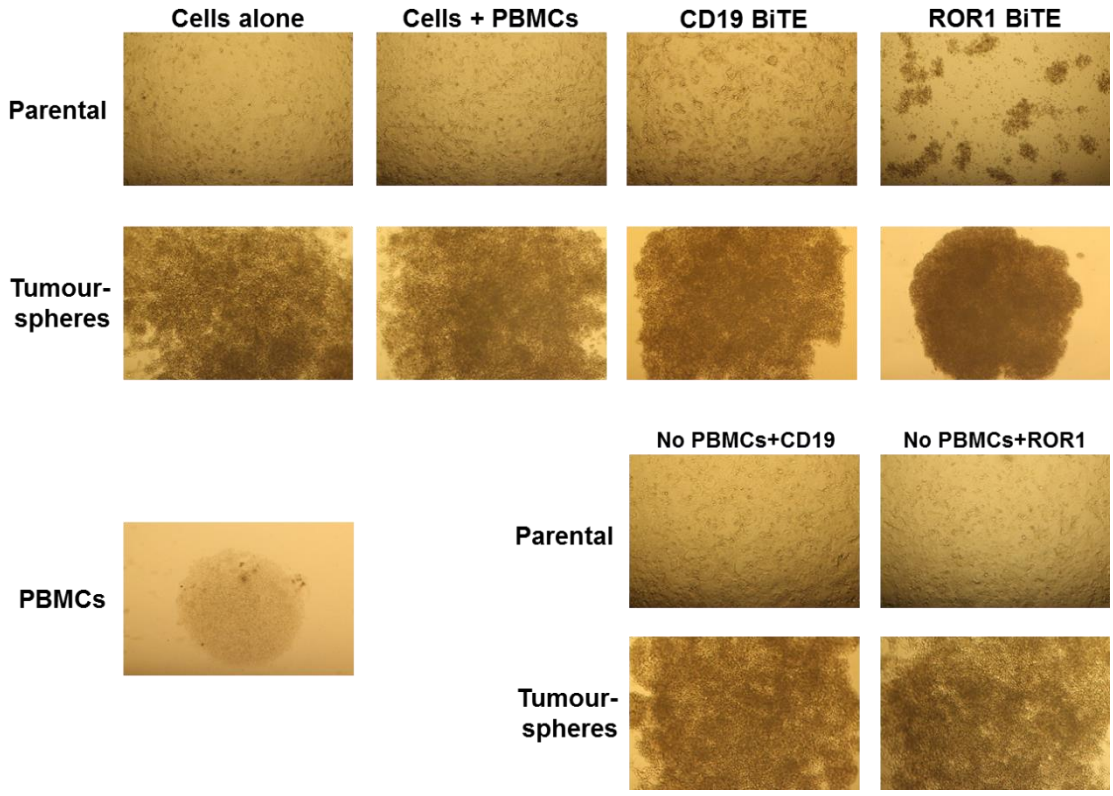

Fig. 6. 14. Cytotoxicity assay on CSC96 cells after ROR1 BiTE therapy. CSC96 tumourspheres were seeded in suspension 96-well plates. On the next day, cells were treated with 1ug/ml ROR1 BiTE, followed by addition of effector cells (activated PBMCs) at a 1:1 ratio. After 72h, images were taken with a 4x microscope objective lens. Shown are representative images of targets and effectors alone, and targets treated with ROR1 BiTE therapy or controls (PBMCs alone, CD19 or ROR1 BiTE alone, and CD19 BiTE therapy). Experiments were performed in triplicates.

For illustrative purposes, images of targets and effectors alone as well as targets treated with ROR1 BiTE therapy or different controls are shown. Consistent with the findings observed in the cell viability experiments, ROR1

BiTE-treated tumourspheres displayed in **Fig. 6. 14** showed a much more contracted cell population compared to those cells treated with CD19 BiTE therapy and other controls.

To determine whether our ROR1 BiTE approach was able to elicit specific cytotoxicity of $ROR1^+$ cells present within CSC subpopulations and the bulk of the tumour, CD19 or ROR1 BiTE-treated cells were harvested and processed for immunocytochemistry. Cells were stained with ROR1 (green) and either Vimentin (red) or ALDH1-A1 (red). Immunostaining was analysed by confocal microscopy. CD19 and ROR BiTE-treated cells were then counted, classified according to their biomarker expression and compared for statistical analyses (**Fig. 6. 15**).

Fig. 6. 15A shows the single or double expression of ROR1 and Vimentin on CSC96 tumourspheres after CD19 or ROR1 BiTE therapy. Similarly, single or double expression of ROR1 and ALDH1-A1 on those same tumourspheres is presented in **Fig. 6. 15B**. Remarkably, expression of ROR1 as a single biomarker or in combination with Vim or ALDH1 is drastically reduced on ROR1 BiTE treated-cells compared to those exposed to CD19 therapy.

Furthermore, **Fig. 6. 15C** displays the quantification of CSC96 classified by their biomarker expression after CD19 or ROR1 BiTE therapy, namely: Vim^+, $ROR1^+$ and $ALDH1^+$ (for single biomarker expression); Vim^+ROR1^+ and $ALDH1^+ROR1^+$ (for double-positive cells); and Vim^-ROR1^- and $ALDH1^-ROR1^-$ (for double-negative cells). Categorised cells were presented as the percentage of total cells counted (at least 550 per condition). Importantly, as mentioned earlier and based on previous reports (Mitra et al., 2015, Martinez-Cruzado et al., 2016, Nakahata et al., 2015, Zhang et al., 2014), $ALDH1^+$ and $ALDH1^+ROR1^+$ cells were considered potential CSC subsets cells within the tumourspheres.

As expected and in line with previous findings reported here and elsewhere (Gohil et al., 2017), a reduction on the percentage of cells expressing ROR1 as a single biomarker after ROR1 BiTE therapy compared to CD19 BiTE treatment was observed. Notably, this reduction became significant when double positive cells were analysed. This is of particular importance as these results would suggest that ROR1 BiTE therapy is not only able to deplete $ROR1^{+}$ cells comprising the bulk of tumours but also $ROR1^{+}$ cancer stem cell-like cells derived from a pancreatic cancer cell line. Furthermore, a significant increase of $Vim^{-}ROR1^{-}$ cells was detected after ROR1 BiTE therapy. This data is consistent with the observation that immunotherapies targeting ROR1 decrease the expression of Vimentin, thereby suggesting an association between both biomarkers (Cui et al., 2013, Zhang et al., 2014). Although not significant, a similar reduction was observed on $ALDH1^{+}$ cells.

All in all, these data suggest that although ROR1 gene expression was downregulated on PANC-1-derived tumourspheres compared to Parental cells, the protein levels of ROR1 could still be detected. In keeping with this, it has been showed that therapy with our ROR1 BiTE was able to target both cancer cells and cancer stem cell-like cells positive for ROR1 expression. It is envisaged that immunotherapies, such as the ROR1 BiTE developed in our lab, able to target not only the bulk of tumours but also CSC offer real prospects of decreased risk of metastasis. Evaluation of this type of therapies in clinical trials used as single agents and in combination with other anti-cancer treatments, such as PD-1 blocking antibodies and/or small molecule inhibitors, will ultimately reveal the clinical benefit ROR1 immunotherapy can achieve.

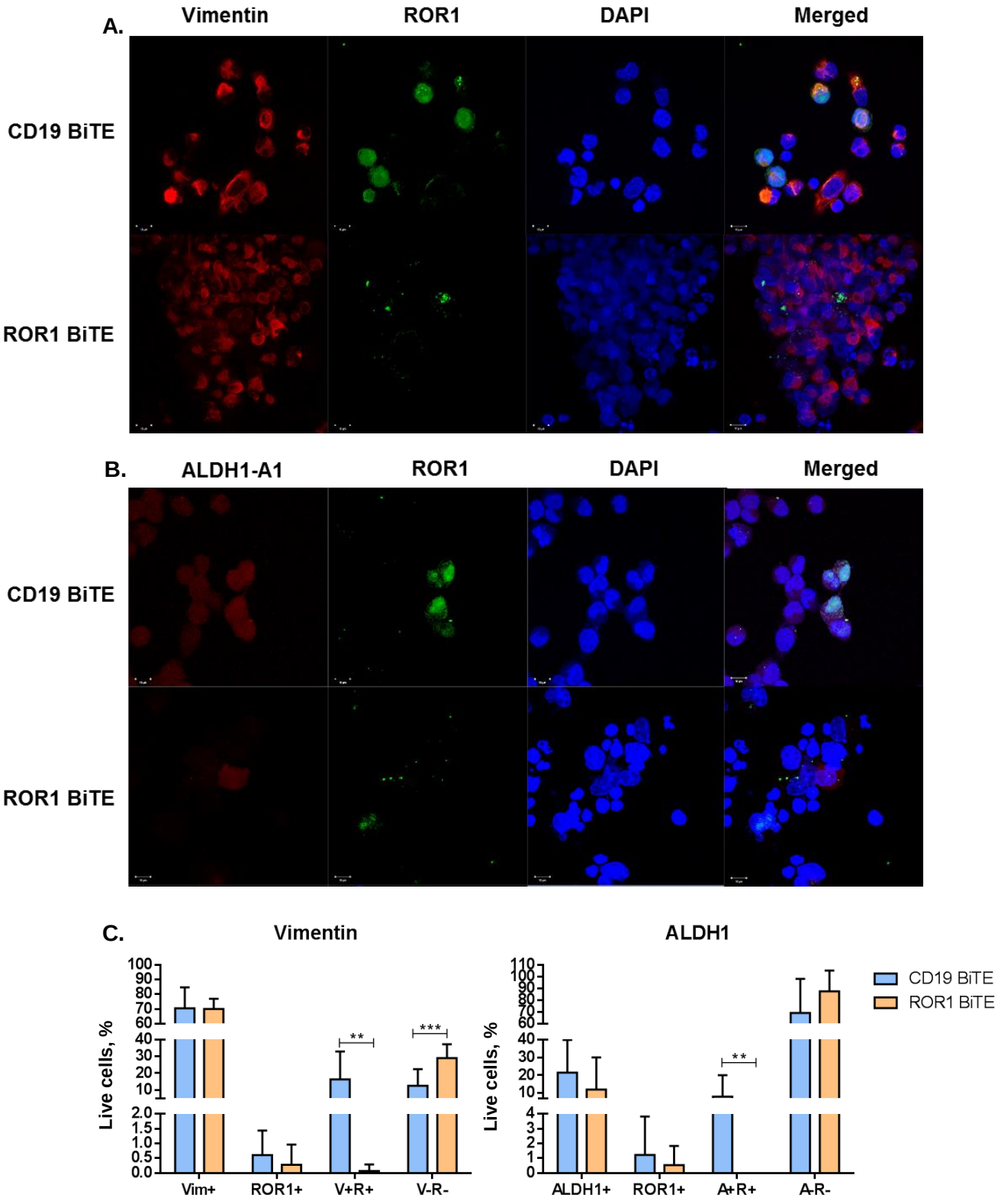

Fig. 6. 15. Immunocytochemistry by confocal microscopy on CD19 or ROR1 BiTE-treated CSC96 tumourspheres. 72h post BiTE therapy, cells were seeded in matrigel-coated coverslips, fixed and stained with a commercial antibody against ROR1 (green) and either (A) Vimentin (red) or (B) ALDH1-A1 (red). Nuclei was counterstained with DAPI (blue). (C) More than 500 cells per treatment and biomarker staining were counted. Cells were classified according to their single or double biomarker expression and conveyed as % of the total cell count. % of ROR1 BiTE-treated cells was compared to that of CD19 BiTE for statistical calculations. Images were taken with a 63x microscope objective lens. Scale represents 10um. Number of spheres imaged: CD19 BiTE Vim, n=619; ROR1 BiTE Vim, n=692; CD19 BiTE ALDH1, n=594; ROR1 BiTE ALDH1, n=550. Error bars represent SD. Statistical test: *Multiple t-tests.* **$p \leq 0.01$, ***$p \leq 0.001$. Unless indicated, other comparisons were not statistically significant. V= Vimentin, R= ROR1, A= ALDH1-A1.

6.4 Discussion

Several studies have identified subpopulations of cells within malignant tumours able to drive tumour initiation, progression and recurrence, termed CSCs. To date, most types of chemo and radiotherapy eliminate the bulk of the tumour but fail to eliminate CSCs; which survive and mediate relapse and metastasis. The development of a reliable model for the study of CSCs is therefore essential for preclinical cancer research.

A number of methods have been tried to isolate and study CSCs, of which the use of specific markers has been the most popular. The main pitfall of this strategy however is the contradictory results from different studies where cells negative for so-called stem cell markers were still able to form tumourspheres and give rise to aggressive tumours *in vivo* (Singh et al., 2015). Recently, several reports have demonstrated that CSCs from primary tumours and cancer cell lines can be enriched within tumourspheres when cultured in serum-free media and in a low adhesion environment (Dalla Pozza et al., 2015, Gaviraghi et al., 2011, Ponti et al., 2005, Fitzgerald and McCubrey, 2014).

In this study, two different types of media (MEBM and CSC) were tested in order to generate tumourspheres derived from PANC-1 cells. After a few passages it became evident that spheroids grown with MEBM were fewer and smaller compared to those cultured with CSC. This could be explained by the presence of antibiotics in MEBM medium. A study by (Relier et al., 2016), showed that antibiotics had no impact on monolayer cultures but inhibited the sphere-forming ability of six cancer cell lines. Furthermore, their data suggests that the number of cells with self-renewal potential were significantly decreased.

In contrast, the CSC medium did not contain antibiotics; and tumourspheres grown in this media were successfully cultured for more than 20 passages, exhibiting consistently good cell viability.

It is worth mentioning that a potential limitation of this approach was the use of a pancreatic cancer cell line (PANC-1) instead of primary tumours, as it has been suggested that efficient enrichment of CSCs by sphere formation assay is not universal and is highly cell line-dependent (Calvet et al., 2014). Fortunately, in the past few years, there has been some reports indicating successful isolation and expansion of CSCs from pancreatic cancer cell lines, particularly PANC-1 (Dalla Pozza et al., 2015, Gaviraghi et al., 2011). Furthermore, the use of cancer cell lines is supported by the recently accepted concept of CSC plasticity, whereby CSCs and non-CSCs co-exist in the tumour in a dynamic equilibrium, and both types are able to interconvert in response to microenvironmental stimuli (Cabrera et al., 2015, Chaffer et al., 2011, Varga et al., 2014).

Accordingly, tumourspheres showed anoikis-resistance, a key feature of CSCs. Anoikis is a form of regulated cell death induced when anchorage-dependent cells detach from their extracellular matrix. It is effectively a physiological barrier to metastasis; therefore, resistance to anoikis is pivotal for the survival of CSCs entering the bloodstream, thereby facilitating secondary tumour formation in distant organs (Kim et al., 2016a). Additionally, PANC-1 tumourspheres were subjected to a limiting dilution assay *in vitro* in order to assess their self-renewal capability. Cells able to form new tumourspheres from a single cell under anchorage-independent growth were named CSC96. Notably, the sphere formation assay coupled with serial passages seems to allow the enrichment of CSC subpopulations, particularly when CSC biomarkers are not well defined (Cao et al., 2011).

In the context of pancreatic cancer, several biomarkers have been proposed for CSC identification, including: CD133, SOX2, CD24, CD44, CXCR4, EpCAM, ABCG2, ALDH1, Nestin, among others. Their use however remains controversial (Matsuda et al., 2012).

Gene expression comparing biomarker levels of both CSC96 and PANC-1 Parental cells revealed significant upregulation of stemness genes CD133 and SOX2, but downregulation of Nestin on tumourspheres. Interestingly, co-expression of both CD133 and SOX2 has been found on CSCs from various tumours, particularly of neurogenic origin (Hussein et al., 2011). Also, Hermann *et al*. (Hermann et al., 2007) reported that the $CD133^{+}CXCR4^{+}$ CSC subpopulation in pancreatic tumours was essential for metastasis. In keeping with this, CXCR4 was also overexpressed on CSC96 spheroids.

Nestin expression has been described in neural stem/progenitor cells and in a variety of mesenchymal and epithelial tumours, including PDAC. Moreover, a correlation between Nestin expression and clinical course has been reported for breast and ovarian carcinomas, gastrointestinal tumours, melanoma, etc. No such relationship however was found for PDAC (Neradil and Veselska, 2015). Therefore, although Nestin has been considered a tissue stem/progenitor and CSC marker in various tissues -according to Matsuda, Y *et al.* (Matsuda et al., 2012)- it is not yet clear whether $Nestin^{+}$ cells in PDAC are also pancreatic CSCs. Additional studies are needed to clarify the relationship between Nestin and PaCa CSCs.

Biomarkers involved in high invasiveness, metastasis and EMT processes were also evaluated. One of the most important CSC markers, whose upregulation has been detected on CSCs from virtually all cancer subtypes studied so far, is ALDH1. ALDH is a family of enzymes responsible for detoxifying the cells and it has been involved in chemotherapy resistance. It is been also involved in the expansion and differentiation of stem cells and CSCs (Martinez-Cruzado et al., 2016). Of the various isoforms, ALDH1-A1 is thought to play an important functional role in stem cells (Nakahata et al., 2015). Also, overexpression of SOX2 and ALDH1-A1 is associated with enhanced malignant potential of spheroids (Martinez-Cruzado et al., 2016). Crucially, both genes were significantly upregulated on CSC96 tumourspheres compared to adherent cells.

An unexpected result was the downregulation of ABCG2 detected on PANC-1-derived tumourspheres. However, the upregulation observed on both ABCA2 and ABCC1 suggest that CSC96 spheroids could have the potential to be resistant to chemotherapy as these ABC transporters are known to mediate the efflux of antimitotic drugs (Fitzgerald and McCubrey, 2014, Calcagno and Ambudkar, 2010, Mack et al., 2008). The study of tumourspheres derived from a human pancreatic cancer tumour would potentially lead us to confirm if these findings are reproducible on CSC from primary cells or if it is rather a limitation of the current model.

Since ROR1 overexpression has been detected on CSCs derived from ovarian cancer and glioblastoma (Jung et al., 2016, Zhang et al., 2014), I investigated whether this was the case on pancreatic CSCs. Surprisingly, a significant reduction of ROR1 was observed. This was consistent, however, with the established concept that the use of CSC biomarkers cannot be generalised and their expression needs to be evaluated in a tissue-dependent manner (Clarke et al., 2006). In line with this, a recent report on nasopharyngeal carcinoma (NPC) revealed that, although ROR1 was detectable on NPC-derived spheroids, there was no significant upregulation of this gene compared to NPC cell lines (Guo et al., 2017).

In light of ROR1 downregulation, I hypothesised that the other member of the ROR family, ROR2, could be overtaking the role that ROR1 has on CSCs derived from other malignancies. As expected, gene expression data confirmed the overexpression of ROR2 on CSC96 spheroids compared to Parental cells. Importantly, the crosstalk between these two genes has been previously reported on melanoma, where ROR1 and ROR2 are inversely expressed and negatively regulate each other (O'Connell et al., 2013). Moreover, O'Connell MP *et al*. indicated that, exposure to hypoxia shifted $ROR1^{+}$ melanoma cells to a more invasive $ROR2^{+}$ phenotype. Similarly, according to Umebayashi, M. *et al*. (Umebayashi et al., 2014), hypoxia has also a strong effect on PaCa cell biology as it reduces its sensitivity to cell

death signals and promotes angiogenesis, proliferation and metastasis. Hence, hypoxia culture has been proposed as an alternative method of CSC isolation (Keith and Simon, 2007). Interestingly, high ROR2 expression has been correlated with poor prognosis in PDAC by Huang, J. *et al.* (Huang et al., 2015). Researchers investigated ROR2 expression in both stromal and cancer cells and its role as a prognostic marker of survival in PDAC patients. However, PDAC CSCs were not specifically addressed. Together, these findings suggest that, as in melanoma, ROR2 expression might be associated with a more aggressive phenotype in PDAC. Whether this ROR1 to ROR2 shift is dependent on hypoxic conditions that drive non-CSCs to CSCs state remains to be addressed and elucidated.

In this study, gene expression analyses were followed by protein expression evaluation. To this end, CSC96 spheroids were assessed by immunocytochemistry and confocal microscopy, whilst PANC-1 Parental cells were used as control. Based on another study that investigated ROR1 on ovarian cancer CSCs and reported an association between this marker and both Vimentin and ALDH1 (Zhang et al., 2014), my investigation focused on these proteins. As mentioned above, Vimentin is an EMT biomarker involved in metastasis, whilst ALDH1 is a widely accepted CSC marker. Results obtained by confocal microscopy showed that protein levels of ROR1, Vimentin and ALDH1 were consistent with gene expression data; whereby ROR1 expression was reduced on tumourspheres, expression of Vimentin on spheroids was not considerably different from Parental cells, and ALDH1 was clearly detected on CSC96 but not on PANC-1 adherent cells. Hence, unlike data from Zhang, S. *et al*. (Zhang et al., 2014), no clear association of these markers was observed.

Considering that prior studies found that ROR1 could mediate proliferation, migration/invasion and tumourigenicity of cancer cells, downregulation of ROR1 on the pancreatic tumourspheres was puzzling. Recently, (Henry et al., 2016), reported that silencing of both ROR1 and ROR2 was required in order

to inhibit cell migration and invasion in chemoresistant ovarian cancer. Based on this and other studies (Henry et al., 2017, Huang et al., 2015, O'Connell et al., 2013, Rebagay et al., 2012), I decided to assess the protein expression of ROR2 on CSC96 spheroids. Notably, confocal microscopy data confirmed that whilst ROR1 protein levels were reduced, ROR2 was overexpressed on CSC96 compared to Parental cells. Although further investigation of the dynamics between these two molecules in PaCa CSCs are needed; this is, to my knowledge, the first time that ROR1 and ROR2 are simultaneously studied in the context of pancreatic CSCs. Furthermore, this observation could be of significance as it supports recent studies that indicate Wnt5a signalling –the sole ligand of both ROR1 and ROR2– is key for the regulation of normal and cancer stem cell self-renewal, proliferation, migration and invasion (Zhou et al., 2017b).

Another interesting observation was the presence of mixed cell subpopulations within CSC96 spheroids. Unlike PANC-1 Parental samples –where cells showed uniform expression of Vimentin and ROR1 and virtually none for ALDH1– CSC96 tumourspheres displayed different cell subsets expressing none, one or two biomarkers. It is considered that this heterogeneity further supports the validity of this *in vitro* model as the existence of different cell subpopulations were potentially caused by the enriched presence of pancreatic CSCs.

In terms of functional characterisation, CSC96 spheroids showed a significantly higher ability to migrate than PANC-1 adherent cells when exposed to R0 (serum-free media). A slight increase in the number of migrating cells, however, was observed when Parental cells were exposed to R10 or conditioned media compared to R0. This is likely explained by the stimulus that the presence of serum exerted on starved cells. In contrast, less migration of CSC96 tumourspheres was detected when cultured in R10 or conditioned media compared to R0. It is believed that the continued exposure to serum for 72h could have been enough to trigger a differentiation process on CSC96

spheroids, which could possibly explain the decrease in migration levels when compared to tumourspheres culture in R0. This observation would be in keeping with tumour cell plasticity and the bidirectional conversion that is possible between non-CSC and CSC, discussed earlier.

A limitation of the migration assay however was the absence of a chemokine as a positive control. The inclusion of a stimulant such as CXCL12 would have been relevant in order to produce conclusive results; particularly in the current scenario where upregulation of CXCR4 at a gene expression level was identified. Also, the functional evaluation of CSCs would greatly benefit from the inclusion of invasion and chemoresistance assays.

BiTEs represent a novel immunotherapy that bridges T-cells to tumour cells, thereby inducing target cell-dependent polyclonal T-cell activation, leading to the elimination of bound cancer cells (Klinger et al., 2016). We have already demonstrated the specific cytotoxicity that our own ROR1 BiTE elicits on a range of $ROR1^+$ solid malignancies, including PaCa (Gohil et al., 2017). In this study, co-culture data have shown that ROR1 BiTE therapy significantly reduces cell viability of PaCa tumourspheres compared to controls. This was quantified by WST1 reagent as per Dalla Pozza et al., 2015; this approach however could be supplemented with other evaluations such as the colony formation assay.

When ROR1 BiTE-treated tumourspheres from a coculture assay were assessed by immunocytochemistry, confocal microscopy data indicated significant elimination of $ROR1^+$ subsets, including $ALDH1^+ROR1^+$, a potential CSC compartment. It is worth mentioning however that the co-culture approach followed by immunocytochemistry was not taken from other reports in the literature and therefore further method validation would be needed in order to reach conclusive results.

Interestingly, whilst gene and protein expression data of Vimentin on CSC96 suggested there was no significant difference with their adherent counterparts, targeting of ROR1 on CSC96 spheroids with our ROR1 BiTE showed significant reduction on the percentage of Vim^+ cells compared to tumourspheres treated with CD19 BiTE. This is in keeping with previous reports (Cui et al., 2013, Zhang et al., 2014) which showed that ROR1 targeting with a ROR1 MAb (Cirmtuzumab) led to the concomitant reduction of both ROR1 and Vim expression. Similarly, an association between ROR1 and ALDH1 has been suggested by the same group (Zhang et al., 2014). Although downregulation on ALDH1 expression after ROR1 BiTE therapy was observed, this was not significant. Hence, further experiments are needed to confidently conclude this is the case.

Collectively, these data suggest that establishment of PANC-1-derived tumourspheres exhibiting anchorage-independent growth and self-renewal properties was achieved. Moreover, gene and protein expression results as well as functional characterisation indicated significant enrichment of cancer stem cell-like cells within CSC96 spheroids compared to PANC-1 Parental cells. Notably, protein expression data also suggested high levels of heterogeneity within the tumourspheres.

Although evaluation of ROR1 expression on tumourspheres at a gene and protein levels indicated significant reduction compared to Parental cells, presence of ROR1 protein was still detectable by confocal microscopy. Moreover, it has been shown that our ROR1 BiTE therapy is able to target both $ROR1^+$ cells within the bulk of the tumour and a subset of $ROR1^+$ cancer stem cell-like cells.

Importantly, the 3D pancreatic cancer *in vitro* model has revealed upregulation of ROR2, consistent with other studies that report ROR2 as a poor prognosis marker in pancreatic ductal adenocarcinomas. It is proposed that both ROR1 and ROR2 are excellent targets for the treatment of minimal residual disease,

which represents the final hurdle in the curative approach to many cancers (Rebagay et al., 2012).

Lastly, I aimed to evaluate if our ROR1 BiTE was an effective therapeutic option able to provide both debulking of tumours and targeting of CSCs. With a spheroid *in vitro* model, it has been shown that targeting of ROR1$^+$ cells present in different compartments of the tumour, including CSCs, was achieved. Additional pre-clinical and clinical work is required to conclusively demonstrate the therapeutic benefit that ROR1 BiTE alone and in combination might achieve for the management of ROR1$^+$ malignancies. Furthermore, it is envisaged that a combined targeting of ROR molecules and checkpoint antibodies, such as anti-PD-1, would be of special interest as a recent study demonstrated that cancer cells that undergo EMT overexpress immune inhibitory molecules, among them PD-L1 and CTL4 (Lou et al., 2016). Moreover, recent findings in resistance mechanisms to BiTE therapy showed overexpression of PD-L1 and T-cell exhaustion (Kohnke et al., 2015, Krupka, 2015). Therefore, combination studies of ROR1 BiTE and anti-PD-1 antibodies represent an exciting prospect yet to be investigated.

6.4.1 Summary & Conclusions

- Tumourspheres from a PDAC cancer cell line (PANC-1) were generated by 3D spheroid formation assay.
- Comparison between MEBM and CSC media revealed that, after several passages, the latter consistently produced more and bigger spheroids compared to MEBM.
- Both culture with ultra-low attachment plates and *in vitro* limiting dilution allowed the generation of “CSC96”; tumourspheres with self-renewal capability and able to grow under anchorage-independent growth conditions.
- Gene expression analyses showed significant upregulation of stemness biomarkers such as CD133 and SOX2 on CSC96 spheroids compared

to PANC-1 Parental cells; Nestin expression, however, was downregulated.

- Similarly, biomarkers associated with self-renewal such as Notch1 and Bmi1 were upregulated on tumourspheres.
- Genes associated with high invasiveness and metastasis such as ALDH1-A1, ALDH1-L2, CD24 and CXCR4 were also overexpressed on CSC96 but not on adherent cells.
- No significant changes on the gene expression of the B1 isoform of ALDH1 and Vimentin were detected.
- Surprisingly, gene expression of ROR1 was found to be significantly reduced on tumourspheres.
- Combined analysis of qPCR, agarose gel and sequencing data confirmed that, although downregulated, ROR1 gene was still expressed on CSC96.
- Further gene expression studies showed that Lgr4, a CSC-related biomarker, was overexpressed on spheroids. This was also the case for drug efflux genes ABCA2 and ABCC1, but not ABCG2.
- Remarkably, ROR2 gene expression was found to be overexpressed on tumourspheres compared to PANC-1 Parental cells.
- Protein expression analysis confirmed the reduced presence of ROR1 but upregulation of ALDH1 and ROR2 on tumourspheres.
- Importantly, confocal microscopy showed the high heterogeneity within CSC96 spheroids, constituted of a mixture of cell subpopulations. Of these, it was hypothesised that both $ALDH1^+$ and $ALDH1^+ROR1^+$ cells represented different CSC compartments.
- Transwell migration assay data showed that CSC96 tumourspheres had a higher migration capability than PANC-1 adherent cells.
- CSC96 spheroids treated with ROR1 BiTE and PBMCs displayed significantly reduced cell viability.
- ROR1 BiTE therapy followed by immunocytochemistry and confocal microscopy showed specific elimination of $ROR1^+$ cell subpopulations,

where the number of $ALDH1^{+}ROR1^{+}$ cells was significantly decreased compared to CD19 BiTE.

- Interestingly, ROR1 targeting with our ROR1 BiTE seemed to be associated with the reduction of both Vimentin and ALDH1 protein expression, an observation consistent with other reports (Cui et al., 2013, Zhang et al., 2014).

6.4.2 Future work

In terms of BiTE technology, a recent study has shown that current manufacturing challenges and short serum half-life of BiTEs could be circumvented by generating these bispecific antibodies *in vivo*. Systemic transfer of a nucleoside-modified mRNA-encoded BiTE resulted in sustained production of so-called RiboMAbs, with half-lives similar to those attained by conventional monoclonal antibodies (Stadler et al., 2017). Another promising option would be to further engineer BiTEs so they can become trifunctional antibodies, with the ability to bind FcγR in order to promote a potent vaccinal effect and attain a long-term immune response (Arce Vargas and Quezada, 2015).

In terms of the tumoursphere model, I propose to generate PaCa primary cells-derived spheroids, characterise both models (cell line- and primary tumour-derived) and test them *in vivo*. In parallel, based on the biomarkers proposed in the literature and those found to be upregulated on our own PANC-1-derived tumourspheres, it would be interesting to perform cell sorting on PaCa primary tumours and inject them in NOD/SCID mice, as per (Fitzgerald and McCubrey, 2014). As mentioned earlier, the gold standard for CSC identification is to test for tumourigenicity *in vivo*. Comparison of these models would ascertain relevant differences and determine which CSC model would be the best for preclinical research.

Also, it would be worth testing our range of ROR1 MAbs for cross-reactivity with ROR2, as it would provide us with an additional therapeutic tool.

Chapter 7 General discussion

7.1 Discussion of results

ROR1 is expressed in a wide range of solid and haematological malignancies with low expression in normal adult tissue. Similar to the physiological functions of ROR1 during embryogenesis; in cancer, ROR1 can have kinase activity-dependent or –independent function, which may come as a result of tissue specific expression of co-receptors or effector proteins (Borcherding et al., 2014).

The discovery of ROR1 overexpression in CLL and other malignancies coupled with: i) different studies showing the induction of apoptosis by knocking down ROR1, ii) ROR1-mediated upregulation of EMT genes and iii) overexpression of this biomarker on CSCs, strongly support the notion that ROR1 it is not merely a bystander but rather plays an important role in cancer progression, metastasis and relapse.

These unique features make ROR1 an ideal drug target for cancer immunotherapy. In line with this, the overriding aim of my research was to generate a ROR1-based immunotherapy using monoclonal antibody technologies. In this chapter, the findings of this thesis and their broader implications will be briefly summarised and discussed. Additionally, future directions for this work will be suggested.

7.1.1 MAb-based ROR1 immunotherapy

As mentioned earlier, ROR1 is an onco-foetal antigen, and as such might be recognised by the immune system. Accordingly, in 2008 Fukuda *et al*. (Fukuda et al., 2008) described for the first time a humoral immune response against ROR1 in CLL patients after vaccination with an adenovirus encoding CD154 (Ad-CD154), a CD40 ligand which reverses the immune-suppressive

phenotype of CLL. Similarly, CLL patients treated with immune-modulating drug Lenalidomide presented anti-ROR1 antibodies in their sera (Lapalombella et al., 2010). More recently, spontaneous humoral and T-cell responses against ROR1 was reported in CLL patients (Hojjat-Farsangi et al., 2015). Together, these results support the concept that ROR1 might behave as a neoantigen and may represent a valuable target for cancer immunotherapy.

In this context, in **Chapter 3**, I reported the generation of 16 novel antibodies against ROR1. These binders were then engineered in order to produce rat-human chimeric antibodies. Binding assays by flow cytometry revealed that only 12 MAbs were still able to target ROR1 in a human IgG1 isotype format. As one of the aims of this thesis was to develop therapeutic MAbs, the IgG1 isotype was chosen for this purpose due to its extended half-life and ability to trigger potent effector mechanisms through Fc-FcγR interactions (Natsume et al., 2009).

It is noteworthy to mention that the isotype of choice can have critical effects not only on antibody activity, but also on specificity, structure and affinity. Consistently, it is hypothesised that this change of isotype might have affected the binding of clones U, Psi, K2 and X, previously able to bind to ROR1 when they were in rat isotypes. A further illustration of isotype influence comes from a recent study of PD-1 therapy *in vivo*. Arlauckas *et al.* (Arlauckas et al., 2017) show that blocking anti-PD-1 antibodies in IgG4 –thought to have no major effect on CDC or ADCC/ADCP– were still able to attract macrophages, which in turn sequestered $CD8^+$ T-cell bound PD-1 antibodies. These findings underline the importance of Fc-FcγR interactions and their role in immune-modulation and immunotherapies.

Notably, the generation of these novel antibody sequences also represented availability of new tools for developing MAb-derivatives such as CARs, ADCs, BiTEs, among others (Mackall, 2014). Since conventional antibodies mainly

rely on the immune system of the patient, which is often compromised (Ramsay et al., 2008), armed antibodies and derivatives have been recently exploited in order to increase cytotoxicity. In our research group, we were also intrigued by these therapeutic approaches. In order to decide which MAb-based approach to choose, antibodies were characterised in terms of cytotoxicity, epitope mapping, K_D determination and internalisation capability.

Characterisation of all ROR1 chimeric MAbs is reported in **Chapter 4**, and with a particular focus on clones SA1 and F in **Chapter 5**. Binding assays using stable cell lines, expressing either full-length extracellular ROR1 or truncated domains, showed that out of 12 ROR1 MAbs, 10 detected the Ig-like domain of ROR1. In contrast, clone F was the only MAb able to bind to the Fz domain; whilst no antibodies were found to bind to the Kringle domain. This might be explained by the high sequence identity (99%) between rat and human for both Fz and Kg domains.

In terms of K_D determination, clones B5, Pi and SA1 exhibited the strongest affinities. Notably, clone SA1 also showed the slowest K_{off} rate which could potentially explain the good CDC activity exerted on CLL cells. As explained by Glennie *et al*. (Glennie et al., 2007), the slow off-rate would provide stable binding which would favour enhanced recruitment of C1q molecules.

Data from different internalisation assays suggested that clone SA1 was also able to get internalised by primary CLL cells and $ROR1^+$ suspension cell lines. This is not in disagreement with the cytotoxicity potential of this clone as a similar profile in terms of internalisation and cytotoxicity was reported for clone D10, the prototype of Cirmtuzumab (Cui et al., 2013, Widhopf et al., 2014).

In light of these findings, I focused my studies on both clone SA1 and F. On the one hand, SA1 offered the possibility to be developed as a conventional, naked antibody due to its low K_D value (1.81nM) and potent cytotoxicity. Additionally, due to its internalisation capabilities, it had the potential to be

further engineered in order to produce an ADC. On the other hand, clone F recognised a unique epitope in the Fz domain. Its membrane proximal epitope coupled with its K_D value (5.46nM) –which was strong but not as potent as SA1's– made clone F a suitable candidate for cancer therapy using antibody-derivative technologies, such as CARs or BiTEs.

7.1.2 ROR1 targeting in CLL: MAb therapy

For CLL and other non-Hodgkin lymphomas, monoclonal antibodies have proven to be effective agents in the treatment of several cancers, particularly when used in combination with chemotherapy. They have been shown to improve response rates and prolonged overall survival (Hallek et al., 2010). To date, most MAbs currently used in the treatment of CLL are directed against CD20. This antigen, however, is expressed on normal B-cells and may lead to hypogammaglobulinemia. Other antigens such as CD19, CD37 and CD52 are also being investigated in the clinic (Robak, 2014), yet none of these antigens are unique to CLL cells.

ROR1 is overexpressed on CLL cells but not healthy, critical tissue. Not surprisingly, a number of groups have recently developed MAbs targeting ROR1 (Baskar et al., 2008, Cui et al., 2013, Daneshmanesh et al., 2012, Yang et al., 2011). For therapeutic purposes, most of these antibodies have been generated against the extracellular portion of ROR1. Nonetheless, the results reported from these MAbs in CLL have been mixed, with Cirmtuzumab being the only ROR1 antibody currently under investigation in the clinic. Some groups have reported no CDC or ADCC activity with ROR1 MAbs (Baskar et al., 2012, Yang et al., 2011); probably because there is an estimate of only 10^3 - 10^4 molecules of ROR1 on the surface of CLL cells (Baskar et al., 2008), which is 10-100 folds lower than conventional targets of MAb therapies (Yang et al., 2011). In contrast, researchers who developed MAbs directed against the Fz and Kg domains have reported cytotoxicity on CLL cells by direct apoptosis (Daneshmanesh et al., 2012). These results, however, were

attained by using IgG and IgM murine antibodies and none of these clones are currently in clinical trials.

In this study, although clone SA1 was able to elicit significant CDC activity, the latter was reduced after humanisation of this clone (**Chapter 5**). Therefore, in an effort to bypass the lack of significant cytotoxicity, a bispecific antibody in full IgG targeting both ROR1 (chimeric SA1 clone) and CD3ε molecules on T-cells was designed and engineered. Unfortunately, when tested on cytotoxicity assays, data revealed non-specific binding to ROR1 negative cell lines. In view of these results, no further studies were carried out with SA1 and instead focused on the development of clone F as a BiTE therapy.

7.1.3 ROR1 targeting in PaCa tumourspheres: BiTE therapy

Due to its unique epitope within the Fz domain of ROR1, our group developed clone F as a humanised BiTE and assessed its cytotoxicity potential on a range of solid cancer malignancies, including pancreatic cancer (PaCa) (Gohil et al., 2017).

PaCa is a lethal disease, often diagnosed when metastatic events have occurred. Despite therapy, the median survival rate is approximately 6 months (Society, 2015). The high mortality rate of PaCa is thought to be caused by its aggressive nature, local and advanced metastasis and intrinsic resistance to chemotherapeutics, including Gemcitabine (Ercan et al., 2017). Since cancer stem cell-like cells play a crucial role not only in tumour initiation but also in cancer progression, drug resistance and relapse (Adorno-Cruz et al., 2015), they represent excellent targets for effective novel therapeutic strategies.

Expression of ROR1 on CSCs from ovarian cancer and glioblastoma was recently reported (Jung et al., 2016, Zhang et al., 2014). Thus, I next sought to investigate whether our ROR1 BiTE was able to target CSCs derived from a pancreatic cancer cell line (PANC-1) (**Chapter 6**). Of note, CSCs can be

identified by their self-renewal and tumour propagation potential. The gold standard assay for this is serial transplantation in animal models. The challenges that this assay presents in terms of feasibility, cost and time, however, rise the necessity of developing alternative *in vitro* models, such as tumourspheres generated by 3D sphere formation assay (Qureshi-Baig et al., 2016). The spheroid formation assay utilises the anchorage-independent growth properties of cancer stem cells-like cells and it has shown to better preserve the characteristics of original tumours in terms of: gene expression profile, tumour heterogeneity and morphology, compared to adherent cultures (Lee et al., 2015, Weiswald et al., 2015, Lee et al., 2006).

In this study, PANC-1 derived tumourspheres were generated *in vitro*. Characterisation data suggested relevant CSC biomarkers were upregulated at both gene and protein levels. Contrary to my expectations, however, ROR1 was downregulated on PaCa spheroids compared to parental, adherent cells. Although surprising, this finding was consistent with the notion that CSC biomarkers described in a particular cancer type, cannot be extrapolated to other malignancies. In fact, these biomarkers need to be evaluated in a tissue-dependent manner (Clarke et al., 2006).

These data led me to evaluate the gene and protein expression of the other member of the ROR family, namely ROR2. As hypothesised, ROR2 was overexpressed on tumourspheres. Of note, both ROR1 and ROR2 share the same ligand, Wnt5a. These results are consistent with previous studies reporting that Wnt5a signalling plays a key role in the regulation of normal and cancer stem cell self-renewal, proliferation, migration and invasion (Zhou et al., 2017b).

Although reduced, expression of ROR1 was still detectable on PaCa spheroids. Therefore, tumourspheres were treated with ROR1 BiTE therapy followed by immunocytochemistry analysis in order to ascertain whether this approach was able to specifically eliminate ROR1^{+} CSCs. Confocal

microscopy data revealed significant elimination of cells expressing both ROR1 and ALDH1. Moreover, in line with previous reports, a reduction on the expression of both Vimentin and ALDH1 after ROR1 targeting (Cui et al., 2013, Zhang et al., 2014) was observed. Further studies and method validation of both immunocytochemistry and confocal microscopy undertaken in this study are required in order to conclusively determine an association between ROR1 and both Vimentin and ALDH1.

Collectively, these data suggest that our ROR1 BiTE therapy is able to target both ROR1$^+$ cells present in PaCa tumours as well as ROR1$^+$ cells within CSC subsets. Additional preclinical studies using a tumoursphere model derived from PaCa primary cells as well as *in vivo* models of CSCs would help further validate the findings obtained in this study. Furthermore, it is anticipated that ROR1 BiTE therapy used in combination with checkpoint blockade antibodies would provide PaCa patients with a much-needed therapeutic option able to significantly enhance their clinical prospects, as the addition of an anti-PD-1 antibody would potentially circumvent the BiTE therapy-driven T-cell exhaustion and increased expression of PD-L1 (Kohnke et al., 2015, Topp et al., 2017). More extensive preclinical and clinical studies will ultimately reveal the true therapeutic potential that ROR1 BiTEs alone or in combination will achieve.

7.2 Summary of results/General conclusions

As a whole, findings reported in this thesis confirmed the primary hypothesis. It was proposed that, due to its exquisite expression on malignant cells including CSCs but not adult, critical tissue, ROR1 is a druggable target for cancer immunotherapy.

Although none of our ROR1 MAbs could be developed as a therapeutic antibody in full IgG, it was identified that clone F was able to bind to the Fz domain of ROR1. This made it a unique candidate for antibody-derivative

therapy, such as BiTEs or CARs. Moreover, it has been recently demonstrated that membrane proximal epitopes facilitate more potent cytotoxicity than membrane distal regions (Hudecek et al., 2013, Jensen and Riddell, 2014). Consequently, having developed a humanised F BiTE and established potent and specific cytotoxicity on a range of solid cancer cell lines, including pancreatic cancer (Gohil et al., 2017), I tested our ROR1 BiTE on ROR1$^+$ PaCa CSCs.

By using an *in vitro* model of PaCa tumourspheres, I have demonstrated that, contrary to previous assumptions, ROR1 expression was downregulated on PaCa tumourspheres compared to adherent cells; and instead, ROR2 expression was found to be upregulated. Although ROR1 downregulation followed by ROR2 upregulation has been described in melanoma under hypoxic conditions (O'Connell et al., 2013); this is, to my knowledge, the first time both receptors are studied in the context of PaCa. Furthermore, it is proposed that overexpression of ROR2 might be overtaking the usual role of ROR1 on PaCa CSCs and might explain the increased migration capability of tumourspheres compared to parental cells.

Despite ROR1 downregulation, protein expression assays revealed that its presence on the cell surface of spheroids was still detectable. By treating these tumourspheres with ROR1 BiTE therapy, followed by immunocytochemistry and confocal microscopy, specific targeting of ROR1$^+$ cells, including cells expressing both ALDH1 (a CSC biomarker) and ROR1 has been shown. In light of this evidence, it is suggested that ROR1 therapy, particularly when used with BiTE technology, may prove a relevant and much needed addition to the currently available options for cancer treatment. The possibility of targeting and eliminating ROR1$^+$ cells within the bulk of the tumour and CSC subpopulations warrants further preclinical and clinical evaluation.

7.3 Further work

For optimal exploitation of our monoclonal antibodies against ROR1, I propose further evaluation of these reagents using different assay systems, such as ELISA, Western blot, immunohistochemistry, flow cytometry, etc. By performing a thorough characterisation of these MAbs and assessing in which system they work best, it would be possible to identify relevant tools for research and/or diagnostic applications. Additionally, due to the cross-talk between ROR1 and ROR2, it would be worth testing our range of ROR1 MAbs against ROR2.

In order to truly assess the cytotoxicity potential of the ROR1 MAbs generated in this study, I suggest performing *in vivo* studies that would allow us to fully evaluate the distinct mechanisms of action exerted by these MAbs. Furthermore, antibody production using CHO/FUT8$^{-/-}$ cells would result in afucosylated antibodies, which have demonstrated strong ADCC activity and a potential vaccine effect.

With regards to CSC models for preclinical research, a recent study from (Giustacchini et al., 2017), has shown that a single cell transcriptomics approach unravelled intratumoral heterogeneity and selective resistance of cancer stem cell subpopulations to molecularly targeted cancer therapies. It is envisaged that this strategy might become commonplace in order to better study and identify subpopulations of therapy-resistant CSCs –that are not apparent through cell-population analysis. Certainly, this approach offers an exciting opportunity to evaluate the therapeutic potential of our ROR1 BiTE at a preclinical level.

Also, taking into consideration that it is unlikely that a single pathway is operative in all CSC subsets (Cabrera et al., 2015), a therapeutic approach targeting multiple pathways essential to CSCs and/or EMT plasticity would theoretically attain substantial clinical benefit. In this context, it is believed that

our ROR1 BiTE therapy represents a pivotal addition to the therapeutic arsenal against both CSC and EMT pathways. Furthermore, since it has been suggested that a more effective anti-tumour response might be achieved by including strategies that enhance T-cell priming, the use of checkpoint blockade antibodies could further boost T-cell proliferation and function (Arce Vargas and Quezada, 2015).

Chapter 8 References

1999. Chemotherapeutic options in chronic lymphocytic leukemia: a meta-analysis of the randomized trials. CLL Trialists' Collaborative Group. *J Natl Cancer Inst,* 91**,** 861-8.

2016. Tumoursphere culture of cancer stem cells (CSC) with the PromoCell Cancer Stem Cell medium. *In:* GMBH, P. (ed.).

ABCAM A comparison between polyclonal and monoclonal: Key differences, advantages and disadvantages.

ABCAM. 2017. *KD value: a quantitative measurement of antibody affinity* [Online]. Available: http://www.abcam.com/primary-antibodies/kd-value-a-quantitive-measurement-of-antibody-affinity [Accessed 2017].

ADAMSKA, A., DOMENICHINI, A. & FALASCA, M. 2017. Pancreatic Ductal Adenocarcinoma: Current and Evolving Therapies. *Int J Mol Sci,* 18.

ADORNO-CRUZ, V., KIBRIA, G., LIU, X., DOHERTY, M., JUNK, D. J., GUAN, D., HUBERT, C., VENERE, M., MULKEARNS-HUBERT, E., SINYUK, M., ALVARADO, A., CAPLAN, A. I., RICH, J., GERSON, S. L., LATHIA, J. & LIU, H. 2015. Cancer stem cells: targeting the roots of cancer, seeds of metastasis, and sources of therapy resistance. *Cancer Res,* 75**,** 924-9.

ADUSUMILLI, P. S., CHERKASSKY, L., VILLENA-VARGAS, J., COLOVOS, C., SERVAIS, E., PLOTKIN, J., JONES, D. R. & SADELAIN, M. 2014. Regional delivery of mesothelin-targeted CAR T cell therapy generates potent and long-lasting CD4-dependent tumor immunity. *Sci Transl Med,* 6**,** 261ra151.

AGUILAR-HERNANDEZ, M. M., BLUNT, M. D., DOBSON, R., YEOMANS, A., THIRDBOROUGH, S., LARRAYOZ, M., SMITH, L. D., LINLEY, A., STREFFORD, J. C., DAVIES, A., JOHNSON, P. M., SAVELYEVA, N., CRAGG, M. S., FORCONI, F., PACKHAM, G., STEVENSON, F. K. & STEELE, A. J. 2016. IL-4 enhances expression and function of surface IgM in CLL cells. *Blood,* 127**,** 3015-25.

ALGARRA, I., CABRERA, T. & GARRIDO, F. 2000. The HLA crossroad in tumor immunology. *Hum Immunol,* 61**,** 65-73.

ALISON, M. R., LIM, S. M. & NICHOLSON, L. J. 2011. Cancer stem cells: problems for therapy? *J Pathol,* 223**,** 147-61.

AMEDEI, A., NICCOLAI, E. & PRISCO, D. 2014. Pancreatic cancer: role of the immune system in cancer progression and vaccine-based immunotherapy. *Hum Vaccin Immunother,* 10**,** 3354-68.

ANSARI, D., TINGSTEDT, B., ANDERSSON, B., HOLMQUIST, F., STURESSON, C., WILLIAMSSON, C., SASOR, A., BORG, D., BAUDEN, M. & ANDERSSON, R. 2016. Pancreatic cancer: yesterday, today and tomorrow. *Future Oncol,* 12**,** 1929-46.

ARCE VARGAS, F. & QUEZADA, S. A. 2015. Fcgamma-receptor tag team boosts anti-tumor immunity. *Trends Immunol,* 36**,** 388-9.

ARLAUCKAS, S. P., GARRIS, C. S., KOHLER, R. H., KITAOKA, M., CUCCARESE, M. F., YANG, K. S., MILLER, M. A., CARLSON, J. C., FREEMAN, G. J., ANTHONY, R. M., WEISSLEDER, R. & PITTET, M. J. 2017. In vivo imaging reveals a tumor-associated macrophage-mediated resistance pathway in anti-PD-1 therapy. *Sci Transl Med,* 9.

BADOUX, X. C., KEATING, M. J., WEN, S., WIERDA, W. G., O'BRIEN, S. M., FADERL, S., SARGENT, R., BURGER, J. A. & FERRAJOLI, A. 2013. Phase II study of lenalidomide and rituximab as salvage therapy for patients with relapsed or refractory chronic lymphocytic leukemia. *J Clin Oncol,* 31**,** 584-91.

BAERGA-ORTIZ, A., HUGHES, C. A., MANDELL, J. G. & KOMIVES, E. A. 2002. Epitope mapping of a monoclonal antibody against human thrombin by H/D-exchange mass spectrometry reveals selection of a diverse sequence in a highly conserved protein. *Protein Sci,* 11**,** 1300-8.

BAILEY, J. M., SWANSON, B. J., HAMADA, T., EGGERS, J. P., SINGH, P. K., CAFFERY, T., OUELLETTE, M. M. & HOLLINGSWORTH, M. A. 2008. Sonic hedgehog promotes desmoplasia in pancreatic cancer. *Clin Cancer Res,* 14**,** 5995-6004.

BALAKRISHNAN, A., GOODPASTER, T., RANDOLPH-HABECKER, J., HOFFSTROM, B. G., JALIKIS, F. G., KOCH, L. K., BERGER, C., KOSASIH, P. L., RAJAN, A., SOMMERMEYER, D., PORTER, P. L. & RIDDELL, S. R. 2017. Analysis of ROR1 Protein Expression in Human Cancer and Normal Tissues. *Clin Cancer Res,* 23**,** 3061-3071.

BALATTI, V., RIZZOTTO, L., MILLER, C., PALAMARCHUK, A., FADDA, P., PANDOLFO, R., RASSENTI, L. Z., HERTLEIN, E., RUPPERT, A. S., LOZANSKI, A., LOZANSKI, G., KIPPS, T. J., BYRD, J. C., CROCE, C. M. & PEKARSKY, Y. 2015. TCL1 targeting miR-3676 is codeleted with tumor protein p53 in chronic lymphocytic leukemia. *Proc Natl Acad Sci U S A,* 112**,** 2169-74.

BARCLAY, A. N. 2003. Membrane proteins with immunoglobulin-like domains--a master superfamily of interaction molecules. *Semin Immunol,* 15**,** 215-23.

BARTH, M. J., MAVIS, C., CZUCZMAN, M. S. & HERNANDEZ-ILIZALITURRI, F. J. 2015. Ofatumumab Exhibits Enhanced In Vitro and In Vivo Activity Compared to Rituximab in Preclinical Models of Mantle Cell Lymphoma. *Clin Cancer Res,* 21**,** 4391-7.

BARTLETT, D. L., LIU, Z., SATHAIAH, M., RAVINDRANATHAN, R., GUO, Z., HE, Y. & GUO, Z. S. 2013. Oncolytic viruses as therapeutic cancer vaccines. *Mol Cancer,* 12**,** 103.

BASKAR, S., KWONG, K. Y., HOFER, T., LEVY, J. M., KENNEDY, M. G., LEE, E., STAUDT, L. M., WILSON, W. H., WIESTNER, A. & RADER, C. 2008. Unique cell surface expression of receptor tyrosine kinase ROR1 in human B-cell chronic lymphocytic leukemia. *Clin Cancer Res,* 14**,** 396-404.

BASKAR, S., WIESTNER, A., WILSON, W. H., PASTAN, I. & RADER, C. 2012. Targeting malignant B cells with an immunotoxin against ROR1. *MAbs,* 4**,** 349-61.

BEERS, S. A., GLENNIE, M. J. & WHITE, A. L. 2016. Influence of immunoglobulin isotype on therapeutic antibody function. *Blood,* 127**,** 1097-101.

BELLOSILLO, B., VILLAMOR, N., LOPEZ-GUILLERMO, A., MARCE, S., ESTEVE, J., CAMPO, E., COLOMER, D. & MONTSERRAT, E. 2001. Complement-mediated cell death induced by rituximab in B-cell lymphoproliferative disorders is mediated in vitro by a caspase-independent mechanism involving the generation of reactive oxygen species. *Blood,* 98**,** 2771-7.

BERGER, C., SOMMERMEYER, D., HUDECEK, M., BERGER, M., BALAKRISHNAN, A., PASZKIEWICZ, P. J., KOSASIH, P. L., RADER, C. & RIDDELL, S. R. 2015. Safety of targeting ROR1 in primates with chimeric antigen receptor-modified T cells. *Cancer Immunol Res,* 3**,** 206-16.

BERMAN, D., KORMAN, A., PECK, R., FELTQUATE, D., LONBERG, N. & CANETTA, R. 2015. The development of immunomodulatory monoclonal antibodies as a new therapeutic modality for cancer: the Bristol-Myers Squibb experience. *Pharmacol Ther,* 148**,** 132-53.

BERNHARDT, S. L., GJERTSEN, M. K., TRACHSEL, S., MOLLER, M., ERIKSEN, J. A., MEO, M., BUANES, T. & GAUDERNACK, G. 2006. Telomerase peptide vaccination of patients with non-resectable pancreatic cancer: A dose escalating phase I/II study. *Br J Cancer,* 95**,** 1474-82.

BHOI, S., LJUNGSTROM, V., BALIAKAS, P., MATTSSON, M., SMEDBY, K. E., JULIUSSON, G., ROSENQUIST, R. & MANSOURI, L. 2016. Prognostic impact of epigenetic classification in chronic lymphocytic leukemia: The case of subset #2. *Epigenetics,* 11**,** 449-55.

BIANKIN, A. V., WADDELL, N., KASSAHN, K. S., GINGRAS, M. C., MUTHUSWAMY, L. B., JOHNS, A. L., MILLER, D. K., WILSON, P. J., PATCH, A. M., WU, J., CHANG, D. K., COWLEY, M. J., GARDINER, B. B., SONG, S., HARLIWONG, I., IDRISOGLU, S., NOURSE, C., NOURBAKHSH, E., MANNING, S., WANI, S., GONGORA, M., PAJIC, M., SCARLETT, C. J., GILL, A. J., PINHO, A. V., ROOMAN, I., ANDERSON, M., HOLMES, O., LEONARD, C., TAYLOR, D., WOOD, S., XU, Q., NONES, K., FINK, J. L., CHRIST, A., BRUXNER, T., CLOONAN, N., KOLLE, G., NEWELL, F., PINESE, M., MEAD, R. S., HUMPHRIS, J. L., KAPLAN, W., JONES, M. D., COLVIN, E. K., NAGRIAL, A. M., HUMPHREY, E. S., CHOU, A., CHIN, V. T., CHANTRILL, L. A., MAWSON, A., SAMRA, J. S., KENCH, J. G., LOVELL, J. A., DALY, R. J., MERRETT, N. D., TOON, C., EPARI, K., NGUYEN, N. Q., BARBOUR, A., ZEPS, N., AUSTRALIAN PANCREATIC CANCER GENOME, I., KAKKAR, N., ZHAO, F., WU, Y. Q., WANG, M., MUZNY, D. M., FISHER, W. E., BRUNICARDI, F. C., HODGES, S. E., REID, J. G., DRUMMOND, J., CHANG, K., HAN,

Y., LEWIS, L. R., DINH, H., BUHAY, C. J., BECK, T., TIMMS, L., SAM, M., BEGLEY, K., BROWN, A., PAI, D., PANCHAL, A., BUCHNER, N., DE BORJA, R., DENROCHE, R. E., YUNG, C. K., SERRA, S., ONETTO, N., MUKHOPADHYAY, D., TSAO, M. S., SHAW, P. A., PETERSEN, G. M., GALLINGER, S., HRUBAN, R. H., MAITRA, A., IACOBUZIO-DONAHUE, C. A., SCHULICK, R. D., WOLFGANG, C. L., et al. 2012. Pancreatic cancer genomes reveal aberrations in axon guidance pathway genes. *Nature,* 491**,** 399-405.

BINDON, C. I., HALE, G., BRUGGEMANN, M. & WALDMANN, H. 1988. Human monoclonal IgG isotypes differ in complement activating function at the level of C4 as well as C1q. *J Exp Med,* 168**,** 127-42.

BIOLABS, C. 2017. *Anti-ROR1 (R11) scFv-Fc-Sec ADC* [Online]. http://www.creativebiolabs.net/R11-scFv-Fc-Sec-21579.htm. Available: http://www.creativebiolabs.net/R11-scFv-Fc-Sec-21579.htm [Accessed 2017 2017].

BLACKBURN, S. D., SHIN, H., HAINING, W. N., ZOU, T., WORKMAN, C. J., POLLEY, A., BETTS, M. R., FREEMAN, G. J., VIGNALI, D. A. & WHERRY, E. J. 2009. Coregulation of CD8+ T cell exhaustion by multiple inhibitory receptors during chronic viral infection. *Nat Immunol,* 10**,** 29-37.

BLUNT, M. D. & STEELE, A. J. 2015. Pharmacological targeting of PI3K isoforms as a therapeutic strategy in chronic lymphocytic leukaemia. *Leuk Res Rep,* 4**,** 60-3.

BOISSARD, F., FOURNIE, J. J., LAURENT, C., POUPOT, M. & YSEBAERT, L. 2015. Nurse like cells: chronic lymphocytic leukemia associated macrophages. *Leuk Lymphoma,* 56**,** 1570-2.

BOON, T., COULIE, P. G., VAN DEN EYNDE, B. J. & VAN DER BRUGGEN, P. 2006. Human T cell responses against melanoma. *Annu Rev Immunol,* 24**,** 175-208.

BORCHERDING, N., KUSNER, D., LIU, G. H. & ZHANG, W. 2014. ROR1, an embryonic protein with an emerging role in cancer biology. *Protein Cell,* 5**,** 496-502.

BOULIANNE, G. L., HOZUMI, N. & SHULMAN, M. J. 1984. Production of functional chimaeric mouse/human antibody. *Nature,* 312**,** 643-6.

BOWLES, J. A., WANG, S. Y., LINK, B. K., ALLAN, B., BEUERLEIN, G., CAMPBELL, M. A., MARQUIS, D., ONDEK, B., WOOLDRIDGE, J. E., SMITH, B. J., BREITMEYER, J. B. & WEINER, G. J. 2006. Anti-CD20 monoclonal antibody with enhanced affinity for CD16 activates NK cells at lower concentrations and more effectively than rituximab. *Blood,* 108**,** 2648-54.

BOWLES, J. A. & WEINER, G. J. 2005. CD16 polymorphisms and NK activation induced by monoclonal antibody-coated target cells. *J Immunol Methods,* 304**,** 88-99.

BRAHMER, J. R., TYKODI, S. S., CHOW, L. Q., HWU, W. J., TOPALIAN, S. L., HWU, P., DRAKE, C. G., CAMACHO, L. H., KAUH, J., ODUNSI, K., PITOT, H. C., HAMID, O., BHATIA, S., MARTINS, R., EATON, K., CHEN, S., SALAY, T. M., ALAPARTHY, S., GROSSO, J. F.,

KORMAN, A. J., PARKER, S. M., AGRAWAL, S., GOLDBERG, S. M., PARDOLL, D. M., GUPTA, A. & WIGGINTON, J. M. 2012. Safety and activity of anti-PD-L1 antibody in patients with advanced cancer. *N Engl J Med,* 366**,** 2455-65.

BRISCHWEIN, K., SCHLERETH, B., GULLER, B., STEIGER, C., WOLF, A., LUTTERBUESE, R., OFFNER, S., LOCHER, M., URBIG, T., RAUM, T., KLEINDIENST, P., WIMBERGER, P., KIMMIG, R., FICHTNER, I., KUFER, P., HOFMEISTER, R., DA SILVA, A. J. & BAEUERLE, P. A. 2006. MT110: a novel bispecific single-chain antibody construct with high efficacy in eradicating established tumors. *Mol Immunol,* 43**,** 1129-43.

BROCHET, X., LEFRANC, M. P. & GIUDICELLI, V. 2008. IMGT/V-QUEST: the highly customized and integrated system for IG and TR standardized V-J and V-D-J sequence analysis. *Nucleic Acids Res,* 36**,** W503-8.

BROOME, H. E., RASSENTI, L. Z., WANG, H. Y., MEYER, L. M. & KIPPS, T. J. 2011. ROR1 is expressed on hematogones (non-neoplastic human B-lymphocyte precursors) and a minority of precursor-B acute lymphoblastic leukemia. *Leuk Res,* 35**,** 1390-4.

BRUNSCHWIG, A. 1937. Resection of the head of pancreas and duodenum for carcinoma – pancreatoduodenectomy. *Surg. Gynecol. Obstet,* 65**,** 681-684.

BUENSALIDO, J. A. & CHANDRASEKAR, P. H. 2014. Prophylaxis against hepatitis B reactivation among patients with lymphoma receiving rituximab. *Expert Rev Anti Infect Ther,* 12**,** 151-4.

BURGER, J. A., LANDAU, D. A., TAYLOR-WEINER, A., BOZIC, I., ZHANG, H., SAROSIEK, K., WANG, L., STEWART, C., FAN, J., HOELLENRIEGEL, J., SIVINA, M., DUBUC, A. M., FRASER, C., HAN, Y., LI, S., LIVAK, K. J., ZOU, L., WAN, Y., KONOPLEV, S., SOUGNEZ, C., BROWN, J. R., ABRUZZO, L. V., CARTER, S. L., KEATING, M. J., DAVIDS, M. S., WIERDA, W. G., CIBULSKIS, K., ZENZ, T., WERNER, L., DAL CIN, P., KHARCHENCKO, P., NEUBERG, D., KANTARJIAN, H., LANDER, E., GABRIEL, S., O'BRIEN, S., LETAI, A., WEITZ, D. A., NOWAK, M. A., GETZ, G. & WU, C. J. 2016. Clonal evolution in patients with chronic lymphocytic leukaemia developing resistance to BTK inhibition. *Nat Commun,* 7**,** 11589.

BURGER, J. A., TEDESCHI, A., BARR, P. M., ROBAK, T., OWEN, C., GHIA, P., BAIREY, O., HILLMEN, P., BARTLETT, N. L., LI, J., SIMPSON, D., GROSICKI, S., DEVEREUX, S., MCCARTHY, H., COUTRE, S., QUACH, H., GAIDANO, G., MASLYAK, Z., STEVENS, D. A., JANSSENS, A., OFFNER, F., MAYER, J., O'DWYER, M., HELLMANN, A., SCHUH, A., SIDDIQI, T., POLLIACK, A., TAM, C. S., SURI, D., CHENG, M., CLOW, F., STYLES, L., JAMES, D. F., KIPPS, T. J. & INVESTIGATORS, R.-. 2015. Ibrutinib as Initial Therapy for Patients with Chronic Lymphocytic Leukemia. *N Engl J Med,* 373**,** 2425-37.

BURGER, J. A., TSUKADA, N., BURGER, M., ZVAIFLER, N. J., DELL'AQUILA, M. & KIPPS, T. J. 2000. Blood-derived nurse-like cells protect chronic lymphocytic leukemia B cells from spontaneous apoptosis through stromal cell-derived factor-1. *Blood,* 96**,** 2655-63.

BURNET, F. M. 1967. Immunological aspects of malignant disease. *Lancet,* 1**,** 1171-4.

BURRIS, H. A., 3RD, MOORE, M. J., ANDERSEN, J., GREEN, M. R., ROTHENBERG, M. L., MODIANO, M. R., CRIPPS, M. C., PORTENOY, R. K., STORNIOLO, A. M., TARASSOFF, P., NELSON, R., DORR, F. A., STEPHENS, C. D. & VON HOFF, D. D. 1997. Improvements in survival and clinical benefit with gemcitabine as first-line therapy for patients with advanced pancreas cancer: a randomized trial. *J Clin Oncol,* 15**,** 2403-13.

BYRD, J. C., BROWN, J. R., O'BRIEN, S., BARRIENTOS, J. C., KAY, N. E., REDDY, N. M., COUTRE, S., TAM, C. S., MULLIGAN, S. P., JAEGER, U., DEVEREUX, S., BARR, P. M., FURMAN, R. R., KIPPS, T. J., CYMBALISTA, F., POCOCK, C., THORNTON, P., CALIGARIS-CAPPIO, F., ROBAK, T., DELGADO, J., SCHUSTER, S. J., MONTILLO, M., SCHUH, A., DE VOS, S., GILL, D., BLOOR, A., DEARDEN, C., MORENO, C., JONES, J. J., CHU, A. D., FARDIS, M., MCGREIVY, J., CLOW, F., JAMES, D. F., HILLMEN, P. & INVESTIGATORS, R. 2014. Ibrutinib versus ofatumumab in previously treated chronic lymphoid leukemia. *N Engl J Med,* 371**,** 213-23.

BYRD, J. C., HARRINGTON, B., O'BRIEN, S., JONES, J. A., SCHUH, A., DEVEREUX, S., CHAVES, J., WIERDA, W. G., AWAN, F. T., BROWN, J. R., HILLMEN, P., STEPHENS, D. M., GHIA, P., BARRIENTOS, J. C., PAGEL, J. M., WOYACH, J., JOHNSON, D., HUANG, J., WANG, X., KAPTEIN, A., LANNUTTI, B. J., COVEY, T., FARDIS, M., MCGREIVY, J., HAMDY, A., ROTHBAUM, W., IZUMI, R., DIACOVO, T. G., JOHNSON, A. J. & FURMAN, R. R. 2016. Acalabrutinib (ACP-196) in Relapsed Chronic Lymphocytic Leukemia. *N Engl J Med,* 374**,** 323-32.

CABRERA, M. C., HOLLINGSWORTH, R. E. & HURT, E. M. 2015. Cancer stem cell plasticity and tumor hierarchy. *World J Stem Cells,* 7**,** 27-36.

CALCAGNO, A. M. & AMBUDKAR, S. V. 2010. Analysis of expression of drug resistance-linked ABC transporters in cancer cells by quantitative RT-PCR. *Methods Mol Biol,* 637**,** 121-32.

CALIN, G. A., DUMITRU, C. D., SHIMIZU, M., BICHI, R., ZUPO, S., NOCH, E., ALDLER, H., RATTAN, S., KEATING, M., RAI, K., RASSENTI, L., KIPPS, T., NEGRINI, M., BULLRICH, F. & CROCE, C. M. 2002. Frequent deletions and down-regulation of micro- RNA genes miR15 and miR16 at 13q14 in chronic lymphocytic leukemia. *Proc Natl Acad Sci U S A,* 99**,** 15524-9.

CALVET, C. Y., ANDRE, F. M. & MIR, L. M. 2014. The culture of cancer cell lines as tumorspheres does not systematically result in cancer stem cell enrichment. *PLoS One,* 9**,** e89644.

CAO, L., ZHOU, Y., ZHAI, B., LIAO, J., XU, W., ZHANG, R., LI, J., ZHANG, Y., CHEN, L., QIAN, H., WU, M. & YIN, Z. 2011. Sphere-forming cell subpopulations with cancer stem cell properties in human hepatoma cell lines. *BMC Gastroenterol,* 11**,** 71.

CARBALLIDO, E., VELIZ, M., KOMROKJI, R. & PINILLA-IBARZ, J. 2012. Immunomodulatory drugs and active immunotherapy for chronic lymphocytic leukemia. *Cancer Control,* 19**,** 54-67.

CASADEVALL, A. & JANDA, A. 2012. Immunoglobulin isotype influences affinity and specificity. *Proc Natl Acad Sci U S A,* 109**,** 12272-3.

CASCINU, S., FALCONI, M., VALENTINI, V., JELIC, S. & GROUP, E. G. W. 2010. Pancreatic cancer: ESMO Clinical Practice Guidelines for diagnosis, treatment and follow-up. *Ann Oncol,* 21 Suppl 5**,** v55-8.

CERVANTES-GOMEZ, F., LAMOTHE, B., WOYACH, J. A., WIERDA, W. G., KEATING, M. J., BALAKRISHNAN, K. & GANDHI, V. 2015. Pharmacological and Protein Profiling Suggests Venetoclax (ABT-199) as Optimal Partner with Ibrutinib in Chronic Lymphocytic Leukemia. *Clin Cancer Res,* 21**,** 3705-15.

CEYHAN, G. O. & FRIESS, H. 2015. Pancreatic disease in 2014: Pancreatic fibrosis and standard diagnostics. *Nat Rev Gastroenterol Hepatol,* 12**,** 68-70.

CHAFFER, C. L., BRUECKMANN, I., SCHEEL, C., KAESTLI, A. J., WIGGINS, P. A., RODRIGUES, L. O., BROOKS, M., REINHARDT, F., SU, Y., POLYAK, K., ARENDT, L. M., KUPERWASSER, C., BIERIE, B. & WEINBERG, R. A. 2011. Normal and neoplastic nonstem cells can spontaneously convert to a stem-like state. *Proc Natl Acad Sci U S A,* 108**,** 7950-5.

CHEN, D. S. & MELLMAN, I. 2013. Oncology meets immunology: the cancer-immunity cycle. *Immunity,* 39**,** 1-10.

CHEN, L. & FLIES, D. B. 2013. Molecular mechanisms of T cell co-stimulation and co-inhibition. *Nat Rev Immunol,* 13**,** 227-42.

CHENEY, C. M., STEPHENS, D. M., MO, X., RAFIQ, S., BUTCHAR, J., FLYNN, J. M., JONES, J. A., MADDOCKS, K., O'REILLY, A., RAMACHANDRAN, A., TRIDANDAPANI, S., MUTHUSAMY, N. & BYRD, J. C. 2014. Ocaratuzumab, an Fc-engineered antibody demonstrates enhanced antibody-dependent cell-mediated cytotoxicity in chronic lymphocytic leukemia. *MAbs,* 6**,** 749-55.

CHEUNG, N. K., GUO, H., HU, J., TASSEV, D. V. & CHEUNG, I. Y. 2012. Humanizing murine IgG3 anti-GD2 antibody m3F8 substantially improves antibody-dependent cell-mediated cytotoxicity while retaining targeting in vivo. *Oncoimmunology,* 1**,** 477-486.

CHIEN, H. P., UENG, S. H., CHEN, S. C., CHANG, Y. S., LIN, Y. C., LO, Y. F., CHANG, H. K., CHUANG, W. Y., HUANG, Y. T., CHEUNG, Y. C., SHEN, S. C. & HSUEH, C. 2016. Expression of ROR1 has prognostic significance in triple negative breast cancer. *Virchows Arch,* 468**,** 589-95.

CHINNASAMY, D., YU, Z., KERKAR, S. P., ZHANG, L., MORGAN, R. A., RESTIFO, N. P. & ROSENBERG, S. A. 2012. Local delivery of

interleukin-12 using T cells targeting VEGF receptor-2 eradicates multiple vascularized tumors in mice. *Clin Cancer Res,* 18**,** 1672-83.

CHIOCCA, E. A. & RABKIN, S. D. 2014. Oncolytic viruses and their application to cancer immunotherapy. *Cancer Immunol Res,* 2**,** 295-300.

CHIORAZZI, N. 2007. Cell proliferation and death: forgotten features of chronic lymphocytic leukemia B cells. *Best Pract Res Clin Haematol,* 20**,** 399-413.

CHIORAZZI, N., RAI, K. R. & FERRARINI, M. 2005. Chronic lymphocytic leukemia. *N Engl J Med,* 352**,** 804-15.

CHMIELEWSKI, M., HOMBACH, A. A. & ABKEN, H. 2014. Of CARs and TRUCKs: chimeric antigen receptor (CAR) T cells engineered with an inducible cytokine to modulate the tumor stroma. *Immunol Rev,* 257**,** 83-90.

CHMIELEWSKI, M., KOPECKY, C., HOMBACH, A. A. & ABKEN, H. 2011. IL-12 release by engineered T cells expressing chimeric antigen receptors can effectively Muster an antigen-independent macrophage response on tumor cells that have shut down tumor antigen expression. *Cancer Res,* 71**,** 5697-706.

CHOI, M. Y., WIDHOPF, G. F., 2ND, WU, C. C., CUI, B., LAO, F., SADARANGANI, A., CAVAGNARO, J., PRUSSAK, C., CARSON, D. A., JAMIESON, C. & KIPPS, T. J. 2015. Pre-clinical Specificity and Safety of UC-961, a First-In-Class Monoclonal Antibody Targeting ROR1. *Clin Lymphoma Myeloma Leuk,* 15 Suppl**,** S167-9.

CHOUDHURY, A., DERKOW, K., DANESHMANESH, A. H., MIKAELSSON, E., KIAII, S., KOKHAEI, P., OSTERBORG, A. & MELLSTEDT, H. 2010. Silencing of ROR1 and FMOD with siRNA results in apoptosis of CLL cells. *Br J Haematol,* 151**,** 327-35.

CHUDASAMA, V., MARUANI, A. & CADDICK, S. 2016. Recent advances in the construction of antibody-drug conjugates. *Nat Chem,* 8**,** 114-9.

CID-ARREGUI, A. & JUAREZ, V. 2015. Perspectives in the treatment of pancreatic adenocarcinoma. *World J Gastroenterol,* 21**,** 9297-316.

CILIBERTO, D., BOTTA, C., CORREALE, P., ROSSI, M., CARAGLIA, M., TASSONE, P. & TAGLIAFERRI, P. 2013. Role of gemcitabine-based combination therapy in the management of advanced pancreatic cancer: a meta-analysis of randomised trials. *Eur J Cancer,* 49**,** 593-603.

CIMMINO, A., CALIN, G. A., FABBRI, M., IORIO, M. V., FERRACIN, M., SHIMIZU, M., WOJCIK, S. E., AQEILAN, R. I., ZUPO, S., DONO, M., RASSENTI, L., ALDER, H., VOLINIA, S., LIU, C. G., KIPPS, T. J., NEGRINI, M. & CROCE, C. M. 2005. miR-15 and miR-16 induce apoptosis by targeting BCL2. *Proc Natl Acad Sci U S A,* 102**,** 13944-9.

CLARK, C. E., HINGORANI, S. R., MICK, R., COMBS, C., TUVESON, D. A. & VONDERHEIDE, R. H. 2007. Dynamics of the immune reaction to pancreatic cancer from inception to invasion. *Cancer Res,* 67**,** 9518-27.

CLARK, M. R. 1997. IgG effector mechanisms. *Chem Immunol,* 65**,** 88-110.

CLARKE, M. F., DICK, J. E., DIRKS, P. B., EAVES, C. J., JAMIESON, C. H., JONES, D. L., VISVADER, J., WEISSMAN, I. L. & WAHL, G. M. 2006. Cancer stem cells--perspectives on current status and future directions: AACR Workshop on cancer stem cells. *Cancer Res,* 66**,** 9339-44.

CLINICALTRIALS.GOV 2017. ClinicalTrials.gov. https://clinicaltrials.gov/ct2/results?cond=&term=ror1&cntry1=&state1=&SearchAll=Search+all+studies&recrs.

CLYNES, R., TAKECHI, Y., MOROI, Y., HOUGHTON, A. & RAVETCH, J. V. 1998. Fc receptors are required in passive and active immunity to melanoma. *Proc Natl Acad Sci U S A,* 95**,** 652-6.

COHEN, C. J., GARTNER, J. J., HOROVITZ-FRIED, M., SHAMALOV, K., TREBSKA-MCGOWAN, K., BLISKOVSKY, V. V., PARKHURST, M. R., ANKRI, C., PRICKETT, T. D., CRYSTAL, J. S., LI, Y. F., EL-GAMIL, M., ROSENBERG, S. A. & ROBBINS, P. F. 2015. Isolation of neoantigen-specific T cells from tumor and peripheral lymphocytes. *J Clin Invest,* 125**,** 3981-91.

COLEY, W. 1893. The treatment of malignant tumors by repeated inoculations of erysipelas: with a report of ten original cases. *Am. J. Med. Sci***,** 487–511.

COLLURA, A., MARISA, L., TROJAN, D., BUHARD, O., LAGRANGE, A., SAGET, A., BOMBLED, M., MECHIGHEL, P., AYADI, M., MULERIS, M., DE REYNIES, A., SVRCEK, M., FLEJOU, J. F., FLORENT, J. C., MAHUTEAU-BETZER, F., FAUSSAT, A. M. & DUVAL, A. 2013. Extensive characterization of sphere models established from colorectal cancer cell lines. *Cell Mol Life Sci,* 70**,** 729-42.

CONNER, S. D. & SCHMID, S. L. 2003. Regulated portals of entry into the cell. *Nature,* 422**,** 37-44.

CONROY, T., DESSEIGNE, F., YCHOU, M., BOUCHE, O., GUIMBAUD, R., BECOUARN, Y., ADENIS, A., RAOUL, J. L., GOURGOU-BOURGADE, S., DE LA FOUCHARDIERE, C., BENNOUNA, J., BACHET, J. B., KHEMISSA-AKOUZ, F., PERE-VERGE, D., DELBALDO, C., ASSENAT, E., CHAUFFERT, B., MICHEL, P., MONTOTO-GRILLOT, C., DUCREUX, M., GROUPE TUMEURS DIGESTIVES OF, U. & INTERGROUP, P. 2011. FOLFIRINOX versus gemcitabine for metastatic pancreatic cancer. *N Engl J Med,* 364**,** 1817-25.

COSTA, J. M. D. 1858. *On the Morbid Anatomy and Symptoms of Cancer of the Pancreas,* Philadelphia, PA, USA JB Lippincott & Company.

COSTELLO, E., GREENHALF, W. & NEOPTOLEMOS, J. P. 2012. New biomarkers and targets in pancreatic cancer and their application to treatment. *Nat Rev Gastroenterol Hepatol,* 9**,** 435-44.

COSTINEAN, S., ZANESI, N., PEKARSKY, Y., TILI, E., VOLINIA, S., HEEREMA, N. & CROCE, C. M. 2006. Pre-B cell proliferation and lymphoblastic leukemia/high-grade lymphoma in E(mu)-miR155 transgenic mice. *Proc Natl Acad Sci U S A,* 103**,** 7024-9.

CUI, B., CHEN, L., ZHANG, S., MRAZ, M., FECTEAU, J. F., YU, J., GHIA, E. M., ZHANG, L., BAO, L., RASSENTI, L. Z., MESSER, K., CALIN, G. A., CROCE, C. M. & KIPPS, T. J. 2014. MicroRNA-155 influences B-cell receptor signaling and associates with aggressive disease in chronic lymphocytic leukemia. *Blood,* 124**,** 546-54.

CUI, B., GHIA, E. M., CHEN, L., RASSENTI, L. Z., DEBOEVER, C., WIDHOPF, G. F., 2ND, YU, J., NEUBERG, D. S., WIERDA, W. G., RAI, K. R., KAY, N. E., BROWN, J. R., JONES, J. A., GRIBBEN, J. G., FRAZER, K. A. & KIPPS, T. J. 2016. High-level ROR1 associates with accelerated disease progression in chronic lymphocytic leukemia. *Blood,* 128**,** 2931-2940.

CUI, B., ZHANG, S., CHEN, L., YU, J., WIDHOPF, G. F., 2ND, FECTEAU, J. F., RASSENTI, L. Z. & KIPPS, T. J. 2013. Targeting ROR1 inhibits epithelial-mesenchymal transition and metastasis. *Cancer Res,* 73**,** 3649-60.

CUI B., W. I. G. F., PRUSSAK C.E., WU C. C. N., SADARANGANI A., ZHANG S., LAO F., JAMIESON C. H. M., CARSON D. A. AND KIPPS T. J. 2015. Cirmtuzumab Vedotin (UC-961ADC3), An Anti-ROR1-Monomethyl Auristatin E Antibody-Drug Conjugate, Is a Potential Treatment For ROR1-Positive Leukemia and Solid Tumors. *55th Annual Meeting and Exposition.*

CURTI, A., RUGGERI, L., D'ADDIO, A., BONTADINI, A., DAN, E., MOTTA, M. R., TRABANELLI, S., GIUDICE, V., URBANI, E., MARTINELLI, G., PAOLINI, S., FRUET, F., ISIDORI, A., PARISI, S., BANDINI, G., BACCARANI, M., VELARDI, A. & LEMOLI, R. M. 2011. Successful transfer of alloreactive haploidentical KIR ligand-mismatched natural killer cells after infusion in elderly high risk acute myeloid leukemia patients. *Blood,* 118**,** 3273-9.

DALL'ACQUA, W. F., DAMSCHRODER, M. M., ZHANG, J., WOODS, R. M., WIDJAJA, L., YU, J. & WU, H. 2005. Antibody humanization by framework shuffling. *Methods,* 36**,** 43-60.

DALLA POZZA, E., DANDO, I., BIONDANI, G., BRANDI, J., COSTANZO, C., ZORATTI, E., FASSAN, M., BOSCHI, F., MELISI, D., CECCONI, D., SCUPOLI, M. T., SCARPA, A. & PALMIERI, M. 2015. Pancreatic ductal adenocarcinoma cell lines display a plastic ability to bidirectionally convert into cancer stem cells. *Int J Oncol,* 46**,** 1099-108.

DAMKE, H., BABA, T., VAN DER BLIEK, A. M. & SCHMID, S. L. 1995. Clathrin-independent pinocytosis is induced in cells overexpressing a temperature-sensitive mutant of dynamin. *J Cell Biol,* 131**,** 69-80.

DAMM, F., MYLONAS, E., COSSON, A., YOSHIDA, K., DELLA VALLE, V., MOULY, E., DIOP, M., SCOURZIC, L., SHIRAISHI, Y., CHIBA, K., TANAKA, H., MIYANO, S., KIKUSHIGE, Y., DAVI, F., LAMBERT, J., GAUTHERET, D., MERLE-BERAL, H., SUTTON, L., DESSEN, P., SOLARY, E., AKASHI, K., VAINCHENKER, W., MERCHER, T., DROIN, N., OGAWA, S., NGUYEN-KHAC, F. & BERNARD, O. A.

2014. Acquired initiating mutations in early hematopoietic cells of CLL patients. *Cancer Discov,* 4**,** 1088-101.

DANESHMANESH, A. H., HOJJAT-FARSANGI, M., KHAN, A. S., JEDDI-TEHRANI, M., AKHONDI, M. M., BAYAT, A. A., GHODS, R., MAHMOUDI, A. R., HADAVI, R., OSTERBORG, A., SHOKRI, F., RABBANI, H. & MELLSTEDT, H. 2012. Monoclonal antibodies against ROR1 induce apoptosis of chronic lymphocytic leukemia (CLL) cells. *Leukemia,* 26**,** 1348-55.

DANESHMANESH, A. H., PORWIT, A., HOJJAT-FARSANGI, M., JEDDI-TEHRANI, M., TAMM, K. P., GRANDER, D., LEHMANN, S., NORIN, S., SHOKRI, F., RABBANI, H., MELLSTEDT, H. & OSTERBORG, A. 2013. Orphan receptor tyrosine kinases ROR1 and ROR2 in hematological malignancies. *Leuk Lymphoma,* 54**,** 843-50.

DAVE, H., ANVER, M. R., BUTCHER, D. O., BROWN, P., KHAN, J., WAYNE, A. S., BASKAR, S. & RADER, C. 2012. Restricted cell surface expression of receptor tyrosine kinase ROR1 in pediatric B-lineage acute lymphoblastic leukemia suggests targetability with therapeutic monoclonal antibodies. *PLoS One,* 7**,** e52655.

DAVIDS, M. S. & BROWN, J. R. 2012. Targeting the B cell receptor pathway in chronic lymphocytic leukemia. *Leuk Lymphoma,* 53**,** 2362-70.

DE JONG, L. A., UGES, D. R., FRANKE, J. P. & BISCHOFF, R. 2005. Receptor-ligand binding assays: technologies and applications. *J Chromatogr B Analyt Technol Biomed Life Sci,* 829**,** 1-25.

DE SOUSA, E. M. F. & VERMEULEN, L. 2016. Wnt Signaling in Cancer Stem Cell Biology. *Cancers (Basel),* 8.

DENIGER, D. C., YU, J., HULS, M. H., FIGLIOLA, M. J., MI, T., MAITI, S. N., WIDHOPF, G. F., 2ND, HURTON, L. V., THOKALA, R., SINGH, H., OLIVARES, S., CHAMPLIN, R. E., WIERDA, W. G., KIPPS, T. J. & COOPER, L. J. 2015. Sleeping Beauty Transposition of Chimeric Antigen Receptors Targeting Receptor Tyrosine Kinase-Like Orphan Receptor-1 (ROR1) into Diverse Memory T-Cell Populations. *PLoS One,* 10**,** e0128151.

DIEBOLDER, C. A., BEURSKENS, F. J., DE JONG, R. N., KONING, R. I., STRUMANE, K., LINDORFER, M. A., VOORHORST, M., UGURLAR, D., ROSATI, S., HECK, A. J., VAN DE WINKEL, J. G., WILSON, I. A., KOSTER, A. J., TAYLOR, R. P., SAPHIRE, E. O., BURTON, D. R., SCHUURMAN, J., GROS, P. & PARREN, P. W. 2014. Complement is activated by IgG hexamers assembled at the cell surface. *Science,* 343**,** 1260-3.

DIGHE, A. S., RICHARDS, E., OLD, L. J. & SCHREIBER, R. D. 1994. Enhanced in vivo growth and resistance to rejection of tumor cells expressing dominant negative IFN gamma receptors. *Immunity,* 1**,** 447-56.

DILILLO, D. J. & RAVETCH, J. V. 2015. Differential Fc-Receptor Engagement Drives an Anti-tumor Vaccinal Effect. *Cell,* 161**,** 1035-45.

DILILLO, D. J., WEINBERG, J. B., YOSHIZAKI, A., HORIKAWA, M., BRYANT, J. M., IWATA, Y., MATSUSHITA, T., MATTA, K. M., CHEN,

Y., VENTURI, G. M., RUSSO, G., GOCKERMAN, J. P., MOORE, J. O., DIEHL, L. F., VOLKHEIMER, A. D., FRIEDMAN, D. R., LANASA, M. C., HALL, R. P. & TEDDER, T. F. 2013. Chronic lymphocytic leukemia and regulatory B cells share IL-10 competence and immunosuppressive function. *Leukemia,* 27**,** 170-82.

DING, W., LAPLANT, B. R., CALL, T. G., PARIKH, S. A., LEIS, J. F., HE, R., SHANAFELT, T. D., SINHA, S., LE-RADEMACHER, J., FELDMAN, A. L., HABERMANN, T. M., WITZIG, T. E., WISEMAN, G. A., LIN, Y., ASMUS, E., NOWAKOWSKI, G. S., CONTE, M. J., BOWEN, D. A., AITKEN, C. N., VAN DYKE, D. L., GREIPP, P. T., LIU, X., WU, X., ZHANG, H., SECRETO, C. R., TIAN, S., BRAGGIO, E., WELLIK, L. E., MICALLEF, I., VISWANATHA, D. S., YAN, H., CHANAN-KHAN, A. A., KAY, N. E., DONG, H. & ANSELL, S. M. 2017. Pembrolizumab in patients with CLL and Richter transformation or with relapsed CLL. *Blood,* 129**,** 3419-3427.

DISTLER, M., AUST, D., WEITZ, J., PILARSKY, C. & GRUTZMANN, R. 2014. Precursor lesions for sporadic pancreatic cancer: PanIN, IPMN, and MCN. *Biomed Res Int,* 2014**,** 474905.

DOHERTY, G. J. & MCMAHON, H. T. 2009. Mechanisms of endocytosis. *Annu Rev Biochem,* 78**,** 857-902.

DOHNER, H., STILGENBAUER, S., BENNER, A., LEUPOLT, E., KROBER, A., BULLINGER, L., DOHNER, K., BENTZ, M. & LICHTER, P. 2000. Genomic aberrations and survival in chronic lymphocytic leukemia. *N Engl J Med,* 343**,** 1910-6.

DOTTI, G., GOTTSCHALK, S., SAVOLDO, B. & BRENNER, M. K. 2014. Design and development of therapies using chimeric antigen receptor-expressing T cells. *Immunol Rev,* 257**,** 107-26.

DUELL, J., DITTRICH, M., BEDKE, T., MUELLER, T., EISELE, F., ROSENWALD, A., RASCHE, L., HARTMANN, E., DANDEKAR, T., EINSELE, H. & TOPP, M. S. 2017. Frequency of regulatory T cells determines the outcome of the T-cell-engaging antibody blinatumomab in patients with B-precursor ALL. *Leukemia,* 31**,** 2181-2190.

DUHREN-VON MINDEN, M., UBELHART, R., SCHNEIDER, D., WOSSNING, T., BACH, M. P., BUCHNER, M., HOFMANN, D., SUROVA, E., FOLLO, M., KOHLER, F., WARDEMANN, H., ZIRLIK, K., VEELKEN, H. & JUMAA, H. 2012. Chronic lymphocytic leukaemia is driven by antigen-independent cell-autonomous signalling. *Nature,* 489**,** 309-12.

DUNN, G. P., BRUCE, A. T., IKEDA, H., OLD, L. J. & SCHREIBER, R. D. 2002. Cancer immunoediting: from immunosurveillance to tumor escape. *Nat Immunol,* 3**,** 991-8.

DUNN, G. P., OLD, L. J. & SCHREIBER, R. D. 2004. The immunobiology of cancer immunosurveillance and immunoediting. *Immunity,* 21**,** 137-48.

DUTTA, D. & DONALDSON, J. G. 2012. Search for inhibitors of endocytosis: Intended specificity and unintended consequences. *Cell Logist,* 2**,** 203-208.

DVORAK, H. F. 1986. Tumors: wounds that do not heal. Similarities between tumor stroma generation and wound healing. *N Engl J Med,* 315**,** 1650-9.

EHRLICH, P. 1909. Über den jetzigen stand der karzinomforschung. *Tijdschr. Geneeskd***,** 273–290.

EMENS, L. A. & JAFFEE, E. M. 2005. Leveraging the activity of tumor vaccines with cytotoxic chemotherapy. *Cancer Res,* 65**,** 8059-64.

EMOLE, J. N., LOCKE, F. L. & PINILLA-IBARZ, J. 2015. An update on current and prospective immunotherapies for chronic lymphocytic leukemia. *Immunotherapy,* 7**,** 455-66.

ENDO, T., NISHIO, M., ENZLER, T., COTTAM, H. B., FUKUDA, T., JAMES, D. F., KARIN, M. & KIPPS, T. J. 2007. BAFF and APRIL support chronic lymphocytic leukemia B-cell survival through activation of the canonical NF-kappaB pathway. *Blood,* 109**,** 703-10.

ENE-OBONG, A., CLEAR, A. J., WATT, J., WANG, J., FATAH, R., RICHES, J. C., MARSHALL, J. F., CHIN-ALEONG, J., CHELALA, C., GRIBBEN, J. G., RAMSAY, A. G. & KOCHER, H. M. 2013. Activated pancreatic stellate cells sequester CD8+ T cells to reduce their infiltration of the juxtatumoral compartment of pancreatic ductal adenocarcinoma. *Gastroenterology,* 145**,** 1121-32.

ERCAN, G., KARLITEPE, A. & OZPOLAT, B. 2017. Pancreatic Cancer Stem Cells and Therapeutic Approaches. *Anticancer Res,* 37**,** 2761-2775.

FABBRI, M., BOTTONI, A., SHIMIZU, M., SPIZZO, R., NICOLOSO, M. S., ROSSI, S., BARBAROTTO, E., CIMMINO, A., ADAIR, B., WOJCIK, S. E., VALERI, N., CALORE, F., SAMPATH, D., FANINI, F., VANNINI, I., MUSURACA, G., DELL'AQUILA, M., ALDER, H., DAVULURI, R. V., RASSENTI, L. Z., NEGRINI, M., NAKAMURA, T., AMADORI, D., KAY, N. E., RAI, K. R., KEATING, M. J., KIPPS, T. J., CALIN, G. A. & CROCE, C. M. 2011. Association of a microRNA/TP53 feedback circuitry with pathogenesis and outcome of B-cell chronic lymphocytic leukemia. *JAMA,* 305**,** 59-67.

FAN, G., WANG, Z., HAO, M. & LI, J. 2015. Bispecific antibodies and their applications. *J Hematol Oncol,* 8**,** 130.

FARIS, J. E., BLASZKOWSKY, L. S., MCDERMOTT, S., GUIMARAES, A. R., SZYMONIFKA, J., HUYNH, M. A., FERRONE, C. R., WARGO, J. A., ALLEN, J. N., DIAS, L. E., KWAK, E. L., LILLEMOE, K. D., THAYER, S. P., MURPHY, J. E., ZHU, A. X., SAHANI, D. V., WO, J. Y., CLARK, J. W., FERNANDEZ-DEL CASTILLO, C., RYAN, D. P. & HONG, T. S. 2013. FOLFIRINOX in locally advanced pancreatic cancer: the Massachusetts General Hospital Cancer Center experience. *Oncologist,* 18**,** 543-8.

FARKONA, S., DIAMANDIS, E. P. & BLASUTIG, I. M. 2016. Cancer immunotherapy: the beginning of the end of cancer? *BMC Med,* 14**,** 73.

FEIG, C., JONES, J. O., KRAMAN, M., WELLS, R. J., DEONARINE, A., CHAN, D. S., CONNELL, C. M., ROBERTS, E. W., ZHAO, Q., CABALLERO, O. L., TEICHMANN, S. A., JANOWITZ, T., JODRELL,

D. I., TUVESON, D. A. & FEARON, D. T. 2013. Targeting CXCL12 from FAP-expressing carcinoma-associated fibroblasts synergizes with anti-PD-L1 immunotherapy in pancreatic cancer. *Proc Natl Acad Sci U S A,* 110**,** 20212-7.

FIDLER, I. J. & HART, I. R. 1982. Biological diversity in metastatic neoplasms: origins and implications. *Science,* 217**,** 998-1003.

FITZGERALD, T. L. & MCCUBREY, J. A. 2014. Pancreatic cancer stem cells: association with cell surface markers, prognosis, resistance, metastasis and treatment. *Adv Biol Regul,* 56**,** 45-50.

FLAMAND, V., SORNASSE, T., THIELEMANS, K., DEMANET, C., BAKKUS, M., BAZIN, H., TIELEMANS, F., LEO, O., URBAIN, J. & MOSER, M. 1994. Murine dendritic cells pulsed in vitro with tumor antigen induce tumor resistance in vivo. *Eur J Immunol,* 24**,** 605-10.

FREEMAN, S. A., GOYETTE, J., FURUYA, W., WOODS, E. C., BERTOZZI, C. R., BERGMEIER, W., HINZ, B., VAN DER MERWE, P. A., DAS, R. & GRINSTEIN, S. 2016. Integrins Form an Expanding Diffusional Barrier that Coordinates Phagocytosis. *Cell,* 164**,** 128-40.

FRIEDBERG, J. W., SHARMAN, J., SWEETENHAM, J., JOHNSTON, P. B., VOSE, J. M., LACASCE, A., SCHAEFER-CUTILLO, J., DE VOS, S., SINHA, R., LEONARD, J. P., CRIPE, L. D., GREGORY, S. A., STERBA, M. P., LOWE, A. M., LEVY, R. & SHIPP, M. A. 2010. Inhibition of Syk with fostamatinib disodium has significant clinical activity in non-Hodgkin lymphoma and chronic lymphocytic leukemia. *Blood,* 115**,** 2578-85.

FROHMAN, M. A. 1993. Rapid amplification of complementary DNA ends for generation of full-length complementary DNAs: thermal RACE. *Methods Enzymol,* 218**,** 340-56.

FUKUDA, T., CHEN, L., ENDO, T., TANG, L., LU, D., CASTRO, J. E., WIDHOPF, G. F., 2ND, RASSENTI, L. Z., CANTWELL, M. J., PRUSSAK, C. E., CARSON, D. A. & KIPPS, T. J. 2008. Antisera induced by infusions of autologous Ad-CD154-leukemia B cells identify ROR1 as an oncofetal antigen and receptor for Wnt5a. *Proc Natl Acad Sci U S A,* 105**,** 3047-52.

FURMAN, R. R., SHARMAN, J. P., COUTRE, S. E., CHESON, B. D., PAGEL, J. M., HILLMEN, P., BARRIENTOS, J. C., ZELENETZ, A. D., KIPPS, T. J., FLINN, I., GHIA, P., ERADAT, H., ERVIN, T., LAMANNA, N., COIFFIER, B., PETTITT, A. R., MA, S., STILGENBAUER, S., CRAMER, P., AIELLO, M., JOHNSON, D. M., MILLER, L. L., LI, D., JAHN, T. M., DANSEY, R. D., HALLEK, M. & O'BRIEN, S. M. 2014. Idelalisib and rituximab in relapsed chronic lymphocytic leukemia. *N Engl J Med,* 370**,** 997-1007.

GABRILOVICH, D. 2004. Mechanisms and functional significance of tumour-induced dendritic-cell defects. *Nat Rev Immunol,* 4**,** 941-52.

GALON, J., COSTES, A., SANCHEZ-CABO, F., KIRILOVSKY, A., MLECNIK, B., LAGORCE-PAGES, C., TOSOLINI, M., CAMUS, M., BERGER, A., WIND, P., ZINZINDOHOUE, F., BRUNEVAL, P., CUGNENC, P. H., TRAJANOSKI, Z., FRIDMAN, W. H. & PAGES, F.

2006. Type, density, and location of immune cells within human colorectal tumors predict clinical outcome. *Science,* 313**,** 1960-4.
GARIKAPATI, K. R., PATEL, N., MAKANI, V. K., CILAMKOTI, P., BHADRA, U. & BHADRA, M. P. 2017. Down-regulation of BORIS/CTCFL efficiently regulates cancer stemness and metastasis in MYCN amplified neuroblastoma cell line by modulating Wnt/beta-catenin signaling pathway. *Biochem Biophys Res Commun,* 484**,** 93-99.
GASCH, C., FFRENCH, B., O'LEARY, J. J. & GALLAGHER, M. F. 2017. Catching moving targets: cancer stem cell hierarchies, therapy-resistance & considerations for clinical intervention. *Mol Cancer,* 16**,** 43.
GATTINONI, L., FINKELSTEIN, S. E., KLEBANOFF, C. A., ANTONY, P. A., PALMER, D. C., SPIESS, P. J., HWANG, L. N., YU, Z., WRZESINSKI, C., HEIMANN, D. M., SURH, C. D., ROSENBERG, S. A. & RESTIFO, N. P. 2005. Removal of homeostatic cytokine sinks by lymphodepletion enhances the efficacy of adoptively transferred tumor-specific CD8+ T cells. *J Exp Med,* 202**,** 907-12.
GAVIRAGHI, M., TUNICI, P., VALENSIN, S., ROSSI, M., GIORDANO, C., MAGNONI, L., DANDREA, M., MONTAGNA, L., RITELLI, R., SCARPA, A. & BAKKER, A. 2011. Pancreatic cancer spheres are more than just aggregates of stem marker-positive cells. *Biosci Rep,* 31**,** 45-55.
GENTILE, A., LAZZARI, L., BENVENUTI, S., TRUSOLINO, L. & COMOGLIO, P. M. 2011. Ror1 is a pseudokinase that is crucial for Met-driven tumorigenesis. *Cancer Res,* 71**,** 3132-41.
GENTILE, A., LAZZARI, L., BENVENUTI, S., TRUSOLINO, L. & COMOGLIO, P. M. 2014. The ROR1 pseudokinase diversifies signaling outputs in MET-addicted cancer cells. *Int J Cancer,* 135**,** 2305-16.
GERSHONI, J. M., ROITBURD-BERMAN, A., SIMAN-TOV, D. D., TARNOVITSKI FREUND, N. & WEISS, Y. 2007. Epitope mapping: the first step in developing epitope-based vaccines. *BioDrugs,* 21**,** 145-56.
GEUKES FOPPEN, M. H., DONIA, M., SVANE, I. M. & HAANEN, J. B. 2015. Tumor-infiltrating lymphocytes for the treatment of metastatic cancer. *Mol Oncol,* 9**,** 1918-35.
GIBSON, A. E., NOEL, R. J., HERLIHY, J. T. & WARD, W. F. 1989. Phenylarsine oxide inhibition of endocytosis: effects on asialofetuin internalization. *Am J Physiol,* 257**,** C182-4.
GILHAM, D. E., ANDERSON, J., BRIDGEMAN, J. S., HAWKINS, R. E., EXLEY, M. A., STAUSS, H., MAHER, J., PULE, M., SEWELL, A. K., BENDLE, G., LEE, S., QASIM, W., THRASHER, A. & MORRIS, E. 2015. Adoptive T-cell therapy for cancer in the United kingdom: a review of activity for the British Society of Gene and Cell Therapy annual meeting 2015. *Hum Gene Ther,* 26**,** 276-85.
GIUSTACCHINI, A., THONGJUEA, S., BARKAS, N., WOLL, P. S., POVINELLI, B. J., BOOTH, C. A. G., SOPP, P., NORFO, R., RODRIGUEZ-MEIRA, A., ASHLEY, N., JAMIESON, L., VYAS, P.,

ANDERSON, K., SEGERSTOLPE, A., QIAN, H., OLSSON-STROMBERG, U., MUSTJOKI, S., SANDBERG, R., JACOBSEN, S. E. W. & MEAD, A. J. 2017. Single-cell transcriptomics uncovers distinct molecular signatures of stem cells in chronic myeloid leukemia. *Nat Med,* 23**,** 692-702.

GLENNIE, M. J., FRENCH, R. R., CRAGG, M. S. & TAYLOR, R. P. 2007. Mechanisms of killing by anti-CD20 monoclonal antibodies. *Mol Immunol,* 44**,** 3823-37.

GOEDE, V., FISCHER, K., ENGELKE, A., SCHLAG, R., LEPRETRE, S., MONTERO, L. F., MONTILLO, M., FEGAN, C., ASIKANIUS, E., HUMPHREY, K., FINGERLE-ROWSON, G. & HALLEK, M. 2015. Obinutuzumab as frontline treatment of chronic lymphocytic leukemia: updated results of the CLL11 study. *Leukemia,* 29**,** 1602-4.

GOH, P. A., CAXARIA, S., CASPER, C., ROSALES, C., WARNER, T. T., COFFEY, P. J. & NATHWANI, A. C. 2013. A systematic evaluation of integration free reprogramming methods for deriving clinically relevant patient specific induced pluripotent stem (iPS) cells. *PLoS One,* 8**,** e81622.

GOHIL, S. H., PAREDES-MOSCOSSO, S. R., HARRASSER, M., VEZZALINI, M., SCARPA, A., MORRIS, E., DAVIDOFF, A. M., SORIO, C., NATHWANI, A. C. & DELLA PERUTA, M. 2017. An ROR1 bi-specific T-cell engager provides effective targeting and cytotoxicity against a range of solid tumors. *Oncoimmunology,* 6**,** e1326437.

GOLAY, J., CITTERA, E., DI GAETANO, N., MANGANINI, M., MOSCA, M., NEBULONI, M., VAN ROOIJEN, N., VAGO, L. & INTRONA, M. 2006. The role of complement in the therapeutic activity of rituximab in a murine B lymphoma model homing in lymph nodes. *Haematologica,* 91**,** 176-83.

GOLAY, J., LAZZARI, M., FACCHINETTI, V., BERNASCONI, S., BORLERI, G., BARBUI, T., RAMBALDI, A. & INTRONA, M. 2001. CD20 levels determine the in vitro susceptibility to rituximab and complement of B-cell chronic lymphocytic leukemia: further regulation by CD55 and CD59. *Blood,* 98**,** 3383-9.

GOODMAN, M. D. & SAIF, M. W. 2014. Adjuvant therapy for pancreatic cancer. *JOP,* 15**,** 87-90.

GREEN, J. L., KUNTZ, S. G. & STERNBERG, P. W. 2008. Ror receptor tyrosine kinases: orphans no more. *Trends Cell Biol,* 18**,** 536-44.

GROS, A., ROBBINS, P. F., YAO, X., LI, Y. F., TURCOTTE, S., TRAN, E., WUNDERLICH, J. R., MIXON, A., FARID, S., DUDLEY, M. E., HANADA, K., ALMEIDA, J. R., DARKO, S., DOUEK, D. C., YANG, J. C. & ROSENBERG, S. A. 2014. PD-1 identifies the patient-specific CD8(+) tumor-reactive repertoire infiltrating human tumors. *J Clin Invest,* 124**,** 2246-59.

GUO, X., ZHENG, H., LUO, W., ZHANG, Q., LIU, J. & YAO, K. 2017. 5T4-specific chimeric antigen receptor modification promotes the immune efficacy of cytokine-induced killer cells against nasopharyngeal carcinoma stem cell-like cells. *Sci Rep,* 7**,** 4859.

HA, K. D., BIDLINGMAIER, S. M. & LIU, B. 2016. Macropinocytosis Exploitation by Cancers and Cancer Therapeutics. *Front Physiol,* 7**,** 381.

HAAS, C., KRINNER, E., BRISCHWEIN, K., HOFFMANN, P., LUTTERBUSE, R., SCHLERETH, B., KUFER, P. & BAEUERLE, P. A. 2009. Mode of cytotoxic action of T cell-engaging BiTE antibody MT110. *Immunobiology,* 214**,** 441-53.

HAHNEFELD, C., DREWIANKA, S. & HERBERG, F. W. 2004. Determination of kinetic data using surface plasmon resonance biosensors. *Methods Mol Med,* 94**,** 299-320.

HALLEK, M. 2013. Signaling the end of chronic lymphocytic leukemia: new frontline treatment strategies. *Hematology Am Soc Hematol Educ Program,* 2013**,** 138-50.

HALLEK, M., FISCHER, K., FINGERLE-ROWSON, G., FINK, A. M., BUSCH, R., MAYER, J., HENSEL, M., HOPFINGER, G., HESS, G., VON GRUNHAGEN, U., BERGMANN, M., CATALANO, J., ZINZANI, P. L., CALIGARIS-CAPPIO, F., SEYMOUR, J. F., BERREBI, A., JAGER, U., CAZIN, B., TRNENY, M., WESTERMANN, A., WENDTNER, C. M., EICHHORST, B. F., STAIB, P., BUHLER, A., WINKLER, D., ZENZ, T., BOTTCHER, S., RITGEN, M., MENDILA, M., KNEBA, M., DOHNER, H., STILGENBAUER, S., INTERNATIONAL GROUP OF, I. & GERMAN CHRONIC LYMPHOCYTIC LEUKAEMIA STUDY, G. 2010. Addition of rituximab to fludarabine and cyclophosphamide in patients with chronic lymphocytic leukaemia: a randomised, open-label, phase 3 trial. *Lancet,* 376**,** 1164-74.

HAMBLETT, K. J., LE, T., ROCK, B. M., ROCK, D. A., SIU, S., HUARD, J. N., CONNER, K. P., MILBURN, R. R., O'NEILL, J. W., TOMETSKO, M. E. & FANSLOW, W. C. 2016. Altering Antibody-Drug Conjugate Binding to the Neonatal Fc Receptor Impacts Efficacy and Tolerability. *Mol Pharm,* 13**,** 2387-96.

HANAHAN, D. & WEINBERG, R. A. 2000. The hallmarks of cancer. *Cell,* 100**,** 57-70.

HANAHAN, D. & WEINBERG, R. A. 2011. Hallmarks of cancer: the next generation. *Cell,* 144**,** 646-74.

HANSFORD, L. M., MCKEE, A. E., ZHANG, L., GEORGE, R. E., GERSTLE, J. T., THORNER, P. S., SMITH, K. M., LOOK, A. T., YEGER, H., MILLER, F. D., IRWIN, M. S., THIELE, C. J. & KAPLAN, D. R. 2007. Neuroblastoma cells isolated from bone marrow metastases contain a naturally enriched tumor-initiating cell. *Cancer Res,* 67**,** 11234-43.

HEINEMANN, V., HAAS, M. & BOECK, S. 2013. Neoadjuvant treatment of borderline resectable and non-resectable pancreatic cancer. *Ann Oncol,* 24**,** 2484-92.

HELDIN, C. H., RUBIN, K., PIETRAS, K. & OSTMAN, A. 2004. High interstitial fluid pressure - an obstacle in cancer therapy. *Nat Rev Cancer,* 4**,** 806-13.

HENRY, C. E., EMMANUEL, C., LAMBIE, N., LOO, C., KAN, B., KENNEDY, C. J., DE FAZIO, A., HACKER, N. F. & FORD, C. E. 2017. Distinct

Patterns of Stromal and Tumor Expression of ROR1 and ROR2 in Histological Subtypes of Epithelial Ovarian Cancer. *Transl Oncol,* 10**,** 346-356.

HENRY, C. E., LLAMOSAS, E., DJORDJEVIC, A., HACKER, N. F. & FORD, C. E. 2016. Migration and invasion is inhibited by silencing ROR1 and ROR2 in chemoresistant ovarian cancer. *Oncogenesis,* 5**,** e226.

HERISHANU, Y., PEREZ-GALAN, P., LIU, D., BIANCOTTO, A., PITTALUGA, S., VIRE, B., GIBELLINI, F., NJUGUNA, N., LEE, E., STENNETT, L., RAGHAVACHARI, N., LIU, P., MCCOY, J. P., RAFFELD, M., STETLER-STEVENSON, M., YUAN, C., SHERRY, R., ARTHUR, D. C., MARIC, I., WHITE, T., MARTI, G. E., MUNSON, P., WILSON, W. H. & WIESTNER, A. 2011. The lymph node microenvironment promotes B-cell receptor signaling, NF-kappaB activation, and tumor proliferation in chronic lymphocytic leukemia. *Blood,* 117**,** 563-74.

HERMAN, S. E., GORDON, A. L., HERTLEIN, E., RAMANUNNI, A., ZHANG, X., JAGLOWSKI, S., FLYNN, J., JONES, J., BLUM, K. A., BUGGY, J. J., HAMDY, A., JOHNSON, A. J. & BYRD, J. C. 2011. Bruton tyrosine kinase represents a promising therapeutic target for treatment of chronic lymphocytic leukemia and is effectively targeted by PCI-32765. *Blood,* 117**,** 6287-96.

HERMANN, P. C., HUBER, S. L., HERRLER, T., AICHER, A., ELLWART, J. W., GUBA, M., BRUNS, C. J. & HEESCHEN, C. 2007. Distinct populations of cancer stem cells determine tumor growth and metastatic activity in human pancreatic cancer. *Cell Stem Cell,* 1**,** 313-23.

HERTER, S., BIRK, M. C., KLEIN, C., GERDES, C., UMANA, P. & BACAC, M. 2014. Glycoengineering of therapeutic antibodies enhances monocyte/macrophage-mediated phagocytosis and cytotoxicity. *J Immunol,* 192**,** 2252-60.

HERTER, S., HERTING, F., MUNDIGL, O., WALDHAUER, I., WEINZIERL, T., FAUTI, T., MUTH, G., ZIEGLER-LANDESBERGER, D., VAN PUIJENBROEK, E., LANG, S., DUONG, M. N., RESLAN, L., GERDES, C. A., FRIESS, T., BAER, U., BURTSCHER, H., WEIDNER, M., DUMONTET, C., UMANA, P., NIEDERFELLNER, G., BACAC, M. & KLEIN, C. 2013. Preclinical activity of the type II CD20 antibody GA101 (obinutuzumab) compared with rituximab and ofatumumab in vitro and in xenograft models. *Mol Cancer Ther,* 12**,** 2031-42.

HEZEL, A. F., KIMMELMAN, A. C., STANGER, B. Z., BARDEESY, N. & DEPINHO, R. A. 2006. Genetics and biology of pancreatic ductal adenocarcinoma. *Genes Dev,* 20**,** 1218-49.

HINRICHS, C. S. & ROSENBERG, S. A. 2014. Exploiting the curative potential of adoptive T-cell therapy for cancer. *Immunol Rev,* 257**,** 56-71.

HODI, F. S., O'DAY, S. J., MCDERMOTT, D. F., WEBER, R. W., SOSMAN, J. A., HAANEN, J. B., GONZALEZ, R., ROBERT, C.,

SCHADENDORF, D., HASSEL, J. C., AKERLEY, W., VAN DEN EERTWEGH, A. J., LUTZKY, J., LORIGAN, P., VAUBEL, J. M., LINETTE, G. P., HOGG, D., OTTENSMEIER, C. H., LEBBE, C., PESCHEL, C., QUIRT, I., CLARK, J. I., WOLCHOK, J. D., WEBER, J. S., TIAN, J., YELLIN, M. J., NICHOL, G. M., HOOS, A. & URBA, W. J. 2010. Improved survival with ipilimumab in patients with metastatic melanoma. *N Engl J Med,* 363**,** 711-23.

HOFFMANN, P., HOFMEISTER, R., BRISCHWEIN, K., BRANDL, C., CROMMER, S., BARGOU, R., ITIN, C., PRANG, N. & BAEUERLE, P. A. 2005. Serial killing of tumor cells by cytotoxic T cells redirected with a CD19-/CD3-bispecific single-chain antibody construct. *Int J Cancer,* 115**,** 98-104.

HOJJAT-FARSANGI, M., JEDDI-TEHRANI, M., DANESHMANESH, A. H., MOZAFFARI, F., MOSHFEGH, A., HANSSON, L., RAZAVI, S. M., SHARIFIAN, R. A., RABBANI, H., OSTERBORG, A., MELLSTEDT, H. & SHOKRI, F. 2015. Spontaneous Immunity Against the Receptor Tyrosine Kinase ROR1 in Patients with Chronic Lymphocytic Leukemia. *PLoS One,* 10**,** e0142310.

HONIGBERG, L. A., SMITH, A. M., SIRISAWAD, M., VERNER, E., LOURY, D., CHANG, B., LI, S., PAN, Z., THAMM, D. H., MILLER, R. A. & BUGGY, J. J. 2010. The Bruton tyrosine kinase inhibitor PCI-32765 blocks B-cell activation and is efficacious in models of autoimmune disease and B-cell malignancy. *Proc Natl Acad Sci U S A,* 107**,** 13075-80.

HRUBAN, R. H., TAKAORI, K., KLIMSTRA, D. S., ADSAY, N. V., ALBORES-SAAVEDRA, J., BIANKIN, A. V., BIANKIN, S. A., COMPTON, C., FUKUSHIMA, N., FURUKAWA, T., GOGGINS, M., KATO, Y., KLOPPEL, G., LONGNECKER, D. S., LUTTGES, J., MAITRA, A., OFFERHAUS, G. J., SHIMIZU, M. & YONEZAWA, S. 2004. An illustrated consensus on the classification of pancreatic intraepithelial neoplasia and intraductal papillary mucinous neoplasms. *Am J Surg Pathol,* 28**,** 977-87.

HRUBAN, R. H. P., MARTHA BISHOP; KLIMSTRA, DAVID S. 2007. Tumors of the pancreas. *AFIP Atlas of Tumor Pathology Fourth Series, Fascicle 6.* Washington, DC: American Registry of Pathology/Armed Forces Institute of Pathology.

HSU, P. J., WU, F. J., KUDO, M., HSIAO, C. L., HSUEH, A. J. & LUO, C. W. 2014. A naturally occurring Lgr4 splice variant encodes a soluble antagonist useful for demonstrating the gonadal roles of Lgr4 in mammals. *PLoS One,* 9**,** e106804.

HU, J. C., COFFIN, R. S., DAVIS, C. J., GRAHAM, N. J., GROVES, N., GUEST, P. J., HARRINGTON, K. J., JAMES, N. D., LOVE, C. A., MCNEISH, I., MEDLEY, L. C., MICHAEL, A., NUTTING, C. M., PANDHA, H. S., SHORROCK, C. A., SIMPSON, J., STEINER, J., STEVEN, N. M., WRIGHT, D. & COOMBES, R. C. 2006. A phase I study of OncoVEXGM-CSF, a second-generation oncolytic herpes

simplex virus expressing granulocyte macrophage colony-stimulating factor. *Clin Cancer Res,* 12**,** 6737-47.

HUANG, J., FAN, X., WANG, X., LU, Y., ZHU, H., WANG, W., ZHANG, S. & WANG, Z. 2015. High ROR2 expression in tumor cells and stroma is correlated with poor prognosis in pancreatic ductal adenocarcinoma. *Sci Rep,* 5**,** 12991.

HUDECEK, M., LUPO-STANGHELLINI, M. T., KOSASIH, P. L., SOMMERMEYER, D., JENSEN, M. C., RADER, C. & RIDDELL, S. R. 2013. Receptor affinity and extracellular domain modifications affect tumor recognition by ROR1-specific chimeric antigen receptor T cells. *Clin Cancer Res,* 19**,** 3153-64.

HUDECEK, M., SCHMITT, T. M., BASKAR, S., LUPO-STANGHELLINI, M. T., NISHIDA, T., YAMAMOTO, T. N., BLEAKLEY, M., TURTLE, C. J., CHANG, W. C., GREISMAN, H. A., WOOD, B., MALONEY, D. G., JENSEN, M. C., RADER, C. & RIDDELL, S. R. 2010. The B-cell tumor-associated antigen ROR1 can be targeted with T cells modified to express a ROR1-specific chimeric antigen receptor. *Blood,* 116**,** 4532-41.

HUSSEIN, D., PUNJARUK, W., STORER, L. C., SHAW, L., OTHMAN, R., PEET, A., MILLER, S., BANDOPADHYAY, G., HEATH, R., KUMARI, R., BOWMAN, K. J., BRAKER, P., RAHMAN, R., JONES, G. D., WATSON, S., LOWE, J., KERR, I. D., GRUNDY, R. G. & COYLE, B. 2011. Pediatric brain tumor cancer stem cells: cell cycle dynamics, DNA repair, and etoposide extrusion. *Neuro Oncol,* 13**,** 70-83.

HWANG, W. Y. & FOOTE, J. 2005. Immunogenicity of engineered antibodies. *Methods,* 36**,** 3-10.

IMANI FOOLADI, A. A., MAHMOODZADEH HOSSEINI, H. & AMANI, J. 2015. An In silico Chimeric Vaccine Targeting Breast Cancer Containing Inherent Adjuvant. *Iran J Cancer Prev,* 8**,** e2326.

JACOBETZ, M. A., CHAN, D. S., NEESSE, A., BAPIRO, T. E., COOK, N., FRESE, K. K., FEIG, C., NAKAGAWA, T., CALDWELL, M. E., ZECCHINI, H. I., LOLKEMA, M. P., JIANG, P., KULTTI, A., THOMPSON, C. B., MANEVAL, D. C., JODRELL, D. I., FROST, G. I., SHEPARD, H. M., SKEPPER, J. N. & TUVESON, D. A. 2013. Hyaluronan impairs vascular function and drug delivery in a mouse model of pancreatic cancer. *Gut,* 62**,** 112-20.

JANDA, A., BOWEN, A., GREENSPAN, N. S. & CASADEVALL, A. 2016. Ig Constant Region Effects on Variable Region Structure and Function. *Front Microbiol,* 7**,** 22.

JANOVSKA, P. & BRYJA, V. 2017. WNT signaling pathways in chronic lymphocytic leukemia and B cell lymphomas. *Br J Pharmacol*.

JANOVSKA, P., POPPOVA, L., PLEVOVA, K., PLESINGEROVA, H., BEHAL, M., KAUCKA, M., OVESNA, P., HLOZKOVA, M., BORSKY, M., STEHLIKOVA, O., BRYCHTOVA, Y., DOUBEK, M., MACHALOVA, M., BASKAR, S., KOZUBIK, A., POSPISILOVA, S., PAVLOVA, S. & BRYJA, V. 2015. Autocrine signaling by Wnt-5a

deregulates chemotaxis of leukemic cells and predicts clinical outcome in chronic lymphocytic leukemia. *Clin Cancer Res*.

JASON-MOLLER, L., MURPHY, M. & BRUNO, J. 2006. Overview of Biacore systems and their applications. *Curr Protoc Protein Sci,* Chapter 19**,** Unit 19 13.

JAVLE, M. M., SHROFF, R. T., XIONG, H., VARADHACHARY, G. A., FOGELMAN, D., REDDY, S. A., DAVIS, D., ZHANG, Y., WOLFF, R. A. & ABBRUZZESE, J. L. 2010. Inhibition of the mammalian target of rapamycin (mTOR) in advanced pancreatic cancer: results of two phase II studies. *BMC Cancer,* 10**,** 368.

JEFFERIS, R., LUND, J. & POUND, J. D. 1998. IgG-Fc-mediated effector functions: molecular definition of interaction sites for effector ligands and the role of glycosylation. *Immunol Rev,* 163**,** 59-76.

JEFFERIS, R., REIMER, C. B., SKVARIL, F., DE LANGE, G., LING, N. R., LOWE, J., WALKER, M. R., PHILLIPS, D. J., ALOISIO, C. H., WELLS, T. W. & ET AL. 1985. Evaluation of monoclonal antibodies having specificity for human IgG sub-classes: results of an IUIS/WHO collaborative study. *Immunol Lett,* 10**,** 223-52.

JENSEN, M. C. & RIDDELL, S. R. 2014. Design and implementation of adoptive therapy with chimeric antigen receptor-modified T cells. *Immunol Rev,* 257**,** 127-44.

JOHNSON, D. B., PUZANOV, I. & KELLEY, M. C. 2015. Talimogene laherparepvec (T-VEC) for the treatment of advanced melanoma. *Immunotherapy,* 7**,** 611-9.

JONES, P. T., DEAR, P. H., FOOTE, J., NEUBERGER, M. S. & WINTER, G. 1986. Replacing the complementarity-determining regions in a human antibody with those from a mouse. *Nature,* 321**,** 522-5.

JONES, S., ZHANG, X., PARSONS, D. W., LIN, J. C., LEARY, R. J., ANGENENDT, P., MANKOO, P., CARTER, H., KAMIYAMA, H., JIMENO, A., HONG, S. M., FU, B., LIN, M. T., CALHOUN, E. S., KAMIYAMA, M., WALTER, K., NIKOLSKAYA, T., NIKOLSKY, Y., HARTIGAN, J., SMITH, D. R., HIDALGO, M., LEACH, S. D., KLEIN, A. P., JAFFEE, E. M., GOGGINS, M., MAITRA, A., IACOBUZIO-DONAHUE, C., ESHLEMAN, J. R., KERN, S. E., HRUBAN, R. H., KARCHIN, R., PAPADOPOULOS, N., PARMIGIANI, G., VOGELSTEIN, B., VELCULESCU, V. E. & KINZLER, K. W. 2008. Core signaling pathways in human pancreatic cancers revealed by global genomic analyses. *Science,* 321**,** 1801-6.

JUNG, E. H., LEE, H. N., HAN, G. Y., KIM, M. J. & KIM, C. W. 2016. Targeting ROR1 inhibits the self-renewal and invasive ability of glioblastoma stem cells. *Cell Biochem Funct,* 34**,** 149-57.

KALOS, M., LEVINE, B. L., PORTER, D. L., KATZ, S., GRUPP, S. A., BAGG, A. & JUNE, C. H. 2011. T cells with chimeric antigen receptors have potent antitumor effects and can establish memory in patients with advanced leukemia. *Sci Transl Med,* 3**,** 95ra73.

KANTOFF, P. W., HIGANO, C. S., SHORE, N. D., BERGER, E. R., SMALL, E. J., PENSON, D. F., REDFERN, C. H., FERRARI, A. C., DREICER,

R., SIMS, R. B., XU, Y., FROHLICH, M. W., SCHELLHAMMER, P. F. & INVESTIGATORS, I. S. 2010. Sipuleucel-T immunotherapy for castration-resistant prostate cancer. *N Engl J Med,* 363**,** 411-22.

KATZ, M. H., PISTERS, P. W., EVANS, D. B., SUN, C. C., LEE, J. E., FLEMING, J. B., VAUTHEY, J. N., ABDALLA, E. K., CRANE, C. H., WOLFF, R. A., VARADHACHARY, G. R. & HWANG, R. F. 2008. Borderline resectable pancreatic cancer: the importance of this emerging stage of disease. *J Am Coll Surg,* 206**,** 833-46; discussion 846-8.

KAUCKA, M., PETERSEN, J., JANOVSKA, P., RADASZKIEWICZ, T., SMYCKOVA, L., DAULAT, A. M., BORG, J. P., SCHULTE, G. & BRYJA, V. 2015. Asymmetry of VANGL2 in migrating lymphocytes as a tool to monitor activity of the mammalian WNT/planar cell polarity pathway. *Cell Commun Signal,* 13**,** 2.

KAUCKA, M., PLEVOVA, K., PAVLOVA, S., JANOVSKA, P., MISHRA, A., VERNER, J., PROCHAZKOVA, J., KREJCI, P., KOTASKOVA, J., OVESNA, P., TICHY, B., BRYCHTOVA, Y., DOUBEK, M., KOZUBIK, A., MAYER, J., POSPISILOVA, S. & BRYJA, V. 2013. The planar cell polarity pathway drives pathogenesis of chronic lymphocytic leukemia by the regulation of B-lymphocyte migration. *Cancer Res,* 73**,** 1491-501.

KAUFMAN, H. L., KOHLHAPP, F. J. & ZLOZA, A. 2015. Oncolytic viruses: a new class of immunotherapy drugs. *Nat Rev Drug Discov,* 14**,** 642-62.

KEARNS, J. D., BUKHALID, R., SEVECKA, M., TAN, G., GERAMI-MOAYED, N., WERNER, S. L., KOHLI, N., BURENKOVA, O., SLOSS, C. M., KING, A. M., FITZGERALD, J. B., NIELSEN, U. B. & WOLF, B. B. 2015. Enhanced Targeting of the EGFR Network with MM-151, an Oligoclonal Anti-EGFR Antibody Therapeutic. *Mol Cancer Ther,* 14**,** 1625-36.

KEATING, M. J., O'BRIEN, S., ALBITAR, M., LERNER, S., PLUNKETT, W., GILES, F., ANDREEFF, M., CORTES, J., FADERL, S., THOMAS, D., KOLLER, C., WIERDA, W., DETRY, M. A., LYNN, A. & KANTARJIAN, H. 2005. Early results of a chemoimmunotherapy regimen of fludarabine, cyclophosphamide, and rituximab as initial therapy for chronic lymphocytic leukemia. *J Clin Oncol,* 23**,** 4079-88.

KEBRIAEI, P. H. H., HARJEET SINGH, SIMON OLIVARES, MATTHEW FIGLIOLA, SOURINDRA MAITI, SU SHIHUANG, PAPPANAICKEN R KUMAR, BIPULENDU JENA, MARIE ANDREE FORGET, SONNY ANG, JACKSON RINEKA, TINGTING LIU, IAN K. MCNIECE, GABRIELA RONDON, PERRY HACKETT, WILLIAM G. WIERDA, SUSAN O'BRIEN, MICHAEL J KEATING, HAGOP M. KANTARJIAN, CHITRA M HOSING, ELIZABETH J SHPALL, RICHARD E. CHAMPLIN AND LAURENCE JN COOPER 2014. Adoptive therapy using sleeping beauty gene transfer system and artificial antigen presenting cells to manufacture T cells expressing CD19 specific chimeric antigen receptor. *American Society of Hematology.* Blood.

KEITH, B. & SIMON, M. C. 2007. Hypoxia-inducible factors, stem cells, and cancer. *Cell,* 129**,** 465-72.

KENNEDY, A. D., BEUM, P. V., SOLGA, M. D., DILILLO, D. J., LINDORFER, M. A., HESS, C. E., DENSMORE, J. J., WILLIAMS, M. E. & TAYLOR, R. P. 2004. Rituximab infusion promotes rapid complement depletion and acute CD20 loss in chronic lymphocytic leukemia. *J Immunol,* 172**,** 3280-8.

KERKAR, S. P., GOLDSZMID, R. S., MURANSKI, P., CHINNASAMY, D., YU, Z., REGER, R. N., LEONARDI, A. J., MORGAN, R. A., WANG, E., MARINCOLA, F. M., TRINCHIERI, G., ROSENBERG, S. A. & RESTIFO, N. P. 2011. IL-12 triggers a programmatic change in dysfunctional myeloid-derived cells within mouse tumors. *J Clin Invest,* 121**,** 4746-57.

KHALIL, D. N., SMITH, E. L., BRENTJENS, R. J. & WOLCHOK, J. D. 2016. The future of cancer treatment: immunomodulation, CARs and combination immunotherapy. *Nat Rev Clin Oncol,* 13**,** 394.

KHONG, H. T. & RESTIFO, N. P. 2002. Natural selection of tumor variants in the generation of "tumor escape" phenotypes. *Nat Immunol,* 3**,** 999-1005.

KIM, S. Y., HONG, S. H., BASSE, P. H., WU, C., BARTLETT, D. L., KWON, Y. T. & LEE, Y. J. 2016a. Cancer Stem Cells Protect Non-Stem Cells From Anoikis: Bystander Effects. *J Cell Biochem,* 117**,** 2289-301.

KIM, Y., YI, H., JUNG, H., RIM, Y. A., PARK, N., KIM, J., JUNG, S. M., PARK, S. H., PARK, Y. W. & JU, J. H. 2016b. A Dual Target-directed Agent against Interleukin-6 Receptor and Tumor Necrosis Factor alpha ameliorates experimental arthritis. *Sci Rep,* 6**,** 20150.

KINDLER, H. L., FRIBERG, G., SINGH, D. A., LOCKER, G., NATTAM, S., KOZLOFF, M., TABER, D. A., KARRISON, T., DACHMAN, A., STADLER, W. M. & VOKES, E. E. 2005. Phase II trial of bevacizumab plus gemcitabine in patients with advanced pancreatic cancer. *J Clin Oncol,* 23**,** 8033-40.

KINDLER, H. L., NIEDZWIECKI, D., HOLLIS, D., SUTHERLAND, S., SCHRAG, D., HURWITZ, H., INNOCENTI, F., MULCAHY, M. F., O'REILLY, E., WOZNIAK, T. F., PICUS, J., BHARGAVA, P., MAYER, R. J., SCHILSKY, R. L. & GOLDBERG, R. M. 2010. Gemcitabine plus bevacizumab compared with gemcitabine plus placebo in patients with advanced pancreatic cancer: phase III trial of the Cancer and Leukemia Group B (CALGB 80303). *J Clin Oncol,* 28**,** 3617-22.

KIPPS, T. J., STEVENSON, F. K., WU, C. J., CROCE, C. M., PACKHAM, G., WIERDA, W. G., O'BRIEN, S., GRIBBEN, J. & RAI, K. 2017a. Chronic lymphocytic leukaemia. *Nat Rev Dis Primers,* 3**,** 16096.

KIPPS, T. J., STEVENSON, F. K., WU, C. J., CROCE, C. M., PACKHAM, G., WIERDA, W. G., O'BRIEN, S., GRIBBEN, J. & RAI, K. 2017b. Chronic lymphocytic leukaemia. *Nat Rev Dis Primers,* 3**,** 17008.

KIPPS, T. J. W., G. F.; CUI, B. 2012. *Therapeutic antibodies against ROR-1 protein and methods for use of same*. United States patent application PCT/US2012/021339.

KLINGER, M., BENJAMIN, J., KISCHEL, R., STIENEN, S. & ZUGMAIER, G. 2016. Harnessing T cells to fight cancer with BiTE(R) antibody constructs--past developments and future directions. *Immunol Rev,* 270**,** 193-208.

KLINKENBIJL, J. H., JEEKEL, J., SAHMOUD, T., VAN PEL, R., COUVREUR, M. L., VEENHOF, C. H., ARNAUD, J. P., GONZALEZ, D. G., DE WIT, L. T., HENNIPMAN, A. & WILS, J. 1999. Adjuvant radiotherapy and 5-fluorouracil after curative resection of cancer of the pancreas and periampullary region: phase III trial of the EORTC gastrointestinal tract cancer cooperative group. *Ann Surg,* 230**,** 776-82; discussion 782-4.

KOCHENDERFER, J. N. & ROSENBERG, S. A. 2013. Treating B-cell cancer with T cells expressing anti-CD19 chimeric antigen receptors. *Nat Rev Clin Oncol,* 10**,** 267-76.

KOEBEL, C. M., VERMI, W., SWANN, J. B., ZERAFA, N., RODIG, S. J., OLD, L. J., SMYTH, M. J. & SCHREIBER, R. D. 2007. Adaptive immunity maintains occult cancer in an equilibrium state. *Nature,* 450**,** 903-7.

KOHLER, G. & MILSTEIN, C. 1975. Continuous cultures of fused cells secreting antibody of predefined specificity. *Nature,* 256**,** 495-7.

KOHNKE, T., KRUPKA, C., TISCHER, J., KNOSEL, T. & SUBKLEWE, M. 2015. Increase of PD-L1 expressing B-precursor ALL cells in a patient resistant to the CD19/CD3-bispecific T cell engager antibody blinatumomab. *J Hematol Oncol,* 8**,** 111.

KONERU, M., O'CEARBHAILL, R., PENDHARKAR, S., SPRIGGS, D. R. & BRENTJENS, R. J. 2015a. A phase I clinical trial of adoptive T cell therapy using IL-12 secreting MUC-16(ecto) directed chimeric antigen receptors for recurrent ovarian cancer. *J Transl Med,* 13**,** 102.

KONERU, M., PURDON, T. J., SPRIGGS, D., KONERU, S. & BRENTJENS, R. J. 2015b. IL-12 secreting tumor-targeted chimeric antigen receptor T cells eradicate ovarian tumors in vivo. *Oncoimmunology,* 4**,** e994446.

KONTERMANN, R. E. & BRINKMANN, U. 2015. Bispecific antibodies. *Drug Discov Today,* 20**,** 838-47.

KRUPKA, C., KÖHNKE, T., KUFER, P., KISCHEL, R., LICHTENEGGER, F. S., BRAUNECK, F., ROHLING, S., ALTMANN, T., HIDDEMANN, W., & SUBKLEWE, M. S. 2015. Identifying Immune Resistance Mechanisms to CD33/CD3 BiTE® Antibody Construct (AMG 330) Mediated Cytotoxicity. Blood, 126(23), 3677. *American Society of Hematology.* Blood.

KUBOTA, T., NIWA, R., SATOH, M., AKINAGA, S., SHITARA, K. & HANAI, N. 2009. Engineered therapeutic antibodies with improved effector functions. *Cancer Sci,* 100**,** 1566-72.

KULIS, M., HEATH, S., BIBIKOVA, M., QUEIROS, A. C., NAVARRO, A., CLOT, G., MARTINEZ-TRILLOS, A., CASTELLANO, G., BRUN-HEATH, I., PINYOL, M., BARBERAN-SOLER, S., PAPASAIKAS, P., JARES, P., BEA, S., RICO, D., ECKER, S., RUBIO, M., ROYO, R.,

HO, V., KLOTZLE, B., HERNANDEZ, L., CONDE, L., LOPEZ-GUERRA, M., COLOMER, D., VILLAMOR, N., AYMERICH, M., ROZMAN, M., BAYES, M., GUT, M., GELPI, J. L., OROZCO, M., FAN, J. B., QUESADA, V., PUENTE, X. S., PISANO, D. G., VALENCIA, A., LOPEZ-GUILLERMO, A., GUT, I., LOPEZ-OTIN, C., CAMPO, E. & MARTIN-SUBERO, J. I. 2012. Epigenomic analysis detects widespread gene-body DNA hypomethylation in chronic lymphocytic leukemia. *Nat Genet,* 44**,** 1236-42.

LAMPSON, B. L., KASAR, S. N., MATOS, T. R., MORGAN, E. A., RASSENTI, L., DAVIDS, M. S., FISHER, D. C., FREEDMAN, A. S., JACOBSON, C. A., ARMAND, P., ABRAMSON, J. S., ARNASON, J. E., KIPPS, T. J., FEIN, J., FERNANDES, S., HANNA, J., RITZ, J., KIM, H. T. & BROWN, J. R. 2016. Idelalisib given front-line for treatment of chronic lymphocytic leukemia causes frequent immune-mediated hepatotoxicity. *Blood,* 128**,** 195-203.

LANDAU, D. A., TAUSCH, E., TAYLOR-WEINER, A. N., STEWART, C., REITER, J. G., BAHLO, J., KLUTH, S., BOZIC, I., LAWRENCE, M., BOTTCHER, S., CARTER, S. L., CIBULSKIS, K., MERTENS, D., SOUGNEZ, C. L., ROSENBERG, M., HESS, J. M., EDELMANN, J., KLESS, S., KNEBA, M., RITGEN, M., FINK, A., FISCHER, K., GABRIEL, S., LANDER, E. S., NOWAK, M. A., DOHNER, H., HALLEK, M., NEUBERG, D., GETZ, G., STILGENBAUER, S. & WU, C. J. 2015. Mutations driving CLL and their evolution in progression and relapse. *Nature,* 526**,** 525-30.

LANNUTTI, B. J., MEADOWS, S. A., HERMAN, S. E., KASHISHIAN, A., STEINER, B., JOHNSON, A. J., BYRD, J. C., TYNER, J. W., LORIAUX, M. M., DEININGER, M., DRUKER, B. J., PURI, K. D., ULRICH, R. G. & GIESE, N. A. 2011. CAL-101, a p110delta selective phosphatidylinositol-3-kinase inhibitor for the treatment of B-cell malignancies, inhibits PI3K signaling and cellular viability. *Blood,* 117**,** 591-4.

LAPALOMBELLA, R., ANDRITSOS, L., LIU, Q., MAY, S. E., BROWNING, R., PHAM, L. V., BLUM, K. A., BLUM, W., RAMANUNNI, A., RAYMOND, C. A., SMITH, L. L., LEHMAN, A., MO, X., JARJOURA, D., CHEN, C. S., FORD, R., JR., RADER, C., MUTHUSAMY, N., JOHNSON, A. J. & BYRD, J. C. 2010. Lenalidomide treatment promotes CD154 expression on CLL cells and enhances production of antibodies by normal B cells through a PI3-kinase-dependent pathway. *Blood,* 115**,** 2619-29.

LAPALOMBELLA, R., YU, B., TRIANTAFILLOU, G., LIU, Q., BUTCHAR, J. P., LOZANSKI, G., RAMANUNNI, A., SMITH, L. L., BLUM, W., ANDRITSOS, L., WANG, D. S., LEHMAN, A., CHEN, C. S., JOHNSON, A. J., MARCUCCI, G., LEE, R. J., LEE, L. J., TRIDANDAPANI, S., MUTHUSAMY, N. & BYRD, J. C. 2008. Lenalidomide down-regulates the CD20 antigen and antagonizes direct and antibody-dependent cellular cytotoxicity of rituximab on primary chronic lymphocytic leukemia cells. *Blood,* 112**,** 5180-9.

LE, D. T., LUTZ, E., URAM, J. N., SUGAR, E. A., ONNERS, B., SOLT, S., ZHENG, L., DIAZ, L. A., JR., DONEHOWER, R. C., JAFFEE, E. M. & LAHERU, D. A. 2013. Evaluation of ipilimumab in combination with allogeneic pancreatic tumor cells transfected with a GM-CSF gene in previously treated pancreatic cancer. *J Immunother,* 36**,** 382-9.

LEDFORD, H. 2015. Cancer-fighting viruses win approval. *Nature,* 526**,** 622-3.

LEE, C. S., CRAGG, M., GLENNIE, M. & JOHNSON, P. 2013. Novel antibodies targeting immune regulatory checkpoints for cancer therapy. *Br J Clin Pharmacol,* 76**,** 233-47.

LEE, J., KOTLIAROVA, S., KOTLIAROV, Y., LI, A., SU, Q., DONIN, N. M., PASTORINO, S., PUROW, B. W., CHRISTOPHER, N., ZHANG, W., PARK, J. K. & FINE, H. A. 2006. Tumor stem cells derived from glioblastomas cultured in bFGF and EGF more closely mirror the phenotype and genotype of primary tumors than do serum-cultured cell lines. *Cancer Cell,* 9**,** 391-403.

LEE, S. H., HONG, J. H., PARK, H. K., PARK, J. S., KIM, B. K., LEE, J. Y., JEONG, J. Y., YOON, G. S., INOUE, M., CHOI, G. S. & LEE, I. K. 2015. Colorectal cancer-derived tumor spheroids retain the characteristics of original tumors. *Cancer Lett,* 367**,** 34-42.

LEONARD, J. P., SHERMAN, M. L., FISHER, G. L., BUCHANAN, L. J., LARSEN, G., ATKINS, M. B., SOSMAN, J. A., DUTCHER, J. P., VOGELZANG, N. J. & RYAN, J. L. 1997. Effects of single-dose interleukin-12 exposure on interleukin-12-associated toxicity and interferon-gamma production. *Blood,* 90**,** 2541-8.

LI, D., SU, D., XUE, L., LIU, Y. & PANG, W. 2015. Establishment of pancreatic cancer stem cells by flow cytometry and their biological characteristics. *Int J Clin Exp Pathol,* 8**,** 11218-23.

LI, F., VIJAYASANKARAN, N., SHEN, A. Y., KISS, R. & AMANULLAH, A. 2010. Cell culture processes for monoclonal antibody production. *MAbs,* 2**,** 466-79.

LITTLE, M., KIPRIYANOV, S. M., LE GALL, F. & MOLDENHAUER, G. 2000. Of mice and men: hybridoma and recombinant antibodies. *Immunol Today,* 21**,** 364-70.

LIU, E., MARINCOLA, P. & OBERG, K. 2013. Everolimus in the treatment of patients with advanced pancreatic neuroendocrine tumors: latest findings and interpretations. *Therap Adv Gastroenterol,* 6**,** 412-9.

LIU, J., MIWA, T., HILLIARD, B., CHEN, Y., LAMBRIS, J. D., WELLS, A. D. & SONG, W. C. 2005. The complement inhibitory protein DAF (CD55) suppresses T cell immunity in vivo. *J Exp Med,* 201**,** 567-77.

LIU, J. K. 2014. The history of monoclonal antibody development - Progress, remaining challenges and future innovations. *Ann Med Surg (Lond),* 3**,** 113-6.

LOBUGLIO, A. F., WHEELER, R. H., TRANG, J., HAYNES, A., ROGERS, K., HARVEY, E. B., SUN, L., GHRAYEB, J. & KHAZAELI, M. B. 1989. Mouse/human chimeric monoclonal antibody in man: kinetics and immune response. *Proc Natl Acad Sci U S A,* 86**,** 4220-4.

LOHR, M., TRAUTMANN, B., GOTTLER, M., PETERS, S., ZAUNER, I., MAILLET, B. & KLOPPEL, G. 1994. Human ductal adenocarcinomas of the pancreas express extracellular matrix proteins. *Br J Cancer,* 69**,** 144-51.

LOISEL, S., ANDRE, P. A., GOLAY, J., BUCHEGGER, F., KADOUCHE, J., CERUTTI, M., BOLOGNA, L., KOSINSKI, M., VIERTL, D., DELALOYE, A. B., BERTHOU, C., MACH, J. P. & BOUMSELL, L. 2011. Antitumour effects of single or combined monoclonal antibodies directed against membrane antigens expressed by human B cells leukaemia. *Mol Cancer,* 10**,** 42.

LOSKOG, A. S. & ELIOPOULOS, A. G. 2009. The Janus faces of CD40 in cancer. *Semin Immunol,* 21**,** 301-7.

LOU, Y., DIAO, L., CUENTAS, E. R., DENNING, W. L., CHEN, L., FAN, Y. H., BYERS, L. A., WANG, J., PAPADIMITRAKOPOULOU, V. A., BEHRENS, C., RODRIGUEZ, J. C., HWU, P., WISTUBA, II, HEYMACH, J. V. & GIBBONS, D. L. 2016. Epithelial-Mesenchymal Transition Is Associated with a Distinct Tumor Microenvironment Including Elevation of Inflammatory Signals and Multiple Immune Checkpoints in Lung Adenocarcinoma. *Clin Cancer Res,* 22**,** 3630-42.

LOWDELL, M. W. & THOMAS, A. 2017. The expanding role of the clinical haematologist in the new world of advanced therapy medicinal products. *Br J Haematol,* 176**,** 9-15.

LOZANSKI, G., HEEREMA, N. A., FLINN, I. W., SMITH, L., HARBISON, J., WEBB, J., MORAN, M., LUCAS, M., LIN, T., HACKBARTH, M. L., PROFFITT, J. H., LUCAS, D., GREVER, M. R. & BYRD, J. C. 2004. Alemtuzumab is an effective therapy for chronic lymphocytic leukemia with p53 mutations and deletions. *Blood,* 103**,** 3278-81.

LTD, M. *Biotinylated PepSets for Epitope Mapping* [Online]. Available: http://www.mimotopes.com/knowledgeBaseDocument.asp?did=59 [Accessed 2017].

MACHIELS, J. P., SPECENIER, P., KRAUSS, J., DIETZ, A., KAMINSKY, M. C., LALAMI, Y., HENKE, M., KEILHOLZ, U., KNECHT, R., SKARTVED, N. J., HORAK, I. D., PAMPERIN, P., BRAUN, S. & GAULER, T. C. 2015. A proof of concept trial of the anti-EGFR antibody mixture Sym004 in patients with squamous cell carcinoma of the head and neck. *Cancer Chemother Pharmacol,* 76**,** 13-20.

MACK, J. T., BROWN, C. B. & TEW, K. D. 2008. ABCA2 as a therapeutic target in cancer and nervous system disorders. *Expert Opin Ther Targets,* 12**,** 491-504.

MACKALL, C. L. 2014. Introduction to the series of reviews on "Antibody derivatives as new therapeutics for hematologic malignancies". *Blood,* 123**,** 2283-4.

MAHASETH, H., BRUTCHER, E., KAUH, J., HAWK, N., KIM, S., CHEN, Z., KOOBY, D. A., MAITHEL, S. K., LANDRY, J. & EL-RAYES, B. F. 2013. Modified FOLFIRINOX regimen with improved safety and maintained efficacy in pancreatic adenocarcinoma. *Pancreas,* 42**,** 1311-5.

MAHONEY, K. M., RENNERT, P. D. & FREEMAN, G. J. 2015. Combination cancer immunotherapy and new immunomodulatory targets. *Nat Rev Drug Discov,* 14**,** 561-84.

MAKKOUK, A. & WEINER, G. J. 2015. Cancer immunotherapy and breaking immune tolerance: new approaches to an old challenge. *Cancer Res,* 75**,** 5-10.

MAKOHON-MOORE, A. & IACOBUZIO-DONAHUE, C. A. 2016. Pancreatic cancer biology and genetics from an evolutionary perspective. *Nat Rev Cancer,* 16**,** 553-65.

MALONEY, D. G., GRILLO-LOPEZ, A. J., WHITE, C. A., BODKIN, D., SCHILDER, R. J., NEIDHART, J. A., JANAKIRAMAN, N., FOON, K. A., LILES, T. M., DALLAIRE, B. K., WEY, K., ROYSTON, I., DAVIS, T. & LEVY, R. 1997. IDEC-C2B8 (Rituximab) anti-CD20 monoclonal antibody therapy in patients with relapsed low-grade non-Hodgkin's lymphoma. *Blood,* 90**,** 2188-95.

MANI, R., MAO, Y., FRISSORA, F. W., CHIANG, C. L., WANG, J., ZHAO, Y., WU, Y., YU, B., YAN, R., MO, X., YU, L., FLYNN, J., JONES, J., ANDRITSOS, L., BASKAR, S., RADER, C., PHELPS, M. A., CHEN, C. S., LEE, R. J., BYRD, J. C., LEE, L. J. & MUTHUSAMY, N. 2015. Tumor antigen ROR1 targeted drug delivery mediated selective leukemic but not normal B-cell cytotoxicity in chronic lymphocytic leukemia. *Leukemia,* 29**,** 346-55.

MANY, A. M. & BROWN, A. M. 2014. Both canonical and non-canonical Wnt signaling independently promote stem cell growth in mammospheres. *PLoS One,* 9**,** e101800.

MARTINEZ-CRUZADO, L., TORNIN, J., SANTOS, L., RODRIGUEZ, A., GARCIA-CASTRO, J., MORIS, F. & RODRIGUEZ, R. 2016. Aldh1 Expression and Activity Increase During Tumor Evolution in Sarcoma Cancer Stem Cell Populations. *Sci Rep,* 6**,** 27878.

MARUANI, A., RICHARDS, D. A. & CHUDASAMA, V. 2016. Dual modification of biomolecules. *Org Biomol Chem,* 14**,** 6165-78.

MARUANI, A., SMITH, M. E., MIRANDA, E., CHESTER, K. A., CHUDASAMA, V. & CADDICK, S. 2015. A plug-and-play approach to antibody-based therapeutics via a chemoselective dual click strategy. *Nat Commun,* 6**,** 6645.

MARUSYK, A. & POLYAK, K. 2010. Tumor heterogeneity: causes and consequences. *Biochim Biophys Acta,* 1805**,** 105-17.

MASAMUNE, A. & SHIMOSEGAWA, T. 2015. Pancreatic stellate cells: A dynamic player of the intercellular communication in pancreatic cancer. *Clin Res Hepatol Gastroenterol,* 39 Suppl 1**,** S98-103.

MASIAKOWSKI, P. & CARROLL, R. D. 1992. A novel family of cell surface receptors with tyrosine kinase-like domain. *J Biol Chem,* 267**,** 26181-90.

MATSUDA, T., NOMI, M., IKEYA, M., KANI, S., OISHI, I., TERASHIMA, T., TAKADA, S. & MINAMI, Y. 2001. Expression of the receptor tyrosine kinase genes, Ror1 and Ror2, during mouse development. *Mech Dev,* 105**,** 153-6.

MATSUDA, Y., KURE, S. & ISHIWATA, T. 2012. Nestin and other putative cancer stem cell markers in pancreatic cancer. *Med Mol Morphol,* 45**,** 59-65.

MAUDE, S. L., FREY, N., SHAW, P. A., APLENC, R., BARRETT, D. M., BUNIN, N. J., CHEW, A., GONZALEZ, V. E., ZHENG, Z., LACEY, S. F., MAHNKE, Y. D., MELENHORST, J. J., RHEINGOLD, S. R., SHEN, A., TEACHEY, D. T., LEVINE, B. L., JUNE, C. H., PORTER, D. L. & GRUPP, S. A. 2014. Chimeric antigen receptor T cells for sustained remissions in leukemia. *N Engl J Med,* 371**,** 1507-17.

MAYOR, S. & PAGANO, R. E. 2007. Pathways of clathrin-independent endocytosis. *Nat Rev Mol Cell Biol,* 8**,** 603-12.

MCCLANAHAN, F., RICHES, J. C., MILLER, S., DAY, W. P., KOTSIOU, E., NEUBERG, D., CROCE, C. M., CAPASSO, M. & GRIBBEN, J. G. 2015. Mechanisms of PD-L1/PD-1-mediated CD8 T-cell dysfunction in the context of aging-related immune defects in the Emicro-TCL1 CLL mouse model. *Blood,* 126**,** 212-21.

MELLMAN, I., COUKOS, G. & DRANOFF, G. 2011. Cancer immunotherapy comes of age. *Nature,* 480**,** 480-9.

MIDDLETON, G., SILCOCKS, P., COX, T., VALLE, J., WADSLEY, J., PROPPER, D., COXON, F., ROSS, P., MADHUSUDAN, S., ROQUES, T., CUNNINGHAM, D., FALK, S., WADD, N., HARRISON, M., CORRIE, P., IVESON, T., ROBINSON, A., MCADAM, K., EATOCK, M., EVANS, J., ARCHER, C., HICKISH, T., GARCIA-ALONSO, A., NICOLSON, M., STEWARD, W., ANTHONEY, A., GREENHALF, W., SHAW, V., COSTELLO, E., NAISBITT, D., RAWCLIFFE, C., NANSON, G. & NEOPTOLEMOS, J. 2014. Gemcitabine and capecitabine with or without telomerase peptide vaccine GV1001 in patients with locally advanced or metastatic pancreatic cancer (TeloVac): an open-label, randomised, phase 3 trial. *Lancet Oncol,* 15**,** 829-40.

MITRA, A., SATELLI, A., XIA, X., CUTRERA, J., MISHRA, L. & LI, S. 2015. Cell-surface Vimentin: A mislocalized protein for isolating csVimentin(+) CD133(-) novel stem-like hepatocellular carcinoma cells expressing EMT markers. *Int J Cancer,* 137**,** 491-6.

MOORE, M. J., GOLDSTEIN, D., HAMM, J., FIGER, A., HECHT, J. R., GALLINGER, S., AU, H. J., MURAWA, P., WALDE, D., WOLFF, R. A., CAMPOS, D., LIM, R., DING, K., CLARK, G., VOSKOGLOU-NOMIKOS, T., PTASYNSKI, M., PARULEKAR, W. & NATIONAL CANCER INSTITUTE OF CANADA CLINICAL TRIALS, G. 2007. Erlotinib plus gemcitabine compared with gemcitabine alone in patients with advanced pancreatic cancer: a phase III trial of the National Cancer Institute of Canada Clinical Trials Group. *J Clin Oncol,* 25**,** 1960-6.

MORGANTI, A. G., FALCONI, M., VAN STIPHOUT, R. G., MATTIUCCI, G. C., ALFIERI, S., CALVO, F. A., DUBOIS, J. B., FASTNER, G., HERMAN, J. M., MAIDMENT, B. W., 3RD, MILLER, R. C., REGINE, W. F., RENI, M., SHARMA, N. K., IPPOLITO, E. & VALENTINI, V.

2014. Multi-institutional pooled analysis on adjuvant chemoradiation in pancreatic cancer. *Int J Radiat Oncol Biol Phys,* 90**,** 911-7.

MOSSNER, E., BRUNKER, P., MOSER, S., PUNTENER, U., SCHMIDT, C., HERTER, S., GRAU, R., GERDES, C., NOPORA, A., VAN PUIJENBROEK, E., FERRARA, C., SONDERMANN, P., JAGER, C., STREIN, P., FERTIG, G., FRIESS, T., SCHULL, C., BAUER, S., DAL PORTO, J., DEL NAGRO, C., DABBAGH, K., DYER, M. J., POPPEMA, S., KLEIN, C. & UMANA, P. 2010. Increasing the efficacy of CD20 antibody therapy through the engineering of a new type II anti-CD20 antibody with enhanced direct and immune effector cell-mediated B-cell cytotoxicity. *Blood,* 115**,** 4393-402.

MUNIRAJ, T., JAMIDAR, P. A. & ASLANIAN, H. R. 2013. Pancreatic cancer: a comprehensive review and update. *Dis Mon,* 59**,** 368-402.

NABHAN, C., ASCHEBROOK-KILFOY, B., CHIU, B. C., SMITH, S. M., SHANAFELT, T. D., EVENS, A. M. & KAY, N. E. 2014. The impact of race, ethnicity, age and sex on clinical outcome in chronic lymphocytic leukemia: a comprehensive Surveillance, Epidemiology, and End Results analysis in the modern era. *Leuk Lymphoma,* 55**,** 2778-84.

NADDAFI, F. & DAVAMI, F. 2015. Anti-CD19 Monoclonal Antibodies: a New Approach to Lymphoma Therapy. *Int J Mol Cell Med,* 4**,** 143-51.

NAGORSEN, D. & BAEUERLE, P. A. 2011. Immunomodulatory therapy of cancer with T cell-engaging BiTE antibody blinatumomab. *Exp Cell Res,* 317**,** 1255-60.

NAKAHATA, K., UEHARA, S., NISHIKAWA, S., KAWATSU, M., ZENITANI, M., OUE, T. & OKUYAMA, H. 2015. Aldehyde Dehydrogenase 1 (ALDH1) Is a Potential Marker for Cancer Stem Cells in Embryonal Rhabdomyosarcoma. *PLoS One,* 10**,** e0125454.

NAKAI, Y., ISAYAMA, H., SASAKI, T., SASAHIRA, N., TSUJINO, T., TODA, N., KOGURE, H., MATSUBARA, S., ITO, Y., TOGAWA, O., ARIZUMI, T., HIRANO, K., TADA, M., OMATA, M. & KOIKE, K. 2012. A multicentre randomised phase II trial of gemcitabine alone vs gemcitabine and S-1 combination therapy in advanced pancreatic cancer: GEMSAP study. *Br J Cancer,* 106**,** 1934-9.

NAKATA, S., PHILLIPS, E. & GOIDTS, V. 2014. Emerging role for leucine-rich repeat-containing G-protein-coupled receptors LGR5 and LGR4 in cancer stem cells. *Cancer Manag Res,* 6**,** 171-80.

NATH, N., GODAT, B., ZIMPRICH, C., DWIGHT, S. J., CORONA, C., MCDOUGALL, M. & URH, M. 2016. Homogeneous plate based antibody internalization assay using pH sensor fluorescent dye. *J Immunol Methods,* 431**,** 11-21.

NATSUME, A., IN, M., TAKAMURA, H., NAKAGAWA, T., SHIMIZU, Y., KITAJIMA, K., WAKITANI, M., OHTA, S., SATOH, M., SHITARA, K. & NIWA, R. 2008. Engineered antibodies of IgG1/IgG3 mixed isotype with enhanced cytotoxic activities. *Cancer Res,* 68**,** 3863-72.

NATSUME, A., NIWA, R. & SATOH, M. 2009. Improving effector functions of antibodies for cancer treatment: Enhancing ADCC and CDC. *Drug Des Devel Ther,* 3**,** 7-16.

NEESSE, A., MICHL, P., FRESE, K. K., FEIG, C., COOK, N., JACOBETZ, M. A., LOLKEMA, M. P., BUCHHOLZ, M., OLIVE, K. P., GRESS, T. M. & TUVESON, D. A. 2011. Stromal biology and therapy in pancreatic cancer. *Gut,* 60**,** 861-8.

NELSON, P. N., REYNOLDS, G. M., WALDRON, E. E., WARD, E., GIANNOPOULOS, K. & MURRAY, P. G. 2000. Monoclonal antibodies. *Mol Pathol,* 53**,** 111-7.

NEOPTOLEMOS, J. P., STOCKEN, D. D., FRIESS, H., BASSI, C., DUNN, J. A., HICKEY, H., BEGER, H., FERNANDEZ-CRUZ, L., DERVENIS, C., LACAINE, F., FALCONI, M., PEDERZOLI, P., PAP, A., SPOONER, D., KERR, D. J., BUCHLER, M. W. & EUROPEAN STUDY GROUP FOR PANCREATIC, C. 2004. A randomized trial of chemoradiotherapy and chemotherapy after resection of pancreatic cancer. *N Engl J Med,* 350**,** 1200-10.

NERADIL, J. & VESELSKA, R. 2015. Nestin as a marker of cancer stem cells. *Cancer Sci,* 106**,** 803-11.

NEWMAN, M. J. & BENANI, D. J. 2016. A review of blinatumomab, a novel immunotherapy. *J Oncol Pharm Pract,* 22**,** 639-45.

NICHOLAS, N. S., APOLLONIO, B. & RAMSAY, A. G. 2016a. Tumor microenvironment (TME)-driven immune suppression in B cell malignancy. *Biochim Biophys Acta,* 1863**,** 471-482.

NICHOLAS, N. S., APOLLONIO, B. & RAMSAY, A. G. 2016b. Tumor microenvironment (TME)-driven immune suppression in B cell malignancy. *Biochim Biophys Acta,* 1863**,** 471-82.

NUNES, J. P., MORAIS, M., VASSILEVA, V., ROBINSON, E., RAJKUMAR, V. S., SMITH, M. E., PEDLEY, R. B., CADDICK, S., BAKER, J. R. & CHUDASAMA, V. 2015. Functional native disulfide bridging enables delivery of a potent, stable and targeted antibody-drug conjugate (ADC). *Chem Commun (Camb),* 51**,** 10624-7.

O'BRIEN, S. M., KANTARJIAN, H., THOMAS, D. A., GILES, F. J., FREIREICH, E. J., CORTES, J., LERNER, S. & KEATING, M. J. 2001. Rituximab dose-escalation trial in chronic lymphocytic leukemia. *J Clin Oncol,* 19**,** 2165-70.

O'CONNELL, M. P., MARCHBANK, K., WEBSTER, M. R., VALIGA, A. A., KAUR, A., VULTUR, A., LI, L., HERLYN, M., VILLANUEVA, J., LIU, Q., YIN, X., WIDURA, S., NELSON, J., RUIZ, N., CAMILLI, T. C., INDIG, F. E., FLAHERTY, K. T., WARGO, J. A., FREDERICK, D. T., COOPER, Z. A., NAIR, S., AMARAVADI, R. K., SCHUCHTER, L. M., KARAKOUSIS, G. C., XU, W., XU, X. & WEERARATNA, A. T. 2013. Hypoxia induces phenotypic plasticity and therapy resistance in melanoma via the tyrosine kinase receptors ROR1 and ROR2. *Cancer Discov,* 3**,** 1378-93.

OBER, R. J., RADU, C. G., GHETIE, V. & WARD, E. S. 2001. Differences in promiscuity for antibody-FcRn interactions across species: implications for therapeutic antibodies. *Int Immunol,* 13**,** 1551-9.

ODOUX, C., FOHRER, H., HOPPO, T., GUZIK, L., STOLZ, D. B., LEWIS, D. W., GOLLIN, S. M., GAMBLIN, T. C., GELLER, D. A. & LAGASSE, E.

2008. A stochastic model for cancer stem cell origin in metastatic colon cancer. *Cancer Res,* 68**,** 6932-41.

OISHI, I., TAKEUCHI, S., HASHIMOTO, R., NAGABUKURO, A., UEDA, T., LIU, Z. J., HATTA, T., AKIRA, S., MATSUDA, Y., YAMAMURA, H., OTANI, H. & MINAMI, Y. 1999. Spatio-temporally regulated expression of receptor tyrosine kinases, mRor1, mRor2, during mouse development: implications in development and function of the nervous system. *Genes Cells,* 4**,** 41-56.

OLIVE, K. P., JACOBETZ, M. A., DAVIDSON, C. J., GOPINATHAN, A., MCINTYRE, D., HONESS, D., MADHU, B., GOLDGRABEN, M. A., CALDWELL, M. E., ALLARD, D., FRESE, K. K., DENICOLA, G., FEIG, C., COMBS, C., WINTER, S. P., IRELAND-ZECCHINI, H., REICHELT, S., HOWAT, W. J., CHANG, A., DHARA, M., WANG, L., RUCKERT, F., GRUTZMANN, R., PILARSKY, C., IZERADJENE, K., HINGORANI, S. R., HUANG, P., DAVIES, S. E., PLUNKETT, W., EGORIN, M., HRUBAN, R. H., WHITEBREAD, N., MCGOVERN, K., ADAMS, J., IACOBUZIO-DONAHUE, C., GRIFFITHS, J. & TUVESON, D. A. 2009. Inhibition of Hedgehog signaling enhances delivery of chemotherapy in a mouse model of pancreatic cancer. *Science,* 324**,** 1457-61.

OWEN, C., ASSOULINE, S., KURUVILLA, J., UCHIDA, C., BELLINGHAM, C. & SEHN, L. 2015. Novel Therapies for Chronic Lymphocytic Leukemia: A Canadian Perspective. *Clin Lymphoma Myeloma Leuk,* 15**,** 627-634 e5.

PADLAN, E. A. 1991. A possible procedure for reducing the immunogenicity of antibody variable domains while preserving their ligand-binding properties. *Mol Immunol,* 28**,** 489-98.

PANDEY, M. & MAHADEVAN, D. 2014. Monoclonal antibodies as therapeutics in human malignancies. *Future Oncol,* 10**,** 609-36.

PARDOLL, D. M. 2012. The blockade of immune checkpoints in cancer immunotherapy. *Nat Rev Cancer,* 12**,** 252-64.

PARK, J. H. & BRENTJENS, R. J. 2013. Immunotherapies in CLL. *Adv Exp Med Biol,* 792**,** 241-57.

PARK, J. H. R., ISABELLE; WANG, XIUYAN; BERNAL, YVETTE J; YOO, SARAH; PURDON, TERRENCE; HALTON, ELIZABETH; QUINTANILLA, HILDA; CURRAN, KEVIN J.; SAUTER, CRAIG S.; DAVILA, MARCO L; SADELAIN, MICHEL AND BRENTJENS, RENIER J. 2014. CD19-Targeted 19-28z CAR Modified Autologous T Cells Induce High Rates of Complete Remission and Durable Responses in Adult Patients with Relapsed, Refractory B-Cell ALL. *American Society of Hematology.* Blood.

PARK, J. H. R., ISABELLE; WANG, XIUYAN; STEFANSKI, JOLANTA; HE, QING; TAYLOR, CLARE; OLSZEWSKA, MALGORZATA; WASIELEWSKA, TERESA; BARTIDO, SHIRLEY; DAVILA, MARCO L; BERNAL, YVETTE; LAMANNA, NICOLE; NOY, ARIELA; SADELAIN, MICHEL AND BRENTJENS, RENIER J. 2012. Impact of the conditioning chemotherapy on outcomes in adoptive T cell

therapy: results from a phase I clinical trial of autologous CD19 targeted T cells for patients with relapsed CLL. *American Society of Hematologists.* Blood.

PARKHURST, M. R., RILEY, J. P., DUDLEY, M. E. & ROSENBERG, S. A. 2011. Adoptive transfer of autologous natural killer cells leads to high levels of circulating natural killer cells but does not mediate tumor regression. *Clin Cancer Res,* 17**,** 6287-97.

PARMIANI, G., CASTELLI, C., DALERBA, P., MORTARINI, R., RIVOLTINI, L., MARINCOLA, F. M. & ANICHINI, A. 2002. Cancer immunotherapy with peptide-based vaccines: what have we achieved? Where are we going? *J Natl Cancer Inst,* 94**,** 805-18.

PATINO, T., SORIANO, J., BARRIOS, L., IBANEZ, E. & NOGUES, C. 2015. Surface modification of microparticles causes differential uptake responses in normal and tumoral human breast epithelial cells. *Sci Rep,* 5**,** 11371.

PAWLUCZKOWYCZ, A. W., BEURSKENS, F. J., BEUM, P. V., LINDORFER, M. A., VAN DE WINKEL, J. G., PARREN, P. W. & TAYLOR, R. P. 2009. Binding of submaximal C1q promotes complement-dependent cytotoxicity (CDC) of B cells opsonized with anti-CD20 mAbs ofatumumab (OFA) or rituximab (RTX): considerably higher levels of CDC are induced by OFA than by RTX. *J Immunol,* 183**,** 749-58.

PEARSE, B. M. 1976. Clathrin: a unique protein associated with intracellular transfer of membrane by coated vesicles. *Proc Natl Acad Sci U S A,* 73**,** 1255-9.

PETERS, C. & BROWN, S. 2015. Antibody-drug conjugates as novel anti-cancer chemotherapeutics. *Biosci Rep,* 35.

PHAN, G. Q., YANG, J. C., SHERRY, R. M., HWU, P., TOPALIAN, S. L., SCHWARTZENTRUBER, D. J., RESTIFO, N. P., HAWORTH, L. R., SEIPP, C. A., FREEZER, L. J., MORTON, K. E., MAVROUKAKIS, S. A., DURAY, P. H., STEINBERG, S. M., ALLISON, J. P., DAVIS, T. A. & ROSENBERG, S. A. 2003. Cancer regression and autoimmunity induced by cytotoxic T lymphocyte-associated antigen 4 blockade in patients with metastatic melanoma. *Proc Natl Acad Sci U S A,* 100**,** 8372-7.

PHILIP, P. A., BENEDETTI, J., CORLESS, C. L., WONG, R., O'REILLY, E. M., FLYNN, P. J., ROWLAND, K. M., ATKINS, J. N., MIRTSCHING, B. C., RIVKIN, S. E., KHORANA, A. A., GOLDMAN, B., FENOGLIO-PREISER, C. M., ABBRUZZESE, J. L. & BLANKE, C. D. 2010. Phase III study comparing gemcitabine plus cetuximab versus gemcitabine in patients with advanced pancreatic adenocarcinoma: Southwest Oncology Group-directed intergroup trial S0205. *J Clin Oncol,* 28**,** 3605-10.

PILLAY, V., GAN, H. K. & SCOTT, A. M. 2011. Antibodies in oncology. *N Biotechnol,* 28**,** 518-29.

PINZON-CHARRY, A., MAXWELL, T. & LOPEZ, J. A. 2005. Dendritic cell dysfunction in cancer: a mechanism for immunosuppression. *Immunol Cell Biol,* 83**,** 451-61.

PONTI, D., COSTA, A., ZAFFARONI, N., PRATESI, G., PETRANGOLINI, G., CORADINI, D., PILOTTI, S., PIEROTTI, M. A. & DAIDONE, M. G. 2005. Isolation and in vitro propagation of tumorigenic breast cancer cells with stem/progenitor cell properties. *Cancer Res,* 65**,** 5506-11.

PORTELL, C. A., WENZELL, C. M. & ADVANI, A. S. 2013. Clinical and pharmacologic aspects of blinatumomab in the treatment of B-cell acute lymphoblastic leukemia. *Clin Pharmacol,* 5**,** 5-11.

PORTER, D. L., HWANG, W. T., FREY, N. V., LACEY, S. F., SHAW, P. A., LOREN, A. W., BAGG, A., MARCUCCI, K. T., SHEN, A., GONZALEZ, V., AMBROSE, D., GRUPP, S. A., CHEW, A., ZHENG, Z., MILONE, M. C., LEVINE, B. L., MELENHORST, J. J. & JUNE, C. H. 2015. Chimeric antigen receptor T cells persist and induce sustained remissions in relapsed refractory chronic lymphocytic leukemia. *Sci Transl Med,* 7**,** 303ra139.

PORTER, D. L., LEVINE, B. L., KALOS, M., BAGG, A. & JUNE, C. H. 2011. Chimeric antigen receptor-modified T cells in chronic lymphoid leukemia. *N Engl J Med,* 365**,** 725-33.

PRANG, N., PREITHNER, S., BRISCHWEIN, K., GOSTER, P., WOPPEL, A., MULLER, J., STEIGER, C., PETERS, M., BAEUERLE, P. A. & DA SILVA, A. J. 2005. Cellular and complement-dependent cytotoxicity of Ep-CAM-specific monoclonal antibody MT201 against breast cancer cell lines. *Br J Cancer,* 92**,** 342-9.

PROVENZANO, P. P., CUEVAS, C., CHANG, A. E., GOEL, V. K., VON HOFF, D. D. & HINGORANI, S. R. 2012. Enzymatic targeting of the stroma ablates physical barriers to treatment of pancreatic ductal adenocarcinoma. *Cancer Cell,* 21**,** 418-29.

PRZEPIORKA, D., KO, C. W., DEISSEROTH, A., YANCEY, C. L., CANDAU-CHACON, R., CHIU, H. J., GEHRKE, B. J., GOMEZ-BROUGHTON, C., KANE, R. C., KIRSHNER, S., MEHROTRA, N., RICKS, T. K., SCHMIEL, D., SONG, P., ZHAO, P., ZHOU, Q., FARRELL, A. T. & PAZDUR, R. 2015. FDA Approval: Blinatumomab. *Clin Cancer Res,* 21**,** 4035-9.

PUENTE, X. S., BEA, S., VALDES-MAS, R., VILLAMOR, N., GUTIERREZ-ABRIL, J., MARTIN-SUBERO, J. I., MUNAR, M., RUBIO-PEREZ, C., JARES, P., AYMERICH, M., BAUMANN, T., BEEKMAN, R., BELVER, L., CARRIO, A., CASTELLANO, G., CLOT, G., COLADO, E., COLOMER, D., COSTA, D., DELGADO, J., ENJUANES, A., ESTIVILL, X., FERRANDO, A. A., GELPI, J. L., GONZALEZ, B., GONZALEZ, S., GONZALEZ, M., GUT, M., HERNANDEZ-RIVAS, J. M., LOPEZ-GUERRA, M., MARTIN-GARCIA, D., NAVARRO, A., NICOLAS, P., OROZCO, M., PAYER, A. R., PINYOL, M., PISANO, D. G., PUENTE, D. A., QUEIROS, A. C., QUESADA, V., ROMEO-CASABONA, C. M., ROYO, C., ROYO, R., ROZMAN, M., RUSSINOL, N., SALAVERRIA, I., STAMATOPOULOS, K., STUNNENBERG, H.

G., TAMBORERO, D., TEROL, M. J., VALENCIA, A., LOPEZ-BIGAS, N., TORRENTS, D., GUT, I., LOPEZ-GUILLERMO, A., LOPEZ-OTIN, C. & CAMPO, E. 2015. Non-coding recurrent mutations in chronic lymphocytic leukaemia. *Nature,* 526**,** 519-24.

QIU, H., FANG, X., LUO, Q. & OUYANG, G. 2015. Cancer stem cells: a potential target for cancer therapy. *Cell Mol Life Sci,* 72**,** 3411-24.

QURESHI-BAIG, K., ULLMANN, P., RODRIGUEZ, F., FRASQUILHO, S., NAZAROV, P. V., HAAN, S. & LETELLIER, E. 2016. What Do We Learn from Spheroid Culture Systems? Insights from Tumorspheres Derived from Primary Colon Cancer Tissue. *PLoS One,* 11**,** e0146052.

RAI, K. R. & JAIN, P. 2015. Chronic lymphocytic leukemia (CLL) - Then and Now. *Am J Hematol*.

RAJ, D., AICHER, A. & HEESCHEN, C. 2015. Concise Review: Stem Cells in Pancreatic Cancer: From Concept to Translation. *Stem Cells,* 33**,** 2893-902.

RAMSAY, A. G., CLEAR, A. J., FATAH, R. & GRIBBEN, J. G. 2012. Multiple inhibitory ligands induce impaired T-cell immunologic synapse function in chronic lymphocytic leukemia that can be blocked with lenalidomide: establishing a reversible immune evasion mechanism in human cancer. *Blood,* 120**,** 1412-21.

RAMSAY, A. G., JOHNSON, A. J., LEE, A. M., GORGUN, G., LE DIEU, R., BLUM, W., BYRD, J. C. & GRIBBEN, J. G. 2008. Chronic lymphocytic leukemia T cells show impaired immunological synapse formation that can be reversed with an immunomodulating drug. *J Clin Invest,* 118**,** 2427-37.

REBAGAY, G., YAN, S., LIU, C. & CHEUNG, N. K. 2012. ROR1 and ROR2 in Human Malignancies: Potentials for Targeted Therapy. *Front Oncol,* 2**,** 34.

RELIER, S., YAZDANI, L., AYAD, O., CHOQUET, A., BOURGAUX, J. F., PRUDHOMME, M., PANNEQUIN, J., MACARI, F. & DAVID, A. 2016. Antibiotics inhibit sphere-forming ability in suspension culture. *Cancer Cell Int,* 16**,** 6.

REYA, T., MORRISON, S. J., CLARKE, M. F. & WEISSMAN, I. L. 2001. Stem cells, cancer, and cancer stem cells. *Nature,* 414**,** 105-11.

RICHES, J. C., DAVIES, J. K., MCCLANAHAN, F., FATAH, R., IQBAL, S., AGRAWAL, S., RAMSAY, A. G. & GRIBBEN, J. G. 2013. T cells from CLL patients exhibit features of T-cell exhaustion but retain capacity for cytokine production. *Blood,* 121**,** 1612-21.

RICHES, J. C. & GRIBBEN, J. G. 2014. Immunomodulation and immune reconstitution in chronic lymphocytic leukemia. *Semin Hematol,* 51**,** 228-34.

ROBAK, T. 2014. Current and emerging monoclonal antibody treatments for chronic lymphocytic leukemia: state of the art. *Expert Rev Hematol,* 7**,** 841-57.

ROBERTS, A. W., MA, S., BRANDER, D. M., KIPPS, T. J., BARRIENTOS, J. C., DAVIDS, M. S., ANDERSON, M. A., TAM, C., MASON-BRIGHT, T., RUDERSDORF, N. K., GRESSICK, L., YANG, J., MUNASINGHE,

W., ZHU, M., CERRI, E., ENSCHEDE, S. H., HUMERICKHOUSE, R. A. & SEYMOUR, J. F. 2014. Determination of Recommended Phase 2 Dose of ABT-199 (GDC-0199) Combined with Rituximab (R) in Patients with Relapsed / Refractory (R/R) Chronic Lymphocytic Leukemia (CLL). *Blood,* 124**,** 325-325.

RODRIGUEZ-VICENTE, A. E., DIAZ, M. G. & HERNANDEZ-RIVAS, J. M. 2013. Chronic lymphocytic leukemia: a clinical and molecular heterogenous disease. *Cancer Genet,* 206**,** 49-62.

ROGERS, L. M., VEERAMANI, S. & WEINER, G. J. 2014. Complement in monoclonal antibody therapy of cancer. *Immunol Res,* 59**,** 203-10.

ROSENBERG, S. A. 1999. A new era for cancer immunotherapy based on the genes that encode cancer antigens. *Immunity,* 10**,** 281-7.

ROSENBERG, S. A., PACKARD, B. S., AEBERSOLD, P. M., SOLOMON, D., TOPALIAN, S. L., TOY, S. T., SIMON, P., LOTZE, M. T., YANG, J. C., SEIPP, C. A. & ET AL. 1988. Use of tumor-infiltrating lymphocytes and interleukin-2 in the immunotherapy of patients with metastatic melanoma. A preliminary report. *N Engl J Med,* 319**,** 1676-80.

ROSZMUSZ, E., PATTHY, A., TREXLER, M. & PATTHY, L. 2001. Localization of disulfide bonds in the frizzled module of Ror1 receptor tyrosine kinase. *J Biol Chem,* 276**,** 18485-90.

ROZOVSKI, U., HAZAN-HALEVY, I., KEATING, M. J. & ESTROV, Z. 2014. Personalized medicine in CLL: current status and future perspectives. *Cancer Lett,* 352**,** 4-14.

SAFDARI, Y., FARAJNIA, S., ASGHARZADEH, M. & KHALILI, M. 2013. Antibody humanization methods - a review and update. *Biotechnol Genet Eng Rev,* 29**,** 175-86.

SAHLIN, S., HED, J. & RUNDQUIST, I. 1983. Differentiation between attached and ingested immune complexes by a fluorescence quenching cytofluorometric assay. *J Immunol Methods,* 60**,** 115-24.

SATHYANARAYANAN, V. & NEELAPU, S. S. 2015. Cancer immunotherapy: Strategies for personalization and combinatorial approaches. *Mol Oncol,* 9**,** 2043-53.

SATO, K., NAGAI, J., MITSUI, N., RYOKO, Y. & TAKANO, M. 2009. Effects of endocytosis inhibitors on internalization of human IgG by Caco-2 human intestinal epithelial cells. *Life Sci,* 85**,** 800-7.

SAULEP-EASTON, D., VINCENT, F. B., QUAH, P. S., WEI, A., TING, S. B., CROCE, C. M., TAM, C. & MACKAY, F. 2016. The BAFF receptor TACI controls IL-10 production by regulatory B cells and CLL B cells. *Leukemia,* 30**,** 163-72.

SCHEEL, C. & WEINBERG, R. A. 2012. Cancer stem cells and epithelial-mesenchymal transition: concepts and molecular links. *Semin Cancer Biol,* 22**,** 396-403.

SCHROFF, R. W., FOON, K. A., BEATTY, S. M., OLDHAM, R. K. & MORGAN, A. C., JR. 1985. Human anti-murine immunoglobulin responses in patients receiving monoclonal antibody therapy. *Cancer Res,* 45**,** 879-85.

SCHUR, P. H. 1988. IgG subclasses. A historical perspective. *Monogr Allergy,* 23**,** 1-11.
SCHWARTZ, R. H. 1992. Costimulation of T lymphocytes: the role of CD28, CTLA-4, and B7/BB1 in interleukin-2 production and immunotherapy. *Cell,* 71**,** 1065-8.
SCIENCES, G. H. L. (ed.) 2012. *Biacore™ Assay Handbook*.
SCIUME, M., VINCENTI, D., REDA, G., OROFINO, N., CASSIN, R., GIANNARELLI, D., GAIDANO, G., ROSSI, D. & CORTELEZZI, A. 2015. Low-dose alemtuzumab in refractory/relapsed chronic lymphocytic leukemia: Genetic profile and long-term outcome from a single center experience. *Am J Hematol*.
SCOTT, A. M., WOLCHOK, J. D. & OLD, L. J. 2012. Antibody therapy of cancer. *Nat Rev Cancer,* 12**,** 278-87.
SEIFFERT, M. 2014. Lenalidomide, an antiproliferative CLL drug. *Blood,* 124**,** 1545-6.
SELIGER, B., WOLLSCHEID, U., MOMBURG, F., BLANKENSTEIN, T. & HUBER, C. 2001. Characterization of the major histocompatibility complex class I deficiencies in B16 melanoma cells. *Cancer Res,* 61**,** 1095-9.
SENZER, N. N., KAUFMAN, H. L., AMATRUDA, T., NEMUNAITIS, M., REID, T., DANIELS, G., GONZALEZ, R., GLASPY, J., WHITMAN, E., HARRINGTON, K., GOLDSWEIG, H., MARSHALL, T., LOVE, C., COFFIN, R. & NEMUNAITIS, J. J. 2009. Phase II clinical trial of a granulocyte-macrophage colony-stimulating factor-encoding, second-generation oncolytic herpesvirus in patients with unresectable metastatic melanoma. *J Clin Oncol,* 27**,** 5763-71.
SERGEANT, G., VANKELECOM, H., GREMEAUX, L. & TOPAL, B. 2009. Role of cancer stem cells in pancreatic ductal adenocarcinoma. *Nat Rev Clin Oncol,* 6**,** 580-6.
SHABANI, M., NASERI, J. & SHOKRI, F. 2015. Receptor tyrosine kinase-like orphan receptor 1: a novel target for cancer immunotherapy. *Expert Opin Ther Targets,* 19**,** 941-55.
SHANKARAN, V., IKEDA, H., BRUCE, A. T., WHITE, J. M., SWANSON, P. E., OLD, L. J. & SCHREIBER, R. D. 2001. IFNgamma and lymphocytes prevent primary tumour development and shape tumour immunogenicity. *Nature,* 410**,** 1107-11.
SHERMAN, M. H., YU, R. T., ENGLE, D. D., DING, N., ATKINS, A. R., TIRIAC, H., COLLISSON, E. A., CONNOR, F., VAN DYKE, T., KOZLOV, S., MARTIN, P., TSENG, T. W., DAWSON, D. W., DONAHUE, T. R., MASAMUNE, A., SHIMOSEGAWA, T., APTE, M. V., WILSON, J. S., NG, B., LAU, S. L., GUNTON, J. E., WAHL, G. M., HUNTER, T., DREBIN, J. A., O'DWYER, P. J., LIDDLE, C., TUVESON, D. A., DOWNES, M. & EVANS, R. M. 2014. Vitamin D receptor-mediated stromal reprogramming suppresses pancreatitis and enhances pancreatic cancer therapy. *Cell,* 159**,** 80-93.
SHURIN, M. R., NAIDITCH, H., GUTKIN, D. W., UMANSKY, V. & SHURIN, G. V. 2012. ChemoImmunoModulation: immune regulation by the

antineoplastic chemotherapeutic agents. *Curr Med Chem,* 19**,** 1792-803.

SINGH, A. K., ARYA, R. K., MAHESHWARI, S., SINGH, A., MEENA, S., PANDEY, P., DORMOND, O. & DATTA, D. 2015. Tumor heterogeneity and cancer stem cell paradigm: updates in concept, controversies and clinical relevance. *Int J Cancer,* 136**,** 1991-2000.

SLEDZINSKA, A., MENGER, L., BERGERHOFF, K., PEGGS, K. S. & QUEZADA, S. A. 2015. Negative immune checkpoints on T lymphocytes and their relevance to cancer immunotherapy. *Mol Oncol,* 9**,** 1936-65.

SMALLWOOD, D. T., APOLLONIO, B., WILLIMOTT, S., LEZINA, L., ALHARTHI, A., AMBROSE, A. R., DE ROSSI, G., RAMSAY, A. G. & WAGNER, S. D. 2016. Extracellular vesicles released by CD40/IL-4-stimulated CLL cells confer altered functional properties to CD4+ T cells. *Blood,* 128**,** 542-52.

SOCIETY, A. C. 2015. Global Cancer Facts & Figures.

STADLER, C. R., BAHR-MAHMUD, H., CELIK, L., HEBICH, B., ROTH, A. S., ROTH, R. P., KARIKO, K., TURECI, O. & SAHIN, U. 2017. Elimination of large tumors in mice by mRNA-encoded bispecific antibodies. *Nat Med,* 23**,** 815-817.

STEINMAN, R. M. & DHODAPKAR, M. 2001. Active immunization against cancer with dendritic cells: the near future. *Int J Cancer,* 94**,** 459-73.

STREBHARDT, K. & ULLRICH, A. 2008. Paul Ehrlich's magic bullet concept: 100 years of progress. *Nat Rev Cancer,* 8**,** 473-80.

STROMNES, I. M., DELGIORNO, K. E., GREENBERG, P. D. & HINGORANI, S. R. 2014. Stromal reengineering to treat pancreas cancer. *Carcinogenesis,* 35**,** 1451-60.

SURYADEVARA, C. M., GEDEON, P. C., SANCHEZ-PEREZ, L., VERLA, T., ALVAREZ-BRECKENRIDGE, C., CHOI, B. D., FECCI, P. E. & SAMPSON, J. H. 2015. Are BiTEs the "missing link" in cancer therapy? *Oncoimmunology,* 4**,** e1008339.

TAEGER, J., MOSER, C., HELLERBRAND, C., MYCIELSKA, M. E., GLOCKZIN, G., SCHLITT, H. J., GEISSLER, E. K., STOELTZING, O. & LANG, S. A. 2011. Targeting FGFR/PDGFR/VEGFR impairs tumor growth, angiogenesis, and metastasis by effects on tumor cells, endothelial cells, and pericytes in pancreatic cancer. *Mol Cancer Ther,* 10**,** 2157-67.

TAN, P., MITCHELL, D. A., BUSS, T. N., HOLMES, M. A., ANASETTI, C. & FOOTE, J. 2002. "Superhumanized" antibodies: reduction of immunogenic potential by complementarity-determining region grafting with human germline sequences: application to an anti-CD28. *J Immunol,* 169**,** 1119-25.

TAO, M. H., SMITH, R. I. & MORRISON, S. L. 1993. Structural features of human immunoglobulin G that determine isotype-specific differences in complement activation. *J Exp Med,* 178**,** 661-7.

TEBBUTT, N., PEDERSEN, M. W. & JOHNS, T. G. 2013. Targeting the ERBB family in cancer: couples therapy. *Nat Rev Cancer,* 13**,** 663-73.

TERABE, M. & BERZOFSKY, J. A. 2004. Immunoregulatory T cells in tumor immunity. *Curr Opin Immunol,* 16**,** 157-62.

THIELE, L., MERKLE, H. P. & WALTER, E. 2003. Phagocytosis and phagosomal fate of surface-modified microparticles in dendritic cells and macrophages. *Pharm Res,* 20**,** 221-8.

THIELE, L., ROTHEN-RUTISHAUSER, B., JILEK, S., WUNDERLI-ALLENSPACH, H., MERKLE, H. P. & WALTER, E. 2001. Evaluation of particle uptake in human blood monocyte-derived cells in vitro. Does phagocytosis activity of dendritic cells measure up with macrophages? *J Control Release,* 76**,** 59-71.

THIJSSEN, R., SLINGER, E., WELLER, K., GEEST, C. R., BEAUMONT, T., VAN OERS, M. H., KATER, A. P. & ELDERING, E. 2015. Resistance to ABT-199 induced by microenvironmental signals in chronic lymphocytic leukemia can be counteracted by CD20 antibodies or kinase inhibitors. *Haematologica,* 100**,** e302-6.

THOMAS, L. 1959. Discussion of cellular and humoral aspects of the hypersensitivity states. *Cellular and Humoral Aspects of Hypersensitivity.* New York: Hoeber-Harper: Lawrence HS.

TOPALIAN, S. L., SZNOL, M., MCDERMOTT, D. F., KLUGER, H. M., CARVAJAL, R. D., SHARFMAN, W. H., BRAHMER, J. R., LAWRENCE, D. P., ATKINS, M. B., POWDERLY, J. D., LEMING, P. D., LIPSON, E. J., PUZANOV, I., SMITH, D. C., TAUBE, J. M., WIGGINTON, J. M., KOLLIA, G. D., GUPTA, A., PARDOLL, D. M., SOSMAN, J. A. & HODI, F. S. 2014. Survival, durable tumor remission, and long-term safety in patients with advanced melanoma receiving nivolumab. *J Clin Oncol,* 32**,** 1020-30.

TOPP, M. S., GOKBUGET, N., ZUGMAIER, G., DEGENHARD, E., GOEBELER, M. E., KLINGER, M., NEUMANN, S. A., HORST, H. A., RAFF, T., VIARDOT, A., STELLJES, M., SCHAICH, M., KOHNE-VOLLAND, R., BRUGGEMANN, M., OTTMANN, O. G., BURMEISTER, T., BAEUERLE, P. A., NAGORSEN, D., SCHMIDT, M., EINSELE, H., RIETHMULLER, G., KNEBA, M., HOELZER, D., KUFER, P. & BARGOU, R. C. 2012. Long-term follow-up of hematologic relapse-free survival in a phase 2 study of blinatumomab in patients with MRD in B-lineage ALL. *Blood,* 120**,** 5185-7.

TOPP, M. S., STELLJES, M., ZUGMAIER, G., BARNETTE, P., HEFFNER, L. T., JR., TRIPPETT, T., DUELL, J., BARGOU, R. C., HOLLAND, C., BENJAMIN, J. E., KLINGER, M. & LITZOW, M. R. 2017. Blinatumomab retreatment after relapse in patients with relapsed/refractory B-precursor acute lymphoblastic leukemia. *Leukemia*.

TSIATAS, M., MOUNTZIOS, G. & CURIGLIANO, G. 2016. Future perspectives in cancer immunotherapy. *Ann Transl Med,* 4**,** 273.

TSUBATA, T. 2001. Molecular mechanisms for apoptosis induced by signaling through the B cell antigen receptor. *Int Rev Immunol,* 20**,** 791-803.

TUDOR, D., YU, H., MAUPETIT, J., DRILLET, A. S., BOUCEBA, T., SCHWARTZ-CORNIL, I., LOPALCO, L., TUFFERY, P. & BOMSEL, M. 2012. Isotype modulates epitope specificity, affinity, and antiviral activities of anti-HIV-1 human broadly neutralizing 2F5 antibody. *Proc Natl Acad Sci U S A,* 109**,** 12680-5.

UENO, H., IOKA, T., IKEDA, M., OHKAWA, S., YANAGIMOTO, H., BOKU, N., FUKUTOMI, A., SUGIMORI, K., BABA, H., YAMAO, K., SHIMAMURA, T., SHO, M., KITANO, M., CHENG, A. L., MIZUMOTO, K., CHEN, J. S., FURUSE, J., FUNAKOSHI, A., HATORI, T., YAMAGUCHI, T., EGAWA, S., SATO, A., OHASHI, Y., OKUSAKA, T. & TANAKA, M. 2013. Randomized phase III study of gemcitabine plus S-1, S-1 alone, or gemcitabine alone in patients with locally advanced and metastatic pancreatic cancer in Japan and Taiwan: GEST study. *J Clin Oncol,* 31**,** 1640-8.

UMEBAYASHI, M., KIYOTA, A., KOYA, N., TANAKA, H., ONISHI, H., KATANO, M. & MORISAKI, T. 2014. An epithelial cell adhesion molecule- and CD3-bispecific antibody plus activated T-cells can eradicate chemoresistant cancer stem-like pancreatic carcinoma cells in vitro. *Anticancer Res,* 34**,** 4509-19.

URBAN, J. L. & SCHREIBER, H. 1992. Tumor antigens. *Annu Rev Immunol,* 10**,** 617-44.

VAN BOCKSTAELE, F., VERHASSELT, B. & PHILIPPE, J. 2009. Prognostic markers in chronic lymphocytic leukemia: a comprehensive review. *Blood Rev,* 23**,** 25-47.

VAN CUTSEM, E., VAN DE VELDE, H., KARASEK, P., OETTLE, H., VERVENNE, W. L., SZAWLOWSKI, A., SCHOFFSKI, P., POST, S., VERSLYPE, C., NEUMANN, H., SAFRAN, H., HUMBLET, Y., PEREZ RUIXO, J., MA, Y. & VON HOFF, D. 2004. Phase III trial of gemcitabine plus tipifarnib compared with gemcitabine plus placebo in advanced pancreatic cancer. *J Clin Oncol,* 22**,** 1430-8.

VAN DEN BROEK, M. E., KAGI, D., OSSENDORP, F., TOES, R., VAMVAKAS, S., LUTZ, W. K., MELIEF, C. J., ZINKERNAGEL, R. M. & HENGARTNER, H. 1996. Decreased tumor surveillance in perforin-deficient mice. *J Exp Med,* 184**,** 1781-90.

VAN DER BURG, S. H., ARENS, R., OSSENDORP, F., VAN HALL, T. & MELIEF, C. J. 2016. Vaccines for established cancer: overcoming the challenges posed by immune evasion. *Nat Rev Cancer,* 16**,** 219-33.

VAN DYKE, D. L., WERNER, L., RASSENTI, L. Z., NEUBERG, D., GHIA, E., HEEREMA, N. A., DAL CIN, P., DELL AQUILA, M., SREEKANTAIAH, C., GREAVES, A. W., KIPPS, T. J. & KAY, N. E. 2016. The Dohner fluorescence in situ hybridization prognostic classification of chronic lymphocytic leukaemia (CLL): the CLL Research Consortium experience. *Br J Haematol,* 173**,** 105-13.

VAN RIKXOORT, M., MICHAELIS, M., WOLSCHEK, M., MUSTER, T., EGOROV, A., SEIPELT, J., DOERR, H. W. & CINATL, J., JR. 2012. Oncolytic effects of a novel influenza A virus expressing interleukin-15 from the NS reading frame. *PLoS One,* 7**,** e36506.

VARGA, J., DE OLIVEIRA, T. & GRETEN, F. R. 2014. The architect who never sleeps: tumor-induced plasticity. *FEBS Lett,* 588**,** 2422-7.
VELDERS, M. P., VAN RHIJN, C. M., OSKAM, E., FLEUREN, G. J., WARNAAR, S. O. & LITVINOV, S. V. 1998. The impact of antigen density and antibody affinity on antibody-dependent cellular cytotoxicity: relevance for immunotherapy of carcinomas. *Br J Cancer,* 78**,** 478-83.
VIDARSSON, G., DEKKERS, G. & RISPENS, T. 2014. IgG subclasses and allotypes: from structure to effector functions. *Front Immunol,* 5**,** 520.
VITALE, C., FALCHI, L., TEN HACKEN, E., GAO, H., SHAIM, H., VAN ROOSBROECK, K., CALIN, G., O'BRIEN, S., FADERL, S., WANG, X., WIERDA, W. G., REZVANI, K., REUBEN, J. M., BURGER, J. A., KEATING, M. J. & FERRAJOLI, A. 2016. Ofatumumab and Lenalidomide for Patients with Relapsed or Refractory Chronic Lymphocytic Leukemia: Correlation between Responses and Immune Characteristics. *Clin Cancer Res,* 22**,** 2359-67.
VOENA, C. & CHIARLE, R. 2016. Advances in cancer immunology and cancer immunotherapy. *Discov Med,* 21**,** 125-33.
VON HOFF, D. D., RAMANATHAN, R. K., BORAD, M. J., LAHERU, D. A., SMITH, L. S., WOOD, T. E., KORN, R. L., DESAI, N., TRIEU, V., IGLESIAS, J. L., ZHANG, H., SOON-SHIONG, P., SHI, T., RAJESHKUMAR, N. V., MAITRA, A. & HIDALGO, M. 2011. Gemcitabine plus nab-paclitaxel is an active regimen in patients with advanced pancreatic cancer: a phase I/II trial. *J Clin Oncol,* 29**,** 4548-54.
VONDERHEIDE, R. H., BAJOR, D. L., WINOGRAD, R., EVANS, R. A., BAYNE, L. J. & BEATTY, G. L. 2013. CD40 immunotherapy for pancreatic cancer. *Cancer Immunol Immunother,* 62**,** 949-54.
WADDELL, N., PAJIC, M., PATCH, A. M., CHANG, D. K., KASSAHN, K. S., BAILEY, P., JOHNS, A. L., MILLER, D., NONES, K., QUEK, K., QUINN, M. C., ROBERTSON, A. J., FADLULLAH, M. Z., BRUXNER, T. J., CHRIST, A. N., HARLIWONG, I., IDRISOGLU, S., MANNING, S., NOURSE, C., NOURBAKHSH, E., WANI, S., WILSON, P. J., MARKHAM, E., CLOONAN, N., ANDERSON, M. J., FINK, J. L., HOLMES, O., KAZAKOFF, S. H., LEONARD, C., NEWELL, F., POUDEL, B., SONG, S., TAYLOR, D., WADDELL, N., WOOD, S., XU, Q., WU, J., PINESE, M., COWLEY, M. J., LEE, H. C., JONES, M. D., NAGRIAL, A. M., HUMPHRIS, J., CHANTRILL, L. A., CHIN, V., STEINMANN, A. M., MAWSON, A., HUMPHREY, E. S., COLVIN, E. K., CHOU, A., SCARLETT, C. J., PINHO, A. V., GIRY-LATERRIERE, M., ROOMAN, I., SAMRA, J. S., KENCH, J. G., PETTITT, J. A., MERRETT, N. D., TOON, C., EPARI, K., NGUYEN, N. Q., BARBOUR, A., ZEPS, N., JAMIESON, N. B., GRAHAM, J. S., NICLOU, S. P., BJERKVIG, R., GRUTZMANN, R., AUST, D., HRUBAN, R. H., MAITRA, A., IACOBUZIO-DONAHUE, C. A., WOLFGANG, C. L., MORGAN, R. A., LAWLOR, R. T., CORBO, V., BASSI, C., FALCONI, M., ZAMBONI, G., TORTORA, G., TEMPERO,

M. A., AUSTRALIAN PANCREATIC CANCER GENOME, I., GILL, A. J., ESHLEMAN, J. R., PILARSKY, C., SCARPA, A., MUSGROVE, E. A., PEARSON, J. V., BIANKIN, A. V. & GRIMMOND, S. M. 2015. Whole genomes redefine the mutational landscape of pancreatic cancer. *Nature,* 518**,** 495-501.

WALTER, H. S., RULE, S. A., DYER, M. J., KARLIN, L., JONES, C., CAZIN, B., QUITTET, P., SHAH, N., HUTCHINSON, C. V., HONDA, H., DUFFY, K., BIRKETT, J., JAMIESON, V., COURTENAY-LUCK, N., YOSHIZAWA, T., SHARPE, J., OHNO, T., ABE, S., NISHIMURA, A., CARTRON, G., MORSCHHAUSER, F., FEGAN, C. & SALLES, G. 2016. A phase 1 clinical trial of the selective BTK inhibitor ONO/GS-4059 in relapsed and refractory mature B-cell malignancies. *Blood,* 127**,** 411-9.

WARSHAW, A. L. & FERNANDEZ-DEL CASTILLO, C. 1992. Pancreatic carcinoma. *N Engl J Med,* 326**,** 455-65.

WEINER, G. J. 2010. Rituximab: mechanism of action. *Semin Hematol,* 47**,** 115-23.

WEINER, G. J. 2015. Building better monoclonal antibody-based therapeutics. *Nat Rev Cancer,* 15**,** 361-70.

WEISWALD, L. B., BELLET, D. & DANGLES-MARIE, V. 2015. Spherical cancer models in tumor biology. *Neoplasia,* 17**,** 1-15.

WHERRY, E. J. 2011. T cell exhaustion. *Nat Immunol,* 12**,** 492-9.

WHIPPLE, A. O., PARSONS, W. B. & MULLINS, C. R. 1935. Treatment of Carcinoma of the Ampulla of Vater. *Ann Surg,* 102**,** 763-79.

WIDHOPF, G. F., 2ND, CUI, B., GHIA, E. M., CHEN, L., MESSER, K., SHEN, Z., BRIGGS, S. P., CROCE, C. M. & KIPPS, T. J. 2014. ROR1 can interact with TCL1 and enhance leukemogenesis in Emu-TCL1 transgenic mice. *Proc Natl Acad Sci U S A,* 111**,** 793-8.

WIEDMANN, M. W. & MOSSNER, J. 2012. Safety and efficacy of sunitinib in patients with unresectable pancreatic neuroendocrine tumors. *Clin Med Insights Oncol,* 6**,** 381-93.

WIESTNER, A. 2012. Emerging role of kinase-targeted strategies in chronic lymphocytic leukemia. *Hematology Am Soc Hematol Educ Program,* 2012**,** 88-96.

WINTER, J. M., BRENNAN, M. F., TANG, L. H., D'ANGELICA, M. I., DEMATTEO, R. P., FONG, Y., KLIMSTRA, D. S., JARNAGIN, W. R. & ALLEN, P. J. 2012. Survival after resection of pancreatic adenocarcinoma: results from a single institution over three decades. *Ann Surg Oncol,* 19**,** 169-75.

WINTER, J. M., TING, A. H., VILARDELL, F., GALLMEIER, E., BAYLIN, S. B., HRUBAN, R. H., KERN, S. E. & IACOBUZIO-DONAHUE, C. A. 2008. Absence of E-cadherin expression distinguishes noncohesive from cohesive pancreatic cancer. *Clin Cancer Res,* 14**,** 412-8.

WOLF, E., HOFMEISTER, R., KUFER, P., SCHLERETH, B. & BAEUERLE, P. A. 2005. BiTEs: bispecific antibody constructs with unique anti-tumor activity. *Drug Discov Today,* 10**,** 1237-44.

WOLFGANG, C. L., HERMAN, J. M., LAHERU, D. A., KLEIN, A. P., ERDEK, M. A., FISHMAN, E. K. & HRUBAN, R. H. 2013. Recent progress in pancreatic cancer. *CA Cancer J Clin,* 63**,** 318-48.

WOOTLA, B., DENIC, A. & RODRIGUEZ, M. 2014. Polyclonal and monoclonal antibodies in clinic. *Methods Mol Biol,* 1060**,** 79-110.

WU, J., LIU, C., TSUI, S. T. & LIU, D. 2016. Second-generation inhibitors of Bruton tyrosine kinase. *J Hematol Oncol,* 9**,** 80.

WUHRER, M., PORCELIJN, L., KAPUR, R., KOELEMAN, C. A., DEELDER, A., DE HAAS, M. & VIDARSSON, G. 2009. Regulated glycosylation patterns of IgG during alloimmune responses against human platelet antigens. *J Proteome Res,* 8**,** 450-6.

YABAR, C. S. & WINTER, J. M. 2016. Pancreatic Cancer: A Review. *Gastroenterol Clin North Am,* 45**,** 429-45.

YACHIDA, S., JONES, S., BOZIC, I., ANTAL, T., LEARY, R., FU, B., KAMIYAMA, M., HRUBAN, R. H., ESHLEMAN, J. R., NOWAK, M. A., VELCULESCU, V. E., KINZLER, K. W., VOGELSTEIN, B. & IACOBUZIO-DONAHUE, C. A. 2010. Distant metastasis occurs late during the genetic evolution of pancreatic cancer. *Nature,* 467**,** 1114-7.

YAMAGUCHI, T., YANAGISAWA, K., SUGIYAMA, R., HOSONO, Y., SHIMADA, Y., ARIMA, C., KATO, S., TOMIDA, S., SUZUKI, M., OSADA, H. & TAKAHASHI, T. 2012. NKX2-1/TITF1/TTF-1-Induced ROR1 is required to sustain EGFR survival signaling in lung adenocarcinoma. *Cancer Cell,* 21**,** 348-61.

YAMPOLSKY, L. Y. & STOLTZFUS, A. 2005. The exchangeability of amino acids in proteins. *Genetics,* 170**,** 1459-72.

YANG, J., BASKAR, S., KWONG, K. Y., KENNEDY, M. G., WIESTNER, A. & RADER, C. 2011. Therapeutic potential and challenges of targeting receptor tyrosine kinase ROR1 with monoclonal antibodies in B-cell malignancies. *PLoS One,* 6**,** e21018.

YOSHIOKA, R., YASUNAGA, H., HASEGAWA, K., HORIGUCHI, H., FUSHIMI, K., AOKI, T., SAKAMOTO, Y., SUGAWARA, Y. & KOKUDO, N. 2014. Impact of hospital volume on hospital mortality, length of stay and total costs after pancreaticoduodenectomy. *Br J Surg,* 101**,** 523-9.

YU, J., CHEN, L., CUI, B., WIDHOPF, G. F., 2ND, SHEN, Z., WU, R., ZHANG, L., ZHANG, S., BRIGGS, S. P. & KIPPS, T. J. 2016. Wnt5a induces ROR1/ROR2 heterooligomerization to enhance leukemia chemotaxis and proliferation. *J Clin Invest,* 126**,** 585-98.

YU, X., MARSHALL, M. J. E., CRAGG, M. S. & CRISPIN, M. 2017. Improving Antibody-Based Cancer Therapeutics Through Glycan Engineering. *BioDrugs,* 31**,** 151-166.

ZENG, J., LIU, R., WANG, J. & FANG, Y. 2015. A bispecific antibody directly induces lymphoma cell death by simultaneously targeting CD20 and HLA-DR. *J Cancer Res Clin Oncol,* 141**,** 1899-907.

ZENT, C. S., LAPLANT, B. R., JOHNSTON, P. B., CALL, T. G., HABERMANN, T. M., MICALLEF, I. N. & WITZIG, T. E. 2010. The

treatment of recurrent/refractory chronic lymphocytic leukemia/small lymphocytic lymphoma (CLL) with everolimus results in clinical responses and mobilization of CLL cells into the circulation. *Cancer,* 116**,** 2201-7.

ZENZ, T., MERTENS, D., KUPPERS, R., DOHNER, H. & STILGENBAUER, S. 2010. From pathogenesis to treatment of chronic lymphocytic leukaemia. *Nat Rev Cancer,* 10**,** 37-50.

ZHANG, C. 2012. Hybridoma technology for the generation of monoclonal antibodies. *Methods Mol Biol,* 901**,** 117-35.

ZHANG, L., CONEJO-GARCIA, J. R., KATSAROS, D., GIMOTTY, P. A., MASSOBRIO, M., REGNANI, G., MAKRIGIANNAKIS, A., GRAY, H., SCHLIENGER, K., LIEBMAN, M. N., RUBIN, S. C. & COUKOS, G. 2003. Intratumoral T cells, recurrence, and survival in epithelial ovarian cancer. *N Engl J Med,* 348**,** 203-13.

ZHANG, S., CHEN, L., CUI, B., CHUANG, H. Y., YU, J., WANG-RODRIGUEZ, J., TANG, L., CHEN, G., BASAK, G. W. & KIPPS, T. J. 2012a. ROR1 is expressed in human breast cancer and associated with enhanced tumor-cell growth. *PLoS One,* 7**,** e31127.

ZHANG, S., CHEN, L., WANG-RODRIGUEZ, J., ZHANG, L., CUI, B., FRANKEL, W., WU, R. & KIPPS, T. J. 2012b. The onco-embryonic antigen ROR1 is expressed by a variety of human cancers. *Am J Pathol,* 181**,** 1903-10.

ZHANG, S., CUI, B., LAI, H., LIU, G., GHIA, E. M., WIDHOPF, G. F., 2ND, ZHANG, Z., WU, C. C., CHEN, L., WU, R., SCHWAB, R., CARSON, D. A. & KIPPS, T. J. 2014. Ovarian cancer stem cells express ROR1, which can be targeted for anti-cancer-stem-cell therapy. *Proc Natl Acad Sci U S A,* 111**,** 17266-71.

ZHANG, X. Y. & ZHANG, P. Y. 2016. Receptor tyrosine kinases in carcinogenesis. *Oncol Lett,* 12**,** 3679-3682.

ZHENG, Y. Z., MA, R., ZHOU, J. K., GUO, C. L., WANG, Y. S., LI, Z. G., LIU, L. X. & PENG, Y. 2016. ROR1 is a novel prognostic biomarker in patients with lung adenocarcinoma. *Sci Rep,* 6**,** 36447.

ZHOU, G., CHIU, D., QIN, D., NIU, L., CAI, J., HE, L., TAN, D. & XU, K. 2013. Expression of CD44v6 and integrin-beta1 for the prognosis evaluation of pancreatic cancer patients after cryosurgery. *Diagn Pathol,* 8**,** 146.

ZHOU, J. K., ZHENG, Y. Z., LIU, X. S., GOU, Q., MA, R., GUO, C. L., CROCE, C. M., LIU, L. & PENG, Y. 2017a. ROR1 expression as a biomarker for predicting prognosis in patients with colorectal cancer. *Oncotarget,* 8**,** 32864-32872.

ZHOU, Y., KIPPS, T. J. & ZHANG, S. 2017b. Wnt5a Signaling in Normal and Cancer Stem Cells. *Stem Cells Int,* 2017**,** 5295286.